# Innate immune cell migration and function in response to damage associated signals

Archer, Sophie

*Award date:*
2015

*Awarding institution:*
University of Bath

# Innate Immune Cell Migration and Function in Response to Damage-Associated Signals

Sophie Louise Archer

A thesis submitted for the degree of Doctor of Philosophy

University of Bath

Department of Pharmacy & Pharmacology

November 2014

## Acknowledgements

I would like to thank Professor Steve Ward, Professor Will Wood and Dr Malcolm Watson for their supervision, and the University of Bath for funding this project. Thanks also go to fellow postgraduates and staff members who I have worked with for their knowledge and guidance. Special thanks are for Jo Carter and Adrian Rogers for their technical assistance.

This thesis would not have been possible without my family: Mum, Dad, Emily, Thomas and Chris. Your support and encouragement have given me the strength to go on through the hard times. This work is dedicated to you.

## Abstract

Tissue damage initiates the release of a complex, interacting collection of chemical signals. The coordinated function of these signals gives rise to an inflammatory event, whereby circulating immune cells are recruited to clear pathogens. Invertebrate models of tissue damage have revealed a key role for damage-associated signals, specifically hydrogen peroxide ($H_2O_2$), in attracting immune cells to sites of tissue damage. The Src family kinase (SFK), Lyn, is oxidised by $H_2O_2$ in zebrafish wound models, and subsequent activation of Lyn triggers directed cell motility. In mammalian systems, $H_2O_2$ is an important second messenger, however, its role as a damage signal and its association with SFK signalling remains unclear.

The aims of this thesis are to investigate how immune cell function and migration in response to damage-associated signals transfers into other models. To address this, we have used an *in vivo Drosophila melanogaster* embryonic wounding model and *in vitro* assays of human innate cell function and migration.

The migration of *Drosophila* hemocytes in response to a wound was impaired in embryos lacking functional Src42A or Shark kinase. However, hemocyte motility was impaired in embryos bathed in exogenous $H_2O_2$. *In vitro*, $H_2O_2$ inhibited human innate cell motility, chemotaxis, actin reorganisation and phagocytosis, but activated intracellular signalling pathways and did not affect receptor expression or cell viability. Exogenous ATP activated chemokinesis and rapid actin reorganisation. The *in vitro* effects of immune-related ligands were inhibited by pharmacological inhibition of SFK, Syk, and PI3K signalling. In particular, inhibition of class IA PI3K isoforms p110β and p110δ, but not p110α, disrupted monocyte MCP-1-mediated actin reorganisation and spreading.

SFKs are required for *Drosophila* immune cell migration to a wound and for human innate cell migration to chemoattractants. While endogenous ROS production is important for immune cell function, exogenous $H_2O_2$ may negatively modulate downstream mediators of chemokine signalling. $H_2O_2$ and ATP are distinct in their abilities to activate immune cells and initiate chemokinesis. Intracellular kinases regulate basal and chemoattractant-mediated motility and are therefore attractive targets for therapeutic management of inflammatory disease.

## Abbreviations

| Abbreviation | Definition |
|---|---|
| 3AC | 3-α-aminocholestane |
| ADP | Adenosine diphosphate |
| ANOVA | Analysis of variance |
| AQP | Aquaporin |
| Asp | Aspartic acid |
| ATP | Adenosine 5'-triphosphate |
| cAMP | Cyclic adenosine monophosphate |
| CFSE | Carboxyfluorescein succinimidyl ester |
| CGD | Chronic granulomatous disease |
| COOH | Carboxylic acid |
| Cys | Cysteine |
| DAG | Diacyl-glycerol |
| DAMP | Damage associated molecular pattern |
| DAPI | 4'-6'-diamidino-2-phenylindole |
| DCFDA | 2',7'-dichlorofluorescein diacetate |
| DMEM | Dulbecco's' modified eagle's medium |
| DPI | Diphenyleneiodonium |
| Duox | Dual oxidase |
| ECM | Extracellular matrix |
| EGF | Epidermal growth factor |
| EMS | Ethyl methanesulfonate |
| ER | Endoplasmic reticulum |
| ERK | Extracellular signal-regulated kinase |
| FAK | Focal adhesion kinase |
| FGF | Fibroblast growth factor |
| fMLP | N-formyl-methionyl-leucyl-phenylalanine |
| FPR | Formyl peptide receptor |
| GAP | Guanine activating protein |
| G-CSF | Granulocyte colony stimulating factor |
| GDI | Guanine dissociation inhibitor |
| GDP | Guanosine diphosphate |
| GEF | Guanine exchange factor |
| GFP | Green fluorescent protein |
| Gly | Glycine |
| GPCR | G protein couple receptor |
| GRK | G protein coupled receptor tyrosine kinase |
| GTP | Guanosine triphosphate |
| $H^+$ | Hydrogen ion |
| $H_2O_2$ | Hydrogen peroxide |
| HBSS | Hank's balanced salt solution |
| IBD | Irritable bowel disease |
| ICAM-1 | Intercellular adhesion molecule-1 |
| IFN | Interferon |
| IL-8 | Interleukin 8 |
| $IP_3$ | Inositol triphosphate |

| | |
|---|---|
| ITAM | Immunoreceptor tyrosine-based activation motif |
| ITIM | Immunoreceptor tyrosine-based inhibition motif |
| LAD | Leukocyte adhesion deficiency |
| LFA-1 | Lymphocyte-function associated antigen-1 |
| LPS | Lipopolysaccharide |
| LT | Leukotriene |
| $LXA_4$ | Lipoxin $A_4$ |
| M-CSF | Monocyte-colony stimulating factor |
| MAPK | Mitogen activate protein kinase |
| MCP-1 | Monocyte chemoattractant protein-1 |
| MMP | Matrix metalloproteinase |
| MO | Morpholino oligonucleotide |
| MTT | 3-(4,5-dimethylthiazol-2-yl)-2,5-diphenyltetrazolium bromide |
| NAD | Nicotinamide adenine dinucleotide |
| NADPH | Nicotinamide adenine dinucleotide phosphate-oxidase |
| NET | Neutrophil extracellular trap |
| NLR | Nod-like receptor |
| NOX | NADPH oxidase |
| $O_2^-$ | Superoxide |
| PAF | Platelet activating factor |
| PAMP | Pathogen associated molecular pattern |
| PBMC | Peripheral blood monocytic cell |
| PBS | Pulbeco's buffered saline |
| Pct | Piceatannol |
| PDGF | Platelet derived growth factor |
| PFA | Paraformaldehyde |
| PH | Pleckstrin homology |
| $PI(3,4,5)P_3$ | Phosphatidylinositol (3,4,5)-triphosphate |
| $PI(3,4)P_2$ | Phosphatidylinositol (3,4)-bisphosphate |
| $PI(4,5)P_2$ | Phosphatidylinositol (4,5)-bisphosphate |
| PI3K | Phosphoinositide 3-kinase |
| pKa | Acid dissociation constant |
| PKC | Protein kinase C |
| PLC | Phospholipase C |
| PRR | Pathogen recognition receptor |
| PS | Phosphatidylserine |
| PSGL-1 | P selectin glycoprotein-1 |
| PTEN | Phosphatase and tensin homologue |
| PTP | Protein tyrosine phosphatase |
| PVF | PDGF/VEGF-like growth factor |
| pY | Phosphotyrosine |
| RA | Rheumatoid arthritis |
| ROCK | Rho kinase |
| ROS | Reactive oxygen species |
| RPMI | Roswell park memorial institute (cell growth medium) |
| SEM | Standard error of the mean |
| Ser | Serine |
| SERCA | Sarco/endoplasmic reticulum $Ca^{2+}$-ATPase |

| | |
|---|---|
| SFK | Src family kinase |
| SH | Src homology |
| Shark | SH2 ankyrin repeat kinase |
| SHIP-1 | SH2 containing inositol phosphatase-1 |
| SOD | Superoxide dismutase |
| Thr | Threonine |
| TIM | T-cell immunoglobulin mucin |
| TLR | Toll-like receptor |
| TNF | Tumour necrosis factor |
| Tyr | Tyrosine |
| UAS | Upstream activating sequence |
| UV | Ultraviolet |
| VCAM-1 | Vascular cell adhesion molecule-1 |
| VEGF-A | Vascular endothelial growth factor-A |
| WAS | Wiskott-Aldrich syndrome |
| WT | Wild type |

## Table of Contents

**Abstract** iii
**Abbreviations** iv
**Table of contents** vii
**Table of figures** xi
**Table of tables** xv

**Chapter 1: Introduction** 1
1.1 Innate immunity and inflammation 2
1.1.1 The immune system 2
1.1.2 The innate immune response and inflammation 2
1.1.3 Cells of the innate immune system 8
1.1.4 Chemoattractants, chemokines, signalling and receptors 12
1.2 Signalling pathways in innate immune cell function 17
1.2.1 SFK signalling 17
1.2.2 PI3K signalling 25
1.2.3 Rho-GTPase signalling 29
1.2.3 Calcium signalling 31
1.3 Mechanisms driving cell motility and migration 31
1.3.1 Cell migration and chemotaxis 31
1.3.2 Establishing a chemoattractant gradient 32
1.3.3 Gradient sensing and polarisation 33
1.3.4 Locomotion 35
1.3.5 Migration in the absence of chemoattractant gradients 36
1.3.6 Physical and environmental influences on motility and chemotaxis 37
1.4 *In vivo* models of inflammation 38
1.4.1 Zebrafish larvae tailfin wound model 38
1.4.2 *Drosophila melanogaster* embryonic wound model 39
1.4.3 $H_2O_2$ is a wound cue in *in vivo* models of inflammation 41
1.4.4 Lyn as a redox sensor 43
1.4.5 $H_2O_2$ may promote phagocytosis via SFKs 44
1.5 Damage cues in mammalian systems 45
1.5.1 Reactive oxygen species 45
1.5.2 Nucleotides as damage signals 52
1.6 Project Aims and Objectives 56

**Chapter 2: Methods and Materials** **58**
2.1 Reagents and materials 59
2.2 Methods and materials for *in vitro* experiments with human cells 59
2.2.1 Cell culture and isolation 59
2.2.2 MTT cell viability assay 60
2.2.3 Fluorescent labelling 60
2.2.4 Wright-Giemsa staining 61
2.2.5 Measurement of intracellular ROS generation 61
2.2.6 Measurement of intracellular calcium 62
2.2.7 Cell surface receptor expression 62
2.2.8 Immunofluorescence 62
2.2.9 Time lapse confocal microscopy 63
2.2.10 Image analysis 63
2.2.11 Migration assays 66
2.2.12 Phagocytosis 68
2.2.13 Western blotting 69
2.3 Methods and materials for *Drosophila* experiments 70
2.3.1 Fly husbandry 70
2.3.2 Embryo collection 70
2.3.3 Gal4-UAS system 71
2.3.4 Stocks and crosses 72
2.3.5 Wounding and imaging live embryos 72
2.3.6 Antibody staining 73
2.3.7 Image analysis 74
2.4 Statistical analysis 74
2.5 Tables 75
2.5.1 Table of reagents and materials 75
2.5.2 Table of antibodies 77
2.5.3 Table of *Drosophila* stocks 77
2.5.4 Table of buffers and solutions 77

**Chapter 3: SFK function and signalling in an embryonic *Drosophila melanogaster in vivo* model of cell migration** **78**
3.1 Rationale 79
3.2 Src42A is required for hemocyte migration to a wound 79
3.3 Shark is required for hemocyte migration to a wound 85
3.4 Phosphotyrosine intensity is increased in activated hemocytes 86

3.5 Exogenous $H_2O_2$ saturation impairs hemocyte random migration 86
3.6 Chapter 3 – Summary of Results 89
3.7 Chapter 3 – Discussion 89

**Chapter 4: The effect of damage-associated signals on innate cell function 93**
4.1 Rationale 94
4.2 $H_2O_2$ does not act as a chemoattractant in the ChemoTx migration assay 95
4.3 Pre-incubation of cells with $H_2O_2$ inhibits monocyte and neutrophil chemotaxis in the ChemoTx migration assay 95
4.4 Inhibition of $H_2O_2$ production and signalling affects monocyte and neutrophil chemotaxis 100
4.5 Neutrophils migrate under agarose towards IL-8, fMLP and $H_2O_2$ 102
4.6 Neutrophil chemotaxis under agarose is not affected by exogenous $H_2O_2$ 104
4.7 $H_2O_2$ does not affect neutrophil chemokinetic velocity 107
4.8 Cell viability is not compromised by sub-milimolar concentrations of exogenous $H_2O_2$, catalase or DPI 109
4.9 $H_2O_2$ does not induce changes in monocyte actin organisation 112
4.10 $H_2O_2$ does not affect monocyte receptor expression 115
4.11 Characterisation of THP-1 derived macrophages and primary human neutrophils 117
4.12 Phagocytosis of latex beads and bacteria is inhibited by $H_2O_2$ 119
4.13 Monocyte and neutrophil stimulation induces transient elevation of intracellular calcium 124
4.14 $H_2O_2$ does not affect ligand-stimulated calcium mobilisation in monocytes or neutrophils 131
4.15 $H_2O_2$ activates PI3K and MAPK signalling pathways in monocytes 134
4.16 $H_2O_2$ does not affect ICAM-1 expression in endothelial cells 136
4.17 fMLP and exogenous $H_2O_2$ increase intracellular ROS in primary human neutrophils 138
4.18 ATP induces migration of monocytes and neutrophils 141
4.19 ATP stimulates actin reorganisation and spreading of THP-1 monocytes 144
4.20 ATP does not affect cell viability 144
4.21 Chapter 4 – Summary of Results 149
4.22 Chapter 4 – Discussion 150

**Chapter 5: Characterisation of SFK and PI3K signalling and function in human innate immune cells 161**
5.1 Rationale 162

5.2 Distinct roles for SFK and Syk during innate cell chemotaxis 165
5.3 SFK and $H_2O_2$ may signal through a common pathway 165
5.4 Neutrophil viability is not affected by PP2 and piceatannol 168
5.5 Syk inhibition, but not SFK inhibition, potentiates MCP-1-induced THP-1 monocyte actin organisation 169
5.6 Phagocytosis of latex beads and bacteria is inhibited by SFK inhibition 171
5.7 SFK inhibition does not affect ligand-stimulated elevation of intracellular calcium 171
5.8 PI3K signalling is required for monocyte and neutrophil chemotaxis 174
5.9 Contributions of negative regulators of PI3K on actin organisation in monocytes 177
5.10 Contributions of individual class IA PI3K isoforms to actin organisation in monocytes 179
5.11 Chapter 5 – Summary of Results 183
5.12 Chapter 5 – Discussion 183

**Chapter 6: General Discussion 191**

**References 199**

**Appendix 232**

## Table of Figures

**Figure 1.1** The inflammatory response 3
**Figure 1.2** Hematopoietic cell lineage tree 8
**Figure 1.3** The structure of SFKs and conformational changes during SFK activation 18
**Figure 1.4** SFK and Syk signalling in the activating signalling pathways utilising ITAM-containing adaptors 21
**Figure 1.5** PI3K signalling cascade and structural domains of class I PI3Ks 26
**Figure 1.6** The Rho GTPase cycle 30
**Figure 1.7** Signalling pathways in leukocyte polarisation 35
**Figure 1.8** Features of leukocyte migration and polarisation 36
**Figure 1.9** Developmental hemocyte migration in *Drosophila* 40
**Figure 1.10** Models of tissue damage *in vivo* 43
**Figure 1.11** Reactive oxygen species and their reactions 45
**Figure 1.12** Redox-dependent signal transduction 48
**Figure 1.13** Extracellular ATP release and signalling during inflammation 54

**Figure 2.1** Primary human neutrophil isolation from peripheral blood 60
**Figure 2.2** Identifying individual cell phenotypes using CellProfiler software 65
**Figure 2.3** Apparatus for Neuroprobe ChemoTx transwell assay 66
**Figure 2.4** Under agarose cell migration assay 68
**Figure 2.5** *Drosophila* embryo collection and mounting for confocal microscopy 71
**Figure 2.6** The GAL4/UAS system in *Drosophila* 72

**Figure 3.1** Src42A drives hemocyte migration to a wound in *Drosophila* embryos 82
**Figure 3.2** Src42A mutant embryos show reduced hemocyte directionality and velocity in *Drosophila* embryos 83
**Figure 3.3** Random migration of hemocytes is not compromised in Src42A mutant *Drosophila* embryos 84
**Figure 3.4** Shark is involved in hemocyte migration to a wound in *Drosophila* embryos 85
**Figure 3.5** Phosphotyrosine (pY) intensity is increased in activated hemocytes at the wound site 87
**Figure 3.6** Exogenous $H_2O_2$ impairs hemocyte random migration in *Drosophila* embryos 88

**Figure 3.7** Proposed models for hemocyte motility in the presence and absence of a $H_2O_2$ gradient ..... 92

**Figure 4.1** THP-1 monocytes and primary human neutrophils migrate towards a range of chemoattractants ..... 97
**Figure 4.2** $H_2O_2$ does not act as a chemoattractant in ChemoTx migration assay ..... 98
**Figure 4.3** Exogenous $H_2O_2$ inhibits THP-1 monocyte and primary neutrophil chemotaxis ..... 99
**Figure 4.4** DPI inhibits THP-1 monocyte and primary neutrophil chemotaxis while catalase inhibits THP-1 monocytes but increases primary neutrophil chemotaxis ..... 101
**Figure 4.5** Primary human neutrophils migrate under agarose towards IL-8, fMLP and $H_2O_2$ ..... 103
**Figure 4.6** Neutrophil chemotaxis under agarose towards IL-8 or fMLP is not affected by exogenous $H_2O_2$ ..... 105
**Figure 4.7** Neutrophil chemotaxis under agarose towards IL-8 or fMLP is not affected by exogenous $H_2O_2$ in either the cell or chemoattractant compartment ..... 106
**Figure 4.8** Neutrophil motility is increased by stimulation with IL-8 and fMLP but not with $H_2O_2$ ..... 108
**Figure 4.9** Monocyte and neutrophil viability is unaffected by sub-milimolar concentrations of $H_2O_2$ ..... 110
**Figure 4.10** Neutrophil viability is unaffected following exposure to catalase or DPI ..... 111
**Figure 4.11** $H_2O_2$ does not induce changes in THP-1 monocyte actin organisation ..... 113
**Figure 4.12** Catalase and DPI induce actin reorganisation in THP-1 monocytes ..... 114
**Figure 4.13** THP-1 monocyte CCR2 surface expression is not affected by $H_2O_2$ ..... 116
**Figure 4.14** Characterisation and identification of PMA-differentiated macrophages and primary human neutrophils ..... 118
**Figure 4.15** Neutrophil phagocytosis of latex beads is inhibited by $H_2O_2$ ..... 121
**Figure 4.16** Neutrophil phagocytosis of latex beads and bacteria is inhibited by $H_2O_2$ ..... 122
**Figure 4.17** Macrophage phagocytosis of latex beads and bacteria is inhibited by $H_2O_2$ ..... 123
**Figure 4.18** MCP-1, $LTB_4$ and ATP increase intracellular calcium mobilisation in monocytic cell lines ..... 125

**Figure 4.19** IL-8, fMLP, $LTB_4$ and ATP increase intracellular calcium mobilisation in primary human neutrophils 126
**Figure 4.20** Ligand induced intracellular calcium mobilisation in monocytes and neutrophils is reduced in low extracellular calcium 127
**Figure 4.21** The effect of exogenous $H_2O_2$ upon intracellular calcium mobilisation in human monocytes and neutrophil 129
**Figure 4.22** $H_2O_2$ induces a biphasic increase in intracellular calcium in primary human neutrophils 130
**Figure 4.23** $H_2O_2$ does not affect chemokine induced intracellular calcium mobilisation in monocytic cell lines 132
**Figure 4.24** Ligand induced intracellular calcium mobilisation in neutrophils is not affected by pre-treatment with $H_2O_2$ 133
**Figure 4.25** fMLP and $H_2O_2$ induce activation of PI3K and ERK signalling pathways in monocytes 135
**Figure 4.26** $H_2O_2$ alone does not induce ICAM-1 expression or affect TNFα induced ICAM-1 expression in endothelial monolayers 137
**Figure 4.27** Intracellular ROS detection in primary human neutrophils 139
**Figure 4.28** Intracellular ROS detection in monocytic cell lines 140
**Figure 4.29** ATP induces migration of monocytes and neutrophils 142
**Figure 4.30** ATP-mediated chemotaxis is inhibited by exogenous $H_2O_2$ 143
**Figure 4.31** ATP increases THP-1 actin reorganisation and spreading 145
**Figure 4.32** Time lapse imaging of THP-1 monocytes seeded on fibronectin reveals changes in shape following stimulation with different agonists 146
**Figure 4.33** Neutrophil viability is unaffected following exposure to ATP 148
**Figure 4.34** Proposed model for redox and ATP-mediated control of cell polarisation and phagocytosis 160

**Figure 5.1** Syk inhibition increases THP-1 monocyte chemotaxis but inhibits neutrophil chemotaxis, SFK inhibition inhibits both monocyte and neutrophil chemotaxis 166
**Figure 5.2** Simultaneous SFK inhibition and exogenous $H_2O_2$ stimulation does not rescue or exacerbate migration in monocytes or neutrophils 167
**Figure 5.3** Neutrophil viability is unaffected following exposure to PP2 or piceatannol 168
**Figure 5.4** Piceatannol, but not PP2, potentiates MCP-1 induced THP-1 monocyte polarisation and spreading 170

**Figure 5.5** Macrophage and neutrophil phagocytosis of latex beads and bacteria is inhibited by SFK inhibitor PP2 ..... 172

**Figure 5.6** Ligand or $H_2O_2$ induced intracellular calcium mobilisation in primary human neutrophils is not affected by inhibition of SFKs ..... 173
**Figure 5.7** PI3K inhibition inhibits monocyte and neutrophil chemotaxis ..... 175
**Figure 5.8** SHIP-1 inhibition and activation, and PTEN inhibition inhibits THP-1 monocyte chemotaxis ..... 176
**Figure 5.9** The effect of modulating PI3K signalling on THP-1 monocyte polarisation and spreading ..... 178
**Figure 5.10** The effect of pan-isoform PI3K inhibitors on THP-1 monocyte actin organisation ..... 180
**Figure 5.11** The effect of p110α, β and δ-selective PI3K inhibitors on THP-1 monocyte actin organisation ..... 181
**Figure 5.12** Inhibition and activation of SHIP-1 lead to the same functional outcome ..... 188
**Figure 5.13** Proposed model of SFK and PI3K signalling in innate cell migration and actin reorganisation ..... 190

## Table of tables

**Table 1.1** The chemokine superfamily ..... 13
**Table 1.2** Selected roles of SFKs and Syk in the regulation of innate cell migration ..... 23
**Table 1.3** $IC_{50}$ values of commonly used PI3K inhibitors ..... 29
**Table 1.4** Advantages and disadvantages of *Drosophila melanogaster* as a model organism ..... 39
**Table 1.5** Features of P2 receptors ..... 53

**Table 2.5.1** Table of reagents and materials ..... 75
**Table 2.5.2** Table of antibodies ..... 77
**Table 2 5.3** Table of *Drosophila* stocks ..... 77
**Table 2.5.4** Table of buffers and solutions ..... 77

**Table 3.1** Mutant *Drosophila* stocks used for the study of Src42A and Shark function in hemocyte migration ..... 81

**Table 4.1** Differences between *in vitro* migration assays ..... 153

**Table 5.1** Summary of the actions of PI3K inhibitors and modulators upon THP-1 monocyte polarisation and spreading on fibronectin ..... 182

**Table 6.1** Differences between monocytic cells and neutrophils ..... 197

# CHAPTER 1: INTRODUCTION

## 1.1 Innate immunity and inflammation

### 1.1.1 The immune system

The immune system is essential for the protection of an organism against tissue damage and invasion from external pathogens. It relies on the coordinated efforts of multiple tissues and organs, specialised cell types and soluble factors whose interactions culminate in the maintenance of a healthy organism, as well as a primed system ready to respond to potential threats to homeostasis. Skin and epithelial membranes form physical barriers to invasion and act in concert with more dynamic, induced components of the immune system, such as activated leukocytes and changes to receptor expression. The immune system has two critical roles: (a) to identify, locate and neutralize external pathogens, and (b) to remove damaged or diseased tissue.

The temporal stages of immunity can be classified into the immediate, first line response, termed innate immunity, and the later, more specific response, termed adaptive immunity. Innate immunity relies heavily on recognition of pathogenic patterns, leukocyte activation and recruitment, and rapid release of soluble neutralizing factors, which is discussed in more detail below. Adaptive immunity also involves both cell-mediated and humoral components, which create an immunological memory following an initial exposure to a specific pathogen. It is dependent on the ability of the body to recognise specific ‘non-self’ antigens in the presence of ‘self’ antigens. The production and storage of antigen specific antibodies gives rise to an acquired immune system, leading to an enhanced response to subsequent exposure to the same pathogen. The dysregulation of any of these processes can give rise to inefficient responses to pathogens and increased susceptibility to infection, or overactive immune responses leading to chronic autoimmune diseases.

### 1.1.2 The innate immune response and inflammation

Inflammation occurs when the immune system is activated. It can be considered a classic stimulation-response system. Inflammation was first described as four cardinal signs: heat, pain, redness and swelling, by Celsus in AD. 25 [1]. These processes have been highly characterised in recent years and are the subject of target validation in many clinical trials. There are two types of inflammatory responses: acute inflammation or chronic inflammation. Acute inflammation is a rapid and temporary host response that delivers leukocytes and plasma proteins to the infected or injured tissues. Chronic inflammation is persistent and characterised by tissue injury and attack with a longer recovery time. The chronic response may increase damage to tissues and organs, resulting in the onset of further disease, such as rheumatoid arthritis (RA), tuberculosis and pulmonary fibrosis. Figure 1.1 illustrates the key initial steps in the inflammatory response.

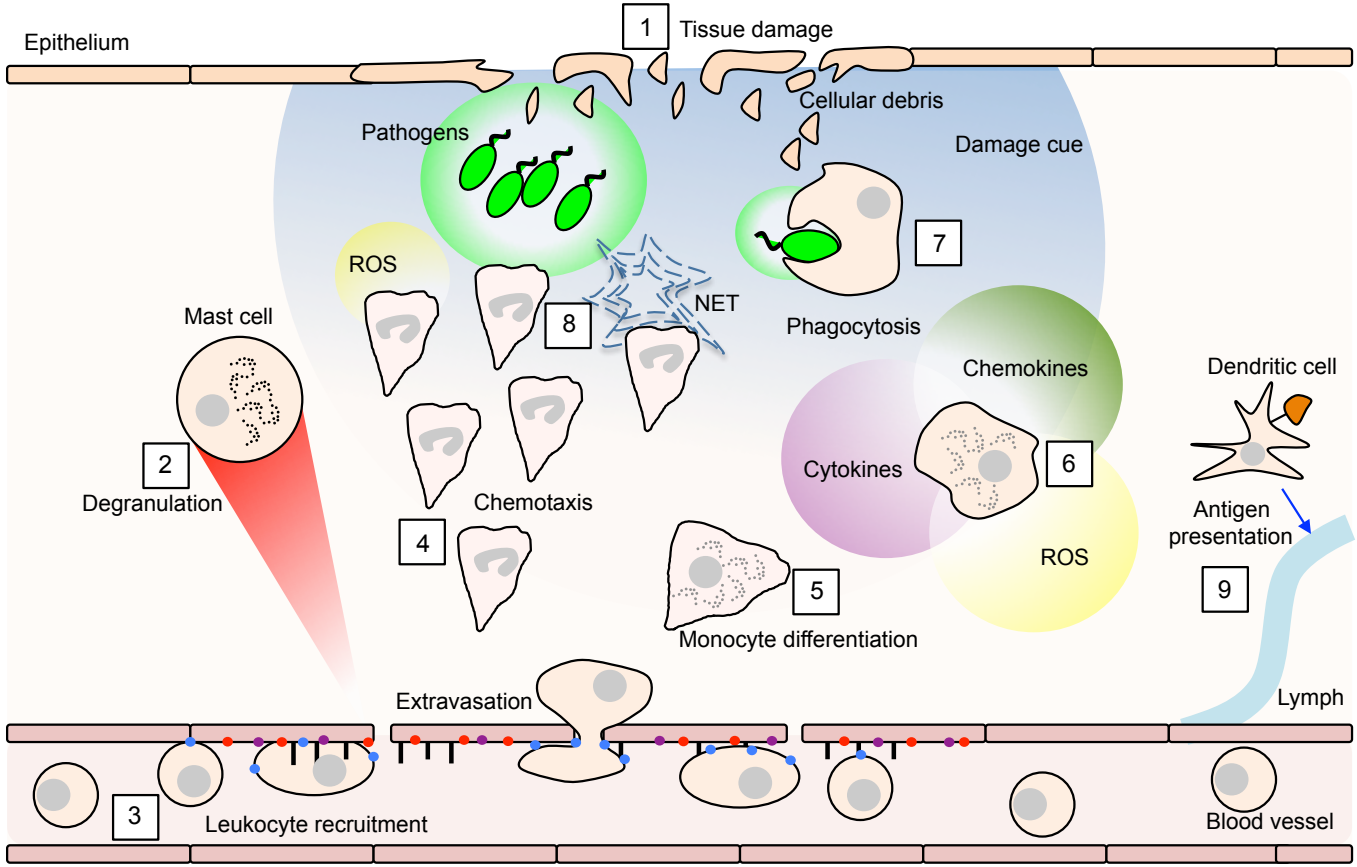


**Figure 1.1: The inflammatory response.** Following epithelial injury and infection (1), the release of damage- and pathogen- associated signals activate tissue resident inflammatory cells. Upon activation, mast cells degranulate (2) and release inflammatory mediators that act on local vasculature to increase permeability and promote endothelial expression of adhesion molecules. Endothelial inflammation promotes leukocyte recruitment from the circulation (3) through a cascade of leukocyte tethering, rolling, firm adhesion and extravasation into the tissue. In the tissue, leukocytes migrate along gradients of chemoattractants (4) towards the source of damage or infection. Monocytes differentiate into macrophages (5), and release key intermediary signals, including ROS, chemokines and cytokines to further amplify the inflammatory response (6). Phagocytes clear damage by engulfing cell debris and pathogens (7). Activated neutrophils release neutrophil extracellular traps (NETs) that capture and immobilise pathogens (8). Finally, tissue dendritic cells capture antigen (9), and travel via the lymph to secondary lymphoid organs where they initiate the adaptive immune response.

### Activation

Leukocytes continuously patrol the vasculature and tissues, monitoring for signs of bacterial infection or tissue damage [2]. When tissue is injured, the loss to skin integrity allows bacteria and other pathogens to enter local tissue. Resident tissue mast cells and macrophages are alerted to the event by detection of damage-associated molecular patterns (DAMPs), e.g. adenosine 5'triphosphate (ATP), and pathogen associated molecular patterns (PAMPs), e.g. lipopolysaccharide (LPS) [3]. DAMPs and PAMPs can initiate signalling via Toll-like receptors (TLRs) and Nod-like receptors (NLRs). TLRs recognise microbial products, for example, TLR4 recognises LPS. NLRs sense peptidoglycan breakdown products and drive caspase activation via assembly and activation of the inflammasome. TLRs and NLRs also sense products of inflamed tissue, such as hyaluronic acid and uric acid [3].

Mast cell activation triggers degranulation and release of inflammatory mediators such as histamine, leukotrienes and prostaglandins [4]. Histamine acts on local vasculature to increase permeability and loosen tight junctions at points of cell contact. If vasculature is ruptured, clotting factors are rapidly activated and dispersed [5]. Activated macrophages release soluble paracrine factors such as cytokines and chemokines that diffuse throughout the tissue, establishing signal gradients to guide the recruitment of leukocytes towards the area of damage and infection. Other chemotactic agents include N-formylated peptides, the complement C5a fragment, leukotriene $B_4$ ($LTB_4$), platelet activating factor (PAF) and the superfamily of chemokines [6].

### Recruitment

Following activation by tissue resident cells, the immune response is amplified by recruitment of more cells to the affected area. Endothelial cells present chemokines on their luminal surface to attract and activate circulating leukocytes and enable their capture and tethering on the vascular wall. Positively charged chemokine molecules are anchored onto the endothelium by binding to negatively charged heparan sulphates, preventing chemokine from being washed away by shear forces [7]. This results in gradients of chemokines becoming established in the vasculature. At the luminal surface, inflammatory mediators act on the endothelium of blood vessels to upregulate the expression of adhesion molecules such as E-cadherin, vascular cell adhesion molecule-1 (VCAM-1) and intercellular adhesion molecule-1 (ICAM-1) [8].

Selectins are required for the rolling phase of leukocyte adhesion and transmigration cascade. Selectins are single chain transmembrane glycoproteins that recognise carbohydrate moieties and mediate transient interactions between leukocytes and the vessel wall [9]. L-selectin is expressed on leukocytes and its primary role appears to be in promoting lymphocyte homing to lymph nodes [10]. E-selectin is expressed on endothelial cells and P-selectin is expressed on platelets and endothelial cells during inflammation. Upon detection of inflammation, selectin expression is upregulated, either from pre-stored sources or synthesised *de novo* [11]. Various selectin ligands bind to selectin receptors, most notably P-selectin glycoprotein-1 (PSGL-1) which is

expressed on leukocytes [12]. These interactions lead to tethering and rolling of circulating leukocytes to the surface of the endothelium. Despite the brief nature of the selectin receptor-ligand interactions, they can trigger intracellular signal transduction processes. A prime example of this is when PSGL-1 binds to E-selectin to induce the activation of CD11a/CD18 integrin and induce slow rolling of leukocytes on the vessel wall [13].

Integrins are heterodimeric transmembrane glycoproteins that are required for leukocyte slow rolling, firm adhesion to the vessel wall and chemotaxis [14]. Leukocytes express $\beta_2$ integrin family members, formed by the $\beta_2$ (CD18) integrin chain plus a unique α chain. Mac-1 ($\alpha_M\beta_2$ – CD11b/CD18) is expressed on myeloid cells such as neutrophils, monocytes and macrophages. LFA-1 ($\alpha_L\beta_2$ – CD11a/CD18) is expressed on all circulating leukocytes. Mac-1 and LFA-1 bind to endothelial ICAM-1 and are involved in different phases of neutrophil adhesion and transmigration [15]. LFA-1 binding to ICAM-1 is essential for firm adhesion [16]. Leukocytes also express VLA-4 ($\alpha_4\beta_1$) integrin that binds to VCAM-1 on endothelial cells.

Integrin signalling can be triggered by integrin ligation (outside-in signalling) and the regulation of integrin ligand binding by intracellular signals (inside-out signalling). Integrin outside-in signalling can be triggered by placing cells on integrin ligand-coated surfaces (e.g. fibronectin) in the presence of a pro-inflammatory stimulus [17]. This triggers cell spreading and respiratory burst, which is dependent on cell surface β integrins. Activation of chemokine receptors on leukocyte surfaces induces changes in the conformation of cell surface integrins that subsequently show higher affinity for their ligands [18].

**Extravasation**

To leave the vasculature, leukocytes must cross the endothelium, followed by the basement membrane. Transmigration involves integrins, adhesion molecules, and junctional molecules. Transmigration can occur paracellularly, between endothelial cells, or transcellularly, through an endothelial cell. During transmigration, cells undergo cytoskeletal changes and rearrange their attachment to the extracellular matrix (ECM) via focal adhesions [19]. The basement membrane comprises collagens and laminins and poses a barrier through which transmigrating leukocytes must pass. Neutrophils contain specific proteases including matrix metalloproteinases (MMPs) and serine proteases which enzymatically digest ECM molecules [20]. However, protease inhibitors have failed to show that this is the only mechanism by which leukocytes can penetrate the basement membrane. Intravital microscopy has revealed that neutrophils preferentially migrated through regions of basement membrane that exhibit low levels of ECM molecules [21]. Interestingly, these regions overlapped with gaps between pericyte regions, suggesting that they represent a path of least resistance for emigrating neutrophils [22].

Following transmigration, emigrated neutrophils or monocytes must move away from any endothelium associated gradients and towards new tissue related gradients. This suggests that leukocytes are able to prioritise different chemokine signals. In fact, when

placed in opposing gradients *in vitro*, neutrophils prioritise end target chemoattractants derived from pathogenic sources, (e.g. bacterial derived N-formyl-methionyl-leucyl-phenylalanine (fMLP)), over intermediary chemoattractants produced by activated leukocytes, (e.g. neutrophil derived IL-8) [23]. This process is described in more detail in section 1.3.

**Phagocytosis**

Phagocytosis is defined as the ingestion by cells of large (≥0.5μm) particles [24] and encompasses a diverse range of related yet distinct molecular mechanisms. Phagocytosis is important in homeostasis and tissue remodelling, as well as in innate immune responses where pathogens, cell corpses and cell debris are cleared and destroyed. Professional phagocytes can also present antigens derived from the degradation of engulfed particles to lymphoid cells and activate adaptive immunity. Fibroblasts, epithelial cells and endothelial cells are able to ingest apoptotic bodies, but not microbes [24]. Phagocytosis is a very complex process and typically involves three key steps: a) particle recognition, b) particle internalisation and c) phagosome maturation.

Phagocytosis is a receptor-mediated event. Given the huge variety of particles that can be ingested, many receptors types are involved. Receptors that engage foreign bodies include pathogen recognition receptors (PRRs) [25] and opsonic receptors (e.g. FcγRs) that recognise soluble molecules such as extraneous antigens and complement components circulating in the blood and interstitial fluid [26]. Apoptotic cells release mediators such as ATP and lysophosphatidylcholine, and these act as 'find me' signals to recruit phagocytes. Apoptotic cells also display 'eat me' signals on their surfaces; phosphatidylserine (PS) is the most characterised example [27]. Multiple receptors bind PS, e.g. TIMs (T-cell immunoglobulin mucin family) and stabilin-2 [28].

Phagocytic receptors drive different intracellular signalling cascades; in some conditions several receptors are activated in parallel so multiple cascades are triggered concomitantly. Internalisation of IgG-opsonised particles by FcγRs is the most well understood model of phagocytosis. This involves binding of ligand-coated particles to receptors, clustering of FcγRs, which induces a signalling cascade, and the engulfment of the particle by an actin driven process. Receptor activation and extension of pseudopods is replicated at many sites surrounding the pathogen [29]. Aggregation of FcγRs leads to activation of tyrosine kinases including Src family kinases (SFKs), followed by recruitment of adaptor proteins (e.g. Grb2, LAT). The resulting signalling platforms activate multiple lipid-modification enzymes (e.g. phosphoinositide 3-kinase (PI3K)) and guanine exchange factors (GEFs) that drive pseudopod extension [24].

The internalisation process culminates in the formation of a membrane-bound vacuole termed the phagosome. Following scission from the plasma membrane, the phagosome becomes a potent microbicidal organelle. The phagosome becomes very acidic, pH ~4.5 via delivery of $H^+$ ions into its lumen via the vacuolar ATPase [30]. The phagosome is also highly oxidative [31]. Phagocytosis is accompanied by the production of two types of free radicals by neutrophils: reactive oxygen intermediates

formed by the activity of NADPH oxidase; and reactive nitrogen intermediates including nitric oxide produced by nitric oxide synthase. Phagosomes are enriched with hydrolytic enzymes (e.g. lactoferran, lysozyme) that ultimately degrade their contents [32].

**Resolution of inflammation**

Once the main threat has been cleared, inflammatory processes are terminated and resolution programs begin. Resolution of inflammation involves remodelling and repair of damaged tissues and vasculature, and clearance of leukocytes. Resolution involves (a) withdrawal of survival signals; (b) normalisation of chemokine gradients; (c) induction of resolution mechanisms that promote leukocyte apoptosis or exit through draining lymphatics [33]. Here, antigen presenting cells opsonise bacteria and travel through draining lymph towards secondary lymphatic organs to activate the adaptive immune response. Fibroblasts begin remodelling damaged tissue. Macrophages release anti-inflammatory mediators to halt cell recruitment and activated neutrophils die by apoptosis. In addition to leukocytes, parenchymal and stromal cells revert back to a non-inflamed phenotype.

Resolution begins with an anti-inflammatory phase involving the release of IL-10 and down regulation of NF-κB activity and production of cytokine receptor antagonists (e.g. IL-1Ra) [33]. This is followed by the resolving phase. Here, leukocytes release 'pro-resolving' lipid mediators, such as lipoxin $A_4$ ($LXA_4$). This inhibits neutrophil migration and initiates phagocytosis of apoptotic neutrophils by macrophages. $LXA_4$ also induces changes in phosphorylation of cytoskeletal proteins, leading to inhibition of neutrophil migration [34]. Other pro-resolving mediators include resolvins and protectins produced by neutrophils, and maresins produced by macrophages [34].

Resolution is strictly controlled to protect the host from overt tissue damage and prevent the development of chronic, on-going inflammation and its associated complications. Leukocytes must be removed from the tissue before they cause excessive damage. Pro-apoptotic neutrophils release 'find me' signals that attract phagocytes and eventually lead to phagocytosis of the dying neutrophil [35]. This can be via macrophages and dendritic cells in the tissue, or by Kuppfer cells in the liver vasculature [36]. Neutrophils therefore promote their own removal by contributing to the resolution of inflammation and promoting tissue repair. Leukocytes can also leave an inflamed site by returning to systemic circulation. Studies in mice and zebrafish larvae have identified a novel mechanism of inflammation by reverse migration of neutrophils from wounded tissue back toward the vasculature [37], [38]. This represents a novel target for managing inflammatory resolution, and is the focus of continuing studies.

If resolution of inflammation is absent, wound healing and regeneration will not occur and severe inflammatory pathologies such as irritable bowel disease (IBD), RA and Crohn's disease may ensue. Inherited human diseases including leukocyte adhesion deficiency (LAD) are associated with impaired wound healing due to persistent infection and have been successfully recapitulated in the zebrafish [39]. Some pathological states present unresolved inflammation despite the absence of inciting

triggers. An ideal drug to target inflammation would be able to stop the inflammatory response and activate the resolution process. Glucocorticoids, as well as being anti-inflammatory, promote resolution by stimulating macrophages to induce the uptake of apoptotic neutrophils [40]. Similarly, aspirin (which has an anti-inflammatory role in blocking prostaglandin production via modulation of cyclooxygenase activity) is also pro-resolving by upregulating lipid mediator generation e.g. lipoxins, resolvins and protectins [41].

### 1.1.3 Cells of the innate immune system

The innate immune system comprises many different cell types with complementary and contrasting functional duties. A lineage tree depicting cells of the immune system is illustrated in figure 1.2. Neutrophils, monocytes and macrophages are key mediators of innate inflammation and the focus of studies described in this thesis. These cells are defined in more detail below.

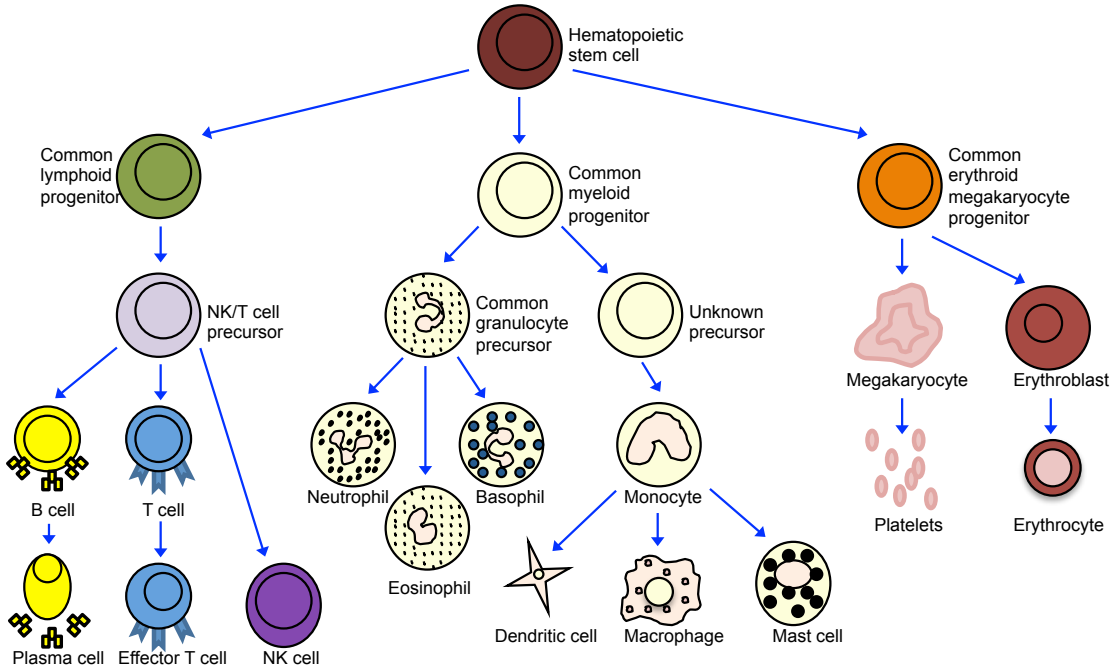


**Figure 1.2: Hematopoietic cell lineage tree**. Stemming from a common hematopoietic stem cell progenitor, three main branches are generated: lymphoid cells (left branch), myeloid cells (central branch), and erythroid cells (right branch). NK= natural killer cell.

#### Neutrophils

Neutrophils are the most abundant cell of the immune system, the fastest responding leukocyte to a pathogen and are critical effectors of innate immunity. Neutrophils are continuously generated in the bone marrow from myeloid precursors, a process controlled by granulocyte colony stimulating factor (G-CSF) [42], with daily production reaching up to $2x10^{11}$ cells [43]. Neutrophils are polymorphonuclear leukocytes and have a segmented nucleus and cytoplasm enriched with granules and secretory

vesicles [43]. Neutrophil granules contain pro-inflammatory proteins including myeloperoxidase, lactoferran and MMPs. These proteins play a key role in neutrophil migration through tissues, as proteases can digest basement membrane or ECM [20].

Several classes of receptors are expressed on the surface of neutrophils, including chemokine G-protein coupled receptors (GPCRs), adhesion molecules, cytokine receptors and C-type lectins [15]. Neutrophils also express TLRs and can directly detect foreign pathogens. Activation of neutrophil surface receptors leads to a plethora of events including phagocytosis, degranulation, reactive oxygen species (ROS) generation, NETosis and chemokine release. In the absence of inflammation, neutrophils can be found in the bone marrow, spleen, liver and lung. This pool of cells is considered to be a reservoir of mature neutrophils ready to be deployed to sites of tissue damage or infection. Tissue resident neutrophils may also be patrolling organs and have a homeostatic function. Recently, this has been observed using intravital microscopy of the mouse lung [44]. There has been speculation as to the existence of distinct neutrophil subsets and whether these represent distinct lineages or instead develop from a single neutrophil precursor. In a human study, differential subsets of neutrophils were shown to be present in the circulation of volunteers following LPS injection compared with untreated controls [45], [46]. It was demonstrated that this $CD11c^{bright}/CD62L^{dim}/CD11b^{dim}/CD16^{bright}$ subset of neutrophils was capable of suppressing human T cell proliferation [46].

Neutrophils have multiple killing mechanisms to eliminate pathogens during inflammation. Neutrophils phagocytose pathogens and kill them intracellularly using NADPH-oxidase dependent mechanisms or antibacterial proteins such as defensins [47]. Antibacterial proteins can also be released from granules into the extracellular space and act on extracellular pathogens. Additionally, activated neutrophils can release neutrophil extracellular traps (NETs) that comprise a core DNA element to which histones, antibacterial proteins and enzymes are attached. Pathogens are immobilized in NETs and this process limits their spread and also facilitates phagocytosis [48].

Neutrophils also demonstrate regulatory, ‘healing’ features. Neutrophils can clear cell debris and phagocytose dead cells at a wound site. Removing neutrophils from a wound site results in worsened tissue pathology, even in sterile injury [49]. Furthermore, neutrophils directly release growth factors, e.g. vascular endothelial growth factor-A (VEGF-A), which have been shown to promote angiogenesis in a model of pancreatic islet transplantation [49]. Potentially, cancer cells could exploit this pro-angiogenic function of neutrophils to promote their survival and spread [50]. Therefore, the role of neutrophils in the tumour microenvironment is now of renewed attention.

Neutrophils also have a role in regulating adaptive immunity and have been identified in the lymph nodes [51]. Neutrophils can mediate suppression of T cell proliferation and activity, which may be a result of degranulation [4]. Neutrophils can also act as antigen presenting cells. One recent study identified neutrophils carrying injected modified vaccinia Ankara virus from skin to the bone marrow, resulting in an alternative source of primed $CD8^+$ T cells [52]. Generally it appears that neutrophils affect adaptive

immunity by promoting humoral immune responses but suppressing cellular immune responses.

Although neutrophil recruitment during infection is likely to be essential for protective immunity, excessive accumulation and subsequent inflammatory signalling may be detrimental. Upon activation neutrophils release oxidants, proteases and antimicrobial proteins and can cause indirect injury [53]. Over activation of the neutrophil response underlies the pathogenesis of various diseases including ischemia, reperfusion-induced tissue damage, and auto-inflammatory diseases [54]. Neutrophil-specific expression of Fc-receptors, C5a-receptors and LFA-1 [55], as well as Syk kinase [56], have been shown to be required for autoantibody-mediated arthritis. In contrast, absent or reduced neutrophil function in response to inflammation is associated with primary immunodeficiency [57].

**Monocytes and macrophages**

Monocytes are a subset of circulating myeloid cells that are derived from monoblast precursors in the bone marrow. They are amoeboid in shape with clear cytoplasm and bean-shaped nuclei. Monocytes circulate in the blood, bone marrow and spleen before entering tissues [58]. Cells of the monocyte lineage are characterised by considerable phenotypic plasticity and diversity. Monocyte subsets can be identified based on their surface receptor expression. Three types of monocyte subset have been identified in human blood: a) classical monocytes are characterised by high CD14 expression; b) non-classical monocytes have low CD14 and additional co-expression of CD16; c) intermediate monocytes have high CD14 and low CD16 expression [59]. Further studies have shown that in mice, expression of LY6C and CD11b identifies a monocyte subset that expresses high levels of CCR2 but low levels of $CX_3CR1$. These monocytes are often referred to as inflammatory monocytes and are rapidly recruited to sites of infection and inflammation [60].

Monocytes are efficient immune effector cells, equipped with chemokine receptors (e.g. CCR2) and pathogen recognition receptors (e.g. TLRs) that mediate migration from blood to tissues during inflammation and infection. Monocytes replenish tissue macrophages and dendritic cells in the steady state, and are recruited to infected tissues and mediate direct antimicrobial activity at these sites [60]. Monocytes or monocyte-derived cells can also enter draining lymph nodes and promote adaptive immune responses [58]. Monocyte chemoattractant protein-1 (MCP-1/CCL2) is the main chemokine that mediates monocyte chemotaxis via CCR2 binding. CCR2 deficiency reduces inflammatory monocyte trafficking to sites of inflammation, indicating a crucial role for this chemokine receptor in trafficking of these monocytes [61]. The properties of MCP-1 are described in more detail in section 1.1.4.

Blood levels of monocytes can rise during infection or inflammation, or also in response to stress and other factors. A sizable fraction of circulating monocytes enters the tissues of the body during inflammation, differentiating into inflammatory dendritic cells or macrophages [62]. Macrophages evolved in simple multicellular organisms to perform phagocytic clearance of dying cells and to protect the host through innate

immunity, both as resident tissue macrophages and monocyte derived recruited cells during inflammation [63]. Once differentiated, macrophages become long-lived cells and develop specialised functions. Macrophages are resistant to constitutive apoptosis [64] and cell number is further maintained by additional recruitment of monocytes into the tissues [65], [66]. Macrophages show distinct phenotypic heterogeneity and plasticity, even after differentiation, which is dependent upon the environment in which they are placed [67]. Macrophages have different names depending on their location, for example, Kupffer cells in the liver, alveolar macrophages in the lung, microglia in the central nervous system, and osteoclasts in the bone.

Historically, inflammatory macrophages have been divided into two classes: classically activated type 1 (inflammatory/M1 cells) and alternatively activated type 2 (wound-healing/M2 cells) [68]. This was based on the roles of macrophages as key modulator and effector cells in the immune response, and because their activation influences and responds to other arms of the immune system.

Inflammatory macrophages are activated by TLR ligands (e.g. LPS) and cytokines and stimulate increased production of ROS and inflammatory cytokines, and higher expression of MHCII [69]. M1 cells function as inducers and effectors of resistance against intracellular parasites and tumours. These macrophages are able to assemble the inflammasome complex leading to IL-1β production and secretion [70]. IL-4 and IL-13 induce the alternate M2 macrophage population, and these cytokines inhibit M1 macrophages. M2 cells are poor at antigen presentation, suppress Th1 adaptive immunity, actively scavenge debris, have efficient phagocytic activity and contribute to the dampening of inflammation to promote wound healing, angiogenesis, and tissue remodelling [71].

More recent evidence from *in vivo* studies has challenged this simplistic model and it has been suggested that a third class, regulatory macrophages, are also operational in tissues. Regulatory macrophages are able to present antigen and regulate the immune system with specific, targeted responses [72]. Furthermore, a series of other chemokines, cytokines, and growth factors can elicit functional responses which share overlapping properties with M1 and M2 phenotypes [72]. M1 and M2 phenotypes can also be reversed in certain immunological conditions, [73] [74]. These reports indicate that macrophage subclasses are to some extent interconvertible and represent a spectrum of phenotypes. Classification of macrophage activation should therefore consider two important aspects: the *in vitro* effects of immune related ligands on macrophage phenotype; and *in vivo* evidence for distinct macrophage phenotypes in disease. We must consider the context and environment in which the cells are functioning, and their interactions with other macrophage populations. Studying the behaviour of macrophages *in vivo* will uncover more information about different subsets and the plasticity of macrophages.

The study of monocytes and macrophages in disease settings has confirmed their ability to have plasticity in different environments. Antibodies against CCL2 or its receptor CCR2 have been investigated in preclinical models and support a role for anti-CCL2 therapy in some cancers [75]. There is substantial evidence to suggest that macrophages play an important role in wound healing and in tumour progression.

Recent zebrafish studies have indicated that depletion of macrophages results in a build up of debris and impairs regeneration at a wound site [76]. Monocyte and macrophage function has also been implicated in settings as diverse as cardiovascular disease, neurological disorders and atherosclerosis.

### 1.1.4 Chemoattractants, chemokines, signalling and receptors

#### Chemokines

Chemokines are chemotactic cytokines that are small heparin-binding proteins belonging to a large family whose main function is to regulate cell trafficking. Chemokines can be classed into four key subfamilies based on the number and location of cysteine residues at the N-terminus of the molecule (Table 1.1). The structure of chemokines comprises three distinct domains – a highly flexible N-terminal domain that is constrained by disulphide bonding between the N-terminal cysteine, a long loop that leads into three antiparallel β-pleated sheets, and an α-helix that overlies the sheets [77]. Sequence motifs in the vicinity of the first two cysteine residues determine receptor recognition and activation. Most chemokine ligands have a molecular mass between 8-12kDa and contain 1-3 disulfide bonds, although the sequence homology of chemokine ligands is highly variable [78]. In addition to structural classification, chemokines can be categorised according to functional properties. For example, amongst inflammatory chemokines, CXC chemokines with an ELR (Glu-Leu-Arg) motif prior to the first cysteine residue are angiogenic. In contrast, the ligands CXCL4, CXCL9, CXCL10 and CXCL11, which do not contain the ELR motif, function as angiostatic chemokines [79].

| | Chemokine Receptor | Chemokine Ligand<br>Systematic name (Common name) | Receptor Cell Type |
|---|---|---|---|
| CC family | CCR1 | CCL5 (RANTES), CCL3 (MIP1A), CCL7 (MCP-3), CCL8 (MCP-2), CCL13 (MCP-4), CCL14, CCL15, CCL16, CCL23 | T, Mo, Eo, Ba |
| | CCR2 | CCL2 (MCP-1), CCL8 (MCP-2), CCL13 (MCP-4), CCL7, CCL16 | Mo, D, $T_{mem}$ |
| | CCR3 | CCL11 (Eotaxin), CCL5, CCL7, CCL13, CCL14, CCL15, CCL24, CCL26, CCL28 | Eo, Ba, MC, Th2, P |
| | CCR4 | CCL17 (TARC), CCL22 (MDC) | Th2, D, Ba |
| | CCR5 | CCL4 (MIP-1B), CCL3, CCL5, CCL7, CCL11, CCL16 | T, Mo |
| | CCR6 | CCL20 (MIP-3A) | $T_{reg}$, $T_{mem}$, B, D |
| | CCR7 | CCL19 (ELC), CCL21 (SLC) | T, DC |
| | CCR8 | CCL1 (I-309) | Th2, Mo, D |
| | CCR9 | CCL25 | |
| | CCR10 | CCL28 (MEC), CCL27 (CTACK) | T |
| CXC family | CXCR1 | CXCL8 (IL-8), CXCL6 (GCP-2)<br>CXCL7, ACPGP | N, Mo |
| | CXCR2 | CXCL7 (NAP-2), CXCL5 (ENA78), CXCL1 (Gro-a), CXCL2 (Gro-b), CXCL3 (Gro-g), CXCL6 (GCP-2), CXCL8 (IL-8), ACPGP, MIF | N, Mo, En |
| | CXCR3 | CXCL10 (IP-10), CXCL9 (MIG), CXCL11 (I-TAC), CXCL4, CXCL13 | Th, MC |
| | CXCR4 | CXCL12 (SDF-1), MIF, Ubiquitin | Ubiquitous |
| | CXCR5 | CXCL13 (BCA-1) | B, Th |
| | CXCR6 | CXCL16 | CD8+ T, NK, $T_{mem}$ |
| CX3C family | CX3CR1 | CX3CL1 (Fracktaline/Neurotactin), CCL26 | Mac, En, SMC |
| XC family | XCR1 | XCL1 (Lymphotactin), XCL2 | T, NK |
| Atypical receptors | CXCR7 | CXCL11, CXCL12 | En |
| | CCBP2 | CCL2, CCL3, CCL4, CCL5, CCL7, CCL8, CCL11, CCL12, CCL13, CCL14, CCL17, CCL22, CCL23, CCL24 | B |
| | CCRL1 | CCL19, CCL21, CCL25, CXCL13 | |
| | CCRL2 | CCL19 | |
| | DARC | CXCL1, CXCL2, CXCL3, CXCL7, CXCL8, CCL2, CCL5, CCL11, CCL13, CCL14, CCL17 | En |
| | D6 | Agonists of CCR1-CCR5 | Mac, HSc, En, Mo, Neut, B, D |

**Table 1.1: The chemokine superfamily.** Chemokine ligands and their receptors are classed into families based on the location of cysteine residues. Atypical chemokine receptors can influence the activity of other chemokine ligands, but do not signal via classical pathways. T= T cell; Mo= Monocyte; Eo= Eosinophil; Ba=Basophil; D=Dendritic cell; $T_{mem}$= Memory T cell; Th2= Th2 T cell; P= Platelet; $T_{reg}$= Regulatory T cell; MC= Mast cell; N= Neutrophil; En= Endothelial cell; Th= Helper T cell; NK= Natural killer cell; Mac= macrophage; SMC= Smooth muscle cell, HSc= Hematopoietic stem cell. Table adapted from Zlotnik *et al* (2012) [79] and Graham *et al* (2012) [80].

Chemokines are also grouped into two main functional subfamilies – inflammatory and homeostatic, although some chemokines overlap both fields and are called dual-function chemokines. Inflammatory chemokines control the recruitment of leukocytes during inflammation. Homeostatic chemokines navigate leukocytes to and within secondary lymphoid organs as well as in the bone marrow and thymus during hematopoiesis. Chemokines also have critical roles in development, lymphocyte trafficking and homing, angiogenesis and malignancy [78].

During inflammation, chemokines are secreted in response to pro-inflammatory mediators and have an important role in selectively recruiting monocytes, neutrophils and lymphocytes. The directed migration of activated cells expressing appropriate chemokine receptors occurs along a chemokine gradient. Chemokines within each chemokine subfamily can competitively bind to the same receptor on target cells and have common functional activities – therefore redundancy is high [81].

**Interleukin-8 (IL-8/CXCL8)**

IL-8 is the prototypical member of the family of CXC chemokines and is one of the most potent neutrophil chemoattractants in inflammation. IL-8 is synthesised as an inactive 99 amino acid precursor protein, with N-terminal cleavage producing a 77 amino acid (fibroblasts and endothelial cells) or 72 amino acid (leukocytes) protein. The 77 amino acid isoform secreted from non-immune cells is further cleaved to produce the active 72 amino acid IL-8 protein, with a molecular weight of approximately 8kDa

IL-8 is secreted from a range of cell types including leukocytes, fibroblasts, endothelial cells and malignant cancer cells. [82]. IL-8 can exist in monomer or dimer forms, which are capable of differentially activating and regulating its two cell surface receptors [83]. It binds to two different chemokine receptors on leukocytes and endothelial cells – the GPCRs CXCR1 and CXCR2. While CXCR1 is specific for IL-8, CXCR2 also interacts with CXCL1, 2, 3, 5, 6, and 7 [84]. Both receptors are also expressed on cancer cells. Binding of CXCR1 and CXCR2 activates specific intracellular signalling cascades including MAPK, PI3K, protein kinase C (PKC) and Src family kinase (SFK) signalling. This can lead to phosphoinositide hydrolysis, intracellular $Ca^{2+}$ mobilisation, chemotaxis and exocytosis [85]. IL-8 signalling also activates multiple transcription factors including NFκB, AP-1, STAT3 and HIF-1 [86].

As neutrophils are the fastest and most rapidly responding innate cell, IL-8 is consistently among the first signals to be expressed and released by cells during inflammation. IL-8 signalling is induced by inflammatory signals, ROS, death receptors and steroid hormones [86]. As well as many other disease settings, IL-8 expression is increased during IBD where it is a major contributor to the increased numbers of neutrophils found in the mucosa [87].

**Monocyte Chemoattractant Protein-1 (MCP-1/CCL2)**

MCP-1 is a C-C chemokine family member and a potent chemotactic factor for monocytes. It belongs to a family composed of three other members (MCP-2, -3, and -4) [78]. MCP-1 is composed of 76 amino acids and is 13kDa in size. It is produced by a variety of cell types, either constitutively or after induction by cytokines, growth factors or oxidative stress, and include endothelial cells, fibroblasts, epithelial cells, smooth muscle cells, monocytic and microglial cells [78].

MCP-1 has been demonstrated to recruit monocytes into foci of active inflammation, including sites of bacterial, fungal and viral infection, as well as sites of sterile inflammation [88]. Another key role of MCP-1 is in orchestrating monocyte egress from the bone marrow into the circulation. Recent studies have shown that the increase in circulating monocyte number associated with infection or sterile inflammation is mediated by MCP-1-mediated signalling in monocytes in the bone marrow [89].

MCP-1 mediates its effects through its receptor CCR2, which is expressed on multiple cell types. CCR2 can have dual roles in both pro-inflammatory and anti-inflammatory settings. CCR2 deficient mice are resistant to the induction of sensory neuropathies [90]. Furthermore, CCR2 null mice immunised with type II bovine collagen were found to be more susceptible to collagen-induced arthritis than the wild-type mice [91]. MCP-1 has been implicated in a range of inflammatory and cancerous pathologies. MCP-1 is involved in leukocyte recruitment to vessels during formation of atherosclerotic plaques [92], and to target tissues in demyelinating lesions during multiple sclerosis [93].

**N-formyl-methionyl-leucyl-phenylalanine (fMLP)**

fMLF is the correct abbreviation for N-formyl-methionyl-leucyl-phenylalanine, as described by Dorward *et al* (2013) [94]. fMLP is a common misnomer and fMLF will be referred to as fMLP throughout this thesis.

Small formyl peptide derivatives, obtained as bacterial metabolites or derived from disrupted mitochondria, are potent chemoattractants. fMLP is a formylated peptide that was the first to be demonstrated as the natural chemotactic product of *E. coli* [95], and is now the most extensively studied member of the formyl peptide family. fMLP is highly lipophilic and has conformational flexibility which allows efficient interactions with its receptor [96].

Formyl peptides bind to the high affinity formyl peptide receptor (FPR) and its low affinity variant FPR-like 1. FPR is activated by picomolar to low nanomolar concentrations of fMLP and is functionally coupled to G proteins. FPR activation results in phospholipase C (PLC) and PI3K signalling leading to $Ca^{2+}$ mobilisation from intracellular stores and tyrosine phosphorylation [97]. $Ca^{2+}$ release into the cytoplasm is the earliest evidence of neutrophil stimulation by fMLP and occurs in close association with an apparent membrane hyperpolarisation [98].

fMLP can activate directed cell movement, phagocytosis, release of proteolytic enzymes and generation of ROS. fMLP activates the transcription factor $NF_KB$ in leukocytes [99]. This appears to be essential for pro-inflammatory cytokine synthesis in phagocytes and is cell-specific and different to TNFα-mediated NFκB activation [100]. fMLP induces the secretion of IL-1 and IL-6 in human mononuclear cells [101]. Upon exposure to fMLP neutrophils develop a characteristic surface ruffling and adopt an elongated shape in which modifications in the actin cytoskeleton are implicated [102]. Mitochondrial formyl peptides are potent immune activators and are septic mediators implicated in clinical systemic inflammatory response syndrome [103].

Neutrophils from patients with localised juvenile periodontitis (LJP) show decreased binding and responsiveness to various chemotactic agents, including fMLP, possibly due to a polymorphism in the FPR [104]. FPR-deficient mice display increased bacterial burden in the liver and spleen, and earlier death, when challenged with *L. monocytogenes*, versus healthy littermates, suggesting a role for fMLP signalling in host defence through regulation of innate immunity [105].

**Leukotriene $B_4$ ($LTB_4$)**

Leukotrienes are a family of eicosanoid inflammatory mediators. Leukotrienes are named after their cells of origin (leukocytes) and the presence of three positional conserved double bonds (trienes). The leukotriene family includes leukotriene $A_4$ ($LTA_4$), a short-living intermediate product of the leukotriene synthesis pathway, leukotriene $B_4$ ($LTB_4$) and the group of cysteinyl leukotrienes: $C_4$ ($LTC_4$), $D_4$ ($LTD_4$) and $E_4$ ($LTE_4$) [106]. Leukotrienes are produced by the oxidation of arachidonic acid by arachidonate 5-lipoxygenase. Neutrophils mainly produce $LTB_4$ while monocytes and macrophages can generate $LTB_4$ and cysteinyl leukotrienes. Other cell types, such as epithelial cells, can synthesise leukotrienes, but to a lesser extent [107].

$LTB_4$ has three receptors with different binding affinity. BLT1 is a high affinity receptor for $LTB_4$ and is expressed by neutrophils, monocytes, T lymphocytes, eosinophils and mast cells. BLT is a low affinity receptor for $LTB_4$ that is expressed on $CD8^+$ and $CD4^+$ T lymphocytes and monocytes [108]. Thirdly, peroxisome proliferator-activated receptors (PPARs) are another group of $LTB_4$ receptors that are expressed in the nucleus and function as lipid homeostasis factors and controllers of inflammatory responses [109].

All leukotriene receptors link to G proteins upon activation and decrease intracellular cAMP, increase cytosolic $Ca^{2+}$, and stimulate MAPK and ERK phosphorylation. $LTB_4$ stimulation leads to a number of functional responses important during inflammation, including degranulation, ROS production, chemotaxis and phagocytosis [110]. $LTB_4$ also stimulates expression of $\beta_2$ integrins (CD11b/CD18), likely related to leukocyte migration [106]. $LTB_4$ has been implicated in a variety of inflammatory disorders, including RA [109]. $LTB_4$ stimulates neutrophil infiltration resulting in emphysematous lung tissue and is significantly implicated in the progression of chronic obstructive pulmonary disease [111].

## 1.2 Signalling pathways in innate immune cell function

Innate cells must be able to effectively recognise and eliminate pathogens and dying cells. This relies on complex intracellular signal transduction pathways that inform the cells of their environment or drive necessary processes, such as chemotaxis, that are required for the restoration of homeostasis. Therefore, intracellular signal transduction processes need to convey a large amount of complex information to support an efficient inflammatory response. SFK and PI3K signalling are heavily involved in immune responses and are described in more detail below.

### 1.2.1 Src family kinase (SFK) signalling

Cytoplasmic tyrosine kinases are crucial for innate immune cell signalling. Two major kinase families that operate in the proximal intracellular signalling pathways in innate cells are the Src-family kinases and the Syk-ZAP70 family [112]. Src family kinases are signalling enzymes that have long been recognised to regulate critical cellular processes such as proliferation, survival, migration and metastasis.

#### SFK family members, structure and discovery

Src kinase is a proto-oncogene encoding a non-receptor protein tyrosine kinase. The Src gene is similar to the v-Src from the Rous sarcoma virus [113]. Subsequent studies of viral and constitutively active forms of Src have increased our understanding of the processes involved in malignant transformation. In addition, studies of signalling pathways leading to the activation of Src and its closely related SFK homologues have been central towards understanding normal growth-regulatory processing, including proliferation, apoptosis, cell cycle control, angiogenesis and cell-cell adhesion and communication [114].

SFKs are classified as non-receptor tyrosine kinases consisting of nine structurally related molecules: Src, Blk, Fyn, Yes, Lyn, Hck, Fgr, Yrk and Lck [115]. SFK expression can differ between different innate cell types [116]. Monocytes, macrophages, granulocytes and dendritic cells primarily express Hck, Fgr, Lyn and to a lesser extent, Src. These SFKs have been implicated as primary signalling molecules downstream of a host of immune cell receptors, such as immunoreceptors, cytokine receptors, integrins and pathogen receptors.

Each SFK member has conserved peptide domains, termed Src homology (SH) domains, four of which have been defined in all SFKs [117]. The structural components of SFK are illustrated in figure 1.3. SH domains allow SFK participation in signalling complexes and also regulate SFK kinase activity through intramolecular interactions. SH-1 is the enzymatic domain of the molecule and possesses intrinsic tyrosine kinase activity [118]. The SH-1 domain also contains an activation loop that has an autophosphorylation site at Tyr416 and regulates the association with substrates. The SH-2 domain allows interaction with phosphotyrosine residues on proteins, specifically with its own C-terminal tyrosine phosphorylated amino acid (Tyr527) in its inactive

conformation [116]. The SH-3 domain recognises proline rich motifs, present on many signalling and structural molecules [119]. Analysis of crystal structures have indicated that SH-2 and SH-3 domains facilitate intermolecular interactions between Src and proteins with which it forms complexes [120]. The NH2-terminal domain, or the SH-4 domain, can be myristoylated and is responsible for membrane association of SFKs and determination of cellular localisation [121].

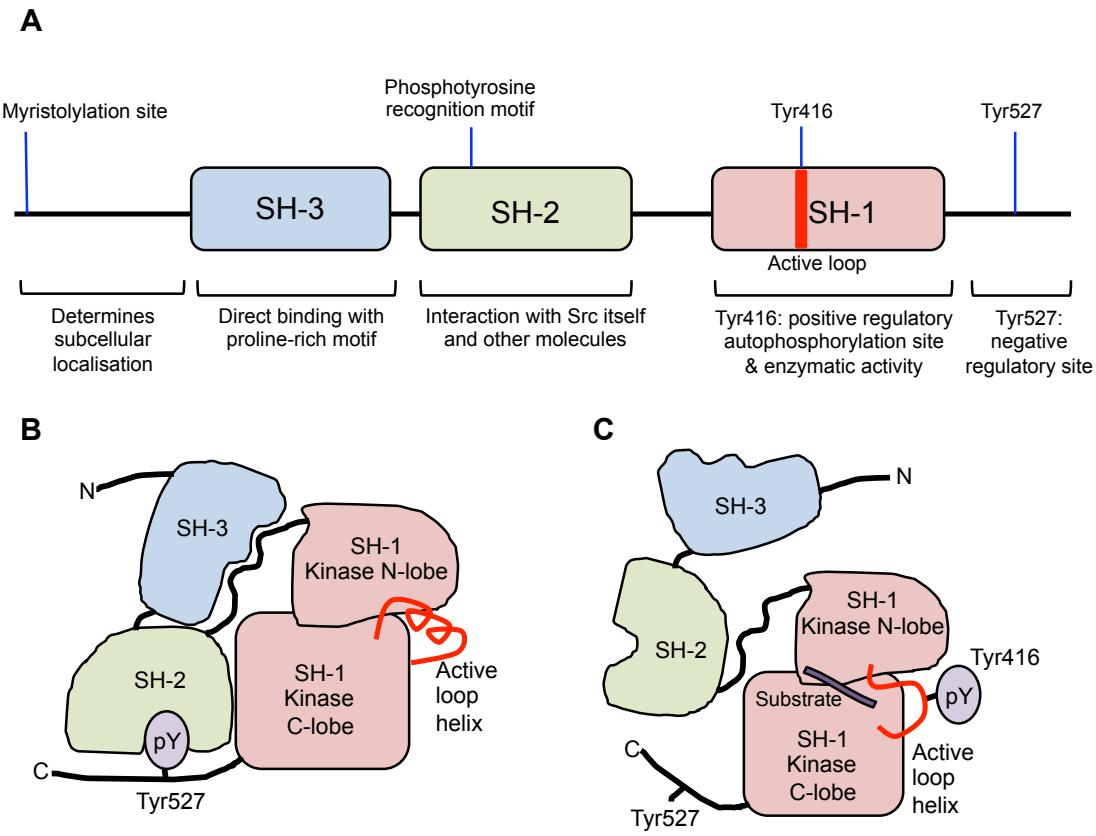


**Figure 1.3: The structure of SFKs and conformational changes during SFK activation.** (A) The SFK structure comprises regulatory SH-1 domain, interactive SH-2 domain and the SH-3 domain that coordinates substrate binding. (B) During the inactive conformation, C-terminal Tyr527 is phosphorylated and bound to SH-2 domain. (B) Phosphorylation of active loop Tyr416 leads to activation of SFKs, with an extended conformation and open structure.

### SFK activation and signalling

SFK activity is regulated by the autophosphorylation and dephosphorylation of their own tyrosine residues [122]. Through interaction of the SH-2 or SH-3 domain with the other domains, SFKs change their structure and exhibit different levels of activity. In the inactive state, C-terminal Tyr527 is phosphorylated and interacts with the SH-2 domain, resulting in a closed conformation. Autophosphorylation at Tyr416 in the SH-1 domain results in an open conformation and active state protein [122]. Figure 1.3 illustrates conformational changes in SFKs during activation.

SFK activity can be regulated by other tyrosine kinases. The C-terminal Src kinase (Csk) and the Csk homology kinase (Chk) are two main tyrosine kinases responsible for the phosphorylation of the auto-inhibitory Tyr527 in Src [123]. Chk forms a non-covalent bond with the auto-phosphorylated form of SFKs that blocks kinase activity. Many other phosphatases, e.g. phosphatase-1B and phosphatase-α, are capable of removing the Tyr527 phosphate group from the C-terminal tyrosine and 'opening up' the catalytic SH-1 site. This is often after the C-terminal phosphorylated tyrosine is 'exposed' following intermolecular interaction of Src with binding proteins in signalling complexes [120].

SFKs phosphorylate tyrosine residues on target proteins. Historically, the study of SFK signalling has focused on immunoreceptor and integrin signalling, however SFKs were later shown to participate in other signal transduction pathways including at chemoattractant receptors and integrin receptors. Figure 1.4 illustrates the role of SFKs at various receptor types. SFKs communicate to various downstream mediators, including Tec-family members, e.g. Btk, Bmx and Tex in innate cells [112]. SFKs also activate the FAK/Pyk2 tyrosine kinase family, which plays a major role in integrin signalling [124]. Pathways can be initiated in different spatial and temporal rates or activated indirectly, for example through the production of cytokines and not through direct intracellular biochemical interactions. Regulation through distinct protein domains and post translational modifications accounts, in part, for the multiple roles SFKs play in signalling complexes, where they serve both as a scaffolding protein and as a protein tyrosine kinase.

SFKs control NADPH oxidase activation and ROS production. Activated NADPH oxidase is a multimeric protein consisting of at least three cytosolic subunits: p47phox, p67phox, and p40phox. The p47phox subunit displays a significant role in the acute activation of NADPH oxidase; the phosphorylation of p47phox by Src kinase is thought to inhibit intracellular interactions and to promote the binding of p47phox to p22phox, thereby inducing the activation of NADPH oxidase [125]. SFKs also promote endothelial permeability in inflammatory processes. Excessive cytokine production and growth factor release can result in vascular endothelial damage and may incite dysfunction of paracellular and transcellular transport mechanisms, leading to diminished ability to regulate trans-endothelial passage of fluid, protein and solute [114].

**SFK signalling at immunoreceptors**

Typically, immunoreceptor engagement leads to activation of SFKs, which in turn phosphorylate immunoreceptor tyrosine-based activation motifs (ITAMs) present on the receptor or associated subunits [126]. This leads to recruitment of Syk via binding of the Syk SH-2 domain to the phospho-ITAM residues, and activation of Syk allowing it to phosphorylate downstream substrates. These substrates include PI3K, which in turn generates $PI(3,4,5)P_3$ and FAK/Pyk2 kinases that activate the Rho/WASP pathway of actin polymerisation. Together all of these pathways can impact many downstream factors, including MAP kinases (leading to gene transcription), Rac/Rho (modulating cytoskeletal function), and inositol triphosphate ($IP_3$) and diacyl-glycerol (DAG)

(regulating $Ca^{2+}$ entry and PKC activation). This prototypical immunoreceptor pathway is similar in both innate and adaptive immune cells [127], [128]. SFKs and Syk tyrosine kinases also activate inhibitory signalling pathways. Lyn is primarily responsible for immunoreceptor tyrosine-based inhibitory motif (ITIM) phosphorylation, which serves as a docking site for phosphatases such as SHP-1 or SHIP-1 [129].

Phagocytosis occurs through the binding of FcγR to immunoglobulins [24]. FcγR cross-linking is induced by the phosphorylation of ITAMs located in the cytoplasmic tail of the tyrosine kinase receptors. SFKs expressed in phagocytes form complexes with inactivated FcγRs. Src deficient cells are less effective than WT cells at mediating phagocytosis [130].

**SFK signalling at non-ITAM containing receptors**

SFKs also have important signalling roles in pathways where ITAMs are not involved. Some studies suggest that SFKs work with Jak kinases in supporting cytokine responses, possibly by phosphorylation of receptor subunits or STAT molecules [131]. In the case of growth factor receptors, such as GM-CSF receptors, SFKs have been found to physically associate with the receptor via SH-3 interactions [132]. In other cytokine responses, SFKs may be acting further downstream of the receptor, for example through TRAF signalling molecules. A number of studies have demonstrated the involvement of SFKs downstream of the M-CSF receptor in macrophages and myeloid progenitors, with their function being to couple receptor activation to downstream PI3K pathways [133]. SFKs have also been shown to signal downstream of selectin receptors, membrane bound receptors and TLRs [112].

Recent developments have led to the demonstration that many innate immune receptors utilise the ‘immunoreceptor pathway’ despite lacking ITAMs and not actually being immunoreceptors. This has evolved from studies of innate cells lacking the ITAM-signalling adaptors DAP12 and the FcγR [134]. Typically, DAP12 and FcγR are coupled to immunoreceptors through charged amino acid interaction within the transmembrane regions of each protein. A number of non-immunoreceptor pathways, for example neutrophil integrin signalling or basophil IL-3 responses, are lost in innate cells derived from mice lacking DAP12 or FcγR [14], [135]. The mechanisms by which these non-immunoreceptors couple to DAP12 and/or FcγR to initiate signalling remain unclear.

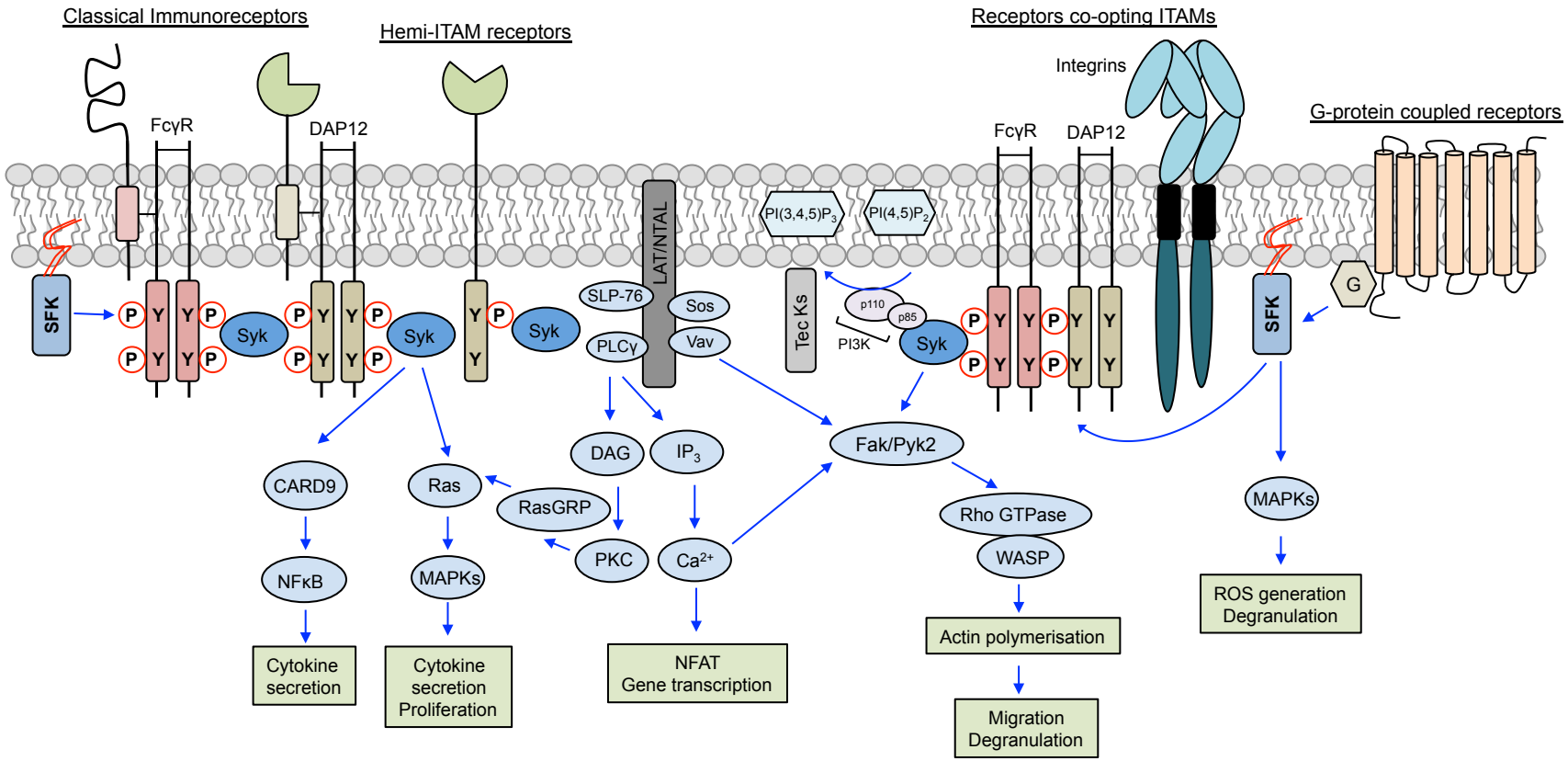


**Figure 1.4: SFK and Syk signalling in the activating signalling pathways utilizing ITAM-containing adaptors.** Examples of immunoreceptors, hemi-ITAM C-type lectin receptors, and non-immunoreceptors that utilize ITAM-signalling adapters and the cytoplasmic tyrosine kinases. Classical immunoreceptors refers to those signalling molecules that are directly coupled to ITAM adaptors FcγR or DAP12. Dectin-1 is an example of a C-type lectin receptor that has ITAM-like sequences as imbedded domains with its cytoplasmic tail. Leukocyte integrins are the best example of receptors that link to or co-opt the ITAM pathway. Typically, SFKs phosphorylate the ITAM adaptors, creating docking sites for Syk kinase that then phosphorylates a number of substrates including scaffolding proteins LAT and NTAL that subsequently recruit further proteins to initiate downstream responses. Syk function is also critical for PI3K activation, which leads to generation of $PIP_3$ and recruitment of Tec-family kinases. Together, these all contribute to downstream pathways of calcium signalling, MAPK activation and NFκB activation. SFKs and Syk also contribute to FAK/Pyk2 activation, leading to actin polymerisation required for migration and adhesion processes. Additionally, SFKs can act downstream of GPCRs by binding to G proteins, and possibly via linking to ITAM-containing receptors. SFKs may link GPCRs to MAPK pathways. Figure adapted from Lowell *et al* (2011) [112].

### SFK signalling at GPCRs

SFKs have also been implicated in the regulation of chemokine signalling, mediated by GPCRs. Ma *et al* (2000) report that G proteins Gαs and Gαi directly stimulate Src kinase activity of down-regulated c-Src, and similarly modulate Hck. This was proposed to be via direct binding to the catalytic domain and a subsequent conformational change, leading to increased accessibility of the active site to substrates [136]. SFK activation has been identified downstream of several chemokine receptors. For example, Lyn kinase is activated in macrophages downstream of both CXCR4 and CCR5, and is thought to couple these GPCRs to the MAPK and PI3K pathways [137]-[139]. Furthermore, recent reports using pharmacological inhibitors have suggested that SFKs may act downstream of MCP-1 signalling via CCR2 [140], and downstream of IL-8 signalling via CXCR1 [141]. Neutrophils derived from $Hck^{-/-}Fgr^{-/-}$ double mutant mice show significant functional defects following fMLP stimulation, which involves signalling through GPCR-coupled FPRs [142]. fMLP-induced degranulation is decreased significantly in neutrophils treated with the Src inhibitor PP1 and in Src-deficient cell lines [143].

### SFK signalling in migration and adhesion

SFKs and Syk play a positive role in regulation of migration of different leukocyte subtypes including granulocytes and macrophages/monocytes [115]. Roles of SFKs in innate immune cell migration are summarised in table 1.2.

$\beta_2$ integrin ligation leads to SFK activation [144] and $\beta_2$ integrin-mediated neutrophil activation also requires the Syk tyrosine kinase. Integrin mediated Syk activation is facilitated by two ITAM-bearing adaptor molecules, DAP12 and FcγR, in a classical phospho-ITAM-mediated manner [14]. Loss of SFK activity results in complete deficiency of $\beta_1$, $\beta_2$ and $\beta_3$ integrin function in innate cells.

| Kinase | Cell Type | Role in migration | Reference |
|---|---|---|---|
| Fgr | Neutrophils, Macrophages, cell lines | Fgr-/- Hck -/- neutrophils display normal chemotactic responses to chemokines. Fgr-/- Hck-/- macrophages display a reduced chemokinetic and chemotactic ability. FcγR-mediated responses were diminished in Fgr-/-Hck-/- macrophages. | [145]-[148] |
| Hck | Neutrophils, Macrophages, cell lines | Hck expression in U937 monocytic cell line enhances cell migration. Neutrophils expressing constitutively active Hck display enhanced chemotaxis toward fMLP. | [149], [150] |
| Lyn | Neutrophils, Mast cells, hematopoietic precursors, cell lines | Neutrophil stimulation with chemoattractants activates a Lyn/Shc/PI3K pathway. SDF-induced cell migration is defective in Lyn-deficient bone marrow cells. Lyn-deficient neutrophils and macrophages display a hyper adhesive integrin signalling-dependent phenotype. | [137], [151]-[153] |
| Fyn | Mast cells, cell lines | CSF-induced cell migration is reduced in Fyn-deficient mast cells | [154], [155] |
| Yes | Ubiquitous | Yes activation drives $LTB_4$-mediated degranulation of human neutrophils. | [156] |
| | | | |
| Syk | Lymphocytes, cell lines | Syk is required for cytoskeleton remodelling and cell migration of macrophage cell line RAW264.7 in response to $CX_3CL1$. | [157] |

**Table 1.2: Selected roles of SFKs and Syk in the regulation of innate cell migration.**

Focal adhesion kinase (FAK) and Pyk2 are expressed in innate cells, amongst other cell types. FAK can drive cell adhesion signalling downstream of integrin activation [158]. FAK and Pyk2 are both substrates for SFKs following integrin ligation and their subsequent phosphorylation leads to protein unfolding and activation of their enzymatic activity. In innate cells, FAK and Pyk2 are found in podosomes, the main contact sites in leukocytes [159]. Macrophages lacking FAK display elevated protrusive activity, altered adhesion dynamics, elevated Rac activity and impaired chemotaxis, all of which greatly impairs directional migration [160], [161]. A similar phenotype is observed in macrophages derived from Pyk2-deficient mice [160]. This involvement of FAK and Pyk2 could also affect phagocytosis mechanisms, because siRNA mediated knock down of FAK and/or Pyk2 can reduce uptake of bacteria [162]. The story is similar in neutrophils, where FAK and/or Pyk2 deficiency leads to impaired adhesion, migration, and bacterial uptake [163], [164]. These reports strongly suggest FAK/Pyk2 signalling is via integrin-mediated events and proposes a role for SFK in this setting.

### Syk kinase

The Syk-ZAP70 family of tyrosine kinases has two members and only Syk is found in innate cells. Syk kinase is involved in all innate immune cell signalling involving ITAM or ITAM-like signalling adaptors [112]. This includes signalling from classical

immunoreceptors, non-immunoreceptors (e.g. integrins, selectins), and those C-type lectin receptors that have hemi-ITAMs embedded in their C-terminal domains (e.g. dectin). Syk is activated by engagement of its two SH-2 domains by phospho-ITAM domains, so it functions only in ITAM-like pathways. It is also likely that Syk is only involved in pathways that also include SFKs. However, differences in phenotypes have been observed when Syk and SFKs are separately inhibited. For example, SFK deficient macrophages have a moderate defect in phagocytosis, caused by a reduction in initial actin polymerisation at the phagocytic cup [148]. In Syk deficient cells, however, phagocytosis is completely blocked due to a block in fusion of the arms of the phagocytic cup, a step subsequent to actin polymerisation events [165]. In light of this, SFKs could be signalling to other pathways besides ITAM-mediated Syk activation. Syk has also been linked to activation of intracellular pattern recognition receptors, which in turn activate the inflammasome leading to IL-1β production [166]. Genetic deficiency of Syk, as well as a novel Syk inhibitor, protects mice from auto-antibody induced arthritis but also prevents neutrophil activation in various assay systems [15]. Interestingly, some reports suggest that it is likely that Syk does not signal in cytokine or GPCR linked pathways. Lack of functional Syk has no effect on neutrophil, macrophage or mast cell recognition of several cytokine growth factors or GPCR agonists, including fMLP or ATP [167].

SFKs have broad effects on overall signalling, while Syk has more defined roles. This is echoed in the fact that deficiencies in single SFKs tend to produce limited signalling defects in innate cells. However, loss of Syk has very defined broad functional effects. SFKs tune responses in a graded fashion, whereas Syk acts more like a signalling switch – being an absolute requirement in certain pathways.

**Targeting SFKs for therapeutics**

Given the wide ranging roles of SFKs and the more defined role of Syk in signalling pathways, targeting Syk may be a more rational therapeutic strategy with reduced side effects. Importantly, the production of Syk kinase inhibitors is underway for the treatment of immune-mediated disease such as RA and type 1 diabetes [168], [169]. SFK inhibitors have proved to be far more broadly acting and target enzymes besides just SFKs, which is problematic for the treatment of immune diseases [112]. A future target is to create inhibitors that can distinguish between SFK members, although this seems particularly chemically challenging.

Novel inhibitors of Src have been designed for therapeutic purposes particularly for use in tumorigenesis. Bosutinib (SKI-606), dasatinib (BMS-354825), saracatinib (AZD0530), KX2-391, and NVP-BHG712 are examples of recently developed Src inhibitors exhibiting $IC_{50}$ values ranging from 1nM-300nM. Most of these have been tested in cancer disease settings [170]. Fostamatinib, an orally active pro-drug of a Syk inhibitor has recently produced promising effects in a phase II clinical trial in human rheumatoid arthritis [171]. Dasatinib, a combined Abl/Src inhibitor used for the treatment of chronic myelogenous leukaemia also shows robust inhibitory effects on certain neutrophil functions and may prove to be a suitable starting point of development of novel tyrosine kinase inhibitor anti-inflammatory molecules [172].

### 1.2.2 Phosphoinositide 3-kinase (PI3K) signalling

Phosphoinositide 3-kinase (PI3K) is a conserved family of lipid kinase enzymes known to play non-redundant roles in multiple cell processes. PI3K isoforms can be divided into three classes (class I, II and III) based on their structure and lipid substrate specificities. While class I PI3Ks are the most extensively studied, less is known about class II PI3Ks. Class III PI3Ks have been implicated in vesicle trafficking and phagocytosis [173].

The structural domains of class I PI3K are illustrated in figure 1.5. Class I PI3Ks are composed of a p110 catalytic subunit and a tightly associated regulatory subunit, which is responsible for the recruitment of the complex to the plasma membrane upon receptor ligation [174]. Class I PI3Ks are composed of four isoenzymes subdivided into class IA (p110α,β,δ) and class 1B (p110γ) which pair with five (p85α, p50α, p55α, p85β and p55γ) and two (p101 and p84) regulatory subunits, respectively [175]. Class IA isoforms are activated downstream of a variety of receptors that are phosphorylated by tyrosine kinases upon cognate stimulation. The class IB PI3Kγ is activated by G-protein βγ subunits and signals downstream of GPCRs. However, recent evidence suggests that PI3Kβ can couple to GPCRs and PI3Kγ can couple to tyrosine-kinase coupled receptors [176], [177].

#### Class I PI3K signalling

Class I PI3K enzymes phosphorylate the D3 position on the inositol ring of phosphatidylinositol 4,5-bisphosphate [$PI(4,5)P_2$] to generate $PI(3,4,5)P_3$ which controls signalling cascades in many cellular responses. $PI(3,4,5)P_3$ is located in the plasma membrane and acts as a docking site to recruit and activate pleckstrin homology (PH) domain containing proteins (see figure 1.5). PH-domain containing proteins that are activated by PI3K signalling include PKB/Akt, PDK1, guanine nucleotide exchange factors, and a range of adaptors and scaffolding proteins [174].

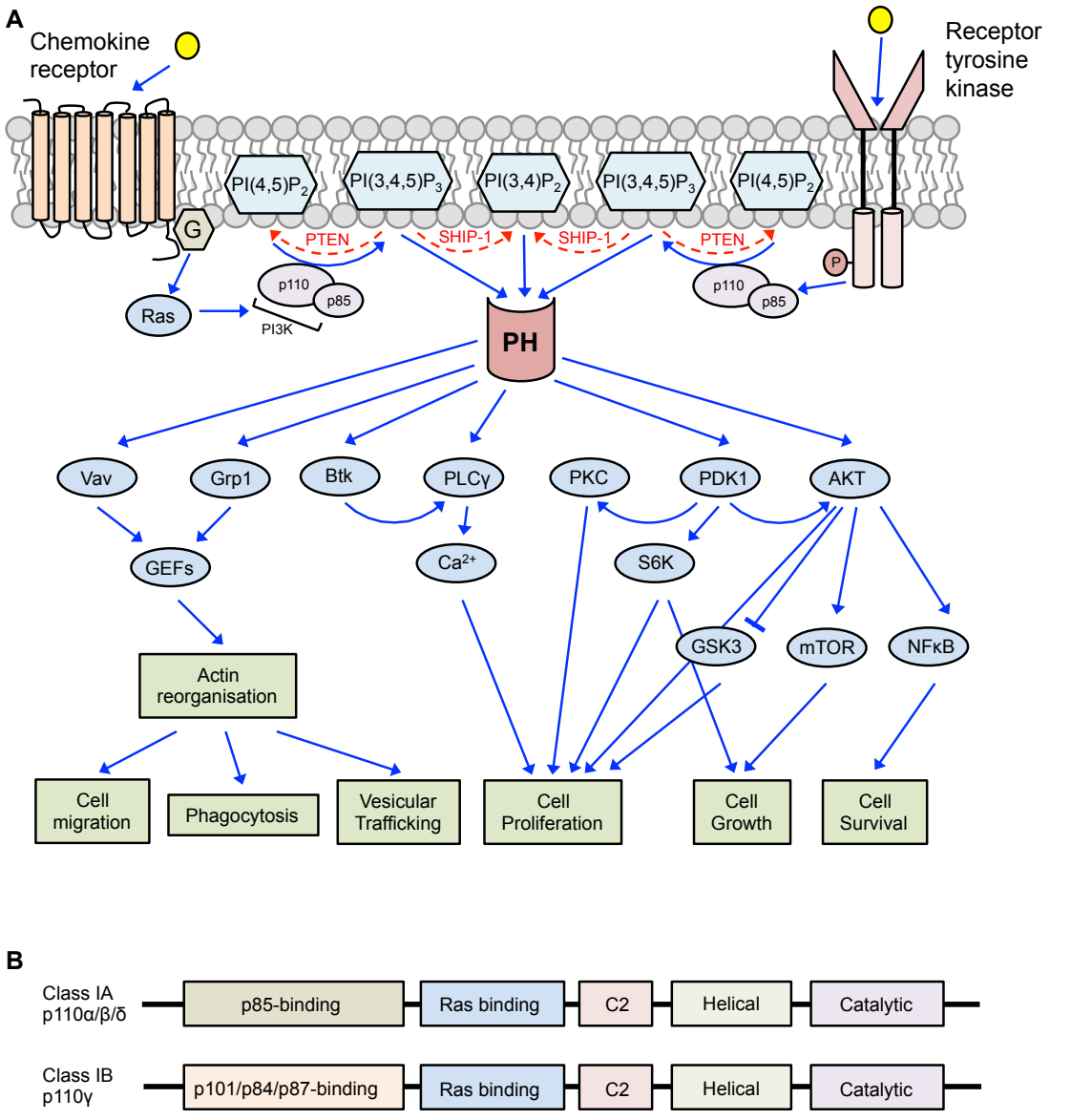


**Figure 1.5: PI3K signalling cascade and structural domains of class I PI3Ks.** (A) Following GPCR or RTK activation, class I PI3K enzymes phosphorylate the D3 position on the inositol ring of $PI(4,5)P_2$ to generate $PI(3,4,5)P_3$ which is located in the plasma membrane and acts as a docking site to recruit and activate pleckstrin homology (PH)-domain-containing proteins that in turn regulate downstream effector proteins and promote a host of cellular responses. (B) Structural domains of PI3K class I enzymes. Class IA and IB share core domain structure of single Ras binding, C2, helical and catalytic domains. Class IA has a p85 regulatory subunit-binding (p110a/b/d) domain, whereas class IB enzymes have p101/p84/p87-binding (p110g) domains.

The PI3K/Akt/mTOR cascade is the most common effector pathway downstream of $PI(3,4,5)P_3$. $PI(3,4,5)P_3$ recruits 3-phosphoinositide-dependent protein kinase 1 (PDK1) which in turn phosphorylates and activates Akt at Thr308 [178]. Akt signals to mTOR, a complex of proteins that functions as serine/threonine kinases. mTORC2 can phosphorylate Akt at Ser473 and this leads to the complete activation of Akt, which exhibits fivefold more activity than phosphorylation at Thr308 alone [179].

PI3K signalling is regulated by at least two lipid phosphatases – SH2-domain containing inositol 5-phosphatase (SHIP) and phosphatase and tensin homologue (PTEN). SHIP dephosphorylates $PI(3,4,5)P_3$ at the D5 position of the inositol ring to create phosphatidylinositol 3,4-bisphosphate [$PI(3,4)P_2$]. Multiple forms of SHIP have been reported. Importantly, SHIP-1 expression is restricted to differentiated cells of the hematopoietic system, endothelial cells and stem cells [180]. PTEN dephosphorylates the D3 position to create $PI(4,5)P_2$ [181]. PTEN is expressed in both hematopoietic and non-hematopoietic tissues.

**PI3K signalling in the immune system**

PI3Ks are activated by an array of receptors expressed on leukocytes across innate and adaptive immunity. The significance of PI3K during inflammation was highlighted by the generation of kinase inactive PI3Kγ or PI3Kδ mice. Although the mice appear viable and healthy, upon immune challenge the mice are unable to mount sufficient inflammatory responses, indicating that these kinases have non-redundant functions in leukocytes, and that they play a critical part in inflammatory disease [173]. It appears that PI3Kγ or PI3Kδ act in partnership to regulate immune cell signalling and function. Several studies have suggested that PI3K inhibition or genetic ablation of PI3Kγ causes a reduction in chemotactic responses of lymphocytes, neutrophils, macrophages and eosinophils in both *in vitro* and *in vivo* migration assays [174]. PI3Kγ is crucial for morphological changes associated with cell polarisation by generating $PI(3,4,5)P_3$ at the leading edge and regulating Rac activity and the cytoskeleton reorganisation [182]. PI3Kδ has also been shown to regulate neutrophil migration as demonstrated by the ability of a PI3Kδ-specific inhibitor to induce directional neutrophil movement in response to chemotactic gradients [183], [184]. PI3K activity in endothelial cells can also regulate neutrophil interactions with an inflamed vessel wall [183]. PI3Kγ and PI3Kδ also coordinate neutrophil respiratory burst [185]

*In vivo* models of neutrophil migration have revealed that while PI3Kγ is important in early chemokine-induced emigration, PI3Kδ replaces PI3Kγ and maintains the delayed chemokine-induced neutrophil recruitment into inflamed tissues [186], suggesting that their coordination is temporally distinct. However, despite this coordination between isoforms, genetic targeting has revealed that each isoform has distinct contributions that are dependent upon the receptor and/or cell type involved. For example, although both PI3Kγ and PI3Kδ are required for neutrophil migration towards $LTB_4$, only PI3Kγ is responsible for migration towards fMLP [187]. The requirement for PI3K during neutrophil chemotaxis is context dependent *in vitro*. PI3Kγ is essential for murine neutrophil migration on fibrinogen-coated surfaces, but is dispensable for migration on glass [188]. Treatment of human neutrophils *in vitro* with PI3K inhibitors abolishes migration towards selected chemoattractants such as IL-8 and $LTB_4$, but not towards others including fMLP or C5a [189].

Using both genetic and pharmacological approaches in zebrafish, it has recently been reported that PI3K activity is required for both random and directed neutrophil motility [190]. This suggests that PI3K and the generation of $PI(3,4,5)P_3$ acts as a key motor at the leading edge that drives cell protrusion and is necessary for motility. Live imaging of the dynamic localisation of $PI(3,4,5)P_3$ and $PI(3,4)P_2$ in zebrafish neutrophils has

revealed that PI3K is activated at the cell front regardless of the direction of cell movement, either towards or away from a wound [190]. Therefore, although accumulation of $PI(3,4,5)P_3$ at the leading cells is an early marker of cell polarity and gradient sensing, it is likely to be a key player in mediating localised protrusion and motility rather than gradient sensing.

Despite their importance in mounting successful inflammatory responses, overactive PI3K signalling can induce immune related pathologies including cancer [191], [192]. This suggests that therapeutic targeting of PI3Ks may be beneficial in these disease settings. Furthermore, there is evidence for a role of PI3K in autoimmune pathology including RA, systemic lupus erythematous, multiple sclerosis and type I diabetes [193].

Negative regulators of PI3K have also been studied in immune settings. Upon receptor stimulation, PI3K negative regulator SHIP-1 translocates to the plasma membrane and hydrolyses the PI3K-generated second messenger $PI(3,4,5)P_3$ to $PI(3,4)P_2$. SHIP-1 is therefore able to influence $PI(3,4,5)P_3$ mediated signalling and control proliferation, differentiation, survival and migration of hematopoietic cells [181]. Analysis of SHIP-1 mutant mice and cells has shown a key role for SHIP-1 in regulating the myeloid cell response to bacterial mitogens and regulating leukocyte polarisation during migratory responses [178], [194].

**Pharmacological targeting of PI3K signalling**

Our understanding of the PI3K signalling pathway has been improved by the development of compounds that can block their activity; the first generation of which include the natural product wortmannin and Eli Lilly compound LY294002. Commonly used PI3K inhibitors are listed in table 1.3. These tools have allowed researchers to explore structural components of PI3K interactions and have influenced the later development of more selective and potent new compounds. Inhibitors targeting the full cohort of PI3K isoforms are currently in trials for the treatment of cancers where the PI3K pathway is a key driver of disease [174].

Due to our increased understanding of specific isoform contribution to immune disorders it is necessary to focus efforts into creating inhibitors with higher isoform selectivity. This will reduce side effects and increase potency of potential therapeutics in the clinic. Such attempts are underway and on going. The ICOS compound IC87114 has an $IC_{50}$ value of approximately 100nM for PI3Kδ lipid kinase activity, but has negligible potency against the PI3Kα and PI3Kβ isoforms [193]. Calistoga, a spinout of ICOS, created CAL101, a PI3Kδ-specific inhibitor that has been successful in proof of concept trials for B cell malignancies [195]. This compound (now owned by Gilead and renamed GS1101) exhibits 40-300 fold selectivity over other isoforms. Inhibitors that are selective for PI3Kγ have also been generated, including Merck Serono SA compound AS605240 [174]. PI3Kγ and PI3Kδ have overlapping roles within inflammation, so it would be very useful to target them together with a single compound. To explore this, TargeGen has described two diaminopteridine-diphenol-based compounds (TG101-110, TG100-115) that have good selectivity for PI3Kδ and PI3Kγ [193].

| | $IC_{50}$ value (nM) | | | | |
|---|---|---|---|---|---|
| | PI3K isoform | | | | |
| **Compound** | **p110α** | **p110β** | **p110δ** | **p110γ** | **Reference** |
| LY294002 | 183 | 98 | 227 | 1967 | [196] |
| ZSTK474 | 16 | 44 | 4.6 | 49 | [197] |
| A66 | 32 | >12,500 | >1250 | 3480 | [198] |
| GSK2636771 | 2000 | 13 | 79 | 1000 | [199] |
| TGX-221 | 5000 | 5 | 100 | >10,000 | [198] |
| IC87114 | >100,000 | 1820 | 70 | 1240 | [200] |
| AS-605240 | 3400 | >20,000 | >20,000 | 190 | [200] |

**Table 1.3: $IC_{50}$ values of commonly used PI3K inhibitors.** Individual $IC_{50}$ values from *in vitro* assays with either purified or recombinant protein.

SHIP-1 is also an ideal target for immune disorders because of its restricted expression in hematopoietic cells. Given the known mechanisms, we would predict that SHIP-1 activation would lead to a reduction of cellular $PI(3,4,5)P_3$ and mimic the effect of PI3K inhibitors. Aquinox Pharmaceutical Inc. is currently developing a small molecule SHIP-1 activator for intended clinical use. Their lead compound, AQX-1125, has been shown to inhibit Akt phosphorylation, inflammatory mediator production and leukocyte chemotaxis *in vitro* [201]. Conversely, a small molecule inhibitor of SHIP-1 has been recently identified – 3 α-aminocholestane (3AC) [202]. SHIP-1 inhibition should lead to activation of PI3K and promote $PI(3,4,5)P_3$ formation. Consistent with observations from SHIP-1 deficient mice, treatment with 3AC led to increased numbers of myeloid suppressor cells and reduced ability of peripheral lymphoid tissues to prime myeloid-associated responses and protected against Graft Versus Host Disease [202]. 3AC also increased the number of granulocytes, red blood cells, and platelets in mice and could therefore be useful in patients with myelodysplastic syndrome or myelosuppressive infection.

### 1.2.3 Rho-GTPase signalling

GTPases are molecular switches that control a wide variety of signal transduction pathways in all eukaryotic cells. They regulate the actin cytoskeleton, cell polarity, microtubule dynamics, membrane transport pathways and transcription factor activity [203].

The association of GTPases with guanosine triphosphate (GTP) or guanosine diphosphate (GDP) controls their activity. GTPases cycle between two conformational states: 'Active' – bound to GTP, and 'inactive' – bound to GDP. GTPases hydrolyse GTP to GDP. In the active state, GTPases recognise target proteins and generate a response until the GTP hydrolysis returns the switch to the inactive state [203]. The exchange of bound GDP for GTP (activation) is regulated by guanine exchange factors (GEFs), which catalyse GDP dissociation and promote GTP binding. GTPase deactivation is catalysed by GTPase activating proteins (GAPs), which stimulate hydrolysis of bound GTP to GDP and inorganic phosphate. Rho GTPases are also regulated by guanine dissociation inhibitors (GDIs), which result in inactivation by

sequestering the GDP-bound GTPase away from the membrane and stabilising GDP binding [204]. These processes are illustrated in summary figure 1.6.

Mammalian cells contain hundreds of different GTPases, but the Ras superfamily is particularly implicated in many aspects of cell behaviour. The Ras superfamily comprises over 60 different GTPases, which can be categorised into five major groups: Ras, Rho, Rab, Arf and Ran. Rho GTPases are of particular interest given the insights they are providing into molecular mechanisms that underlie cell biology [203]. Of these, Rho, Rac and Cdc42 are the three best-characterised members of the Rho GTPase family. Constitutively activated mutants of Rho and Rac were found to induce the assembly of contractile actin and myosin filaments and actin rich surface protrusions when introduced into fibroblasts [205]. Cdc42 was later shown to promote the formation of actin-rich, finger-like membrane extensions (filopodia) [206].

Rho GTPases may also regulate other signal transduction pathways in addition to those linked to the actin cytoskeleton. They participate in the regulation of cell polarity, gene transcription, cell cycle progression, microtubule dynamics, vesicular transport pathways and many enzymatic activities including NADPH oxidase activity in phagocytes. The main targets for Rac and Cdc42 that mediate actin polymerisation in protrusions are the WASP/WAVE family of Arp2/3 complex activators. Rac stimulates lamellipodial extensions by activating WAVE proteins [207], and Cdc42 binds to WASP proteins. *In vitro* this stimulates the Arp2/3 complex to induce dendritic actin polymerisation [208]. WAVE/WASP proteins may themselves regulate the activity of Rac and Cdc42 by binding to GAPs and GEFs. They could thereby generate positive or negative feedback loops to regulate the extent of Cdc42/Rac-induced actin polymerisation [209].

The role of Rho GTPase signalling in leukocyte polarisation is described in more detail in section 1.3.

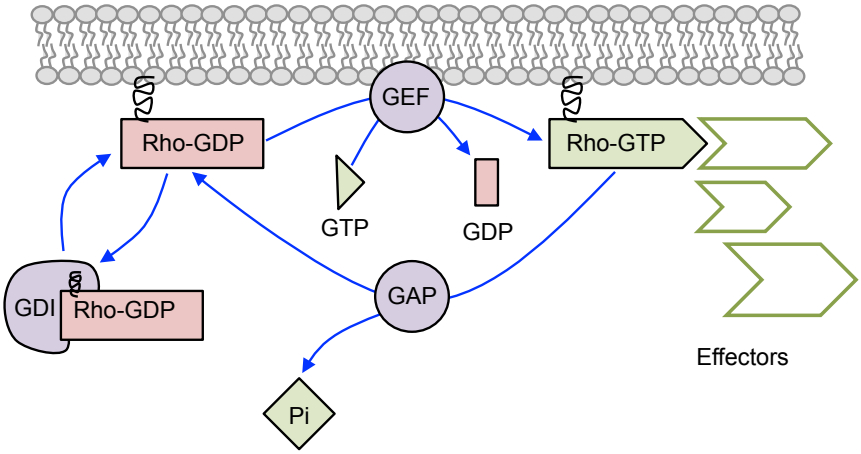


**Figure 1.6: The Rho GTPase cycle.** Rho GTPases cycle between GTP-bound 'active' and GDP-bound 'inactive' conformations. In the active state, they interact with many different effector proteins. Rho GTPase activity is regulated by GEFs, which catalyse nucleotide exchange and mediate activation, and GAPs, which stimulate GTP hydrolysis, leading to inactivation and inorganic phosphate (Pi) production. GDIs extract the inactive GTPase from membranes. Figure adapted from Etienne-Manneville *et al* (2002) [203].

### 1.2.4 Calcium signalling

Calcium acts as a second messenger in a variety of cell processes in different organisms. Transient variations in intracellular calcium have been linked to key immunological processes including ROS production, chemotaxis, phagolysosome formation, degranulation, adherence, and integrin recycling [210].

#### Mobilisation of calcium

Physiological agonists such as chemokines and ATP can induce calcium mobilisation. Receptor agonists activate initial rapid calcium release from intracellular stores, followed by a sustained plateau due to calcium entry through plasma membrane calcium channels. Activation of pertussis toxin-sensitive G-proteins activates several enzymes, including PLCβ [211]. Hydrolysis of $PI(4,5)P_2$ in the plasma membrane by PLC yields the second messengers $IP_3$ and DAG [212]. Binding of $IP_3$ to its receptor causes depletion of calcium stores within the endoplasmic reticulum (ER) and relocation of the calcium-binding type I transmembrane protein STIM-1 from the ER to structures near the plasma membrane [213]. STIM-1 then activates the plasma membrane calcium-release-activated calcium channel (CRAC) to cause an influx of calcium into the cell. Elevated intracellular calcium together with PKC activation by DAG is important for vesicle exocytosis, superoxide production by NADPH oxidases, leukotriene synthesis and JNK activation [214]. A protein tyrosine kinase dependent pathway can also activate PLC. Comparative studies using Syk- and Lyn-negative DT40 cells revealed that Syk and Lyn regulate calcium mobilisation and $IP_3$ production in B cells in response to oxidative stress, most likely through tyrosine phosphorylation of PLCγ2 [215]. In addition to receptor activation, calcium signals have been observed following tissue damage in epithelial cells *in vitro* [216], [217], in the *C. elegans* embryo epidermis [218], the zebrafish larvae [219] and recently in *Drosophila* embryos [220]. These wave-like signals are thought to be propagated through cell-cell contact; gap junctions allow calcium waves to spread via diffusion of $IP_3$ from cell to cell [221].

Calcium release via the $IP_3$ pathways can be blocked using xestopongin-C, or 2-APB which inhibits the $IP_3$-R [222]. Sarco/endoplasmic reticulum $Ca^{2+}$-ATPase (SERCA) blockers such as thapsigargin will deplete the ER calcium stores, and will indirectly block calcium release through $IP_3$-dependent stores [223]. Ethylene glycol tetraacetic acid (EGTA) is a calcium chelator that depletes extracellular calcium [224]. Despite the identification of various pharmacological modulators of calcium signalling that we can use in the laboratory, calcium signalling is not a specific target for therapeutics.

## 1.3 Mechanisms driving cell motility and migration

### 1.3.1 Cell migration and chemotaxis

Cell migration is a fundamental process that occurs in many physiological and pathological settings including development, immune responses and cancer metastasis. In a physiological setting, four key features influence the movement of leukocytes: a) anatomical borders, b) adhesion to other cells or extracellular matrix, c)

signals that trigger motility, and d) directional signals that guide the cells [225]. Leukocytes are able to migrate in the absence of chemoattractants; this ability is fundamental to immunological surveillance by tissue resident macrophages. Hematopoietic cells constantly shuttle between tissue compartments: bone marrow, blood stream, tissues and lymph [226]. Cells have adapted to cope with changing environments by carrying out fast migration. They can survive without being adherent, become autonomous from their environment, and appear to behave like single celled organisms.

Successful, coordinated directional migration depends on the formation of chemoattractant gradients, which are detected and prioritised by individual cells. The cells respond by developing a polarised morphology, from which internal signalling initiates directed locomotion in the direction of the gradient. The processes that drive motility are common throughout most cell types, although migration varies from one cell type to another in terms of speed, directionality and coordination.

Chemotaxis is the ability of a cell to undergo directed locomotion along a chemical gradient. Chemotaxis was first described in leukocytes by Metchnikoff in 1893 [227]. Since then, chemotaxis has been extensively studied in a host of cell types including bacteria, *Dictyostelium*, fibroblasts and neurons. Interestingly, most *in vitro* models of chemotaxis show differences between modes of cell locomotion and signal transduction pathways. However, these models all share several general principles: (a) cells often exhibit intrinsic random motility; (b) exposure to a chemoattractant gradient leads to small spatial or temporal differences in receptor activation that are amplified within the cells to induce Rac-mediated actin polymerisation and protrusion towards the gradient source; (c) cell polarity is stabilised by positive-feedback loops combined with long-range inhibitory signals that restrict protrusion towards the cell front and increase its sensitivity to chemoattractants along the gradient [228].

### 1.3.2 Establishing a chemoattractant gradient

Factors that can influence gradient formation include size, polarity, diffusion rate, and reactivity of the chemoattractant and the nature of the surrounding environment. Chemoattractants may be produced in discrete spatial domains from where they diffuse and exert their graded effect over short or long distances [229]. Additionally, a stable gradient of immobilised chemoattractant is formed after diffusion, as observed for mouse chemokine CCL21, which is released by lymphatic vessels and attracts dendritic cells through a decay-mediated gradient of CCL21 bound to heparin sulphates [230].

Most *in vitro* models (and some *in vivo* models) assume that the chemotactic gradient encountered by cells is at steady state, static and spatially stable, and it is generally assumed that the gradient is created by diffusion of the chemoattractant from the source site towards the target cells. However, in the physiological milieu, gradients of chemoattractants might be a) non linear, with rapid decay of concentration as a function of distance from secreting source, b) sequestered by extracellular matrix, c) degraded, d) self generated and amplified, and e) modified by extracellular enzymes

[229]. These conditions may give rise to unstable, dynamic and discontinuous gradients.

Additionally, cells may encounter more than one chemoattractant with different diffusion rates and must therefore adapt to multiple cues. It has been proposed that secondary chemoattractants (e.g. IL-8) are secreted in sequential waves allowing recruitment of neutrophils far away from primary attractants [231]. Signal relay can also occur between cells. For example, $LTB_4$ is actively secreted by neutrophils as they migrate towards inflammation sites, therefore acting as a signal relay between neutrophils [232]. The release of secondary signals amplifies the chemotactic landscape of primary chemoattractants by relaying signals to neighbouring cells that are too far away to sense the primary signal.

Gradients of small highly diffusible molecules pose a potential problem because of their rapid diffusivity and inability to persist and reach far enough to convey spatial information to target cells. However, $H_2O_2$ has proved contradictory to this theory. $H_2O_2$ has been shown to extend ~100-200μm into injured zebrafish tail fin epithelium [233]. Other diffusible molecules include $H^+$ ions. A gradient of $H^+$ was identified between adenocarcinoma xenografts to blood vessels [234]. Reaction diffusion of chemoattractants by delimiting product concentration is one of the most widely used mechanisms to maintain gradients of highly diffusible molecules, as is the case for the degradation of $H_2O_2$ by extracellular dismutase. Gradients may also be maintained through the spatially graded production of chemoattractants by neighbouring cells. For example, the NADPH oxidase dual oxidase (Duox) produces $H_2O_2$ in a graded manner in tissues and is responsible for $H_2O_2$ generation at wound sites in zebrafish [233].

### 1.3.3 Gradient sensing and polarisation

The ability of a cell to sense an external gradient of chemotactic factors governs directed cell migration. Cells constantly monitor the chemical concentrations over time or through spatial sampling. Directional sensing does not require actin polymerisation and is mediated by recognition of chemoattractants by their cell surface receptors (usually GPCRs). Various theories exist that attempt to explain how receptor activation leads to formation of polarised protrusions. The ‘chemotactic compass’ model suggests that gradient sensing results in local asymmetric accumulation of intracellular signalling molecules, such as $PI(3,4,5)P_3$, towards the highest chemoattractant concentration. This localised signalling occurs upstream of Rac and is used as a compass to adjust the actual cell polarity by turning the cell front towards the gradient [235], [236]. An alternative model describes ‘chemotactic bias’. Here, chemoattractants simply bias the dynamic and self-organising autocatalytic nature of protrusions towards the gradient without the need for a compass [237]. This theory takes into account recent observations that membrane tension resulting from actin polymerisation acts as a long range physical signal that inhibits protrusion formation in regions other than the cell front [238].

Historically, it was understood that activation of a single pathway (PI3K) controlled chemotaxis. When activated by chemoattractant ligands, PI3K phosphorylated $PI(4,5)P_2$ into $PI(3,4,5)P_3$ at the leading edge of migrating cells, and this promoted

directional migration [239]. The asymmetric distribution of the PI3K product $PI(3,4,5)P_3$ at the front of the cell is a hallmark of cell polarisation in neutrophils and other amoeboid cells, and is illustrated in figure 1.7. It is now known that a hierarchy of intracellular signals exists and while intermediate chemoattractants can signal via the PI3K pathway, end-target chemoattractants can induce signals that involve the p38 MAPK pathway [189]. This is summarised in figure 1.8c. Heit *et al* (2002) demonstrated that when faced with opposing gradients of end target (e.g. fMLP) and intermediary (e.g. IL-8) chemoattractants, Akt (protein kinase B) activation was significantly reduced within neutrophils, and cells migrated preferentially toward end-target chemoattractants [189]. Furthermore, p38 MAPK inhibition reversed this hierarchy, and allowed neutrophils to be drawn out of a local end target chemoattractant gradient and towards an intermediary chemoattractant environment [189].

The main characteristic of front-rear polarity in cells migrating on 2D surfaces is the production of membrane protrusions in the form of broad lamellipodia and finger-like filopodia [209]. Lamellipodia have highly branched actin filaments, while filopodia contain long parallel bundles of actin filaments. *In vivo* imaging with actin probes has revealed that dynamic F-actin localises to the leading edge and stable F-actin predominantly localises to the tail of rapidly migrating zebrafish neutrophils *in vivo* [190].

The acquisition of polarity is controlled by small GTPases such as Cdc42, Rac and RhoA. Cdc42 is active towards the front of the cell and both activation and inhibition of Cdc42 can disrupt directional migration [203]. The main output of Cdc42 is local activation of Rac. As active Cdc42 and Rac are at the front of the cell, molecular feedback loops and mechanical tensile forces work together to maintain protrusions in the direction of migration [240]. Working together at the back of the migrating cell are Rho, myosin II and $Ca^{2+}$-activated proteases. Active Rac at the front of the cell suppresses Rho activity, but at the sides and back of the cell Rho is more active and suppresses Rac activity. RhoA affects actomyosin contractility via Rho kinase (ROCK) [241]. Furthermore, strong adhesions at the back of the cell increase tension, open stretch activated $Ca^{2+}$channels and promote subsequent activation of proteases that have the potential to cleave focal adhesion proteins [228]. To move forward, the cell retracts its trailing edge by combining actomyosin contractility and disassembly of adhesions at the rear. These processes are illustrated in figure 1.7.

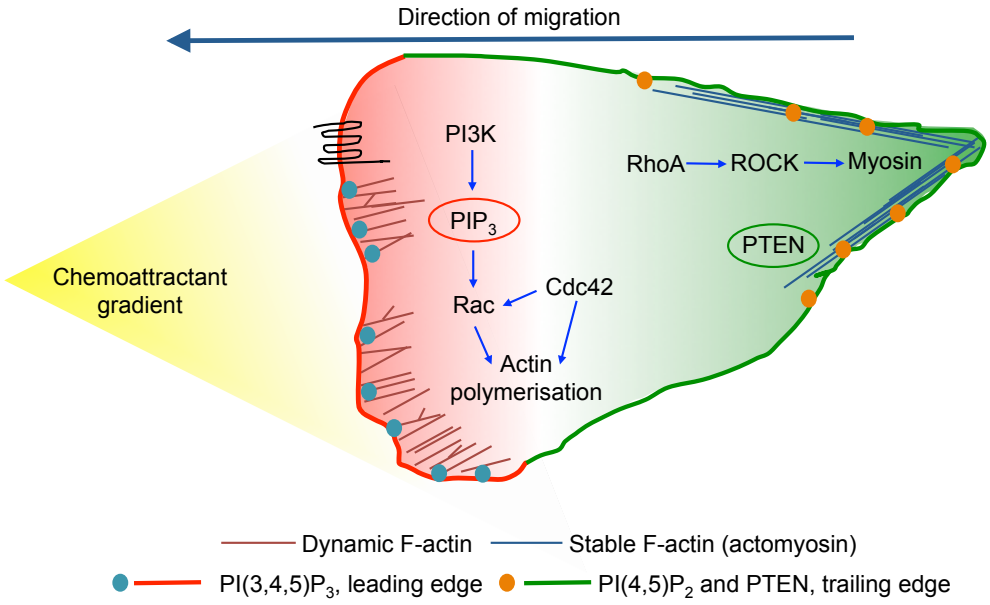


**Figure 1.7: Signalling pathways in leukocyte polarisation.** In the presence of a chemoattractant gradient, $PIP_3$ is enriched at the leading edge, leading to Rac and Cdc42 activation and subsequent actin polymerisation. This generates lamellipodia. At the back of the cell, phosphatase and tensin homologue (PTEN) prevents PI3K-mediated $PIP_3$ accumulation. Here, RhoA drives myosin contraction.

### 1.3.4 Locomotion

Several mechanisms of leukocyte locomotion have been identified. Leukocytes can use retrograde actin flow to migrate. Here, the leading edge pulls the cell forward by coupling the retrograde force of the actin cortex – through transmembrane receptors – to the extracellular environment [242]. Two mechanisms drive the retrograde force of the actin cytoskeleton. First, actin grows at the leading plasma membrane and filaments get pushed backward into the cell body where the actin network is disassembled in a process termed ‘treadmilling’ [243]. Next, myosin II – located behind the leading edge – pulls the cortex backward, supporting the polymerization driven retrograde movement [244].

Locomotion may also be driven by cell blebbing. Here the cell generates hydrostatic pressure by actomyosin contraction [245], which is dependent on myosin II motor activity that contracts the cortical actin network. Increased pressure and increased cortical tension are eventually freed, either by rupture of the actin cortex or by detachment of the cellular membrane from the underlying cortex. This membrane bleb can generate transient membrane protrusion. Leukocytes can also move entirely by deformation of the cell body, stimulated by deformatins that are generated by actin polymerisation [246].

In some models, integrins seem to have a role in locomotion. Neutrophils migrating through interstitium of mouse peritoneum or rat cremaster muscle have been shown to decelerate by 30% in the presence of antibodies against $\beta_1$ integrin [247]. However, in other models integrins seem to be indispensible. New evidence suggests that there exists plasticity of migratory modes, and cells are able to switch between adhesion-dependent and deformation based modes of migration very quickly [248]. This

phenomenon allows cells to efficiently migrate through diverse and changing environments.

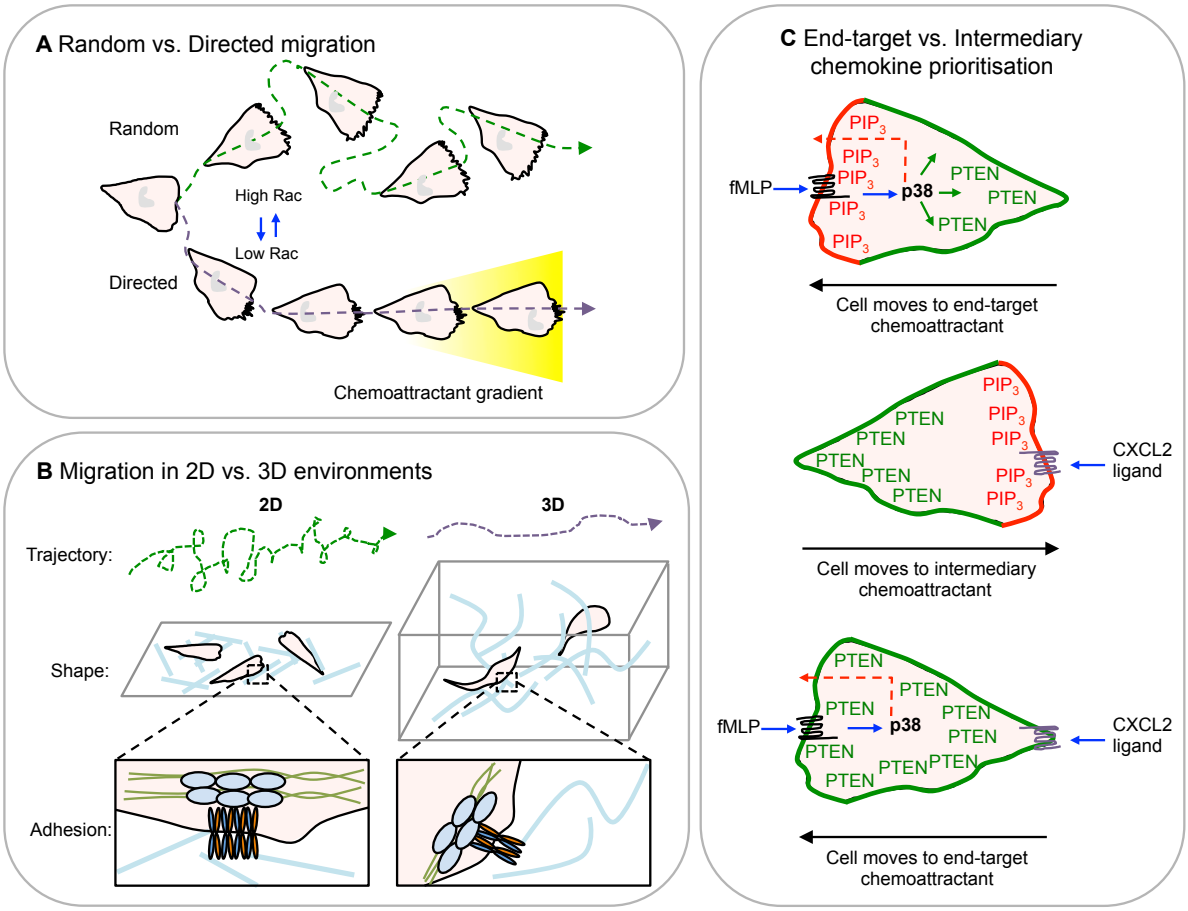


**Figure 1.8: Features of leukocyte migration and polarisation**. (A) Cells on 2D surfaces show intrinsic random migration driven by multiple cell protrusions. This behaviour can be transformed into directed migration via a single lamellipodial projection either by lowering total activated Rac levels, or by local activation of Rac by chemical and physical guidance cues, e.g. chemoattractant gradient. Figure adapted from Reig *et al* (2014) [228]. (B) Cell shape, adhesive structures and migratory behaviour is altered when cells are studied in 2D or 3D environments. In 3D matrices, cells become elongated and display more directional movement than those migrating on 2D surfaces. Fibroblasts on 2D develop prominent and stable focal adhesions with the ECM, however the formation of focal adhesions in 3D is still a matter of debate and can only be detected under particular conditions. Figure adapted from Reig *et al* (2014) [228]. (C) Proposed model of PTEN, PI3K and p38 MAPK function of neutrophil chemotaxis. When cells are placed in opposing gradients, PTEN antagonises any $PIP_3$ accumulation so all chemotaxis occurs through p38 MAPK. Figure adapted from Phillipson and Kubes (2011) [249].

### 1.3.5 Migration in the absence of chemoattractant gradients

Historically, our insight into cell migration has come from time-lapse studies of fibroblasts cultured *in vitro*. Fibroblasts quickly polarise when placed on 2-dimensional (2D) surfaces and migrate in a seemingly random, exploratory fashion. In this environment, they display high levels of activated Rac, which promotes the formation of multiple peripheral lamellae and subsequent random migration [250]. When neutrophils are migrating in the absence of a chemoattractant gradient, they extend pseudopods

that branch, and subsequently one pseudopod can become stabilised to determine the direction of migration [237]. Random motility is also a feature of embryonic cells during tissue morphogenesis and accounts for tissue patterning [251]. Figure 1.8a compares random and directed migration.

Additionally, crawling does not require a chemotactic gradient. *In vitro*, in the absence of gradient, neutrophils were shown to crawl in straight lines that were perpendicular to the shear forces applied and cells returned to a random pattern of migration when shear flow was terminated [18].

### 1.3.6 Physical and environmental influence on motility and chemotaxis

The environment in which a cell is studied can considerably influence phenotypes observed. Besides chemoattractants, guided cell locomotion *in vitro* can be manipulated by topographical features of a substrate, such as grooves, physical forces such as rigidity, and cell-cell contact [228]. Plasticity in migration strategies allows leukocytes to adapt to the geometry and molecular composition of their environment.

When comparing fibroblasts on 2D surfaces (e.g. petri dishes, glass coverslips) and 3-dimensional (3D) surfaces (e.g. gel matrix scaffolds, hanging drops), cells change their shape, adhesive structures and migratory behaviour [252]. Cells are generally more elongated and follow more directional paths when in 3D matrices. Fibroblasts on 2D surfaces develop prominent and stable focal adhesions that associate with stress fibres over the broad lamellipodial region [253]. The existence of such focal adhesions in 3D environments is still unclear. Interestingly, cells plated on soft 2D surfaces show irregular and unstable focal adhesions [254], whereas adhesions similar in structure to those found in 2D can be detected *in vivo* in cells submitted to high tensile forces [255]. These findings indicate that cell adhesion is sensitive to physical properties of substrates such as tension and stiffness. Integrin mediated adhesion is required for leukocyte migration on 2D surfaces *in vitro*. However, murine dendritic cells that have been depleted of all integrin receptors are able to migrate in interstitial tissues in 3D [256]. Figure 1.8b summarises the differences between migration in 2D versus 3D environments.

In addition to integrin signalling, the requirement for PI3K during neutrophil chemotaxis is context dependent *in vitro*. PI3Kγ is essential for murine neutrophil migration on fibrinogen-coated surfaces, but is dispensable for migration on glass [188]. Treatment of human neutrophils *in vitro* with PI3K inhibitors abolishes migration towards selected chemoattractants such as IL-8 and $LTB_4$, but not towards others including fMLP or C5a [189].

In some situations, leukocytes use retrograde flow based mechanisms to drive locomotion. Activated neutrophils adhere to 2D surfaces and form a sheet-like protrusion that is spread out and rich in actin. Movement here is dependent on force coupling by integrins; interference with integrins inhibits 2D migration [256]. However, this changes when leukocytes are embedded into 3D environments. In 3D environments, leukocytes do not adapt to the ECM fibres, but change shape by deforming the cell body, even in suspension [257]. Leukocytes in 3D environments do

not form leading edge protrusions that align with ECM fibres but rather form rounded or cylindrical extensions that protrude between fibres [258]. This suggests that leukocytes do not need to adhere to their substrates in order to migrate. *In vitro* and *in vivo* studies have shown that integrins are unnecessary for 3D leukocyte motility [259]. In this case, frictional forces are generated by alternative force-coupling receptors, such as sydecans and CD44. Taken together, most reports suggest that cells migrating in 2D surfaces appear to form exaggerated versions of adhesive structures found *in vivo*, whereas less rigid 3D matrices favour more discrete adhesions that seem to resemble those most *in vivo* migrating cells. These studies highlight the importance of developing appropriate *in vivo* systems to characterise cell migration in relevant physiological settings.

## 1.4 *In vivo* models of inflammation

Given the complexity of the human immune system and the difficulty of modelling a 3D intact structure to study injury and cell damage, scientists rely on animal models to provide relevant platforms for their research. Model organisms, including *Danio rerio* and *Drosophila melanogaster*, have been used for decades for the study of diverse biological and genetic processes. Despite having simplistic immune systems and being clearly distant on an evolutionary scale, they are advantageous over mammalian models due to their low cost, avoidance of ethical considerations and the possibility of high throughput experimentation. Recent technological advances especially in genetics have made these model organisms more accessible to a wider research community. Two important models used in the study of inflammation and wound repair are described in more detail below.

### 1.4.1 Zebrafish larvae tailfin wound model

Zebrafish, *Danio rerio*, have emerged as a powerful model system to explore many aspects of cellular and molecular biology, including the wound repair process and inflammation. Recently zebrafish studies from various groups have greatly increased our understanding of leukocyte migration mechanisms. Additionally, zebrafish are gaining popularity as a model system to study human disease and drug screening. Support for conservation of innate immune functions can be found in the recapitulation of human immunodeficiency phenotypes in zebrafish models of WAS and LAD-like syndrome [260].

Zebrafish are ideal for live imaging *in vivo* because their embryos develop externally and can be viewed and manipulated at all stages. Zebrafish are transparent during embryonic development and permit non-invasive observation of leukocyte behaviour and subcellular molecular events at a high resolution *in vivo* [261]. Transgenic zebrafish lines with fluorescently labelled neutrophils and macrophages have been developed in addition to reporter lines that label specific tissues including epithelium. This development has revolutionised our ability to study and track live events in real time.

The immune system of the zebrafish and mammals is highly conserved on both the cellular and molecular level [262]. Zebrafish develop immune cells such as

lymphocytes, mast cells, dendritic cells, neutrophils and macrophages, and they produce chemokines and cytokines including TNF and IFN. Zebrafish utilize conserved molecules that are involved in pattern recognition, such as TLRs, NODs and Myd88 [263]. The adaptive immune system does not appear until after the early larval period, so it is ideal to study innate immune system in isolation. Morpholino oligonucleotides (MOs) provide a powerful tool for globally suppressing gene expression. These are stable nucleic acid analogs that bind to pre-mRNA to prevent splicing or the initiation of translation [264].

Modeling tissue damage in zebrafish larvae can be achieved by cutting the embryonic tailfin. Using zebrafish lines that express transgenes that encode fluorescently labeled proteins and are driven by the myeloperoxidase promoter to primarily label neutrophils, a robust and rapid recruitment of neutrophils to the site of tissue injury is observed following tail transection [265]. More recently, it has been shown that leukocytes can be recruited directly from the caudal hematopoietic tissue to sites of tissue injury, thereby bypassing the extravasation process [266]. Neutrophils subsequently migrated between the wound and the vasculature and finally resolve the inflammatory response through reverse migration back to the vasculature [266]. Recently, a population of inflammatory macrophages has also been reported to migrate towards wound sites and phagocytose melanocyte debris and apoptotic neutrophils in the zebrafish model. These macrophages display slower but more directional migration to tissue wounds compared with neutrophils, and dwell more persistently at the wound margin before wound resolution [267]. Characteristics of the zebrafish larval wound model are depicted in figure 1.10.

### 1.4.2 *Drosophila melanogaster* embryonic wound model

Fruit flies, *Drosophila melanogaster*, are an established invertebrate model for scientific research. Well characterised throughout both developmental and adult life cycles, the genetic tractability of *Drosophila* has supported the discovery of many basic principles of heredity, gene mapping and behaviour. Recent advances in labelling and imaging techniques have allowed *Drosophila* to become a robust invertebrate tool for studying cell behaviour and gene expression. In the last decade *Drosophila* have become recognised as a worthy model to study the genetics of tissue repair and inflammation. Table 1.4 summarises the advantages and disadvantages of using *Drosophila* as a model organism.

| Advantages | Disadvantages |
|---|---|
| • Easy to culture<br>• High fecundity<br>• Low cost maintenance<br>• Non-pathogenic<br>• Well established knowledge base<br>• Elegant genetics and tools<br>• Short generation time<br>• Well annotated genomic databases<br>• Live imaging of embryonic events | • Stock keeping<br>• Inability to freeze<br>• Mites<br>• Virgining<br>• Lack of adaptive immune system<br>• Lack of embryonic vasculature<br>• Lack of embryonic fibrosis or scarring<br>• Lack of mammalian chemokine orthologues |

**Table 1.4: Advantages and disadvantages of *Drosophila melanogaster* as a model organism.** Fly stock keeping, virgining and general procedures are described in more detail in section 2.3.

*Drosophila* embryonic hemocytes are macrophage-like innate immune cells, and represent the main immune cell component of the innate response in the fly [268]. During embryonic development, hemocytes arise in the head mesoderm at developmental stage 10 and migrate along the ventral nerve cord before undergoing segmental, lateral migration (as illustrated in figure 1.9). At stage 15 hemocytes are arranged into three parallel lines extending along the full length of the embryo. During developmental migration, hemocytes are steered along gradients of growth factors PDGF/VEGF-like growth factor (PVF) 2 and 3 that are highly expressed in the developing nerve cord [269]. With actin rich protrusions and dynamic motility, the hemocyte's primary function is to patrol the embryo and phagocytose cellular debris or cell corpses [268].

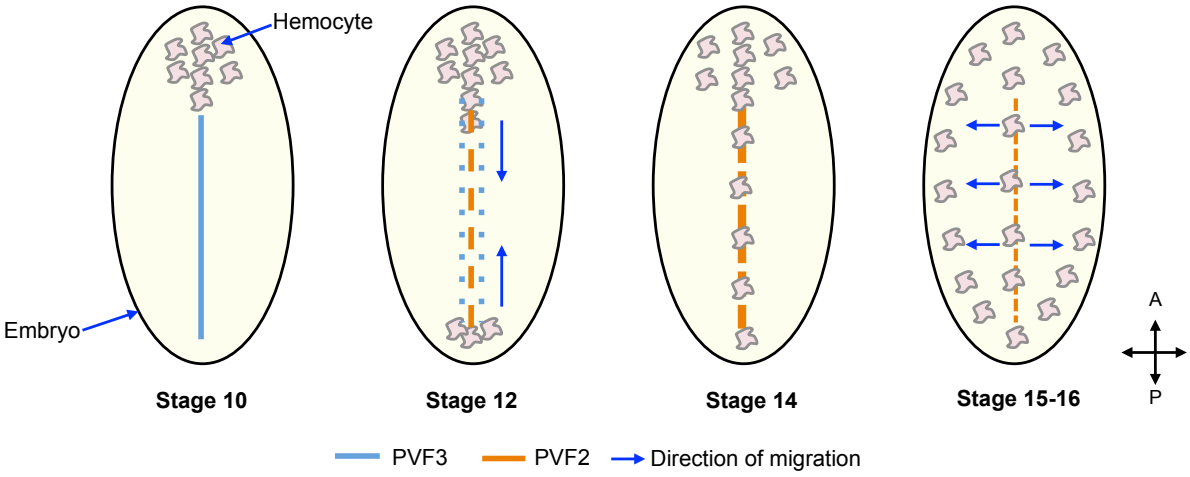


**Figure 1.9: Developmental hemocyte migration in *Drosophila*.** Hemocyte migration along the ventral nerve cord is directed by PVF signals. At stage 10, PVF3 is strongly expressed along the ventral midline. At stage 12, hemocytes migrate along the developing nerve cord from posterior and anterior ends, attracted by the expression of PVF3 and PVF2. These populations migrate until they form a continuous line along the ventral midline. At stage 14, PVF3 has disappeared and expression levels of PVF2 have increased. Hemocytes now rapidly migrate laterally leaving the midline and taking up three parallel lines extending along the whole length of the embryo. PVF= platelet-derived growth factor (PDGF) and vascular endothelial growth factor (VEGF)-related factor.

Following laser induced epidermal damage, hemocytes at late developmental stage 14 are rapidly recruited to the wound site. Hemocytes within close vicinity of the wound (20-30mm of a 40mm diameter wound) abandon their developmental migration position and migrate directly to the wound site [270]. This observation suggests that a local signal is generated at the wound site, and this damage signal can outcompete developmental migration signals. With this in mind, embryos at developmental stage 15 are typically used for wounding studies. Migration of hemocytes to wounds depends on PI3K [269], and also requires GTPases Rho, Rac and Cdc42 [271]. Moreira *et al* (2010) discovered that the wound attractant acts transiently; within two hours post wounding, hemocytes migrate back to the ventral midline away from the wound. Following recruitment to the wound, hemocytes engulf damaged epidermal cells and bacteria if present. Characteristics of the *Drosophila* embryonic wound model are illustrated in figure 1.10.

### 1.4.3 $H_2O_2$ is a wound cue in *in vivo* models of inflammation

The generation of ROS, specifically $H_2O_2$, at sites of tissue damage has been observed in phylogenetically diverse organisms, including plants, *Drosophila*, zebrafish and mammals [233], [270], [272]-[274]. Owing to their fast diffusion and versatile biological activities, ROS are interesting candidates for wound-to-leukocyte signalling. However, $H_2O_2$ is quickly degraded within cells so its effects are rapid and transient; a steep $H_2O_2$ gradient must be maintained for prolonged effects to occur.

The mechanism determining how $H_2O_2$ is generated is not well understood. Historically, most theories assumed $H_2O_2$ was released from ruptured cells after direct injury. New evidence has emerged to suggest ROS release is controlled by an immediate calcium signal triggered in the epithelium. Recent findings in the *Drosophila* hemocyte wound model showed that wounding of the embryo epidermis results in an immediate calcium wave [220]. Reducing the calcium signal with chelators impairs the inflammatory response of hemocyte migration to a wound site. The study proposed that calcium activates NADPH oxidase Duox through its EF hand to direct $H_2O_2$ generation and attract hemocytes to wounds. Another group found that tissue mediated-ATP release activated purinergic receptors that modulate Duox activity through intracellular calcium signalling *in vivo* [275]. This Duox-derived $H_2O_2$ was also able to trigger the NFκB inflammatory signalling pathway. This report suggested the ATP-mediated Duox activity was able to modulate the early recruitment of leukocytes to the wound.

The first studies investigating the action of wound-induced $H_2O_2$ were carried out in the zebrafish larvae tailfin wound model. Niethammer *et al* (2009) sought to investigate whether $H_2O_2$ could signal in a paracrine fashion. They first examined the role of $H_2O_2$ during the early events of wound responses in zebrafish larvae expressing a genetically encoded $H_2O_2$ sensor, HyPer [233]. HyPer is highly selective for $H_2O_2$ over other ROS [276]. Niethammer's study observed a sustained rise in $H_2O_2$ concentration at the wound edge, starting 3 minutes after wounding and peaking at 20 minutes, which extended 100–200mm into the tail-fin epithelium. They hypothesised that wound-induced extracellular $H_2O_2$ may reach concentrations of ~0.5-50μM near the wound margin. Importantly $H_2O_2$ was reported to be required for rapid recruitment of leukocytes to the wound because neutrophils appeared at the scene approximately 17 minutes after the initial injury. This recruitment was blocked in Duox-/- larvae, and following treatment with NADPH oxidase inhibitor diphenyleneiodonium (DPI). They conclude that the $H_2O_2$ gradient produced by Duox is required for rapid recruitment of leukocytes to a wound [233]. To explain their findings, Niethammer *et al* (2009) suggested that leukocytes could be expressing transmembrane receptors for $H_2O_2$. Alternatively, $H_2O_2$ may be directing migration by entering the cytoplasm and locally modifying intracellular mediators, such as redox-sensitive PTEN [277], considered to be an important regulator of chemotaxis. Leukocyte recruitment to a wound via a $H_2O_2$ gradient has also been observed in the *Drosophila* embryonic hemocyte wound model. Moreira *et al* (2010) discovered that *Drosophila* hemocyte migration to a wound was impaired when DPI was inserted into the wound site via a bead [270].

Many cellular and genetic responses occur in wounded tissue, including transcription of effector genes. Duox is required to activate wound reporters after epidermal wounding in *Drosophila* embryos [278]. Even injected $H_2O_2$ is sufficient to activate widespread

epidermal wound gene expression. This indicates the important of $H_2O_2$ not only in immune cell responses, but also in later epidermal repair.

The molecular mechanisms responsible for $H_2O_2$ clearance have subsequently been investigated. Pase *et al* (2012) found that neutrophil delivered myeloperoxidase dampens the $H_2O_2$ burst after tissue wounding in zebrafish [279]. Neutrophils are rich in myeloperoxidase, an enzyme catalysing an $H_2O_2$-consuming reaction. Pase *et al* showed that neutrophil depleted zebrafish have an abnormally sustained wound $H_2O_2$ burst, indicating that leukocytes themselves were required for $H_2O_2$ down regulation. Myeloperoxidase deficient zebrafish also had abnormally sustained high wound $H_2O_2$ concentrations despite similar numbers of arriving neutrophils [279].

As well as an increasingly more well defined role for $H_2O_2$ as a wound cue, studies in mammalian airway epithelium also suggest a regulatory role for enhanced $H_2O_2$ production in the host innate immune response to sensing bacterial triggers [280]. Enhanced production of $H_2O_2$ might be a universal mechanism used by the host to sense the disruption of tissue homeostasis by various insults and to activate the appropriate innate immune response. Subsequent studies have reported that $H_2O_2$ is not required for neutrophil recruitment to sites of bacterial infection, indicating neutrophils can be sensitised by different chemical cues [281]. $H_2O_2$ has also been identified as a key factor that mediates leukocyte attraction to transformed cells in zebrafish [274], implicating $H_2O_2$-mediated migration in cancer. Further studies are still necessary to confirm the physiological relevance of $H_2O_2$ mediated leukocyte attraction to wounds in mammals.

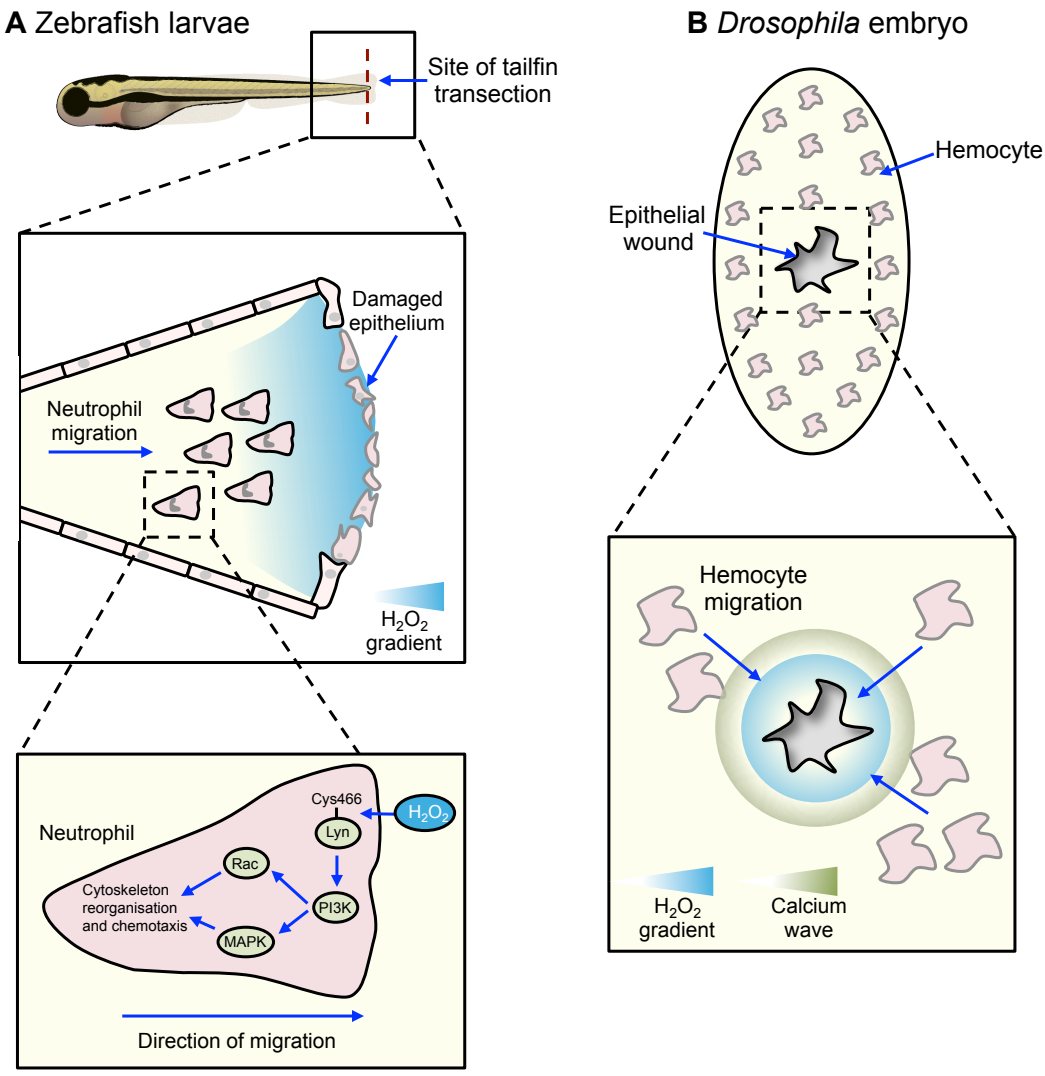


**Figure 1.10: Models of tissue damage *in vivo*.** (A) Transection of the zebrafish larval tailfin triggers the recruitment of neutrophils. Migration occurs along a gradient of damage cue $H_2O_2$. $H_2O_2$ oxidises intracellular neutrophil Lyn kinase and activates a signalling cascade leading to cytoskeleton rearrangement and migration. (B) Laser ablation of *Drosophila* embryo epithelium similarly drives the recruitment of embryonic hemocytes to the wound margin. Tissue damage triggers a rapid and transient calcium wave in cells proximal to the wound edge, followed by an $H_2O_2$ gradient that acts as a chemoattractant.

### 1.4.4 Lyn as a redox sensor

Researchers have been keen to uncover the mechanisms that function downstream of epithelial ROS production following tissue damage. Recently, Lyn, an SFK member, was identified as a neutrophil sensor that directly responds to $H_2O_2$ in injured tissues. Yoo *et al* (2011) used a zebrafish larvae wounding model to reveal that Lyn mediates initial neutrophil recruitment to wounds and Lyn activation was dependent on wound-derived $H_2O_2$ [282]. During this process, a single cysteine residue in Lyn, Cys466, appears to be the direct target of oxidation by $H_2O_2$. Mutation of Cys466 to alanine specifically abolishes $H_2O_2$-induced activation of Lyn. The direct physical implication of Cys466 oxidation on Lyn activation remains unclear. Oxidation may provoke a conformational change in the protein, or the formation of an intramolecular disulphide

bond that results in activation. Activation of Lyn leads to the activation of ERK signalling pathways, which are required for neutrophil wound attraction. Lyn can activate PI3K *in vitro* [283]. Therefore it is highly attractive to speculate that activation of Lyn by $H_2O_2$ can lead to asymmetric PI3K activation in leukocytes, which then drives cell polarisation and migration along a $H_2O_2$ gradient. Cys466 is highly conserved across species (e.g. in *Drosophila* Src42A and human Lyn). Therefore, oxidation-dependent activation may be a general mechanism for all SFK members. It has not yet been established whether *Drosophila* Src42A can also act as a redox sensor in injured tissues. However, elegant genetic studies have indicated that Src42A is transcriptionally activated around a wound site, and is sufficient to inhibit wound-induced transcription in epidermal cells [278].

### 1.4.5 $H_2O_2$ may promote phagocytosis via SFKs

Phagocytosis is a very important component of the inflammatory response. Defects in cell corpse clearance have been associated with autoimmune and inflammatory diseases [284]. An important driver of the phagocytic response in *Drosophila* is the engulfment receptor Draper, which recognizes cell corpses and guides the internal cellular machinery to promote phagocytosis. Various ligands for Draper have been proposed, including Pretaporter, an apoptotic cell ligand [285], and lipoteichoic acid, a bacterial cell ligand from *S. aureus* [286].

Ziegenfuss *et al* (2009) first proposed an association between Draper-dependent phagocytosis and the *Drosophila* SFK Src42A by studying the phagocytic activity of glial cells in adult fly brains [287]. Glial cells, the primary phagocyte in the brain, rapidly engulf neuronal cell corpses during development and during Wallerian degeneration in the adult brain. Wallerian degeneration occurs when axon injury destroys the parent cell body, and the proximal axon stump subsequently disintegrates [288]. Using a model of Wallerian degeneration in adult fly brains, Ziegenfuss *et al* revealed that ligand-dependent Draper activation initiates the Src42A-dependent phosphorylation of Draper, promoting glial phagocytic activity. Furthermore, Ziegenfuss *et al* also reported that following Src42A phosphorylation of Draper, *Drosophila* SH2 ankyrin repeat kinase (Shark), a non-receptor tyrosine kinase and homologue of mammalian Syk, binds to Draper via an intracellular immunoreceptor tyrosine-based activation motif (ITAM) [287]. Previously reported roles of Shark include embryonic dorsal closure [289], and maintenance of epithelial cell apicobasal polarity [290]. Shark activity at Draper is essential for downstream signalling events *in vivo*, including phagocytosis of axonal debris. Ziegenfuss *et al* concluded that both Shark and Src42A were crucial mediators in the activation of the Draper pathway.

This association between Src42A, a potential redox sensor, and Draper, an engulfment receptor, suggests that Draper may also have a part to play in hemocyte migration to a wound and hemocyte phagocytosis at a wound. Both processes require the same functional outputs of internal signalling – actin remodeling aimed at polarisation of the cell towards a gradient. Therefore it is likely that the signalling pathways are overlapping and conserved together.

## 1.5 Damage cues in mammalian systems

### 1.5.1 Reactive oxygen species

#### ROS production and regulation

ROS are considered to be not only the main mediator of pathological tissue injury but also important second messengers for a variety of cellular receptor signal transduction pathways. ROS are a heterogeneous group of molecules that include highly active free oxygen radicals (e.g. superoxide) and non-radical oxidants (e.g. $H_2O_2$). Given that superoxide is rapidly converted to $H_2O_2$ in the cell, $H_2O_2$ is often considered the principal ROS member. Following their generation, ROS can be further converted into other ROS species or they can be neutralised by enzymatic and non-enzymatic reactions inside and outside a cell [291]. Figure 1.11 illustrates ROS family members and their reactions.

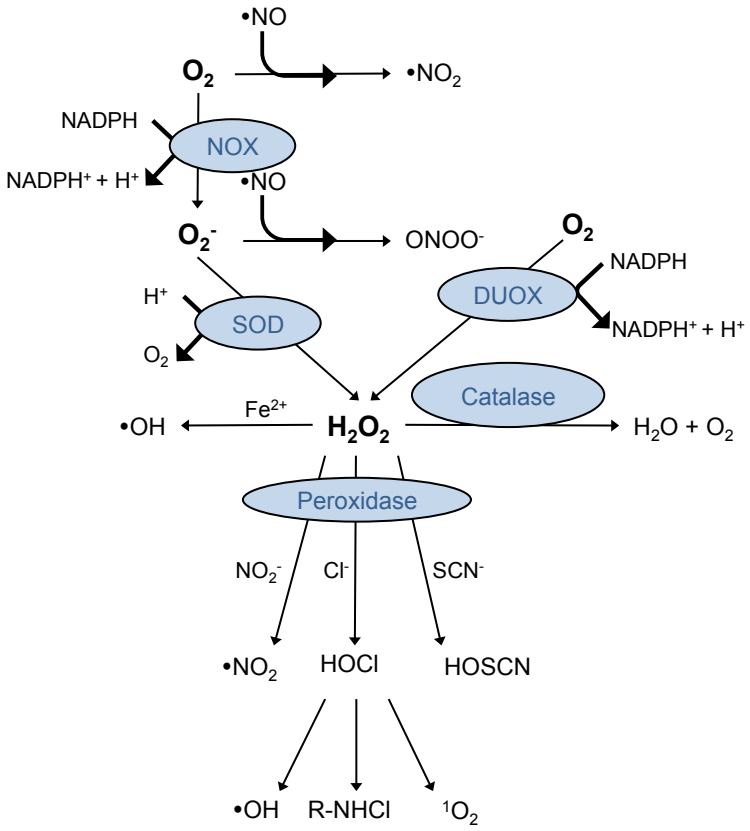


**Figure 1.11: Reactive oxygen species and their reactions.** HOCl, hypochlorous acid; HOSCN, hypothiocyanous acid; •NO, nitric oxide; $•NO_2$ nitrogen dioxide; $^1O_2$, singlet oxygen; •OH, hydroxyl radical; $ONOO^-$, peroxynitrite; R-NHCl, chloramines; DUOX, dual oxidase. Figure modified from Sareila *et al* (2011) [292].

A number of intracellular mediators, including cyclooxygenases, cytochrome P450, lipoxygenases, xanthine oxidase and NADPH oxidases regulate the enzymatic production of ROS. Mitochondrial respiration is also a major source of ROS [291]. Free radicals can arise through chemical processes including oxidation of phenols, aromatic amines and hydrazine by heme proteins. ROS can also be produced by ionising and UV radiation and from the metabolism of drugs. Some compounds undergo

autoxidation catalysed by transition metal ions. For example, metabolites of antimalarial drugs are oxidised by haemoglobin and can be accountable for drug toxicity [293].

The main source of extracellular ROS is likely to be NADPH oxidases. The NOX family of NADPH oxidases produces ROS as a result of electron transfer across membranes. The NOX family comprises NOX1-5 and DUOX1-2. NOX proteins are integral membrane proteins comprising six transmembrane domains that form a channel to allow successive transfer of electrons [292]. NADPH oxidases located in the plasma membrane generate ROS into the extracellular space. They can also be located on the membranes of intracellular vesicles and generate ROS in phagosomes. NOX can generate superoxide that can be dismutated into $H_2O_2$ by separate superoxide dismutase (SOD) enzymes; whereas Duox generates $H_2O_2$ without requiring a separate SOD [294].

ROS are highly reactive and interact with several biological molecules including proteins, lipids, carbohydrates and nucleic acids. Owing to this high reactivity, ROS in high concentrations or at specific locations are likely to promote cellular damage and tissue destruction. $H_2O_2$ can cause oxidative damage at high concentrations and initiate cell death [295]. One possible mechanism for this is that $H_2O_2$ causes DNA strand breaks, leading to the activation of nuclear poly(ADP-ribose) polymerase, which critically depletes the cell of NAD, leading to eventual cell death. Another hypothesis proposes that $H_2O_2$ disrupts the cell membrane integrity in a non-specific manner through lipid peroxidation. $H_2O_2$ formed from superoxide is converted by neutrophil myeloperoxidase or eosinophil peroxidase to more reactive oxidants such as hypochlorous and hypobromous acids [292].

ROS are rapidly produced and removed to avoid sustained signalling and oxidative damage. A complex assortment of antioxidant systems protects cells against ROS damage. These can be enzymatic (e.g. catalase, superoxide dismutase, and peroxiredoxin) or non-enzymatic (e.g. flavonoids, vitamin A, vitamin C) [296]. The activity of antioxidants is necessary to control fluctuations in cellular redox status and to avoid irreversible oxidation of cellular molecules leading to oxidative stress.

**ROS as signalling mediators**

ROS can have a wide array of different biological effects ranging from regulation of specific and fine tuned steps in cell signalling, to harmful nonspecific events such as lipid peroxidation. Damaging functions of ROS occur through uncontrolled excessive production, whereas ROS involved in signalling is tightly regulated and takes place in confined compartments. The known signalling roles of $H_2O_2$ in animals are primarily within the cytoplasm, where it regulates metabolism, phosphatase activity and gene transcription [297].

$H_2O_2$ is a small, diffusible molecule that can be synthesised and destroyed rapidly, making it a useful intracellular messenger [298], [299]. Many cellular responses to growth factors, hormones and inflammatory cytokines involve redox signalling and $H_2O_2$ is likely to be a second messenger acting here [300]. Various studies have

suggested that $H_2O_2$ fulfils the role of messenger by modulating the extent of protein phosphorylation on either serine-threonine or tyrosine residues [301], [302]. Exogenous $H_2O_2$ mimics growth factors by inducing protein tyrosine phosphorylation and MAPK activation [303]. Given the simple structure of $H_2O_2$, it is unlikely to be recognised specifically by a protein, and so it is likely that modulation of protein phosphorylation by $H_2O_2$ is mediated by reversible binding of $H_2O_2$ to protein kinases or phosphatases.

**Redox regulation of proteins**

Proteins are the main targets for ROS within the cell and account for approximately 69% of oxidation events mainly because of their abundance [304]. Oxidation of particular residues can influence the charge, size, hydrophobicity or polarity of amino acids in a polypeptide. This can affect the secondary and tertiary protein structure, which will dictate the stability and activity of the whole protein. Redox regulation of kinases for signalling purposes will impose a degree of structural re-configuration resulting in increased, altered or decreased enzyme activity [305]. Oxidation events that promote phosphorylation or dephosphorylation may increase or decrease the binding of substrates, as well as trigger dimerization or oligomerisation through disulfide bond formation. Additionally, it is possible that oxidative modifications may tag or cue a kinase for trafficking or sequestrations, thus indirectly affecting the activity of the kinase by removing it from the vicinity of its target and perhaps exposing it to novel binding partners [305].

Sulphur-containing cysteine and methionine are the most easily, and reversibly, oxidised amino acids [306]. Intracellular antioxidants can reverse or reduce this reaction [307]. Reversible cysteine modifications are the most physiologically relevant because hyper-oxidation occurs predominantly during conditions of oxidative stress, promoting enzyme inactivation and degradation [305]. A widely accepted hypothesis for how ROS modulate signalling pathways is that they reversibly inhibit protein tyrosine phosphatases (PTPs) through oxidation of redox-sensitive cysteine residues resulting in formation of intermediate sulphenic acid [308]. This is illustrated in figure 1.12. Most cysteine residues contain a sulfhydryl group with a pKa of ~8.5 which is not prone to oxidation by $H_2O_2$, unlike the cysteine thiolate anion. Some protein cysteine residues do exist as thiolate anions at neutral pH because their pKa is lowered by charge interactions between the negatively charged thiolate and nearby positively charged amino acids. One example of this type of low pKa protein is PTPs [300]. All PTPs contain an essential cysteine residue that exists as a thiolate anion at neutral pH [309]. The active site cysteine is the target of specific oxidation by oxidants including $H_2O_2$. This modification can be reversed by incubation with thiol compounds such as dithiothreitol and reduced glutathione [310]-[312]. Together, this suggests that PTPs might undergo $H_2O_2$-dependent inactivation in cells, creating a window of phosphorylation that is un-interrupted by phosphatase activity, resulting in a shift in the equilibrium with protein tyrosine kinases towards protein phosphorylation.

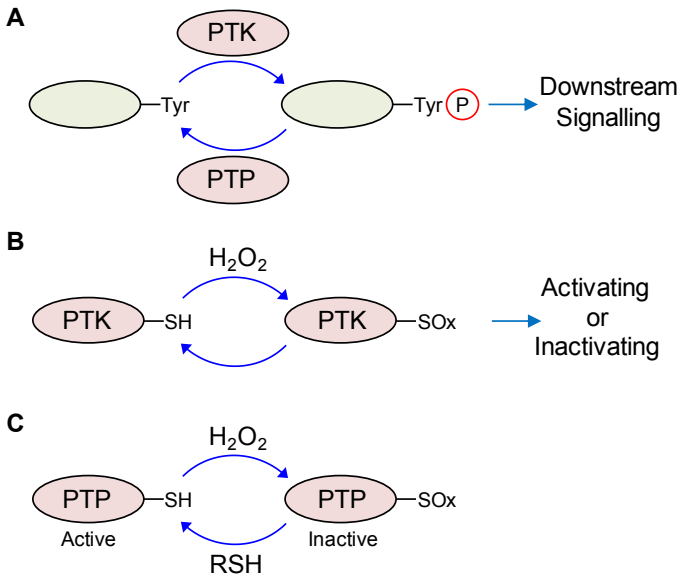


**Figure 1.12: Redox-dependent signal transduction.** (A) PTKs catalyse the transfer of phosphate groups from ATP to tyrosine hydroxyls of proteins. PTPs remove phosphate groups from phosphorylated Tyr residues. (B) PTKs can undergo oxidation/reduction at regulatory cysteines to modulate their function. (C) Oxidation of the active site cysteine residues in PTPs inactivates these enzymes, and can be reversed by reducing the oxidised residue back to its thiol form with RSH. PTP = protein tyrosine kinase; PTP = protein tyrosine phosphatase; RSH = reducing thiol; SOx = oxidised cysteine. Adapted from Truong *et al* (2013) [313].

The redox regulation of PTPs is an area that has been widely studied, however oxidation has also been implicated as a signalling device in the regulation of, amongst others, GTPases [314], and proteases [315]. Other kinases are also susceptible to redox-regulation, e.g. RTKs and Akt, which undergo direct oxidation [316]. cAMP-dependent protein kinase is also regulated by redox activity. The formation of intramolecular disulfide bonds in oxidised cAMP-dependent protein kinase de-stabilises the enzyme and allows de-phosphorylation of its activation loop, resulting in decreased activity [317]. Redox regulation of the MAPK/ERK pathway has been implicated both by oxidative inactivation of regulatory phosphatases and associations with antioxidants [318], [319]. More recently, direct redox regulation of ERK2, JNK2 and p38 has been proposed to occur at different concentrations of $H_2O_2$. It was reported that low concentrations of $H_2O_2$ oxidised ERK2 and caused a conformational change that increased binding to MEK1/2 and leads the system towards proliferation. If the concentration of $H_2O_2$ reaches very high levels, the cysteine residues in ERK2 become redox-insensitive, while JNK2 and p38 are activated and stimulate a cell-cycle arrest programme [320].

### $H_2O_2$ in innate immunology

ROS are a prominent feature of innate immunology in both health and disease. Generation of ROS by phagocytes is an essential process for host defence. Upon engulfment, phagocytes use intracellular ROS to destroy pathogens. ROS produced by phagocytes are often considered to damage surrounding cells as a result of ‘leakage’

during cellular processes [296]. In phagocytic leukocytes, ROS and $H_2O_2$ are produced through NADPH oxidase mechanisms following activation of many cell surface receptors. Ligand stimulated receptors also provoke a $H_2O_2$ response in non-phagocytic cells. Ligands that do this include PDGF, epidermal growth factor (EGF), fibroblast growth factor (FGF), insulin, GM-CSF, cytokines, IL-1, IL-3, IFNγ, TNFα, and agonists of GPCRs [321]. $H_2O_2$ release is triggered from cells stimulated by TNFα when they are plated on serum coated biological surfaces [17]. Several types of NADPH oxidase have been identified in non-phagocytic cells that have been shown to be responsible for receptor stimulated derived $H_2O_2$ production. Activated PI3K has been shown to be necessary for PDGF induced production of $H_2O_2$ [322].

$H_2O_2$ has been reported to affect various processes associated with inflammation. It can increase phagocytosis in human neutrophils [323]. $H_2O_2$ increases ICAM-1 expression and increased neutrophil adhesion to endothelial cells [324]. Experiments studying the directed locomotion of mouse peritoneal neutrophils show that at low micromolar concentrations $H_2O_2$ induces neutrophil chemotaxis [325]. This has been supported by studies showing human neutrophil chemotaxis to gradients of $H_2O_2$ *in vitro* [282]. Furthermore, overexpression of thioredoxin, a ROS decomposing protein thiol, suppresses leukocyte recruitment induced by MCP-1 [326]. Aquaporins (AQP) are a family of highly conserved transmembrane channels that transport water and small solutes. Recently, several AQPs, including AQP3 and AQP8, have been found to mediate membrane $H_2O_2$ uptake, which is used for intracellular signalling in mammalian cells [327]. T cell chemotaxis is dependent on AQP3-mediated $H_2O_2$ uptake [327]. This $H_2O_2$ transport is essential for activation of Cdc42 and subsequent actin rearrangements driving cell migration [328].

**Redox regulation of SFKs**

Cysteine residues in Src are necessary for the enzyme's stability and transformative ability. Consistent with other examples of protein oxidation by ROS, Cys245 and Cys487 undergo intramolecular disulfide bridge linkage upon exposure to ROS, leading to Src activation. Oxidation of Src has been proposed to be crucial for a final 'super-activation' state being achieved. This concept demonstrates that direct redox activation of Src is important in many systems [329]**.** In a disease environment where higher levels of ROS may be present, dysregulated Src activity could be contributing to pathogenesis. For example, in cancer, redox-regulated activation of Src could be an additional avenue for pro-tumorigenic activity (alongside oncogenic activation of Src through constitutive phosphorylation or overexpression).

The first SFK proposed to be redox regulated was lymphocyte-specific Lck [305]. It wasn't until later studies that detail of the oxidation-induced modifications to Lck by ROS was revealed, by examining the phosphotyrosine (pY) profile of T cells following oxidative stress. Lck was phosphorylated at its autophosphorylation site after exposure to an oxidant, and its activity was increased [330]. This study also showed that exposure of Lck to oxidant prompted the association of Lck with PI3K and implies that a conformational change to the enzyme occurs. Despite the presence of a number of cysteine residues in Lck, it is not yet established whether Lck is directly redox-activated. More recently, Lyn in zebrafish was found to go undergo oxidation at Cys466

upon exposure to extracellular $H_2O_2$ [282]. This resulted in the autophosphorylation and activation of the kinase and selective stimulation of its downstream pathways, and was directly linked to driving the directional migration of neutrophils towards a wound.

### The effect of $H_2O_2$ in calcium mobilisation

Recent reports have associated Duox activity and $H_2O_2$ release with calcium signalling. Duox possesses two canonical calcium-binding EF hands on an intracellular loop, which implicates cytosolic calcium as a potential regulator of $H_2O_2$ production [331]. Duox has been shown to act in concert with SFKs and calcium to drive epithelial aspects of the regenerative processes in zebrafish larvae [219]. There is good correlation between oxidative stress, induction of ROS, and an increase in intracellular calcium levels immediately preceding the final destructive events of cell death [224]. There are various theories as to how $H_2O_2$ mediates an increase in calcium, including: a) influx through voltage gated calcium channels, b) non specific changes in membrane permeability, c) alteration of $Ca^{2+}$-$Na^{2+}$ exchange, d) changes in calcium release from intracellular stores.

Exogenous $H_2O_2$ can induce calcium mobilisation and signalling. Across a range of different cell types, $H_2O_2$-induced increase in intracellular calcium has been attributed to either mobilisation from intracellular stores [332], calcium influx across the plasma membrane [333], or both [334]. $H_2O_2$ causes a biphasic rise in intracellular calcium level in insulin-secreting cell line CRI-G1 [335]. These results indicated that the $H_2O_2$-induced early increase in intracellular calcium level results predominantly from mobilisation of calcium from intracellular stores and that the second, late increase in intracellular calcium levels is a result of extracellular calcium influx. Similarly, in rat parotid gland, $H_2O_2$ alone evokes a gradual and concentration dependent increase in intracellular calcium [336]. $H_2O_2$-evoked calcium release from intracellular stores may also be due to inhibition of SERCA [337]. Other studies have shown that extremely high concentrations of $H_2O_2$ (≥1mM) can cause severe oxidative stress in most cells, with the release of calcium from the mitochondrial and non-mitochondrial stores [338].

### ROS in disease

Excessive and uncontrolled production of ROS leads to oxidative modification of cellular and molecular components in host tissues and has been identified in many different pathological settings. Excessive production of ROS has been causally related in the aetiology of inflammatory diseases, ageing and chronic degenerative diseases such as Parkinson's disease, Huntington's disease and Alzheimer's disease [339]. The involvement of ROS and oxidation products is often suggested to be important for the progression of rheumatoid arthritis [340], as well as multiple sclerosis, type I diabetes and thyroiditis [341]-[343]. In light of new evidence placing $H_2O_2$ as an immune cell chemoattractant, excessive production could be a factor in diseases often marked by the elevation of white blood cell levels, e.g. in asthma, chronic obstructive pulmonary disease (COPD) and IBD. In asthma, the lung epithelia might be producing too much $H_2O_2$ because it is chronically irritated, which could explain inappropriate levels of white blood cells [344]. Cancerous cells have also been frequently associated with

overproduction of ROS, possibly due to elevated expression and activity of NOX enzymes downstream of constitutively active growth factor receptors. Elevated ROS production (oxidative stress) promotes genomic instability, and augments favourable growth mutations and chemoresistance [345]. Antioxidants including vitamin C, vitamin E and melatonin are often suggested to decrease inflammatory responses, however *in vivo* studies of antioxidants do not consistently support this [346].

Despite its known role in oxidative stress and cellular damage, topical $H_2O_2$ has been used for generations to sterilise wounds and promote faster healing [347]. Evidence to suggest that ROS can have a more regulatory role in particular disease settings has recently surfaced. Hyper-inflammatory responses in mice lacking functional NOX2 have been found in models of helicobacter gastritis [348], inflammation induced by UV [349], and lung inflammation induced by cigarette smoke [350]. These indicate a new picture of ROS being involved in the regulation and limitation of inflammatory responses. Further evidence for a regulatory role of ROS is seen in patients with chronic granulomatous disease (CGD). CGD patients have a genetic deficiency in the phagocyte NADPH oxidase NOX2 [351]. Phagocytes are unable to kill bacteria and fungi that they have ingested. The role of ROS as a pro-inflammatory mediator is questioned in CGD patients where a lack of ROS, in addition to recurrent bacterial and fungal infections, leads to aseptic inflammation. There is increasing evidence for hyper-inflammatory, non-infectious complications in CGD, suggesting a role for ROS in dampening inflammatory responses. CGD patients suffer from increased frequency of bacterial infections and are more prone to developing other inflammatory diseases, such as granulomas and colitis [352].

**Tools for ROS detection**

The development of methods for the detection of redox-modifications has been essential to the recent advances in the field of redox biology. This has included the development of fluorescent and affinity-labelled probes for the detection and isolation of cysteine residue modifications and the detection and quantification of PTP oxidation. Of note is the synthesis of DYn-2, a new chemo-selective probe for detecting sulphenated proteins in human cells [353], and the ox-PTP antibody, which can recognise sulfonic acid containing PTPs [354].

Accurate localisation and quantification of $H_2O_2$ have previously been huge hurdles for researchers. The most common method of imaging biological ROS is through the use of fluorescent redox-sensitive dyes such as 2',7'-dichlorofluorescein diacetate (DCFDA) or similar dyes MitoSox Red and Amplex Red. Disadvantages of these tools include uncertainties about specificity, cell uptake and subcellular diffusion [355]. Additionally, fluorescent probes such as hydrogen peroxide sensor (HyPer) incorporate redox-sensitive cysteines, becoming fluorescent in the presence of particular ROS. HyPer is a genetically encoded ratiometric sensor that is highly selective for $H_2O_2$ over other ROS [276]. HyPer consists of the bacterial $H_2O_2$-sensitive transcription factor OxyR fused to a circularly permutated yellow fluorescent protein (YFP). Cysteine oxidation of the OxyR part induces a conformational change that increases emission excited at 500nm and decreases emission excited at 420nmm. This change is rapidly reversible within the reducing cytoplasmic environment, allowing dynamic monitoring of intracellular

$H_2O_2$ concentration. HyPer can be introduced into an organism by messenger RNA injection to induce global cytoplasmic expression [233]. These redox sensitive probes have high sensitivity and specificity, signal reversibility and easy modification to allow tissue specific expression [356]. The development of transgenic animals expressing redox-sensitive proteins has provided invaluable *in vivo* models to study ROS [233].

### 1.5.2 Nucleotides as damage signals

Many other endogenous molecules can regulate the function of leukocytes and thereby modulate immune responses (e.g. following tissue damage). Intracellular localised substances can be released into the extracellular space and can therefore be a sign of tissue damage. For such molecules to be considered chemotaxins during an inflammatory event, they must be recognised by cells of the immune system that can migrate. Nucleotides are one example of molecules can that fulfil this role.

#### Adenosine 5'triphosphate

Adenosine 5'triphosphate (ATP) is a naturally occurring nucleotide present in every living cell. ATP is often referred to as the molecular unit of currency in intracellular energy transfer for cell metabolism and can also function as an extracellular mediator [357]. ATP is produced by oxidation of glucose to carbon dioxide in a process known as cellular respiration. It is an unstable molecule with short half life, and is easily hydrolysed into adenosine diphosphate (ADP) and phosphate by the action of ubiquitous ecto-ATPases and ecto-nucleotidases [358]. ATP typically accumulates in lysosomes in the intracellular compartment, resulting in an intracellular concentration of 1-10mM [359]. In the extracellular compartment, ATP contributes to the regulation of many processes, including cardiac function, neurotransmission, vasodilation and bone metabolism. Many reports suggest extracellular nucleotides such as ATP may function as endogenous signalling molecules that control inflammation and immune responses, and are therefore targets for anti-inflammatory and anti-tumour therapy [358].

ATP, ADP or adenosine are recognised by a large family of membrane bound purinergic receptors. P1 purinergic receptors are activated by adenosine and P2 receptors are activated by ATP and other nucleotides (e.g. UTP). P2 receptors are further subdivided based on their signalling properties, and are described in table 1.5. Metabotropic P2Y receptors are G-protein coupled and ionotropic P2X receptors are nucleotide-gated ion channels and respond primarily to ATP [360]. Purinergic receptors are expressed on immune and non-immune cells. Receptor density may change during inflammatory conditions by the action of immunomediators. ATP can act in a feed forward loop possibly amplifying responses to it or other external cues which couple to ATP secretion, as described in epithelial cells [361]. Given its short half-life and high reactivity, ATP is likely to operate only transiently in the local microenvironment in an autocrine or paracrine manner.

| | P2Y | P2X |
|---|---|---|
| **Subtypes** | $P2Y_1$, $P2Y_2$, $P2Y_4$, $P2Y_6$, $P2Y_{11}$, $P2Y_{12}$, $P2Y_{13}$, $P2Y_{14}$ | $P2X_{1-7}$ |
| **Receptor Type** | GPCR | Ion channel |
| **Signalling pathway** | ↑$IP_3$, ↑$Ca^{2+}$, ↑DAG ↓cAMP | $Ca^{2+}$ >> $Na^+$ > $K^+$ Membrane depolarisation $Ca^{2+}$-sensitive signalling |
| **Functional effect in immune cells** | Chemotaxis | Cytokine production |
| **Agonists** | ATP, ADP, UTP | ATP |
| **Antagonists** | Suramin, PPADS | |
| **Immune cell expression** | Neutrophils, monocytes, macrophages, dendritic cells, T cells, B cells, natural killer cells | |

**Table 1.5: Features of P2 receptors.** PPADS = Pyridoxalphosphate-6-azophenyl-2',4'-disulfonic acid

### ATP in innate cells and inflammation

All immune and inflammatory cells express P2 receptors on the plasma membrane which are coupled to an array of different functional outputs such as chemotaxis, generation of nitric oxide or superoxide anion, secretion of lysosomal constituents, release of cytokines, cell differentiation, cytotoxicity and intracellular $Ca^{2+}$ mobilisation [362]. Macrophage and monocyte P2R expression depends on maturation stage and state of activation. A lack of functional $P2X_7$ has been found in monocytes, however the receptor appears during maturation of monocytes to macrophages [363]. Human monocytes secrete ATP in a constitutive manner, leading to activation of cell surface P2 receptors which elevate intracellular $Ca^{2+}$ levels [364]. This ATP 'halo' appears to be important in regulating intracellular $Ca^{2+}$ homeostasis following P2Y receptor activation.

There exists overwhelming evidence to suggest that ATP and their purinergic receptors play a major role in immunity and inflammation. Following cell activation or direct injury, the extracellular ATP concentration is increased massively, especially in the pericellular space [365]. Mechanisms of extracellular ATP release are illustrated in figure 1.13. ATP can be released in an uncontrolled fashion, e.g. in necrosis, or in a more controlled manner through regulated transport. ATP can be released via transmembrane channels such as pannexins in apoptotic cells [366], and connexins [367]. Therefore, nucleotides can generate concentration gradients in tissues that can serve as chemotactic signals for different immune cells, causing migration. ATP breakdown may be delayed during early inflammatory processes due to the down-regulation of hydrolyzing enzymes by pro-inflammatory cytokines (e.g. TNFα) [368]. This results in the accumulation of extracellular ATP at inflammatory sites.

ATP acts as a pro-inflammatory mediator and constitutes a danger signal which triggers several pro-inflammatory effector functions of neutrophils, including the production of ROS and cytokines such as IL-1α, IL-1β, IL-6, IL-18 and TNFα [369]. Additionally, danger signals such as uric acid, complement factor C5a, TLR ligands and IL-8 are stimulated by an autocrine ATP-$P2Y_2$R loop to modulate migration and cytokine production of neutrophils or eosinophils [368]. ATP function in early

inflammation is most likely to involve the $P2X_7$ receptor, whose activation causes production of cytokines by residing immune cells. $P2X_7$ receptors in monocytes and macrophages are down regulated by anti-inflammatory mediators IL-4 and IL-10, whereas they are upregulated by pro-inflammatory regulators TNFα, IFNγ and LPS [357]. Dying tumour cells release ATP, which activates $P2X_7$Rs on dendritic cells, leading to priming of IFNγ-producing CD8+ T cells that kill cancer cells. But, $P2X_7$R signalling and subsequent T cell priming to different T cell lineages can also lead to allergy, graft versus host disease and IBD [368]. Interestingly, ATP at low milimolar concentrations has been shown to upregulate E-selectin through $P2X_7$ receptor mediated activation of NFκB [370]. Furthermore, reports suggests that extracellular ADP may increase surface expression of Mac-1 integrin on monocytes [371]. These findings propose a role for ATP in modulating the adhesive mechanisms behind leukocyte recruitment to sites of inflammation.

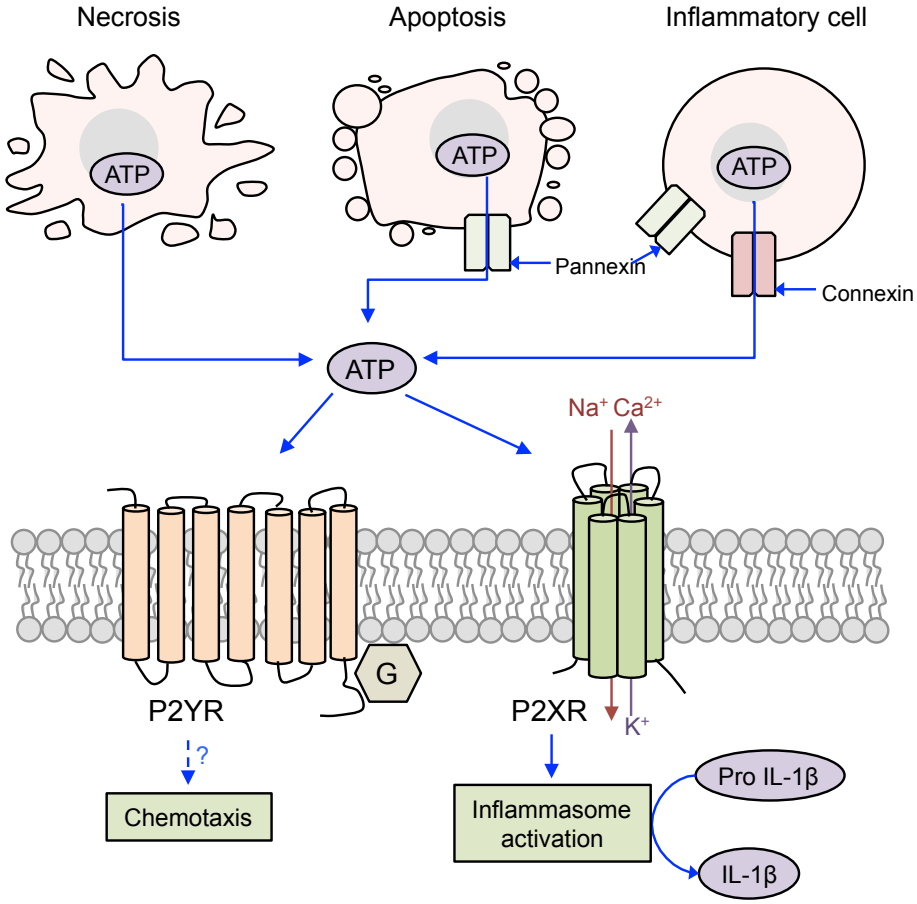


**Figure 1.13: Extracellular ATP release and signalling during inflammation.** During inflammation, multiple cell types release ATP from their intracellular compartments into the extracellular space. ATP can be released by necrotic cells, apoptosing cells, or activated inflammatory cells. ATP signals via the activation of P2 receptors: metabotropic G-protein coupled P2YRs and ATP-gated ionotropic P2XRs. P2XRs bind to ATP in the milimolar range, and this induces ion transport and influx of extracellular $Ca^{2+}$ leading to inflammasome assembly and activation and cytokine production. Figure adapted from Idzko *et al* (2014) [368].

The effects of extracellular ATP on neutrophil function during inflammation are ambiguous. At micromolar ATP concentrations, neutrophil chemotaxis and chemokinesis has been shown either to be unaffected [372], inhibited [373], or promoted via stimulation of $P2Y_2$ receptors [374]. Neutrophils are capable of releasing ATP from their leading edge to amplify chemotactic signals and direct cell orientation by feedback signalling involving $P2Y_2R$ [375]. Thus, effector functions may be subject to autocrine and paracrine control by endogenous ATP. Additionally, promyeloid precursor HL60 cells respond to ATP by increasing intracellular $Ca^{2+}$ concentration via a pertussis toxin-sensitive G-protein receptor that couples to the inositol phospholipid signalling system, suggesting involvement of P2Y subtypes [376]. ATP can also stimulate production of CXCL8 by eosinophils [377]. ATP stimulation of chemokine release by cells near sites of tissue damage may contribute to neutrophil recruitment towards these sites. Upon arriving at inflamed sites where ATP levels are the highest, neutrophil recruitment may be no longer affected, or even inhibited by ATP, allowing the neutrophils to exert their bactericidal functions.

**Targeting nucleotides for therapy**

Current therapeutic targets of nucleotides in inflammation and immune disease include agonist stimulated ATP release or purinergic receptor signalling. A wide array of different compound types is presently under investigation for targeting nucleotides during inflammation. Efforts have been made to develop highly selective antagonists of ATP-gated P2XRs. The $P2X_7R$ antagonist AZ9056 was tested in patients with RA, and initial studies were promising. However, phase IIb/III trials with different $P2X_7R$ antagonists failed to improve long-term clinical outcome [378]. There are on-going clinical trials with $P2X_7R$ and $P2X_3R$ antagonists in chronic pain and chronic cough [368]. Statins have both cholesterol lowering and anti-inflammatory functions. Interestingly, fluvastatin was shown to suppress native and recombinant human $P2X_4R$ function in monocytes through cholesterol depletion [379]. Suramin is a parasiticide and is also a non-specific inhibitor of P2YR and P2XR [380]. Suramin is commonly used as a pharmacological tool in the study of nucleotide biology. Only two types of P2YR specific compounds have been tested clinically: antithrombotic $P2Y_{12}R$ antagonists (e.g. clopidrogel) and $P2Y_2R$ agonist denufosol, which was examined for the treatment of cystic fibrosis but eventually failed in clinical trials [381]. The search for better therapeutics aimed at targeting nucleotides in inflammation will need to be more selective and specific, or involve specific combinations of antagonists to directly target known receptor subtypes.

### 1.6 Project aims and objectives

Inflammatory responses to tissue damage are highly coordinated and rely on efficient communication between cell types. Studies in model organisms have revealed that leukocytes are recruited to sites of tissue damage along gradients of soluble damage cues, including $H_2O_2$. In zebrafish, $H_2O_2$ can activate directed neutrophil migration to a wound via oxidation of the SFK, Lyn. The aims of this thesis are designed to examine how these processes transfer into other models:

1. **To study the role of SFK signalling in hemocyte migration to a wound using a *Drosophila* embryonic wound model.** We hypothesise that SFKs containing the conserved Cys466 residue will be necessary for hemocyte directed migration to a wound, indicating conservation between zebrafish and *Drosophila*. The objectives to explore this are to:
    - Measure the recruitment of hemocytes to a wound site in *Drosophila* embryos and compare responses between wild type embryos and embryos lacking functional SFKs.
    - Analyse parameters of migratory responses, e.g. cell velocity and directionality, and compare responses between wild type embryos and embryos lacking functional SFKs.
    - Compare motility of SFK-mutant hemocytes in the presence and absence of a wound, to determine if the $H_2O_2$ gradient is necessary for SFK activity.
    - Identify markers of kinase activity in embryos at wound site and distal to the wound.

2. **To investigate the effect of damage-associated signals on human innate cell function *in vitro*.** We hypothesise that $H_2O_2$ and ATP will act as chemoattractants *in vitro*, and activate immune cells in a fashion comparable to that induced by known chemoattractants. This aim is accompanied by the following objectives:
    - Identify whether $H_2O_2$ and/or ATP act as chemoattractants *in vitro* models of cell migration using human neutrophils and monocytes.
    - Analyse the effect of damage signals on ligand-mediated cellular responses, including chemotaxis, polarisation, phagocytosis, and ROS generation, in neutrophils and monocytes *in vitro*.
    - Interpret the responses of damage signals on intracellular signalling and receptor expression in monocytes and neutrophils *in vitro*.
    - Measure the effect of $H_2O_2$ on signal prioritisation in neutrophils placed in opposing gradients of chemoattractants using an *in vitro* model of cell migration.

3. **To examine the contribution of SFK and PI3K signalling in human innate cell function *in vitro*.** We hypothesise that SFK and PI3K signalling are essential for monocyte and neutrophil cell function *in vitro*. We will address this aim with the following objectives:
    - Analyse the contribution of SFKs and Syk in models of monocyte and neutrophil chemotaxis and polarisation *in vitro* using pharmacological inhibitors of SFK and Syk kinase signalling components.
    - Use pan-isoform and isoform-selective PI3K pharmacological inhibitors to identify the contribution of PI3K isoforms to models of monocyte and neutrophil chemotaxis and polarisation *in vitro*.
    - Dissect the signalling properties of SFKs in response to $H_2O_2$.

# CHAPTER 2: METHODS AND MATERIALS

## 2.1 Reagents and materials

A full reagents and materials list containing product names, product numbers and supplier information can be found in table 2.5.1.

## 2.2 Methods and materials for *in vitro* experiments with human cells

### 2.2.1 Cell culture and isolation

#### Cell lines

Human THP-1 (monocytic) [382] and U937 (monocytic) [383] cell lines were maintained in RPMI 1640 cell culture medium supplemented with 10% fetal bovine serum (FBS), 2mM L-glutamine, 100U/ml penicillin and 100µg/ml streptomycin. Human EA.hy926 (endothelial) cells [384] were maintained in DMEM:F12 cell culture medium supplemented with 10% fetal bovine serum (FBS), 2mM L-glutamine, 100U/ml penicillin and 100µg/ml streptomycin. All cells were grown in a 37°C 95% air/5% $CO_2$ incubator. Suspension cells were passaged every 2-3 days, maintained at a confluence of 0.1-1x$10^6$ cells/ml and discarded after 3 months. Adherent cells that had reached 80% confluence were trypsinised with 0.25% Trypsin-EDTA and passaged at a subculture ratio of 1:6. Cell stocks were stored in liquid nitrogen at density of 1x$10^6$ cells/ml in cryopreservation media (complete medium + 5% DMSO v/v) until required.

#### Differentiation of THP-1 monocytes

THP-1 monocytes were differentiated as previously described [385]. Briefly, cells were cultured at density of 0.5x$10^6$ cells/ml in complete medium supplemented with 80nM PMA for 48 hours. Cells that had adhered to the culture flask were washed in complete media and cultured for a further 3-5 days in PMA free media to mature. The differentiation process was verified as described in section 4.11.

#### Isolation of primary human neutrophils

Neutrophil isolation was performed as originally described by Böyum (1968) [386] with several modifications. Peripheral heparinised whole blood from healthy human volunteers was mixed 1:1 with RPMI 1640, layered over Lymphoprep™ density gradient medium and centrifuged at 300 g for 30 minutes at room temperature to separate differential layers of cell populations. Plasma, mononuclear cells and Lymphoprep™ layers were discarded using a Pasteur pipette, and remaining granulocyte and red blood cell layers were resuspended in ice cold $Ca^{2+}$-$Mg^{2+}$-free HBSS and 6% dextran ($M_r$ ~100,000) at 1:5 (dextran:HBSS). Sedimentation was allowed to occur at room temperature for 30-45 minutes, after which the top layer was removed and centrifuged at 300 g for 5 minutes. Pellets were resuspended in red blood cell lysis buffer (15.5mM $NH_4Cl$, 1mM $KHCO_3$, 0.01mM EDTA, pH 7.4) and rocked gently for 5 minutes before centrifugation at 300 g for 5 minutes. Supernatant containing lysed red blood cells was discarded, and remaining granulocyte pellet was resuspended in cold $Ca^{2+}$-$Mg^{2+}$-free HBSS before use. Figure 2.1 illustrates the key steps in neutrophil isolation. This procedure yielded a cell viability of at least 95% by trypan blue stain exclusion. A neutrophil population was confirmed by morphology

using Wright-Giemsa (as described in section 2.2.4) and DAPI staining to show lobed nuclei. Neutrophils were used on the day of isolation, unless otherwise stated, and discarded thereafter.

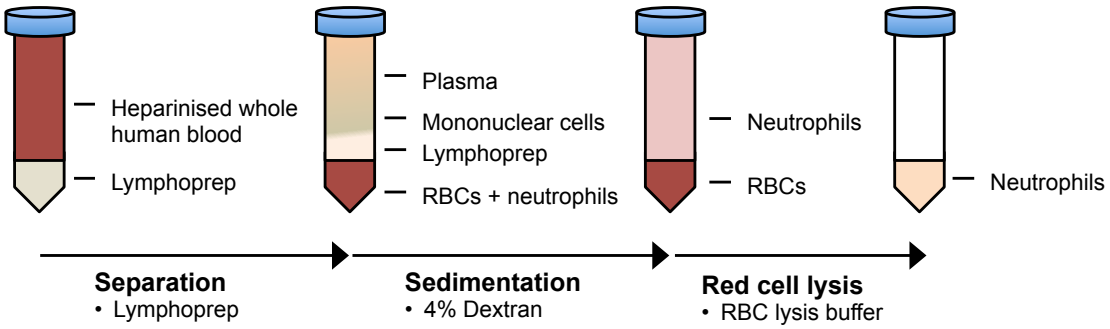


**Figure 2.1: Primary human neutrophil isolation from peripheral blood.** Blood is mixed with RPMI and layered over Lymphoprep. Differential centrifugation yields separate layers of blood cell populations. Neutrophils are present in a band above the red blood cell (RBC) pellet. Plasma, mononuclear cells and remaining Lymphoprep are discarded and neutrophil/RBC layers resuspended in HBSS with 4% dextran. Sedimentation of RBCs occurs whilst tubes are allowed to stand at room temperature for 30 minutes. Finally, RBC pellet is discarded and remaining cells are rocked with RBC lysis buffer for 5 minutes, resulting in a purified neutrophil population.

### 2.2.2 MTT cell viability assay

(4,5-dimethylthiazol-2-yl)-2,5-diphenyly tetrazolium bromide (MTT) can be used to assess the viability of cells. One inside a metabolically active, viable cell, MTT is converted to formazan by mitochondrial succinic dehydrogenase. Formazan can be dissolved by DMSO and releases an intense colour, which is proportional to cell viability and can be measured using a plate reader.

Cells plated in a 96 well flat-bottomed plate were stimulated as described. Non-adhesive cells were centrifuged in the plate at 500 g for 10 minutes, media removed and replaced with 100µl MTT media (1ml MTT (50mg/ml), 1ml FBS, 8ml plain RPMI 1640). Plates were incubated at 37°C for 3-4 hours after which 100µl DMSO was added to each well. Absorbance was read using a FluoStar Optima plate reader at 540nm wavelength.

### 2.2.3 Fluorescent labelling

#### Calcein AM

Calcein AM is a cell permeant dye that is used to determine cell viability and label cells. In live cells the non-fluorescent calcein AM is converted to a green-fluorescent calcein after acetoxymethylester hydrolysis by intracellular esterases. Fluorescence can be recorded using plate reader, flow cytometry or confocal microscopy.

Cells were loaded with 10μM calcein-AM in DMSO for 30 minutes at 37°C before being washed in plain media twice. Fluorescence was read using flow cytometry on a FACSAria with excitation/emission at 495/515nm, using FACSDiva software.

**CFSE**

Carboxyfluorescein succinimidyl ester (CFSE) is a cell tracing reagent that is used to label cells for lineage and proliferation studies [387]. CFSE readily diffuses into healthy viable cells and covalently binds to intracellular amines, resulting in a stable, well-retained fluorescent signal. Excess unconjugated reagent passively diffuses out of the cells and can be quenched and washed away.

Cells were loaded with 10μM Cell Trace$^{TM}$ CFSE in DMSO for 10 minutes at 37°C before being quenched with 5 volumes ice-cold plain media. Cells were incubated on ice for 5 minutes and then washed three times in plain media before use. Fluorescence was read using flow cytometry on a FACSAria with excitation/emission at 495/515nm, using FACSDiva software.

### 2.2.4 Wright-Giemsa staining

Wright-Giemsa stain is a histological Romanowsky stain that is used to perform differential cell counts and may also be used to facilitate diagnosis of diseases [388]. The stain contains components including eosin Y, which stains cytoplasm of cells pink/orange, and methylene blue and azure B, which stain nuclei varying shades of blue to purple.

Whole blood, or blood containing only red cells and granulocytes was pipetted onto a clean microscope slide and a film smear created using a second slide. The slide was allowed to air dry and then submerged in methanol for 5 minutes to fix the cells. Slides were removed from methanol, allowed to air dry, and submerged in Wright-Giemsa stain for 5 minutes. After staining the slide was placed under running $H_2O$ for 2-3 minutes. Slides were imaged immediately using a Zeiss LSM confocal microscope with a 40x oil objective.

### 2.2.5 Measurement of intracellular ROS generation

$H_2$DCFDA (2'-7'dichlorofluorescein diacetate) is used as an indicator of ROS in cells [389]. CM-$H_2$DCFDA passively diffuses into cells, where its acetate groups are cleaved by intracellular esterases and its thiol-reactive chloromethyl (CM) group reacts with intracellular glutathione and other thiols. Subsequent oxidation yields a fluorescent adduct that is trapped inside the cell and can be detected using a plate reader.

Cells were washed twice in plain RPMI 1640, loaded with 10μM CM-$H_2$DCFDA and incubated at 37°C for 30 minutes. Following incubation, cells were washed twice in PBS and density adjusted to $1x10^6$ cells/ml. Cells were plated into black flat bottomed 96 well plates at 100μl per well and allowed to rest at 37°C for at least 30 minutes. Cells were treated with compound or vehicle as described in figure legends.

Immediately after treatment fluorescence was read using a FluoStar Optima plate reader at excitation/emission 490/515nm.

### 2.2.6 Measurement of intracellular calcium

Fluo-4 is a cell permeant, labelled calcium indicator that exhibits an increase in fluorescence upon binding to calcium [390]. Fluo-4, AM (acetoxymethylester) is the ester derivative of the indicator that readily loads into cells because it is an uncharged molecule that can permeate cell membranes. Once inside the cell, the lipophilic blocking groups are cleaved by non-specific esterases, resulting in a charged form that is unable to breach the cell membrane. Changes in free intracellular ion concentration can be measured using a plate reader.

Cells were washed twice in plain RPMI 1640 and loaded with 10μM Fluo-4,AM dissolved in DMSO and incubated at 37°C for 45 minutes. Following incubation, cells were washed twice in $Ca^{2+}$-free HBSS and density adjusted to $1x10^6$ cells/ml. Extracellular calcium concentration was adjusted to 1mM using $CaCl_2$ solution. Cells were plated into black flat bottomed 96 well plates at 100μl per well and allowed to rest at 37°C for at least 30 minutes. The plate was loaded into FluoStar Optima plate reader and fluorescence read at excitation/emission 490/515nm over time at 37°C. Fluorescence at each well was read every 15 seconds. For compound additions, recording was temporarily paused, compounds were manually pipetted into appropriate wells and recording restarted.

### 2.2.7 Cell surface receptor expression

For experiments examining surface receptor expression of CCR2, CD14 or ICAM-1, cells were washed twice in plain RPMI 1640, density adjusted to $1x10^6$ cells per sample, and treated as described in figure legends. Following treatment, cells were washed once in 300μl ice cold PBS and resuspended in ice-cold FACS buffer (5% BSA in PBS). Samples were incubated on ice on a rocker for 20 minutes before being pelleted and resuspended in 50μl PBS containing Alexa-Fluor 488- or phycoerythrin-conjugated primary antibody, or corresponding conjugated IgG control antibody. Samples were incubated at room temperature on a rocker for 30 minutes before being washed twice in ice cold PBS. Finally, the samples were resuspended in 500μl PBS and transferred to FACS tubes for flow cytometry on a FACSAria using FACSDiva software. Live cells were gated using forward and side scatter and mean fluorescence recorded per 10,000 cells.

### 2.2.8 Immunofluorescence

#### Sample preparation

Cells were washed twice in plain RPMI 1640, density adjusted to $1x10^6$ cells/ml and seeded onto coverslips coated with 10μg/ml fibronectin and allowed to adhere for 30 minutes. Cells were treated as indicated in figure legends. After treatment, media was

removed and cells were fixed in 4% paraformaldehyde for 20 minutes at room temperature, and then permeabilised with 0.01% triton-X 100 for 20 minutes on ice.

**Immunofluorescence staining**

Following permeablisation, samples were blocked with 2% BSA in PBS for 30 minutes and then incubated with primary antibody diluted in 2% BSA in PBS for 1 hour at room temperature, or overnight at 4°C. Following incubation, samples were washed in 2% BSA in PBS and then incubated with secondary antibody for 2 hours. Samples were then washed again and finally incubated in a 1µg/ml solution of 4',6-diamidino-2-pheylindole (DAPI) for 20 minutes to label the cell nuclei. Where indicated, cellular F-actin was labelled by incubating the samples for a further 20 minutes with 1µM Alexa-Fluor 488 Phalloidin dye for 30 minutes at room temperature. Excess DAPI or Alexa-Fluor 488 was removed, samples washed in PBS and mounted with Mowiol mounting medium onto microscope slides. Samples were air dried overnight and stored at 4°C until imaging. Fluorescent images were acquired using a Zeiss LSM 510 confocal microscope using a 40x oil objective, unless otherwise indicated.

### 2.2.9 Time lapse confocal microscopy

**Sample preparation**

Cells were seeded at density of 0.5-1x$10^6$ cells/ml onto chambered coverglasses coated in 10µg/ml fibronectin and allowed to adhere for 30 minutes at 37°C. Coverglasses chambers were transferred to Zeiss LSM 510 confocal microscope with an external incubator heated to give air and stage temperature of 37°C. Coverglass chambers were allowed to equilibrate for at least 10 minutes before imaging began. Cells were imaged using a 40x oil objective, unless otherwise indicated. Time-lapse images were acquired using the brightfield channel. For live cell stimulations, recording was temporarily paused and compounds were pipetted manually into the chamber before recording recommenced.

Time lapse movies corresponding to relevant figures are provided on a separate CD as .avi files. Movies legends are provided in Appendix 1.

Images were analysed using ImageJ software as described below.

### 2.2.10 Image analysis

Image analysis using ImageJ

Image J is a public domain Java image processing program [391]. Images recorded on Zeiss LSM 510 confocal microscope were opened as LSM files in ImageJ (version 1.47b) using the LSM reader plugin. Background fluorescence was removed using the 'despeckle' ImageJ function. For single slices with multiple channels, channels were overlayed using 'merge channels' tool. Images were saved as .tif files.

For time lapse migration recordings, the paths of individual cells were manually tracked using the 'manual tracking' plugin and data was analysed using the 'chemotaxis tool' plugin to calculate parameters such as cell velocity and directionality. For each time point, the center of the cell body tracked was manually highlighted, and through its coordinates mean velocity and directionality were calculated. The directionality of a migrating cell is calculated by comparing Euclidian and accumulated distance. It is a measure of directness of cell trajectories. A directionality of 1 means a straight-line migration from start to endpoint. For time lapse recordings, brightfield single channel images were saved as .avi files.

Image analysis using CellProfiler

CellProfiler is free open-source software designed to enable quantitative measurement of phenotypes from multiple images automatically [392]. Using CellProfiler version 2.1.0, single slice images for analysis were split into pairs of separate channels – one for actin (phalloidin) staining and one for nucleic (DAPI) staining. Image pairs were uploaded and the following analysis pipeline applied: Identify primary objects; Identify secondary objects; Measure object size shape; Export to spreadsheet.

'Identify primary object' module uses nucleic (DAPI) input image to identify nuclei of each cell in the image, restricted to diameter of 10-40 pixel units to remove outliers, groups of cells or overlapping cells. 'Identify secondary object' module uses actin (phalloidin) input image and nuclei (DAPI) input object to identify cells and pairs nuclei and actin from each individual cell. 'Measure object size shape' runs quantitative measurement of phenotypes, including 'form factor' and 'area'. Figure 2.2 provides representative images of CellProfiler software.

All quantitative measurements are exported to an Excel spreadsheet, and from this 'form factor' measurements from every individual cell analysed can be obtained. 'Form factor' is a measurement of cell roundedness, given by the equation: $4*\pi*Area/Perimeter^2$. A perfectly round cell is given a score of 1, and as the cell elongates and becomes more irregular, the score tends to 0.

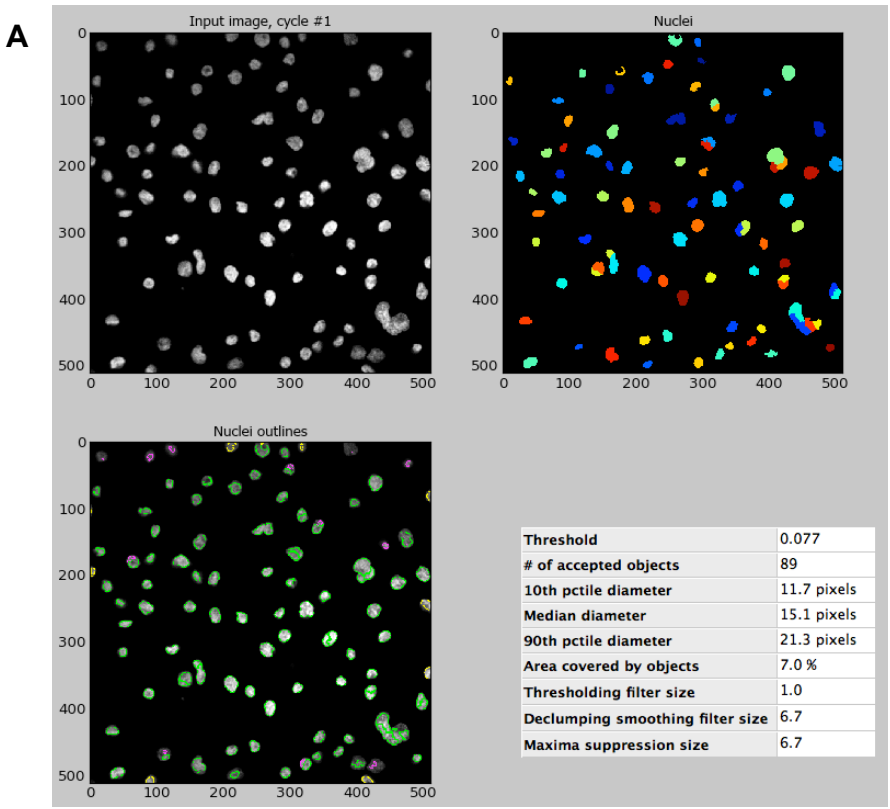


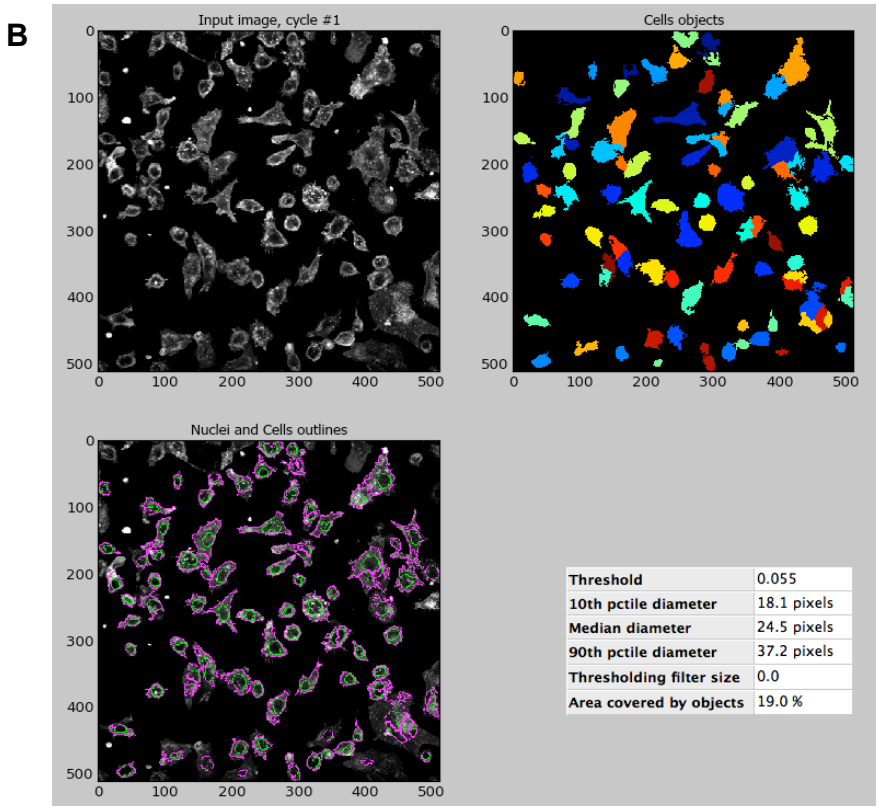


**Figure 2.2: Identifying individual cell phenotypes using CellProfiler software.** Fluorescent images of THP-1 monocyte nuclei (DAPI) (A) and actin (phalloidin) (B) were uploaded into CellProfiler for analysis. (A) Using DAPI signal, the 'identify primary objects' module identifies and outlines the nuclei of all cells (bottom left panel) from the fluorescent image and generates a mask (right panel). (B) The paired phalloidin image is also analysed with 'identify secondary object' module outlining the cell based on the nuclei identified earlier (bottom left panel). From these identifiers, the software generates measurements of cell characteristics spanning shape and size. Images displayed are representative output windows from analysis with one sample image.

### 2.2.11 Migration assays

#### Neuroprobe ChemoTx® migration assay

Cells were washed and resuspended in chemotaxis medium (FBS- and phenol red-free RMPI 1640) at $3.2x10^6$ cells/ml and rested for 1 hour. Chemoattractants were diluted in chemotaxis medium and 29µl placed in the lower wells of a 96-well ChemoTx® chemotaxis plate (Neuroprobe) (Fig 2.3). Polyvinyl-free polycarbonate membranes with 5µm pores were placed over the chemoattractants to separate lower and upper wells of the plate. 25µl cell suspension was placed on top of the filter over each well. After incubation at 37°C for 3 hours in humidified air with 5% $CO_2$, the cell suspension was removed from the top of the membrane with blotting paper. The plate was placed in a centrifuge at spun at 300 g for 10 minutes to collect cells that had migrated into the lower wells. Cells were removed from each well, transferred to 300µl PBS and counted using flow cytometry on FACSAria using FACSDiva software. Viable cells were gated using forward and side scatter. Each tube was counted for 30 seconds on high flow rate. Results are expressed as chemotactic index, i.e. the ratio of migration between stimulated and unstimulated cells. All wells were run in triplicate.

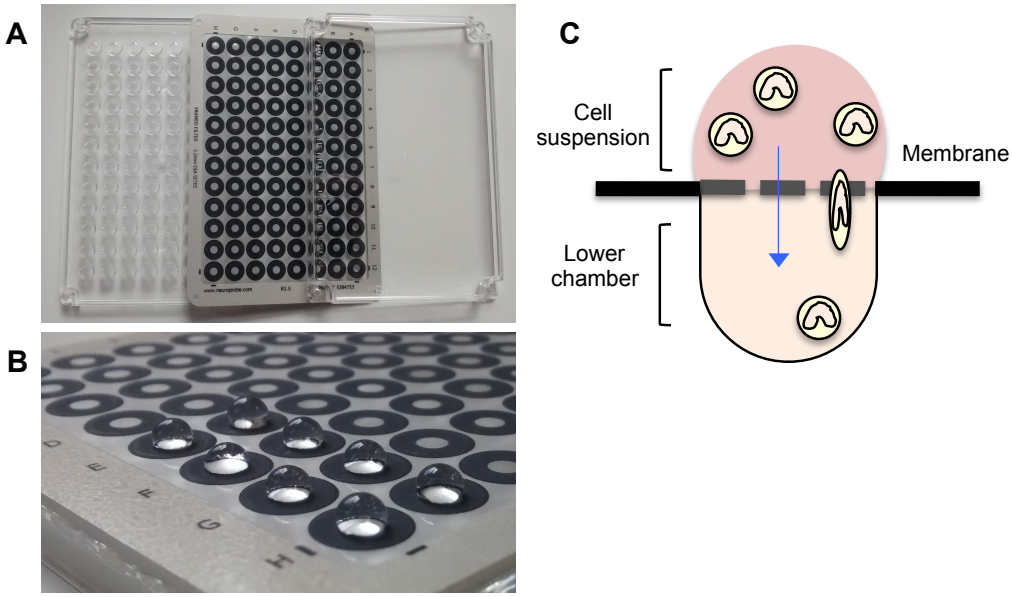


**Figure 2.3: Apparatus for Neuroprobe ChemoTx transwell assay.** (A) Neuroprobe 96 well ChemoTx plate showing (l-r) lower chamber base, filter membrane and lid. (B) Representative photograph showing droplet of cell suspension surrounded by hydrophobic ring on the surface of the filter membrane. (C) Schematic of a single well of Neuroprobe 96 well ChemoTx plate. A droplet of cell suspension is pipetted on the surface of the membrane, with chemoattractant placed in the lower chamber. Cells migrate through the membrane towards the chemoattractant and are retained in the bottom chamber. Migrated cells can be collected and counted.

**Under-agarose cell migration assay**

The under-agarose cell migration assay was prepared as described by Heit and Kubes [393] with a few modifications. Key stages are illustrated in figure 2.4.

Casting the gels

0.48g ultrapure agarose was dissolved in 10ml $H_2O$ and boiled until all agarose had dissolved. This was mixed with a pre-warmed mixture of 10ml HBSS and 20ml RPMI+20% FBS to give a 1.2% agarose solution. 3ml agarose solution was carefully pipetted into each well of a 6 well tissue culture plate, covered and allowed to solidify slowly at room temperature. Slow cooling is vital here to allow serum proteins to coat the bottom of the tissue culture plate.

Once gels were solidified, wells were punched using a hole punch. A hole punch was created using 3 identical plastic tubes each with diameter 3.5mm, configured in a straight line with a 2.2mm equal spacing between tubes. Tubes were mounted on a wooden holder to create a robust, reusable hole punch. Agarose was cleared from the holes using a sterile Pasteur pipette attached to an aspirator to suck the agar from the wells. Gels were equilibrated at 37°C for 1 hour in humidified air with 5% $CO_2$. Following equilibration, any condensation formed in the wells was removed using an aspirator. Gels were inspected for uniform thickness, coloration and lack of bubbles, particles or fissures.

Loading and running the gels

Primary human neutrophils were isolated from peripheral human blood as described above. Cells were resuspended in $Ca^{2+}$/$Mg^{2+}$-free HBSS at a density of $1x10^6$ cells/ml and rested at 37°C for at least 30 minutes. Cells were treated with inhibitors or stimulants for 30 minutes prior to being loaded in the gels, unless otherwise stated.

Gels were first loaded with 10µl chemoattractant or HBSS control per well, followed by 10µl cells per well, equating to $1x10^4$ cells/well. For all experiments, cells were placed in the central well and chemoattractant was placed in either one or two of the outer wells, depending on whether the actions of opposing chemoattractant gradients were being studied. Gels were incubated at 37°C for 2 hours in humidified air with 5% $CO_2$. Once incubation was complete, gels were placed in a refrigerator for 20-30 minutes to ease analysis by increasing contrast between cells and agar.

Analysing the gels

Gels were photographed using a Canon EOS 110D camera mounted on an Olympus CKX41 light microscope with a 4x objective. For each tissue culture plate well, the space between inner and outer wells was photographed. Images were viewed using ImageJ software. On each image, a rectangle with dimensions equating to 5mmx2mm was superimposed over the image to denote the target zone for cell counting. Cells that had migrated were counted in this target zone alone, and compared to the number of cells that had migrated in the other direction using the same rectangle template for target zone.

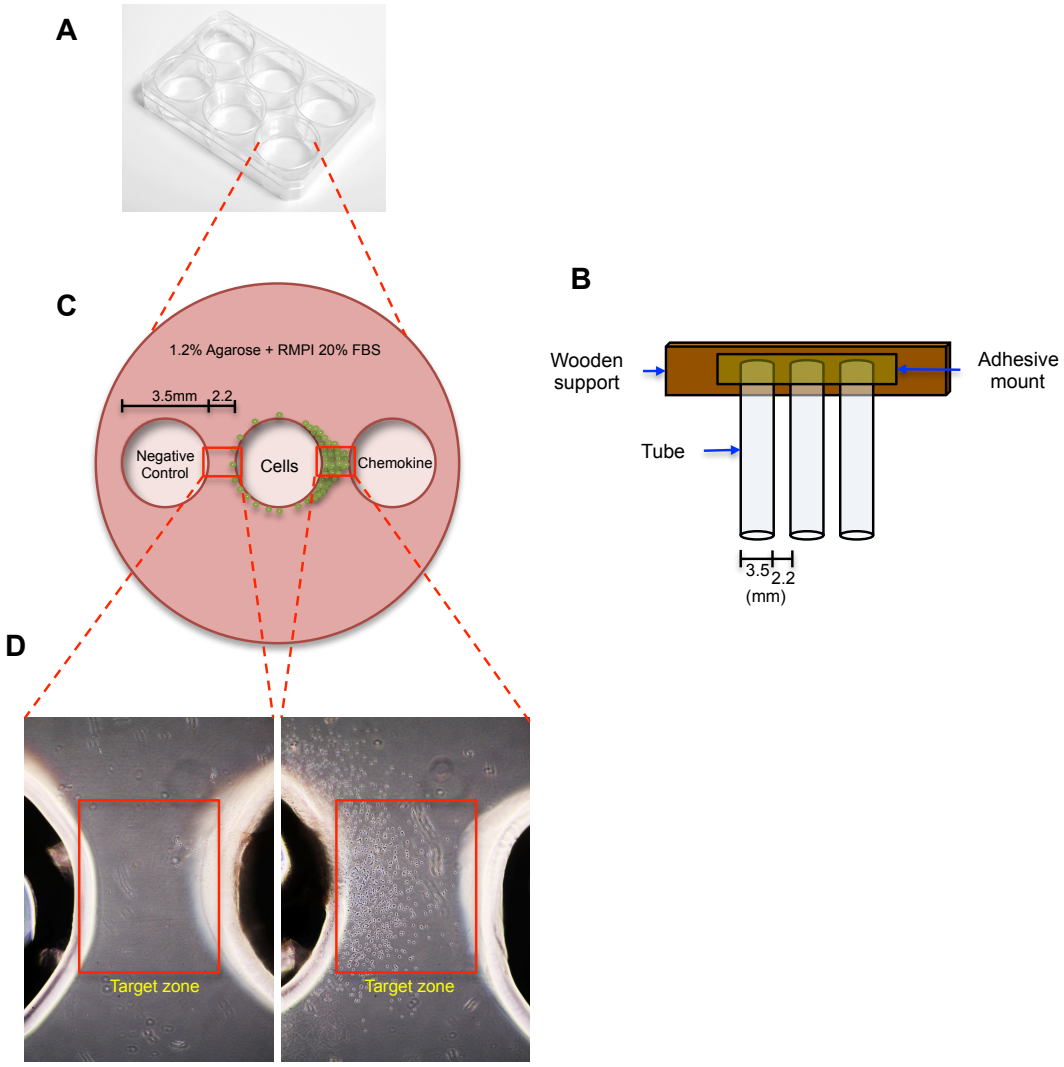


**Figure 2.4: Under agarose cell migration assay**. Agarose gel supplemented with RPMI 20% FBS was cast in a 6 well tissue culture plate (A) and allowed to solidify. 3 parallel holes were punched in the agar using hole punch (B). Cells were pipetted into the central well and chemoattractant or HBSS control was pipetted into the outer wells (C). Plates were incubated 37°C for 2 hours in humidified air with 5% $CO_2$ to allow migration to occur. Following incubation, gels were photographed (D) at the spaces in between wells. Using ImageJ software, a target zone of defined area was superimposed on the photograph and cells that had migrated into the target zone were counted.

### 2.2.12 Phagocytosis

#### Phagocyte preparation

For macrophage experiments, THP-1 monocytes were treated with 80nM PMA for differentiation into macrophages, as previously described. For neutrophil experiments, primary human neutrophils were isolated from peripheral human blood as previously described. All cells were washed in plain RPMI 1640, and rested for at least 1 hour at 37°C prior to phagocytosis experiments.

**IgG opsonisation of latex beads**

Carboxylate-modified polystyrene fluorescent red latex beads were washed in PBS and incubated with 10mg/ml human IgG for 1 hour on a rocker at room temperature. Beads were washed twice in PBS to remove excess IgG and stored at room temperature until use.

**Preparation of bacteria**

Overnight culture of *E. coli* was washed in warm PBS and loaded with 10μM CFSE in DMSO for 30 minutes at 37°C under agitation. Following incubation, bacterial cells were washed three times in PBS and rested.

**Phagocytosis procedure and analysis**

Phagocytes treated with compounds or vehicle as indicated in figure legends were mixed 5:1 (v/v) with latex beads or bacteria and incubated for 30 minutes at 37°C with constant gentle agitation to encourage mixing. Following incubation, samples were washed twice in PBS, transferred to flow cytometry tubes and analysed by flow cytometry on a FACSAria using FACSDiva software. Flow cytometry was performed to demonstrate that single live phagocytes were associated with IgG-coated fluorescent beads or bacteria.

For each phagocyte population, viable cells were gated using forward and side scatter. Mean fluorescence signal of the phagocyte population was measured for 10,000 individual viable cells. If a phagocyte had engulfed a particle, a fluorescent signal would be detected within the viable gate. Controls included phagocytes incubated with no fluorescent particle, which gave mean fluorescence signal of zero, and either latex beads or bacteria alone which, due to their smaller size as determined by side and forward scatter, did not appear in the phagocyte viable gate and obstruct the true signal value. Data analysis was performed using FACSDiva software.

### 2.2.13 Western blotting

**Sample preparation**

Following treatment as indicated in figure legends, cells were washed in ice cold PBS. Cells were then lysed by rotating at 4°C for 30-40 minutes in lysis buffer (50mM Tris-HCl, 150mM NaCl, 1% Non-idet P40, 1mM sodium vanadate, 1mM sodium molybdate, 10mM sodium fluoride, 40μg/ml PMSF, 0.7μg/ml pepstatin A, 10μg/ml aprotinin, 10μg/ml leupeptin and 10μg/ml soybean trypsin inhibitor). Lysates were then centrifuged at 500 g at 4°C for 10 minutes to remove debris and the protein containing supernatant collected. Samples were diluted in sample buffer (60mM Tris-HCl pH 6.8, 2% SDS, 10% glycerol, 5% 2-mercaptoethanol, 0.01% bromophenol blue) and boiled for 5 minutes prior to electrophoresis.

### Immunoblotting

Samples were loaded into a 10% SDS-page gel positioned in a gel tank containing running buffer (25mM Tris-Base, 192mM glycine, 0.1% SDS). Proteins were stacked at 75V for 20 minutes and then resolved at 150V for approximately an hour or until the sample buffer had reached the base of the gel. Proteins were transferred onto nitrocellulose membrane at 40mA per membrane for 1 hour using semi-dry transfer buffer (48mM Tris-Base, 39mM glycine, 0.0375% SDS, 20% methanol). Following transfer, the membrane was blocked in 5% milk in TBS tween (20mM Tris-HCl, 150mM NaCl, 0.1% tween 20) for 1 hour at room temperature. Membranes were then incubated in primary antibody diluted in TBS tween containing 1% BSA and 0.01% sodium azide overnight at 4°C on a rocker. Following incubation, the membrane was washed in TBS tween for 15 minutes before being incubated in a species appropriate horseradish peroxidase conjugated secondary antibody for 1 hour at room temperature. Finally, the membrane was washed in TBS tween for 15 minutes and protein bands visualised using an EZ-ECL chemiluminescence detection kit and developed using an ImageQuant developer. Resulting images were analysed using ImageJ software.

## 2.3 Methods and materials for *Drosophila* experiments

### 2.3.1 Fly husbandry

Unless otherwise stated, all fly stocks were maintained at 25°C in the Fly Room at the University of Bath. Flies were kept in plastic vials containing fly food (17g yeast, 39g malt extract, 60g cornmeal, 9g soya flour, 6g plant agar, 64g sugar, 1.5g in 15ml MeOH Nipagin, 5.3ml in 7.7ml $H_2O$ propionic acid, up to 1.2L $H_2O$) and tipped on to new feed approximately every other day. Larger stocks of flies were maintained in bottles containing the same fly food. For phenotyping and collection, flies were anaesthetised using a $CO_2$ emitting pad and viewed under a dissection microscope. For crosses, virgin females were collected every morning and afternoon and distinguished by a swollen pale abdomen with a visible meconium.

### 2.3.2 Embryo collection

To collect embryos, flies were transferred to a laying cage (Figure 2.5). Cages were constructed out of upturned 100ml plastic beakers with air holes punched into the base. An apple juice agar plate (Agar, Apple Juice, Sugar) was placed to seal the open end and secured with an elastic band. Agar plates were supplemented with a pea-sized amount of yeast paste. Cages were stored in a dark incubator at 23°C.

Fresh apple juice agar plates were placed on cages in the late afternoon. Embryos were then collected from these plates the next morning. For collection, embryos were dislodged from the plate using water and a paintbrush, and sieved through a basket. Embryos were dechorionated in bleach for 1 minute and 45 seconds to allow the chorion to dissolve; this was checked using a dissection microscope. Embryos were

washed thoroughly in water and kept submerged in water to avoid dehydration before mounting for imaging.

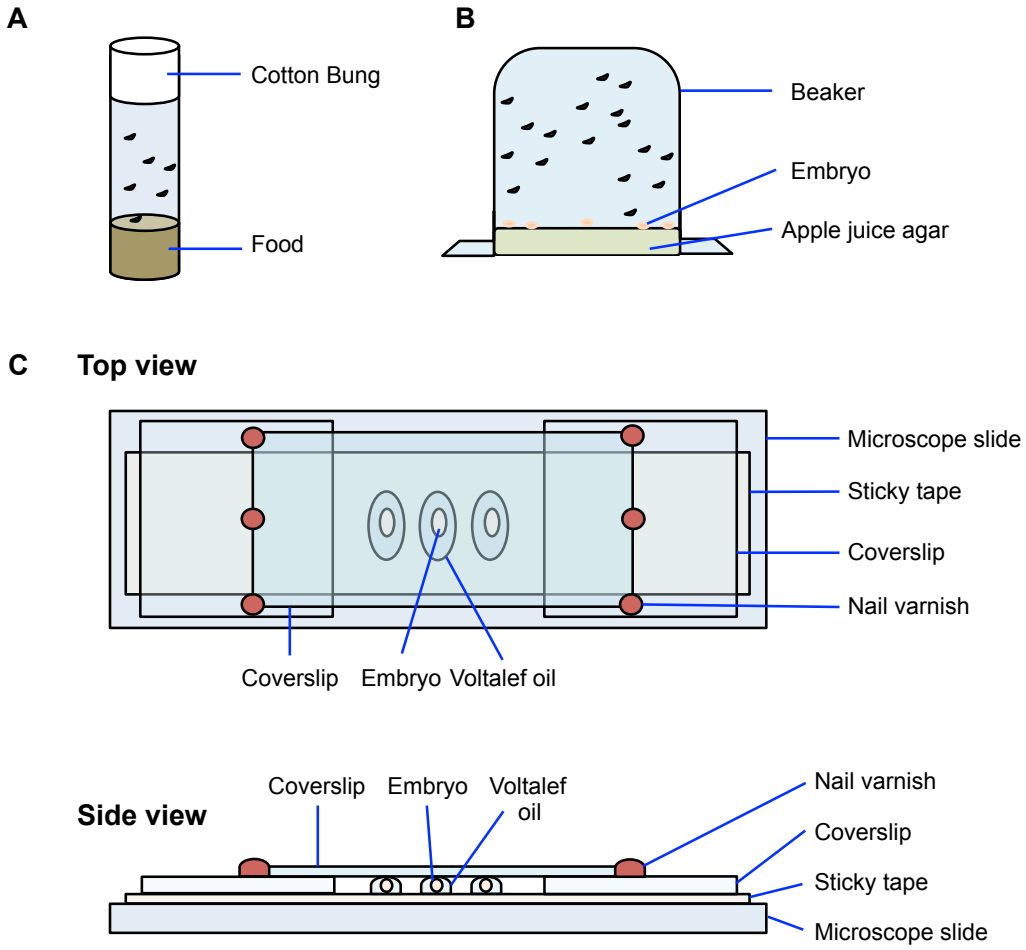


**Figure 2.5: *Drosophila* embryo collection and mounting for confocal microscopy.** (A) Fly stocks were maintained in plastic vials containing fly food. (B) To collect embryos, flies were transferred to a laying cage, comprising an upturned plastic beaker with apple juice agar plate placed to seal the open end. (C) Embryos were collected, dechorionated and mounted ventral side up onto double sided sticky tape attached to a microscope slide and covered in Voltalef oil. Two square coverslips were attached to both ends to form a bridge for a large coverslip to be placed over the embryos, and secured with nail varnish.

### 2.3.3 Gal4-UAS system

Unless otherwise stated, the Gal4-UAS system was used for fluorescent labelling of hemocytes (Figure 2.6). This two-component system contains a Gal4 driver fly line and an upstream activating sequence (UAS) effector fly line. The yeast transcription factor Gal4 contains a DNA binding domain alongside an activation domain, and will be expressed when driven by an upstream promoter. This is crossed to an effector line including an UAS containing CGG-$N_{19}$-CCG motif, where N is equivalent to any base; Gal4 binds here. In these studies, unless otherwise stated, fly lines contained the hemocyte specific promoter croquemort upstream of Gal4 recombined to UAS upstream of green fluorescent protein (GFP) on chromosome three. This cytoplasmic GFP labels the hemocyte body and protrusions.

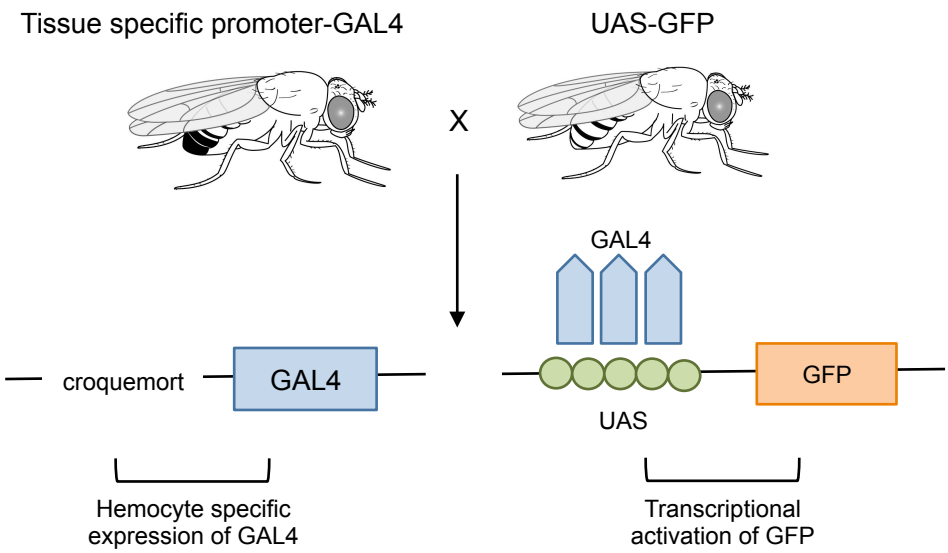


**Figure 2.6: The GAL4/UAS system in *Drosophila*.** When females carrying UAS-GFP are mated to males carrying the yeast transcriptional activator GAL4 under the control of tissue specific promoter croquemort, progeny containing both GAL4 and UAS are produced. The binding of GAL4 at UAS drives GFP expression in the hemocytes only.

### 2.3.4 Stocks and crosses

Fly stocks are described in table 2.5.3. A croquemort-Gal4,UAS-GFP line was used to visualise wild type (WT) hemocyte migration. Fly lines with mutations on chromosome II were crossed with a croquemort-Gal4,UAS-GFP line in order to visualise hemocyte migration. Mutations were kept over balancer CTG on chromosome II. Crosses were performed at 25°C on standard fly food medium supplemented with additional yeast paste in plastic vials.

### 2.3.5 Wounding and Imaging live embryos

#### Mounting embryos

Dechorionated embryos were collected during stage 15 of development and mounted ventral side up using curved forceps onto double side adhesive tape attached to a microscope slide and covered in Voltalef oil. Two square no. 1 coverslips (22mm x 22mm) were attached to both ends of the slide and a large coverslip (32mm x 24mm) was placed over the top using flat forceps. The top coverslip was secured in place using nail varnish. Figure 2.5(c) illustrates fully mounted embryos ready for wounding.

#### Wounding embryos

For wounding, mounted embryos were subjected to laser ablation from a nitrogen laser-pumped dye laser connected to a microscope using the Micropoint system (Photonic Science, Robertsbridge, UK). Wounds were placed close to the ventral lines of hemocytes along the centre of the anterior/posterior axis.

**Confocal microscopy**

Shark embryos and WT controls were wounded and imaged using a Zeiss LSM 510 confocal microscope with 63x objective. Src42A embryos and WT controls were imaged using a Perkin Elmer spinning disc confocal at 40x objective with Volocity (Perkin Elmer) software.

Unless otherwise stated, for time-lapse movies, images were collected at 2-minute intervals for one hour. Recording started immediately after wounding. Time-lapse movies were created from the confocal Z-stacks by using ImageJ software (NIH). Movies were made at room temperature.

Time lapse movies corresponding to relevant figures are provided on a separate CD as .avi files. Movies legends are provided in Appendix 1.

### 2.3.6 Antibody staining

**Fixing embryos**

Embryos were collected and dechorionated as previously described. Unwounded embryos at stage 15 of development were fixed for 20 minutes in a 1.5ml plastic tube containing a 1:1 mix of heptane and 4% paraformaldehyde in PBS, on a roller at room temperature. The fixative phase was removed and replaced with methanol. To remove the vitelline membrane the embryos were shaken vigorously until embryos settled in the bottom of the plastic tube. Embryos were transferred to a fresh plastic tube using a glass Pasteur pipette and washed three times in methanol. Embryos were subsequently stored in 500µl methanol at -20°C.

Wounded embryos were removed from the microscope slide using heptane to dissolve oil and adhesive tape, collected in a basket and transferred to a 1.5ml epindorf containing a 1:1 mix of heptane and 4% paraformaldehyde in PBS. Embryos were fixed for 20 minutes on the roller at room temperature. Fixed embryos were hand-devitellinized in PBS using forceps, washed three times in methanol and transferred to 500µl methanol for storage at -20°C.

**Antibody labelling**

Fixed embryos were transferred to a fresh 1.5ml plastic tube and rinsed three times with 300µl PBT before being washed in 300µl fresh PATx every 20 minutes for an hour, on the roller at room temperature. PATx and PBT are described in table 2.5.4. Embryos were incubated with 200µl primary antibody diluted in PATx overnight at 4°C on a roller. Antibodies and concentration used are listed in Table 2.5.2. Samples were then rinsed several times in PATx before longer washes of 20 minutes in fresh PATx for an hour. Embryos were collected in a fresh plastic tube and incubated in secondary antibody diluted in PATx for 2 hours at room temperature on the roller. Following incubation, secondary antibody was removed and embryos rinsed three times in PATx and then washed for 20 minutes three times in fresh PATx. Finally, PATx was removed and embryos were covered in 100µl DABCO mounting medium. Inversion of the plastic

tube allowed suspension and dispersal of the embryos throughout the DABCO. Samples were stored at 4°C until mounted on microscope slides for imaging.

### 2.3.7 Image analysis

Images recorded on Zeiss confocal and spinning disk confocal were opened as LSM files in ImageJ using the LSM reader plugin. Background fluorescence was removed using the 'despeckle' ImageJ function before stacking the z projections using Grouped_z_projector plugin. Images were saved as .tif files and movies as .avi files.

#### Hemocyte recruitment to a wound

Z stack images using the GFP fluorescent laser were taken of individual wounded embryos 60 minutes post wounding to visualise hemocytes. In addition, brightfield images of the embryo were recorded concurrently to reveal the wounded epithelium. Using ImageJ software, the size of the wound can be measured using freehand selections. From these images, the number of hemocytes at the wound were counted and normalised against the size of the wound.

#### Individual cell tracking

Cell tracking was performed using the 'Manual Tracking' ImageJ plugin on maximum projections of Z slices. For each time point, the centre of the cell body tracked was manually highlighted, and through its coordinates mean velocity and directionality was calculated. The directionality of a migrating cell is calculated by comparing Euclidian and accumulated distance. It is a measure of directness of cell trajectories. A directionality of 1 indicates a straight-line migration from start to endpoint.

#### Phosphotyrosine Intensity

Measurement of phosphotyrosine intensity following immunostaining was carried out using ImageJ measurement tool 'Mean gray value' on individual slices of images corresponding to phosphotyrosine channel.

## 2.4 Statistical analysis

Data were normalised as described above and in figure legends, statistical analysis was performed using GraphPad Prism 6 software. Graphical representations of data include mean values ± standard error of the mean (SEM) for experiments with $n \geq 3$.

For normalised data either a one way-ANOVA followed by Tukey's post test or two way-ANOVA followed by Dunnett's post test was performed to analyse significance between treatment groups. A paired t-test was also used when only comparing 2 groups. A p value of less than 0.05 was considered to be statistically significant.

For all experiments the following annotations are used to indicate the levels of significance: *=$p<0.05$, **=$p<0.01$, ***=$p<0.001$, ****=$p<0.0001$.

## 2.5 Tables

### 2.5.1 Table of reagents and materials

| Product | Catalogue No. | Supplier |
|---|---|---|
| 12-well tissue culture treated polystyrene plate with lid | 665180 | Greiner Bio-One, Gloucester, UK |
| 13mm coverslips | MNJ-500-010G | Fisher Scientific, Loughborough, UK |
| 2-mercaptoethanol | M6250 | Sigma Aldrich, Dorset, UK |
| 30% Acrylamide/Bis Solution | 161-0154 | Bio-Rad, Hertfordshire, UK |
| 3AC | 565835 | Merck Millipore, Billerica, USA |
| 6 well tissue culture treated polystyrene plate with lid | 657160 | Greiner Bio-One, Gloucester, UK |
| A66 | S2636 | SelleckChem, Suffolk, UK |
| Alexa-Fluor 488 Phalloidin dye | A12379 | Life Technologies, Paisley, UK |
| Amersham Protran Supported 0.45µm nitrocellulose | 15220033 | Fisher Scientific, Loughborough, UK |
| Ammonium persulfate | A3678 | Sigma Aldrich, Dorset, UK |
| Ampicillin | A9518 | Sigma Aldrich, Dorset, UK |
| Annexin V | A35111 | Life Technologies, Paisley, UK |
| Aprotinin | A1152 | Sigma Aldrich, Dorset, UK |
| ATP | A2383 | Sigma Aldrich, Dorset, UK |
| Bovine serum albumin | A2153 | Sigma Aldrich, Dorset, UK |
| BpV (HOpic) | 203-701 | Merck Millipore, Billerica, USA |
| Bromophenol blue | B/P620/44 | Fisher Scientific, Loughborough, UK |
| Calcein | C1359 | Sigma Aldrich, Dorset, UK |
| Catalase from bovine liver | C1345 | Sigma Aldrich, Dorset, UK |
| Cell Scrapers | 541070 | Greiner Bio-One, Gloucester, UK |
| CellTrace™ CFSE cell proliferation kit | C34554 | Life Technologies, Paisley, UK |
| ChemoTx Migration plate (Neuroprobe) | 101-5 | Receptor Technologies, Warwick, UK |
| 96 well tissue culture treated polystyrene plate, with lid, clear | 655180 | Greiner Bio-One, Gloucester, UK |
| CM-$H_2$DCFDA | C6827 | Invitrogen, Paisley, UK |
| DABCO (1,4-diazabicyclo[2.2.2]octane) | 290734 | Sigma Aldrich, Dorset, UK |
| DAPI (4',6'-Diamidino-2-phenylindole dihydrochloride) | D9542 | Sigma Aldrich, Dorset, UK |
| Dextran ($M_r$ ~100,000) | 09184 | Sigma Aldrich, Dorset, UK |
| Dimethyl sulfoxide | D8418 | Sigma Aldrich, Dorset, UK |
| DPI (Diphenyleneiodonium chloride) | D2926 | Sigma Aldrich, Dorset, UK |
| DMEM-F12 media | 11330-057 | Invitrogen, Paisley, UK |
| EA.hy926 cells | CRL-2922 | ATCC, Virginia, USA |
| EDTA (Ethylenediaminetetraacetic acid) | BPE2482 | Fisher Scientific, Loughborough, UK |
| EZ-ECL Chemiluminescence Detection Kit for HRP | K1-0170 | Geneflow Ltd, Staffordshire, UK |
| Flat bottomed 96 well plates | 11997944 | Fisher Scientific, Loughborough, UK |
| Fluo-4 AM | F14201 | Life technologies, Paisley, UK |
| Foetal bovine serum, heat inactivated | 7.01 Hi | Source Bioscience, Nottingham, UK |
| Glycerol | G5516 | Sigma Aldrich, Dorset, UK |
| GSK2636771 | S8002 | SelleckChem, Suffolk, UK |
| HBSS, no calcium, no magnesium | 14185052 | Invitrogen, Paisley, UK |

| | | |
|---|---|---|
| Heparin sodium salt | 84020 | Sigma Aldrich, Dorset, UK |
| Human Fibronectin | 1918-FN | R&D Systems, Minneapolis, USA |
| Human M-CSF | 130-093-963 | Miltenyi Biotech, Cologne, Germany |
| Human recombinant IL-8 (CXCL8) | 200-08 | Peprotech, New Jersey, USA |
| Human recombinant MCP-1 (CCL2) | 300-04 | Peprotech, New Jersey, USA |
| Hydrogen peroxide solution | 216763 | Sigma Aldrich, Dorset, UK |
| IC87114 | S1268 | SelleckChem, Suffolk, UK |
| Ionomycin calcium salt | 1704 | Tocris Bioscience, Bristol, UK |
| L-glutamine | 25030-081 | Invitrogen, Paisley, UK |
| LABTEK Chambered coverglass 8 well | 10384221 | Fisher Scientific, Loughborough, UK |
| Latex beads carboxylate-modified polystyrene, fluorescent red | L3030 | Sigma Aldrich, Dorset, UK |
| Leukotriene $B_4$ | 2307 | Tocris Bioscience, Bristol, UK |
| Leupeptin | BPE2662 | Fisher Scientific, Loughborough, UK |
| Lipopolysaccharide from *E. coli* (Serotype O111:B4) | L2630 | Sigma Aldrich, Dorset, UK |
| LY294002 | S1105 | SelleckChem, Suffolk, UK |
| Lymphoprep | 1114547 | Axis Shield, Dundee, UK |
| Microscope Slides | MNJ-700-010N | Fisher Scientific, Loughborough, UK |
| MnTBAP Chloride | ab141496 | Abcam Biochemicals, Cambridge, UK |
| Mouse IgG Alexa Fluor 488 Isotype control | IC0041G | R&D Systems, Minneapolis, USA |
| Mowiol 4-88 | 81381 | Sigma Aldrich, Dorset, UK |
| MTT formazan | M2003 | Sigma Aldrich, Dorset, UK |
| N-formyl-Met-Leu-Phe (fMLP) | F3506 | Sigma Aldrich, Dorset, UK |
| Nonidet P-40 | 56009 | Sigma Aldrich, Dorset, UK |
| PFA (Paraformaldehyde) | P6148 | Sigma Aldrich, Dorset, UK |
| PBS (1mM $KH_2PO_4$, 155mM NaCl, 3mM $Na_2HPO_4$-$7H_2O$) | 10010023 | Invitrogen, Paisley, UK |
| Penicillin-Streptomycin | 15140-122 | Invitrogen, Paisley, UK |
| Pepstatin A | 10011413 | Fisher Scientific, Loughborough, UK |
| Pertussis Toxin | 3097 | R&D Systems, Minneapolis, USA |
| PMA (Phorbol 12-myristrate 13-acetate) | P8139 | Sigma Aldrich, Dorset, UK |
| PMSF (Phenylmethanesulfonyl fluoride) | P7626 | Sigma Aldrich, Dorset, UK |
| Piceatannol | 1554 | Tocris Bioscience, Bristol, UK |
| PP2 | 1407 | Tocris Bioscience, Bristol, UK |
| Protein ladder, pre-stained recombinant for SDS PAGE gel | 11478503 | Fisher Scientific, Loughborough, UK |
| Protein Standard Marker | 161-0375 | Bio-Rad, Hertfordshire, UK |
| RPMI 1640 Medium | 11875-093 | Invitrogen, Paisley, UK |
| SDS (Sodium dodecyl sulphate) | L3771 | Sigma Aldrich, Dorset, UK |
| STI (Soybean trypsin inhibitor) | 17075-029 | Life Technologies, Paisley, UK |
| THP-1 Human monocytic leukaemia cell line | 88081201 | ECACC, Porton Down, UK |
| Triton-X100 | X100 | Sigma Aldrich, Dorset, UK |
| Trypan blue solution, 0.4% | 15250-061 | Invitrogen, Paisley, UK |
| Trypsin-EDTA (0.25%) | 25200-056 | Invitrogen, Paisley, UK |
| Tween-20 | P1379 | Sigma Aldrich, Dorset, UK |
| U937 cells | CRL-1593.2 | ATCC, Virginia, USA |
| Ultra Pure Agarose | 16500100 | Invitrogen, Paisley, UK |
| Wright-Giemsa stain | WG128 | Sigma Aldrich, Dorset, UK |
| ZSTK474 | S1072 | SelleckChem, Suffolk, UK |

### 2.5.2 Table of antibodies

| Antibody | Species | Manufacturer | Product number | Dilution |
|---|---|---|---|---|
| Primary | | | | |
| **ERK1** | Rabbit | Santa Cruz Biotech, TX, USA | SC-93 | 1:1000 (WB) |
| **ICAM-1 (H108)** | Rabbit | Santa Cruz Biotech, TX, USA | SC7891 | 1:1000 (WB)<br>1:100 (IF) |
| **pAkt (S473)** | Rabbit | Cell Signaling Technology, MA, USA | 4060S | 1:1000 (WB) |
| **pERK (Y204)** | Rabbit | Cell Signaling Technology, MA, USA | 4376S | 1:1000 (WB) |
| **CCR2 (Alexa Fluor 488 conjugated)** | Mouse | R&D Systems, MN, USA | FAB151G | 1:10 (FC) |
| **CD14 (Fluorescein conjugated)** | Mouse | R&D System, MN, USA | FAB3832F | 1:10 (FC) |
| **pTyrosine, clone 4G10** | Mouse | Merck Millipore, MA, USA | 05-321 | 1:100 (IF) |
| | | | | |
| Secondary | | | | |
| **HRP-conjugated anti Rabbit** | Goat | DAKO, UK | P0449 | 1:2000 (WB) |
| **Alexa Fluor 568-conjugated anti Rabbit** | Donkey | Invitrogen, UK | A10042 | 1:200 (IF) |
| **Alexa Fluor 568-conjugated anti Mouse** | Donkey | Invitrogen, UK | A10037 | 1:200 (IF) |

(WB= western blot; FC= flow cytometry; IF= immunofluorescence)

### 2.5.3 Table of *Drosophila* stocks

| Fly line | Supplier |
|---|---|
| w;;crq-Gal4,UAS-GFP | W Wood, University of Bath, UK |
| w;shark/CTG;crq-Gal4,UAS-GFP | I Evans, University of Bath, UK |
| w;lf/Cyo;crq-Gal4,UAS-GFP/TM6B | W Wood, University of Bath, UK |
| w;lf/Cyo;MKRS/TM6B | W Wood, University of Bath, UK |
| w;src42a$^{E1}$/Cyo | Bloomington Stock Centre, Indiana, USA |
| w;src42a$^{K10108}$/Cyo | Bloomington Stock Centre, Indiana, USA |
| w;src42a$^{myri}$/Cyo | Bloomington Stock Centre, Indiana, USA |
| w;shark$^{1}$/Cyo | Bloomington Stock Centre, Indiana, USA |

### 2.5.4 Table of buffers and solutions

| Buffer | Contents |
|---|---|
| Phosphate Buffered Saline with Triton X-100 (PBT) | 0.1% Triton X-100 in 1X PBS |
| PBT with BSA (PATx) | 1% BSA diluted in PBT |

# CHAPTER 3: SFK SIGNALLING AND FUNCTION IN AN EMBRYONIC *DROSOPHILA MELANOGASTER IN VIVO* MODEL OF CELL MIGRATION

## 3.1 Rationale

*In vivo* models of tissue damage have revealed that $H_2O_2$ is an early signal generated locally in response to wounding [233], [270]. Using a zebrafish larval model of tissue damage, it has recently been suggested that wound generated damage cue $H_2O_2$ can stimulate neutrophil recruitment to a wound by oxidising and activating an intracellular zebrafish kinase, Lyn [282]. Lyn has consequently been termed a 'redox sensor' in neutrophils. Lyn is a member of the SFK family, a conserved group of enzymes that drive many cellular signalling events. Zebrafish studies identified the critical residue that is oxidised by $H_2O_2$ as cysteine 466. Importantly, this residue is conserved in SFK members between species, including *Drosophila* Src42A, human Lyn, Src, Hck and Lck, and *C. elegans* Src-1 [282].

The damage signal $H_2O_2$ is also important in driving immune cell recruitment to sites of tissue damage in *Drosophila* embryos. Whether this is via a SFK driven mechanism, akin to observations in zebrafish, has yet to be fully elucidated. Therefore, our first aim was to investigate whether *Drosophila* Src42A has a role in driving immune cell recruitment to sites of tissue damage. For this we can use a *Drosophila* embryonic wounding model with embryos lacking functional Src42A to analyse responses of immune cells to laser induced epithelial damage. This is a robust model that harnesses the tractability of *Drosophila* genetics with time-lapse confocal microscopy to measure cellular events in real time.

Human Syk (*Drosophila* Shark) is a key signalling mediator and adaptor protein downstream of SFKs. SFK and Syk interactions have been characterised downstream of human immunoreceptors [126], and the *Drosophila* engulfment receptor Draper, as described in section 1.4.5. Shark is required for embryonic dorsal closure in *Drosophila*, a process which requires the synchronised movement of epithelial cell layers [289]. Additionally, a recent study in *Drosophila* highlighted a potential link between Src42A and Shark signalling downstream of the engulfment receptor Draper in glial cell phagocytosis of apoptotic corpses [287].

The aim of this chapter is to examine the contribution of Src42A and Shark in hemocyte recruitment to a wound by examining individual cell behaviour in response to a wound event in embryos lacking functional Src42A or Shark.

## 3.2 Src42A is required for hemocyte migration to a wound

To investigate whether SFK redox sensitivity is conserved in *Drosophila*, SFK candidates containing the critical cysteine 466 residue were identified in a gene search using FlyBase. *Drosophila* Src42A was a positive hit. To determine whether Src42A was involved in the migration of hemocytes to wound, embryos with mutated Src42A were studied. Three mutant Src42A fly lines were used in the *Drosophila* embryonic wounding assay, as summarised in Table 3.1.

To investigate the migratory response to a wound, developmental stage 15 Src42A mutant embryos expressing the fluorescent cytoplasmic marker GFP under the hemocyte specific driver croquemort were wounded close to the ventral midline and imaged using a spinning disc confocal microscope 60 minutes post wounding (Figure

3.1a). Hemocytes from $Src42A^{E1}$ and $Src42A^{K10108}$ embryos showed significant impairment in migration to the wound after 60 minutes (Figure 3.1b). $Src42A^{myri}$ hemocytes migrated to the wound with greater variance and the mean hemocyte number was not significantly impaired compared to WT responses. Consistent with previous observations from our lab group, the number of WT hemocytes at the wound correlated linearly with the size of the wound (Figure 3.1c). However, for all three Src42A mutants linear regression analysis indicated this correlation was less linear than for WT embryos ($Src42A^{E1}$ $R^2$=0.049, $Src42A^{K10108}$ $R^2$=0.676, $Src42A^{myri}$ $R^2$=0.360, WT $R^2$=0.709). $Src42A^{E1}$ hemocyte number at the wound remained constant (<5 hemocytes) regardless of the wound size.

Time-lapse movies of hemocyte migration were captured using all three GFP-expressing Src42A mutants and compared to WT embryos to gain a better insight into the migratory characteristics of Src42A mutant hemocytes. Images were captured every 2 minutes for one hour. Figure 3.2a contains representative images of embryos before wounding and up to 60 minutes post wounding, as well as individual cell tracks from which hemocyte velocity and directionality were calculated. Src42A mutant hemocyte directionality was significantly impaired in all three mutants compared to WT embryos (Figure 3.2b). This was also true of hemocyte velocity; all Src42A mutant hemocytes were significantly slower when migrating to a wound than WT controls (Figure 3.2b).

We next sought to determine whether mutations in Src42A were affecting migratory responses in unwounded embryos. Embryos were mounted and imaged without wounding for up to 30 minutes. Individual cell tracking revealed that hemocyte random migration was not compromised by Src42A mutations. Interestingly, random migration velocity of $Src42A^{E1}$ and $Src42A^{myri}$ hemocytes was significantly higher than WT hemocytes (Figure 3.3).

| Mutation | Mutagen | Feature | Reference |
|---|---|---|---|
| $Src42A^{myri}$ | EMS | Membrane localisation defect – Point mutation in codon 2 results in amino acid substitution from Gly2 to Asp. Gly2 is conserved in all members of the Src family and must be myristoylated for localization of Src to the cellular membrane in mammals. | [394] |
| $Src42A^{K10108}$ | P-element | Loss of kinase function – P{lacW}$Src42A^{K10108}$ transgene insertion located on chromosome 2. | [395] |
| $Src42A^{E1}$ | EMS | Loss of kinase function – Point mutation at codon 483 eliminates the COOH-terminal part of the kinase domain. | [394] |
| $Shark^{1}$ | EMS | Loss of kinase function – The $Shark^{1}$ locus encodes a truncated form of Shark protein due to a C → T transition at nucleotide 685 that changes Gln210 to a stop codon and truncates Shark open reading frame. | [289] |

**Table 3.1: Mutant *Drosophila* stocks used for the study of Src42A and Shark function in hemocyte migration.** EMS = ethyl methanesulfonate.

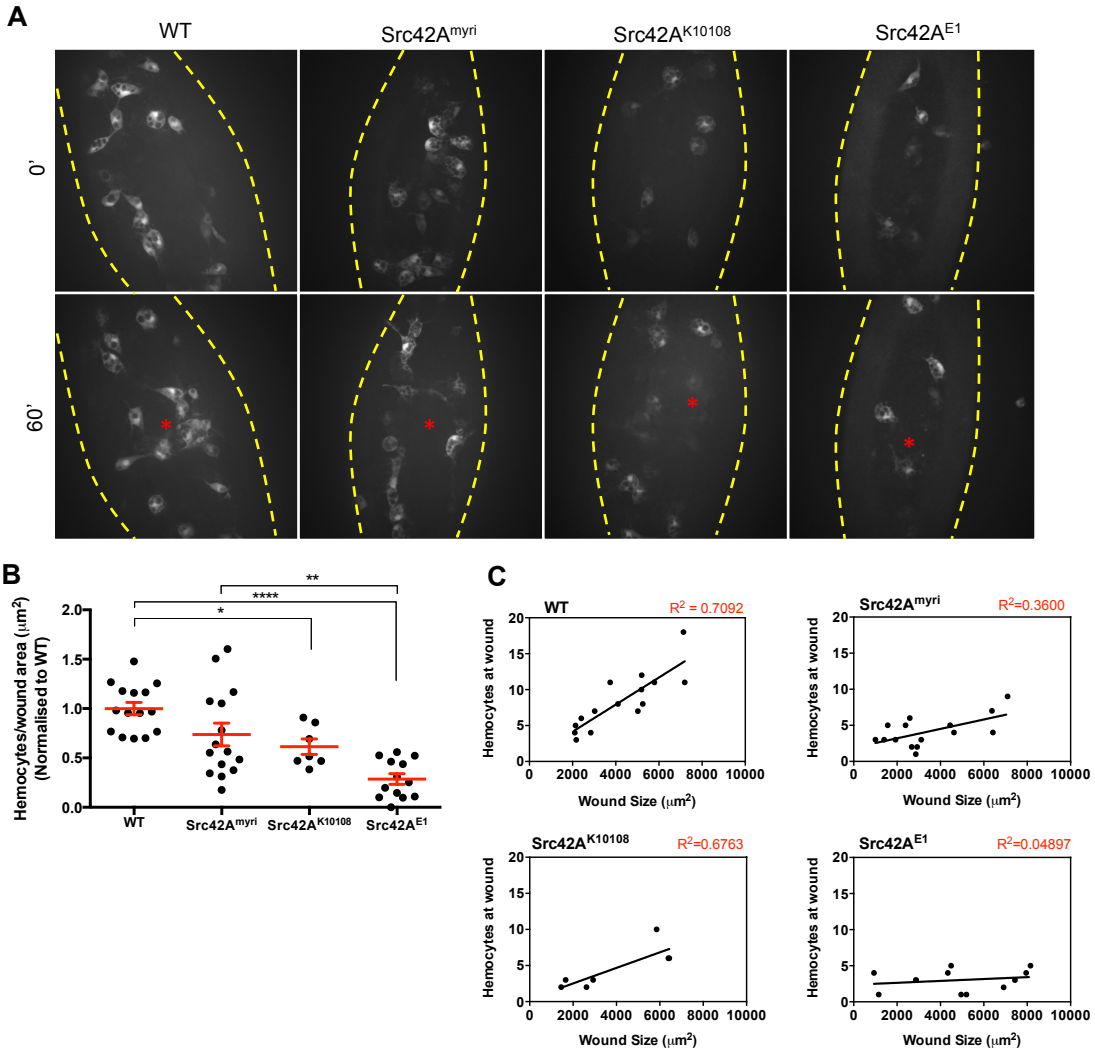


**Figure 3.1: Src42A drives hemocyte migration to a wound in *Drosophila* embryos.** Stage 15 embryos containing hemocyte specific GFP expression were mounted on a microscope slide ventral side up and wounded with a laser along the midline. Embryos were imaged using confocal microscopy with a 20x objective. (A) Images captured pre wound (0') and 60 minutes post wounding (60'). Dashed yellow lines indicate embryo outline, red asterisk denotes site of wound. (B) Quantification of hemocytes at wound 60 minutes post wounding, normalised to WT. Statistical analysis by one way-ANOVA with Tukey's post test, where *=p<0.05, **=p<0.01 and ****=p<0.0001. (C) Correlation plot and linear regression analysis between wound size and number of hemocytes counted at wound 60 minutes post wounding. Data represents means (±SEM) from at least 3 separate experiments with at least 2 embryos per genotype measured per experiment.

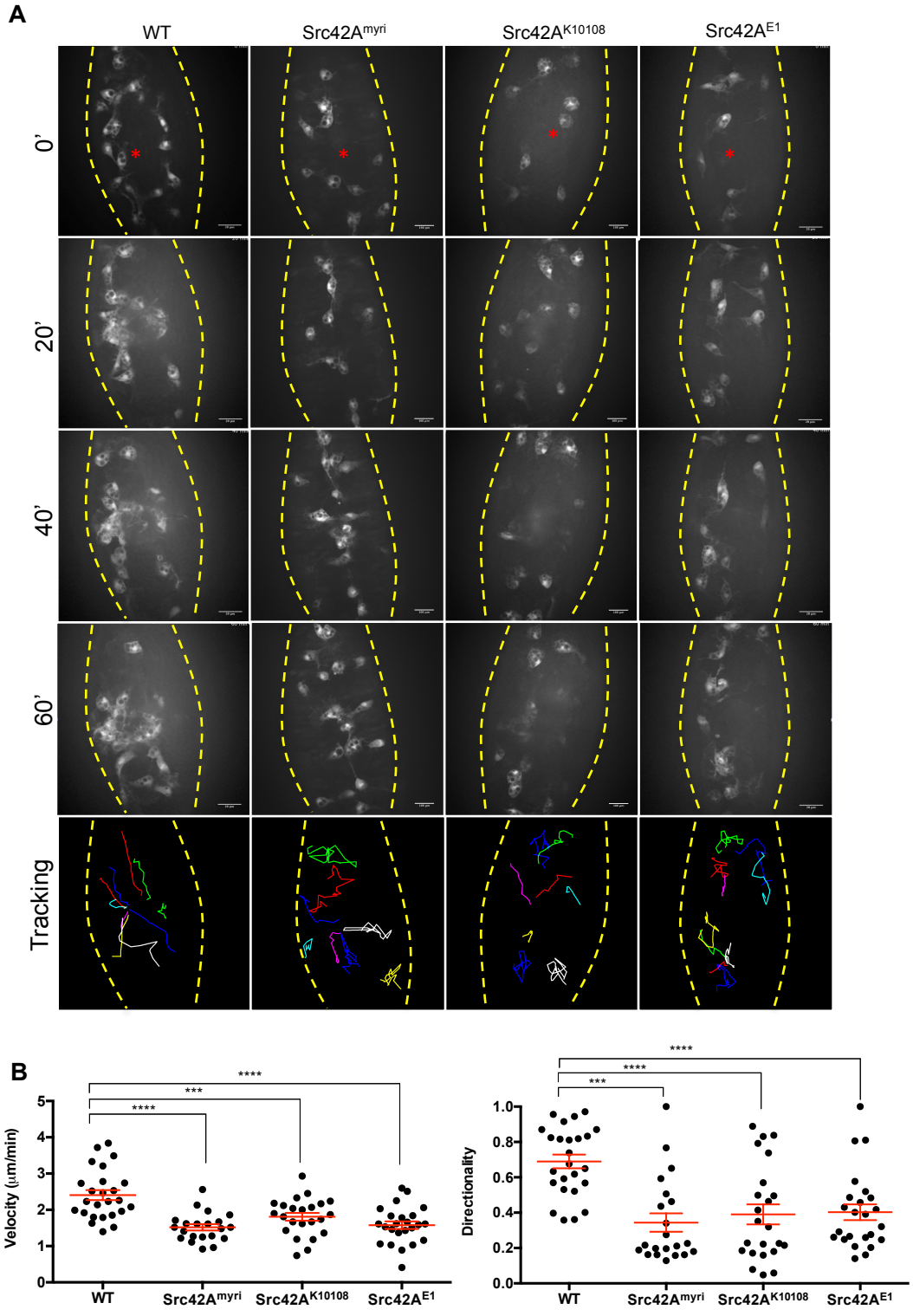


**Figure 3.2: Src42A mutant embryos show reduced hemocyte directionality and velocity in *Drosophila* embryos.** Stage 15 embryos containing hemocyte specific GFP expression were mounted on microscope slides ventral side up and wounded with a laser along the midline. Embryos were imaged using confocal microscopy with a 20x objective with image acquisition every 120 seconds. (A) Stills from time-lapse imaging representing pre-wound (0') and 20, 40 and 60 minutes post wound and manual tracking trajectories. Dashed yellow lines indicate embryo outline, red asterisk denotes site of wound, scale bar = 100µm. (B) Hemocytes were manually tracked and quantification of hemocyte directionality and velocity measured using ImageJ software with 'Manual tracking' plugin. Data represents velocity or directionality (± SEM), normalised to WT, from at least 25 hemocytes pooled from 3 embryos per genotype. Statistical analysis by one way-ANOVA with Tukey's post test, where ***=p<0.001, ****=p<0.0001.

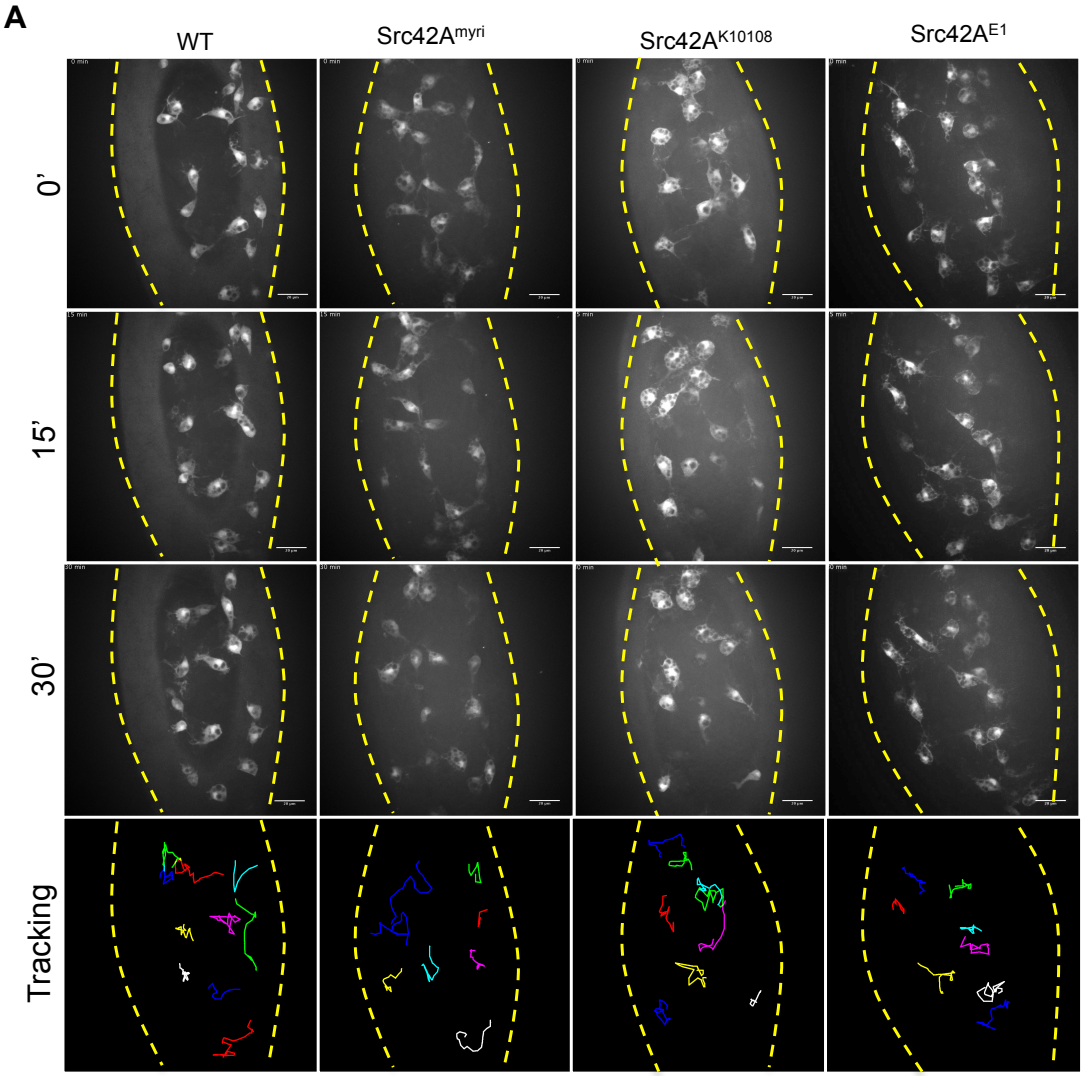


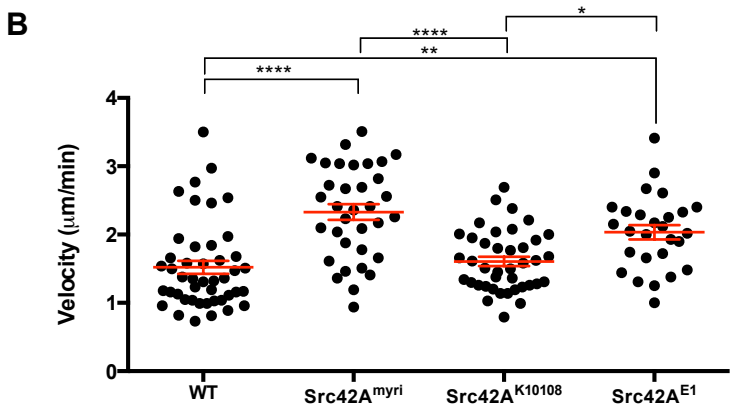


**Figure 3.3: Random migration of hemocytes is not compromised in Src42A mutant *Drosophila* embryos.** Stage 15 embryos containing hemocyte specific GFP expression were mounted on microscope slides ventral side up. Embryos were imaged using confocal microscopy with a 20x objective and images acquired every 60 seconds. (A) Stills from time-lapse imaging representing time points 0, 15 and 30 minutes and manual tracking trajectories. Dashed yellow lines indicate embryo outline. Scale bar = 100μm. (B) Hemocytes were manually tracked and quantification of hemocyte velocity measured using ImageJ software with 'Manual tracking' plugin. Data represents velocity (± SEM), normalised to WT, from at least 25 hemocytes pooled from 3 embryos per genotype. Statistical analysis by one way-ANOVA with Tukey's post test, where *=p<0.05, **=p<0.01 and ****=p<0.0001.

### 3.3 Shark is required for hemocyte migration to a wound

Shark has been associated with the engulfment response seen in glial cells via the Draper receptor pathway and in coordinating actin remodelling [287]. There is potential for Shark to have a wider role in directing hemocyte migration in response to wounds. To investigate this, a Shark mutant fly line, Shark$^{1}$ [289], was tested in the *Drosophila* embryonic wounding assay.

To investigate the migratory response to a wound, developmental stage 15 Shark$^{1}$ mutant embryos expressing the fluorescent cytoplasmic marker GFP under the hemocyte specific driver croquemort were wounded close to the ventral midline and imaged using confocal microscopy 60 minutes post wounding. Shark$^{1}$ mutant embryos showed significantly impaired hemocyte recruitment to the wound versus WT embryos (Figure 3.4a). We also observed weaker correlation between the number of hemocytes at the wound and the wound size: Shark$^{1}$ mutant $R^2$=0.02 when compared to WT $R^2$=0.38 (Figure 3.4b).

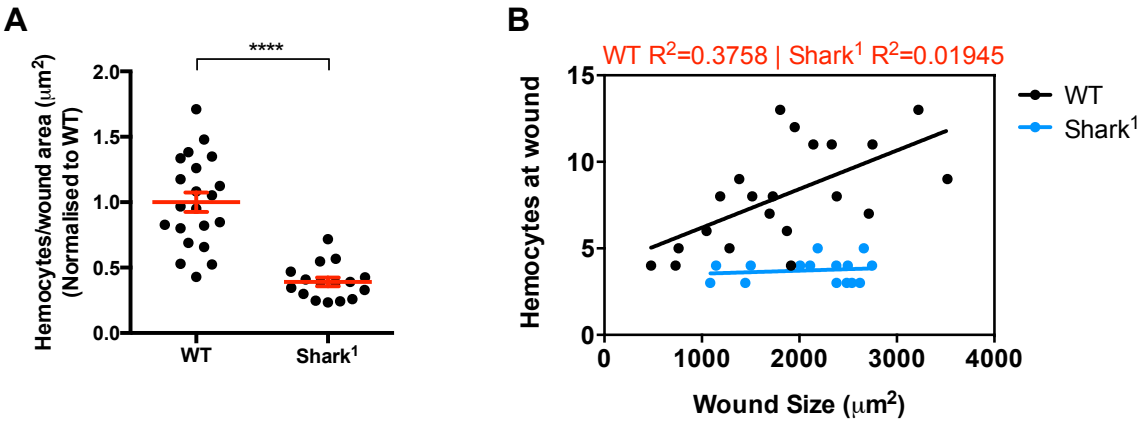


**Figure 3.4: Shark is involved in hemocyte migration to a wound in *Drosophila* embryos.** Stage 15 embryos containing hemocyte specific GFP expression were mounted on microscope slides ventral side up and wounded with a laser along the midline. Embryos were imaged using confocal microscopy with a 20x objective. Confocal images were taken before wounding, and 60 minutes post wounding. (A) Quantification of number of hemocytes at wound in Shark$^{1}$ mutant embryos normalised to WT. (B) Correlation plot and linear regression analysis between wound size and number of hemocytes counted at wound 60 minutes post wounding. Data represents means (± SEM) from at least 3 separate experiments with at least 2 embryos counted per experiment. Statistical analysis by t test, where ****=p<0.0001 versus WT.

### 3.4 Phosphotyrosine intensity is increased in activated hemocytes

SFK activation leads to phosphorylation of various intracellular targets. In order to identify whether SFK activity is upregulated in hemocytes responding to a wound signal, WT embryos with GFP expressing hemocytes were wounded and fixed 30 minutes post wounding. Embryos were stained for phosphotyrosine (pY) and imaged by confocal microscopy. Brightfield imaging revealed the location of the wound site in the epithelium. Microscopy revealed high pY expression throughout the embryo, particularly in epithelial tissue. pY intensity in individual hemocytes was measured and comparisons were made between activated hemocytes (those cells that had responded to wound cues and were present at the wound site), and quiescent hemocytes (non-responders, distal to the wound site). Measurement of pY intensity indicated significantly enhanced pY expression in activated hemocytes at the wound site versus quiescent hemocytes distal to the wound (Figure 3.5).

### 3.5 Exogenous $H_2O_2$ saturation impairs hemocyte random migration

$H_2O_2$ has been identified as an early wound cue generated locally after tissue damage [287]. Immune cells respond to the $H_2O_2$ gradient and migrate towards its source. We examined the effects of saturated $H_2O_2$ environments upon random hemocyte motility to see if exploratory behaviour was influenced by stable concentrations of $H_2O_2$. WT embryos containing GFP expressing hemocytes were incubated with increasing concentrations of $H_2O_2$ for 10 minutes before hemocyte random migration was imaged using time-lapse microscopy for 5 minutes. Individual cell trajectories were tracked and cell velocity and accumulated distance measured. Embryos incubated in $H_2O_2$ had a significant and dose dependent impairment in random migration velocity and total migratory distance versus PBS treated control embryos (Figure 3.6).

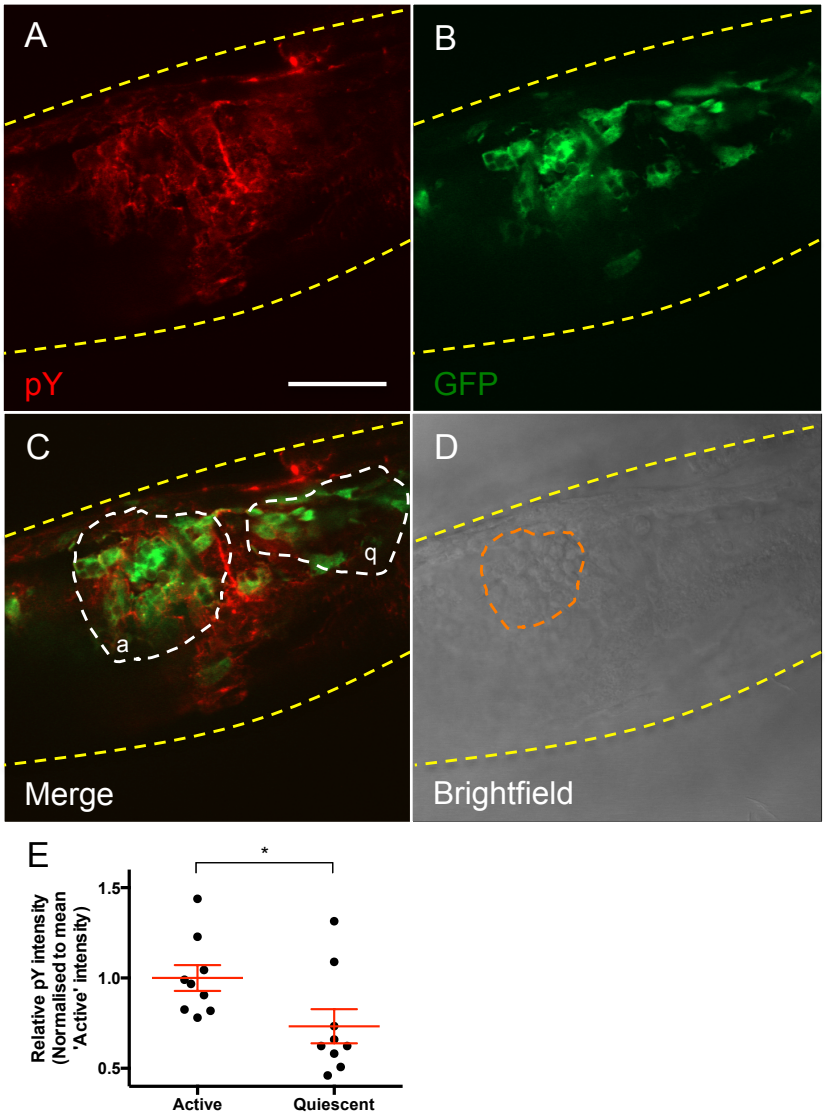


**Figure 3.5: Phosphotyrosine (pY) intensity is increased in activated hemocytes at the wound site.** WT *Drosophila* embryos at developmental stage 15 expressing crq-UAS,Gal4-GFP were wounded with a laser, fixed in PFA and immunostained to visualise pY. The embryo was imaged using confocal microscopy to locate the wounded epithelium. Representative images of (A) pY signal, (B) GFP hemocyte signal and (C) merged channel image. Yellow dashed lines indicates embryo outline. White dashed lines indicate areas sampled for quantification of (a) active hemocytes at the wound, or (q) quiescent hemocytes distal to the wound. (D) Brightfield image of embryo epithelium. Orange dashed line denotes wound site. (E) Quantification of pY signal intensity in hemocytes from an 'active' or 'quiescent' area of the embryo. Data collected from a single embryo. Scale bar = 20μm. Statistical analysis by unpaired t test, where *=$p<0.05$.

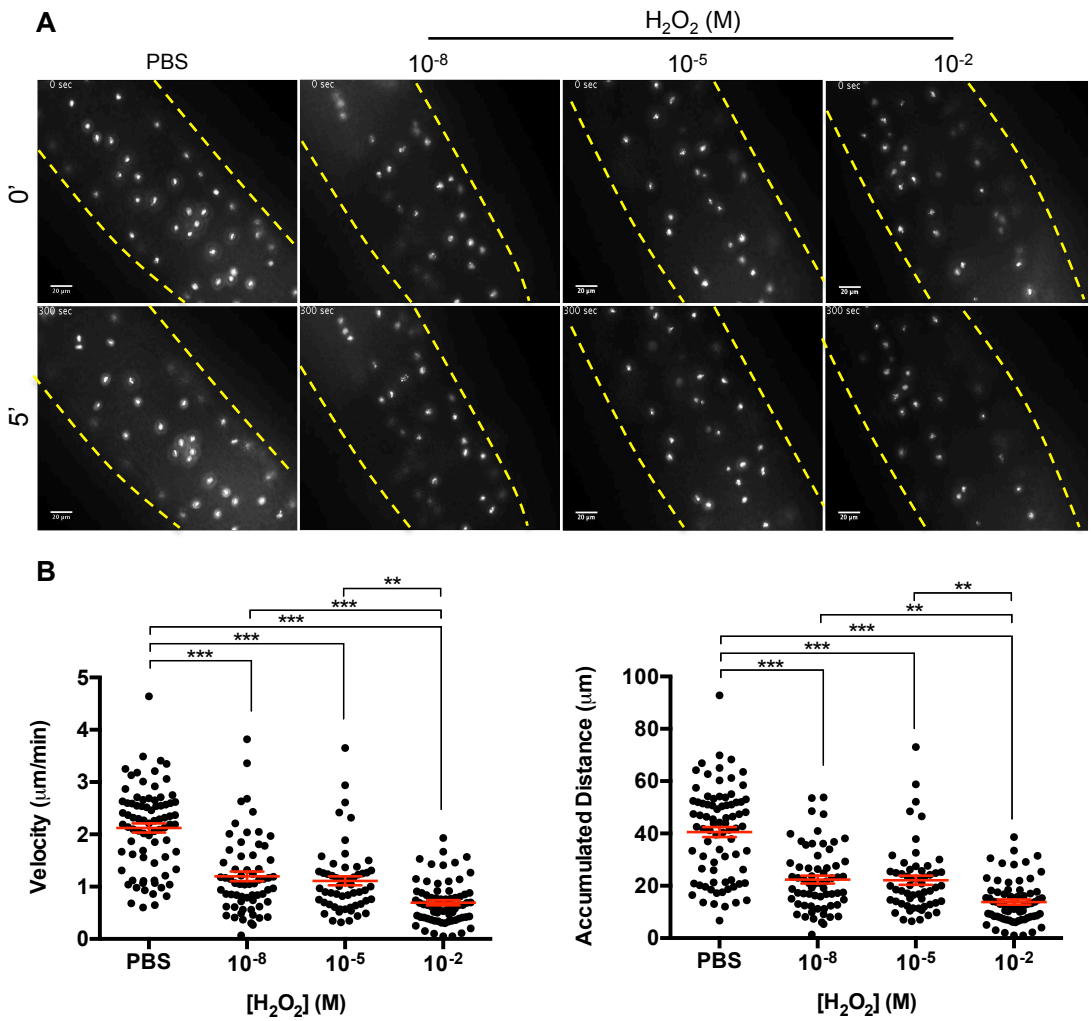


**Figure 3.6: Exogenous $H_2O_2$ impairs hemocyte random migration in *Drosophila* embryos**. WT *Drosophila* embryos at developmental stage 15 expressing crq-UAS,Gal4-GFP were dechorionated, permeabilised in methanol for 5 minutes, and incubated with increasing concentrations of $H_2O_2$ or PBS for 10 minutes. Following treatment, embryos were mounted and imaged over time using a light microscope with GFP filter. Images of each embryo were acquired every 30 seconds. (A) Stills from time-lapse imaging after 0 and 5 minutes, dashed yellow lines indicate embryo outline. (B) Hemocytes were manually tracked and quantification of hemocyte velocity and accumulated distance measured using ImageJ software with 'Manual tracking' plugin. Data represents velocity or distance (± SEM), from at least 25 hemocytes pooled from 3 embryos per genotype. Scale bar = 20μm. Statistical analysis by one way-ANOVA with Tukey's post test, where **=p<0.01, ***=p<0.001.

### 3.6 Summary of results

- Hemocyte accumulation at a wound was significantly impaired in Src42A$^{E1}$ and Src42A$^{K10108}$, but not Src42A$^{myri}$, mutant embryos compared to WT embryos.
- Hemocytes migrated to a wound with significantly reduced velocity and directionality in Src42A mutant embryos compared to WT embryos.
- Hemocyte random migration was not significantly impaired in Src42A mutant embryos compared to WT embryos.
- Hemocyte accumulation at a wound was significantly impaired in Shark$^{1}$ mutant embryos compared to WT embryos.
- pY intensity was increased in 'activated' hemocytes that are present at the wound compared to hemocytes in distal regions of a wounded embryo.
- Hemocyte random migration velocity was significantly impaired following embryo incubation with exogenous $H_2O_2$.

### 3.7 Chapter 3 Discussion

#### Src42A and Shark kinases are required for immune cell migration to a wound

In *Drosophila* embryos lacking functional Src42A, immune cell recruitment to a wound was impaired in comparison to responses in wild type embryos. The speed and directionality of immune cell migration was also compromised. However, migration and motility in the absence of a wound was unaffected by a Src42A mutation. This result agrees with the findings of Yoo *et al* (2011) that SFKs play a role in coordinating neutrophil migration following epithelial damage in zebrafish larvae [282]. Src42A has previously been found to inhibit wound-induced transcriptional events in epidermal cells [278], thus having an anti-inflammatory role in limiting epithelial responses to damage. However, other studies have found that Src42A$^{E1}$ mutant embryos, which gave the strongest phenotype in our experiments, fail to heal and show delayed re-epithelialisation after wounding [396]. The strongest phenotype in our experiments was found in Src42A$^{E1}$ mutant embryos, where the Src42A kinase domain lacks a carboxyl-terminal group. This implies that the kinase domain and ability of Src42A to phosphorylate other proteins is crucial in driving directed cell migration to a wound. The Src42A$^{myri}$ mutant embryos showed the least severe phenotype in the wounding assay, with no significant difference in the number of hemocytes recruited to a wound versus WT embryos. The mutation in Src42A$^{myri}$ embryos results in the protein being unable to localise to the plasma membrane. Our observations therefore suggest that this ability is not essential for detection of a wound cue and activation of Src42A. The Src42A$^{K10108}$ embryos showed an intermediate phenotype in response to wounds, indicating that the transgene insertion does not completely block its ability to function as a mediator downstream of tissue damage. Taken together, our findings show that in the immune cell compartment, at least, Src42A is likely to promote inflammation, while there may be diverging roles for SFKs in different tissues associated with the wound response.

Similarly, immune cell recruitment to a wound in *Drosophila* embryos lacking functional Shark kinase was significantly impaired. This is complementary to other reports demonstrating the role of Shark in cell migration in the setting of embryonic dorsal

closure [289]. Shark tyrosine kinase may be activated directly or indirectly by wound-associated $H_2O_2$. This cannot be concluded from our studies alone, however in other settings $H_2O_2$ has been reported to activate tyrosine kinase signalling and complex formation [397]-[399]. To study whether Src42A and Shark are interacting downstream, heterozygote mutants containing one allele of each mutation could be engineered and studied in the wound model. If the recruitment phenotype was exacerbated in heterozygote mutants, this would suggest that Src42A and Shark are signalling in distinct pathways.

We found no linear correlation between wound size and the number of recruited immune cells in our Src42A or Shark mutant embryos. This suggests the total cell number in these embryos may be reduced and could account for the impaired recruitment we observe following wounding. Additionally, the mutations could affect the development and dispersal of hemocytes – a process that is normally tightly regulated by PVF gradients [270]. The mutant lines used here contained disrupted genes of interest. However, the mutant genes are not expressed specifically in hemocytes but in every cell of the embryo. Embryo wide genetic disruption is likely to have wide-reaching consequences given the infidelity of genes in multiple organ systems. However, our observations confirmed that random exploratory hemocyte velocity is unaffected by the loss of active Src42A. This indicated that while Src42A may be involved in detection of damage cues, it is unlikely to be a key signalling mediator in undirected motility.

How Src42A 'activation' leads to directed cell migration still remains to be uncovered. From our studies alone we cannot identify the downstream targets of Src42A. Because SFKs lie upstream of many other signalling mediators we can predict that it is likely to be targeted by $H_2O_2$ directly, or indirectly via receptors that activate/recruit Src42A. Others have demonstrated that Src42A may serve as a negative regulator of receptor tyrosine kinases (RTKs). [400]. This has been suggested to be Ras-independent, indicating that Src42A works in a parallel pathway alongside Ras/Raf/MAPK signalling to inhibit RTK-mediated responses. Tateno *et al* (2000) suggest that Src42A may function in a synergistic manner with the tyrosine kinase Tec29 during dorsal closure and this pathway could be involved in migratory processes in hemocytes [394]. By localised expression of gain-of-function and dominant-negative forms of Src42A, it was demonstrated that Src42A may be involved in the regulation of cytoskeleton organisation and cell-cell contacts in the *Drosophila* eye [401].

Given the complexity and indistinct functions of Src42A it will be pertinent to investigate the how embryos lacking functional Src42A-downstream mediators, particularly components of the MAPK pathway and Rac/Cdc42a pathway, respond to damage cues. In addition, it cannot be ruled out that other damage signals may also be produced following tissue injury in this model and could be acting in concert with $H_2O_2$ to initiate migration. For example, extracellular ATP is considered a likely wound-associated signal that can alert cells to damage [357]. However, when *Drosophila* embryos lacking functional *Drosophila* purinergic receptor were wounded, normal hemocyte recruitment responses were observed [270], suggesting additional factors could compensate for loss of ATP signalling.

**Kinase activity is upregulated at sites of tissue damage**

Our initial data indicate that kinase activity could be upregulated at the site of tissue damage. This is in agreement with previous reports showing phosphotyrosine up-regulation in epidermal wounds [402] and activation of JNK signalling in wound healing [403]. Immunostaining wounded embryos offers the ability to reveal phosphorylation that may not otherwise be possible via genetically encoded reporters *in vivo.* While our results do indicate a higher phosphotyrosine signal in the vicinity of the wound compared to distal sites, we cannot conclude as to its tissue-specific location. The embryo used for this experiment contained GFP-expressing hemocytes and was immunostained for embryo-wide pY. When overlaid, the pY and GFP signals appear to co-localise particularly in the area where hemocytes have accumulated. However, kinase activity will be embryo wide and is likely to have important roles in many processes involved in the wound response. This approach cannot tell us for certain if the pY is upregulated in the wound hemocytes specifically. It is difficult to pinpoint specific pY expression in hemocytes, especially when images are taken from a fixed, uneven surface of an embryo. To confirm that Src42A is being activated during the wound response, or to identify kinase activity from other mediators, it may be more appropriate to dissect individual cells types and examine phosphorylation events *ex vivo*, or to use a genetic reporter *in vivo,* as live imaging will reveal a more dynamic response in actively migrating cells.

**Exogenous $H_2O_2$ slows hemocyte random exploratory migration**

The wound-generated $H_2O_2$ gradient has been shown to recruit neutrophils in a zebrafish larvae model of tissue injury [233]. To investigate the significance of an established $H_2O_2$ gradient, we were interested to study how exposure to exogenous, stable concentrations of $H_2O_2$ affected hemocyte motility. The effect of exogenous $H_2O_2$ in model organisms has been previously investigated in different settings. Exogenous $H_2O_2$ promotes growth of severed axons in zebrafish following tailfin transection [404]. It is likely that this process occurs in parallel with the neutrophil migratory response and that these are both in fact mediated by tissue damage-generated $H_2O_2$. In adult *Drosophila*, feeding or injection of $H_2O_2$ causes increased adult fly locomotor activity and affects circadian rhythms [405]. Furthermore, in a mouse model of T cell migration, chemokine-dependent AQP3-mediated influx of extracellular $H_2O_2$ was crucial for the activation of Rho GTPase Cdc42 and subsequent actin remodelling, leading to T cell migration [328].

When embryos were permeabilised and bathed in exogenous $H_2O_2$, hemocyte motility was slower and some cells were in fact stationary at the highest $H_2O_2$ concentrations. These results are unexpected and can be interpreted in several ways. Firstly, the stable, $H_2O_2$-saturated conditions created in this assay could reflect the environment at sites closest to tissue damage, where the $H_2O_2$ concentration is greatest. This represents the ‘target’ for migrating cells and could induce their arrest via inhibition of actin-mediated pathways in order to hold the cells at the damage site and allow them to carry out other processes such as phagocytosis. It may also suggest that the $H_2O_2$ signal overrides any other embryonic guidance cues that may be regulating their embryonic dispersal at the time of wounding. This could explain why we have observed

a slowing of hemocyte migration when the $H_2O_2$ gradient is absent. Alternatively, the saturated $H_2O_2$ environment could be toxic to the cells and cause them to engage cell death mechanisms and stop migrating. To explore this further, studying functional processes such as phagocytosis in the presence of exogenous $H_2O_2$ could identify whether all the cell functions are halted. If the $H_2O_2$ is holding the cell at the site, we predict phagocytosis would be increased.

### Proposed mechanism of SFK activity in *Drosophila* embryos

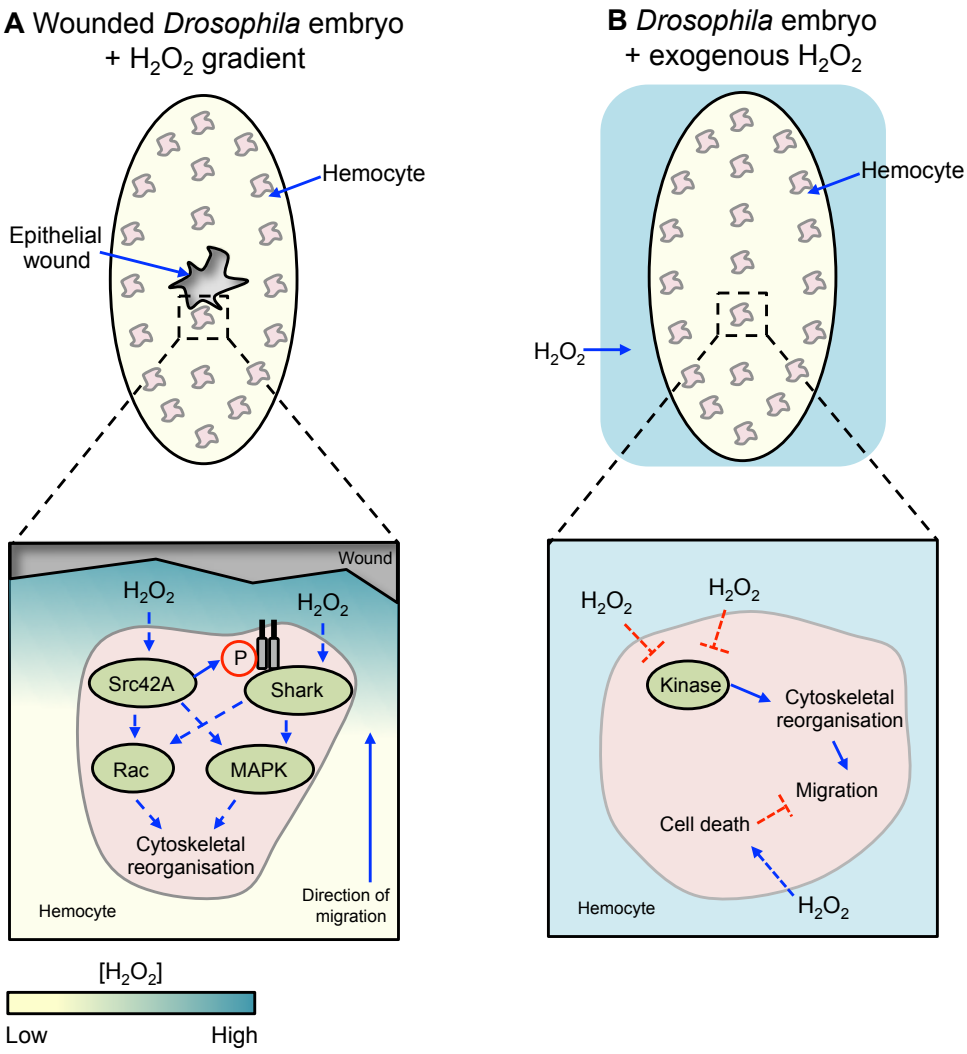


**Figure 3.7: Proposed models for hemocyte motility in the presence and absence of a $H_2O_2$ gradient.** (A) In *Drosophila* embryos, the presence of a $H_2O_2$ gradient leads to Src42A activation and downstream signalling resulting in cytoskeletal reorganisation and directed cell migration. The adaptor kinase, Shark, may function downstream of Src-phosphorylated ITAM-containing receptors via MAPK and Rac pathways to initiate directed cell migration in response to wounds. (B) When unwounded *Drosophila* embryos are bathed in exogenous, stable concentrations of $H_2O_2$, hemocyte random migration is reduced. This may be due to the action of $H_2O_2$ targeting protein kinase mediators of actin reorganisation, or by inducing cell death.

# CHAPTER 4: THE EFFECT OF DAMAGE-ASSOCIATED SIGNALS ON HUMAN INNATE IMMUNE CELL FUNCTION

## 4.1 Rationale

Innate immune cells are exposed to multiple signals throughout their lifetimes – during their development and maturation, their working lives as patrollers, engulfers and communicators, and finally during their end of life death mechanisms. In addition to homeostatic signals, innate cells can also encounter external foreign pathogenic signals and tissue damage-associated danger signals. The ability of innate cells to produce an integrated, signal specific response to all these signals is an essential driving force in inflammation.

Zebrafish models have demonstrated that immune cells can migrate to areas of tissue damage and that $H_2O_2$ is an early wound signal involved in recruiting cells to promote healing [233]. In humans, the role of $H_2O_2$ as a signalling molecule at low concentrations has been associated with various processes. However, at higher concentrations it is a danger signal, involved in the respiratory burst and ROS signalling. Additional danger molecules, such as nucleotides, are also generated at high concentrations at sites of tissue damage and have auxiliary roles in mediating inflammatory responses [406]. In a setting of inflammation, damage signals are generated by the same cells as pro-inflammatory mediators such as chemokines. Therefore, interactions between chemokines and damage signals are likely to occur *in vivo*. It is important to ask whether damage signals could serve to amplify chemoattractant-induced changes in the immunological and inflammatory capacities of leukocytes and the endothelium. Various reports offer conflicting views on the responses of human innate cells to exogenous damage signals. It is important to establish whether the role of damage signals in immune cell recruitment to a wound can be recapitulated in human cells, as this offers a novel strategy for the management of many inflammatory and autoimmune pathologies.

Two human innate immune cell types, neutrophils and monocytes, were employed to represent the innate immune system and to increase the range of known ligand-receptor interactions for comparisons to damage signals. In order to model human physiological processes most representatively, primary human neutrophils have been isolated from healthy human blood. A limitation of working with primary neutrophils is their short life span after purification (6–8 hours), which makes it difficult to manipulate specific signalling pathways other than using inhibitor-based approaches. Due to the difficulties in obtaining large numbers of blood-derived neutrophils and monocytes, and the variations between donors, a monocytic cell line THP-1 was also used in most experiments in this study.

The THP-1 cell line originates from a human child suffering from acute monocytic leukaemia. This pre-monocyte cell line possesses Fc and C3b receptors, as do monocytes [382]. THP-1 cells have a monocytic phenotype and can be differentiated into macrophage-like cells by various transforming factors such as phorbol esters and vitamin $D_3$ [385]. In some cases, an alternative monocytic cell line, U937, was used alongside or in place of THP-1 cells. The U937 monoblastic cell line was originally established from a human patient with diffuse hystiocytic lymphoma and has been used extensively in studies of myeloid differentiation [383]. All cell types were employed in a range of *in vitro* assays covering many known immediate functional responses observed during inflammation. These include chemotaxis, motility,

polarisation, receptor expression, signal prioritisation, calcium signalling, protein phosphorylation, phagocytosis, adhesion molecule expression and viability.

In summary, the aim of this chapter is to examine the effects of exogenous damage-associated signals on human innate immune cells, particularly with regard to key cellular functions triggered during early inflammation, including chemotaxis, polarisation and cell activation. We aim to compare immediate functional responses of innate immune cells following exposure to damage cues against known chemoattractants, in order to dissect their comparative role in the inflammatory environment. This approach will distinguish whether there is conservation between human and model organism responses to tissue damage, and will potentially identify key therapeutic targets that could aid the management of clinical inflammatory events as well as chronic inflammatory disease.

### 4.2 $H_2O_2$ does not act as a chemoattractant in the ChemoTx migration assay

*In vitro* models of cell migration have been employed for many decades to reproducibly show migration across a membrane towards a source of chemoattractant. Here, the ChemoTx migration assay has been used to characterise chemotaxis of the monocytic cell line THP-1 and primary human neutrophils (Figure 4.1). In agreement with many historical reports, monocytes migrated towards MCP-1 and M-CSF1 with optimal chemotaxis occurring with 10nM and 0.1nM chemoattractant respectively (Figure 4.1a). Additionally, primary neutrophils migrated towards fMLP, IL-8, IFNγ and $LTB_4$ with optimal concentrations of chemoattractant at 10nM, 10nM, 10ng/ml and 30nM respectively (Figure 4.1b). In all cases, chemotactic responses appeared to follow a bell-shaped response to increasing concentrations of chemoattractant.

After validating the assay with known chemoattractants, $H_2O_2$ was tested to demonstrate if it was acting in a similar fashion. $H_2O_2$ was placed in the lower well of the chemotaxis plate and cells were plated on top of the filter. For both monocytes and neutrophils, migration across the filter membrane was inhibited when $H_2O_2$ was present in the chemoattractant compartment versus plain media (Figure 4.2). Whilst in monocytes this appears to be a concentration dependent effect, with significant inhibition at micromolar and milimolar concentrations of $H_2O_2$ (Figure 4.2a), in neutrophils the effect is sustained at approximately 50% basal migration across the whole range of concentrations tested, but this is not statistically significant (Figure 4.2b).

### 4.3 Pre-incubation of cells with $H_2O_2$ inhibits monocyte and neutrophil chemotaxis in the ChemoTx migration assay

Given the observation that exogenous $H_2O_2$ did not act as a chemoattractant alone in the ChemoTx migration assay, the next objective was to establish whether exogenous $H_2O_2$ had an effect upon chemoattractant-mediated migration. Cells were pre-exposed to increasing concentrations of $H_2O_2$ before being plated in the upper compartment and exposed to a chemoattractant in the bottom well of the ChemoTx assay.

Monocyte migration towards optimal concentrations of MCP-1 and M-CSF1 was inhibited following exposure to exogenous $H_2O_2$ (Figure 4.3a left panel). Significant inhibition was observed throughout the picomolar to milimolar concentration range of $H_2O_2$ tested. The degree of inhibition appeared to be stronger in cells migrating towards MCSF-1, where 10mM $H_2O_2$ led to almost no cells being detected in the lower chamber. Similarly, neutrophil migration towards optimum concentrations of fMLP, IL-8 and $LTB_4$ was inhibited by approximately 50% following exposure to exogenous $H_2O_2$ (Figure 4.3b left panel), although variation was higher in neutrophils compared to monocytes. The inhibition of neutrophil migration to all chemoattractants did not appear to occur in a concentration dependent manner.

In both cell types basal migration was also inhibited by approximately 40-60% across the whole range of $H_2O_2$ concentrations tested compared to control cells, although this was not significant.

Figure 4.3 (right panels) compares chemotactic indices as a percentage of the control cell response. From this analysis it is possible to compare the effect of $H_2O_2$ treatment on basal and chemoattractant-mediated migration in each experiment. In THP-1 monocytes, basal migration was inhibited to a greater degree than MCP-1-mediated chemotaxis. However, M-CSF-1-mediated chemotaxis was inhibited more strongly by $H_2O_2$ than basal migrating cells, also in THP-1 monocytes. In neutrophils, the magnitude of inhibition of basal and chemoattractant-mediated migration was similar in all cases.

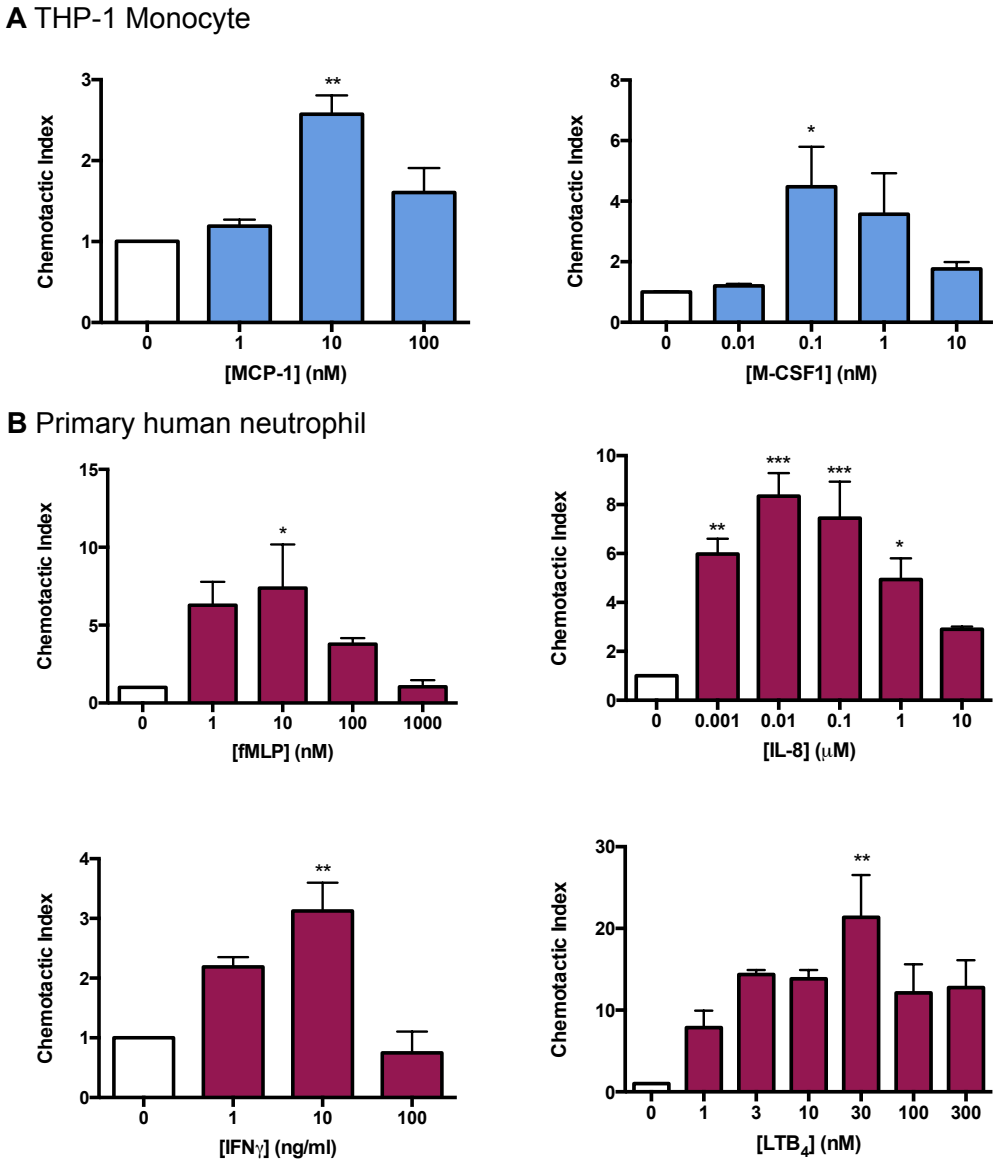


**Figure 4.1: THP-1 monocytes and primary human neutrophils migrate towards a range of chemoattractants.** (A) Chemotaxis of THP-1 monocytes towards increasing concentrations of MCP-1 and M-CSF1. (B) Chemotaxis of primary human neutrophils towards increasing concentrations of fMLP, IL-8, IFNγ and $LTB_4$. Cells were washed in serum free media, resuspended to $3.2x10^6$ cells/ml and plated on top of filter membrane above lower chambers containing chemoattractant or plain media. Chemotaxis across 5μm pore size membrane was determined after a 3 hour incubation at 37°C in 5% $CO_2$ as previously described. Data presented represent means ± SEM from at least three separate experiments. Statistical analyses by one way-ANOVA versus untreated control with Dunnett's multiple comparisons post hoc test where *=p<0.05, **=p<0.01, ***=p<0.001.

**A** THP-1 Monocyte

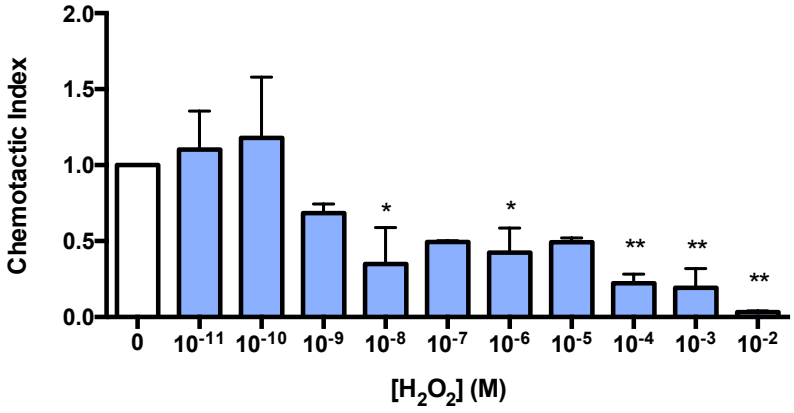


**B** Primary human neutrophil

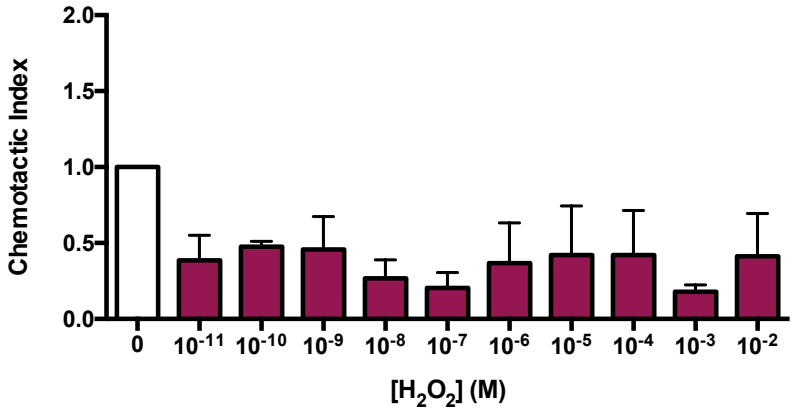


**Figure 4.2: $H_2O_2$ does not act as a chemoattractant in ChemoTx migration assay.** Chemotaxis of (A) THP-1 monocytes or (B) primary human neutrophils towards increasing concentrations $H_2O_2$. Cells were washed in serum free media, resuspended to $3.2x10^6$ cells/ml and plated on top of filter membrane above lower chambers containing $H_2O_2$ or plain media. Chemotaxis across 5μm pore size membrane was determined after a 3 hour incubation at 37°C in 5% $CO_2$ as previously described. Data presented represent means ± SEM from at least three separate experiments. Statistical analyses by one way-ANOVA versus untreated control with Dunnett's multiple comparisons post hoc test where *=p<0.05, **=p<0.01.

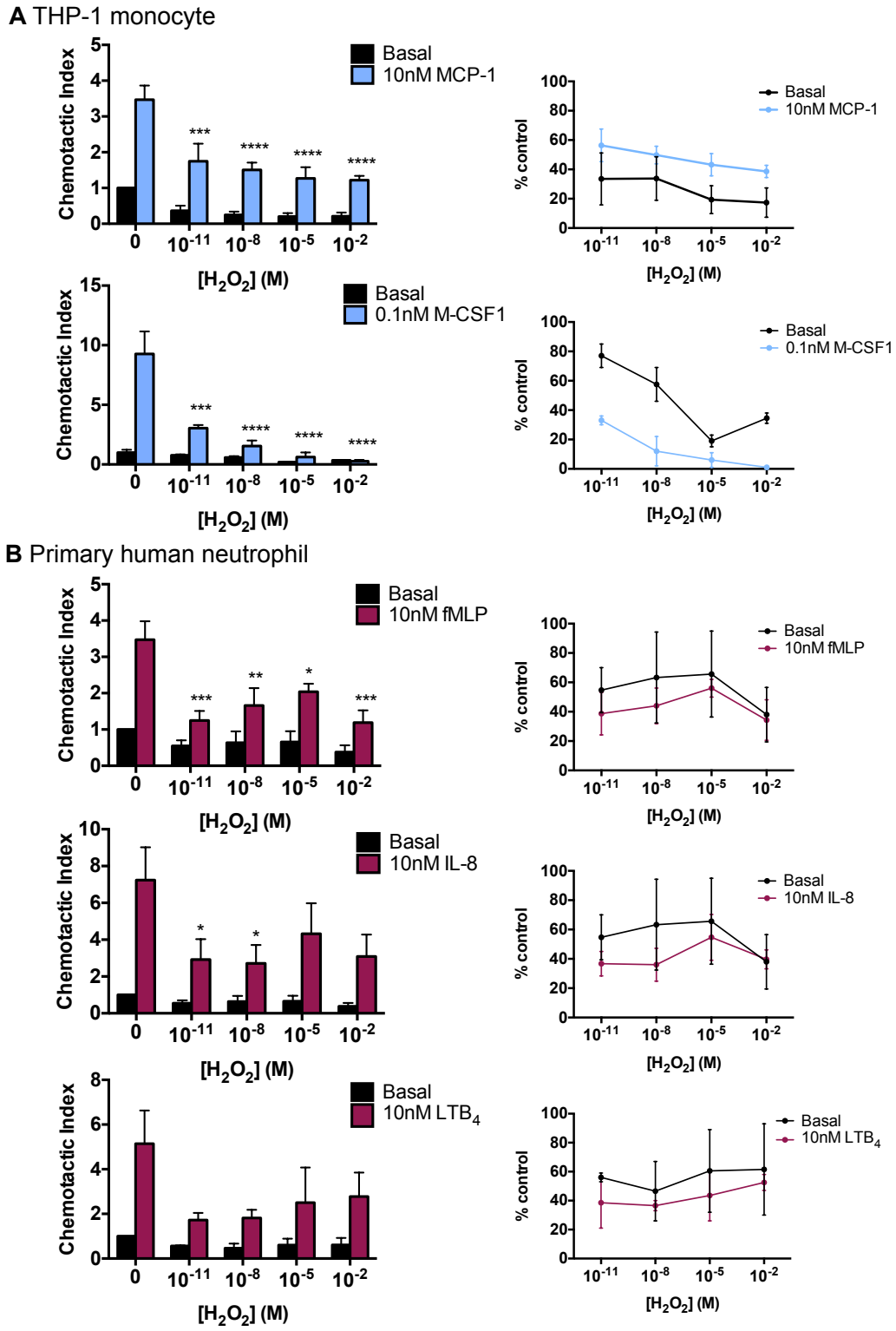


**Figure 4.3: Exogenous $H_2O_2$ inhibits THP-1 monocyte and primary neutrophil chemotaxis.** (A) Chemotaxis of THP-1 monocytes towards MCP-1 and M-CSF1 following pre-treatment with increasing concentrations of $H_2O_2$. (B) Chemotaxis of primary human neutrophils towards 10nM fMLP, IL-8 and $LTB_4$ following pre-treatment with increasing concentrations of $H_2O_2$. Migration expressed as chemotactic index (left panels), and as a percentage of control cells (right panels). Cells were washed in serum free media, resuspended to $3.2x10^6$ cells/ml and incubated with $H_2O_2$ for 30 minutes at 37°C before being plated on top of filter membrane above lower chambers containing attractant or plain media. Migration across 5μm pore size membrane was determined after a 3 hour incubation at 37°C in 5% $CO_2$ as previously described. Data presented represents means (± SEM) from at least three separate experiments, with samples run in triplicate. Statistical analyses by two way-ANOVA versus untreated control with Dunnett's multiple comparisons post hoc test. *=p<0.05, **=p<0.01, ***=p<0.001, ****=p<0.0001.

### 4.4 Inhibition of $H_2O_2$ production and signalling affects monocyte and neutrophil chemotaxis

The use of pharmacological inhibitors offers alternative strategies for investigating the effects of $H_2O_2$ upon cell migration; in particular the cellular events involved in autocrine $H_2O_2$ control and signalling can be dissected. Here two approaches to target the action of $H_2O_2$ have been used: Diphenyleneiodonium (DPI), a potent NADPH oxidase inhibitor, to block $H_2O_2$ generation; and catalase, an enzyme that rapidly catalyses the decomposition of $H_2O_2$ to water and oxygen. O'Donnell *et al* (1993) demonstrated that the inhibition constant ($K_i$) for time-dependent inhibition by DPI of human neutrophil membrane NADPH oxidase was 5.6μM [407], in light of this we have tested DPI in the concentration range of 1-100μM. Similarly, catalase has activity at 2000-5000 units/mg [Sigma Aldrich product information – enzymatic assay of catalase EC 1.11.1.6] therefore we have tested catalase in a concentration range of 0.1-1 mg/ml.

In the ChemoTx migration assay, cells were pre-treated with increasing concentrations of DPI or catalase before being exposed to optimal concentrations of chemoattractant. THP-1 monocyte chemotaxis to MCP-1 was significantly inhibited to approximately 30-40% of the untreated control with DPI treatment (Figure 4.4a). Basal monocyte migration was also inhibited to 20-30% of the untreated control by DPI pre-treatment. Similarly, treatment with increasing concentrations of catalase significantly inhibited MCP-1-mediated monocyte migration. Basal migration was also inhibited to 20-40% of the untreated control, although this was not significant. Inhibition with catalase appeared to be concentration dependent in both cases.

Primary neutrophil migration to IL-8 was inhibited to approximately 20% of the untreated control following treatment with increasing concentrations of DPI (Figure 4.4b). Basal migration was also inhibited in a more variable albeit seemingly concentration dependent manner. Pre-treatment of neutrophils with catalase increased both basal and IL-8 mediated migration in a concentration dependent manner. 1mg/ml catalase increased neutrophil migration to IL-8 by approximately 2-fold.

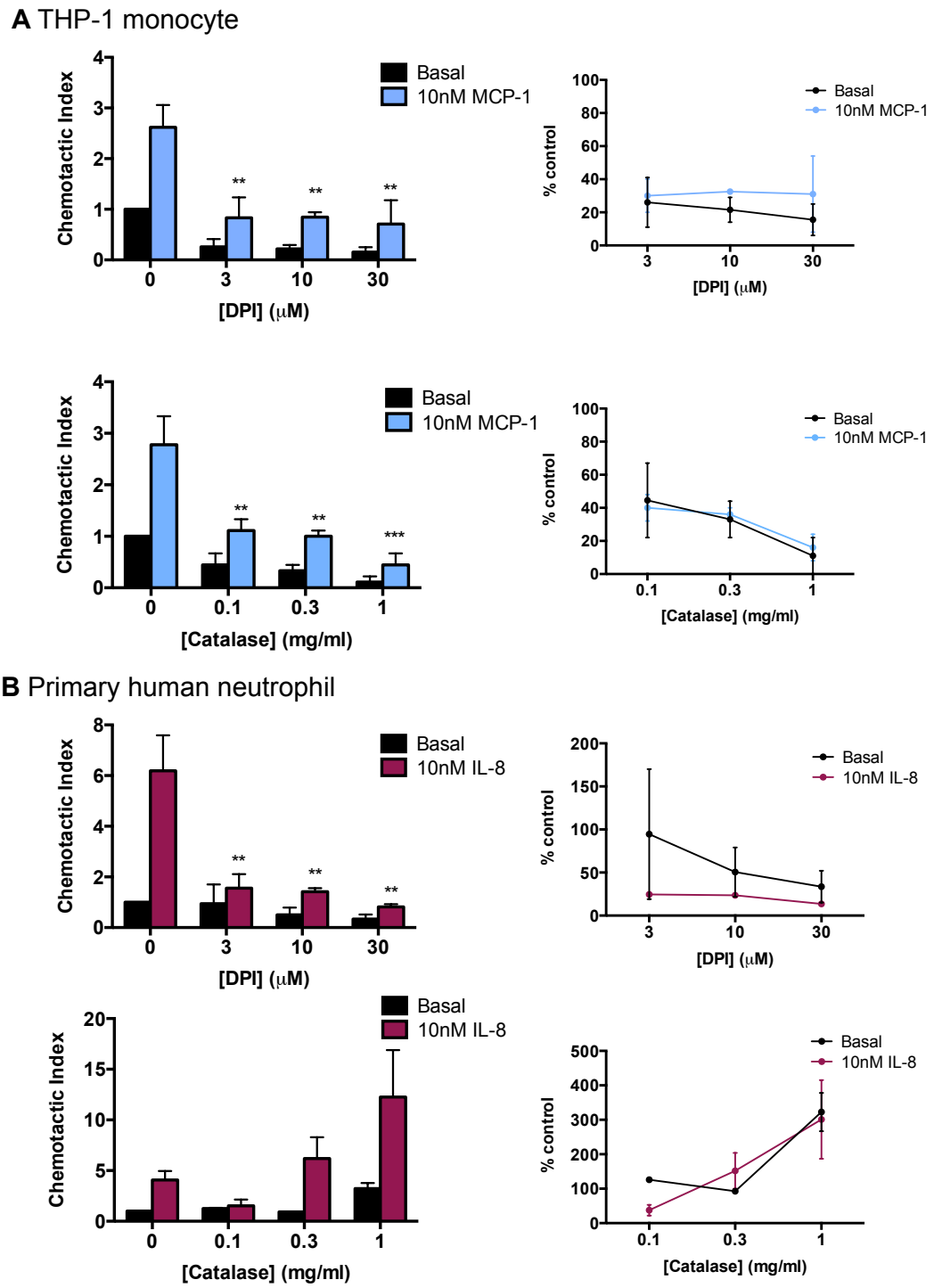


**Figure 4.4: DPI inhibits THP-1 monocyte and primary neutrophil chemotaxis while catalase inhibits THP-1 monocytes but increases primary neutrophil chemotaxis.** (A) Chemotaxis of THP-1 monocytes towards 10nM MCP-1 following pre-treatment with increasing concentrations of DPI or catalase. (B) Chemotaxis of primary human neutrophils towards 10nM IL-8 following pre-treatment with increasing concentrations of DPI or catalase. Migration expressed as chemotactic index (left panels), and as a percentage of control cells (right panels). Cells were washed in serum free media, resuspended to $3.2x10^6$ cells/ml and incubated with DPI or catalase for 30 minutes at 37°C before being plated on top of filter membrane above lower chambers containing chemoattractant or plain media. Migration across 5μm pore size membrane was determined after a 3 hour incubation at 37°C in 5% $CO_2$ as previously described. Data presented represents means (± SEM) from at least three separate experiments, with samples run in triplicate. Statistical analyses by two way-ANOVA versus untreated control with Dunnett's multiple comparisons post hoc test. *=p<0.05, **=p<0.01, ***=p<0.001.

### 4.5 Neutrophils migrate under agarose towards IL-8, fMLP and $H_2O_2$

The under agarose cell migration assay offers an alternative *in vitro* method for quantitative analysis of cell migration. The assay can be used for studying cell chemotaxis, as well as measuring cellular responses to multiple chemotactic gradients. The under agarose assay has been used to show that an intracellular signalling hierarchy determines chemotaxis in opposing gradients using known chemoattractants [189].

Firstly, to examine the nature of neutrophil chemotaxis in the under agarose migration assay, primary human neutrophils were exposed to increasing concentrations of known intermediary or end-target chemoattractants, IL-8 (Figure 4.5a(i)) or fMLP (Figure 4.5a(ii)), with plain buffer used as a control in the opposite well to measure basal migration. For both chemoattractants, neutrophils migrated in a concentration dependent manner towards the source of the chemoattractant, with 100nM IL-8 and 10nM fMLP stimulating strong migration. Despite high variation of migration between human donors, the number of cells that migrated towards optimal concentrations of IL-8 and fMLP was approximately 200-300 cells.

This assay has previously been employed to show the migration of human neutrophils towards 10μM $H_2O_2$ [282]. Here it was used to examine whether this result was reproducible and whether chemotaxis induced by $H_2O_2$ was comparable to that induced by known chemoattractants. 10μM $H_2O_2$ induced a chemotactic response that was on average 2.3 times greater than to HBSS control alone. In the same experiment, 10nM IL-8 and 10nM fMLP stimulated a chemotactic response that was 5.7 and 5.1 times greater, respectively, than to HBSS buffer control alone (Figure 4.5b).

In order to model a more physiologically relevant scenario, the next objective was to explore the effect of multiple chemoattractant signals on a single neutrophil population and determine whether the cells were showing a preference to one signal over another. When exposed to opposing gradients of 10nM IL-8 and 10nM fMLP, cells preferentially migrated towards fMLP (Figure 4.5c). The migratory response to fMLP was approximately 1.3 times greater than to IL-8. When exposed to opposing gradients of 10nM IL-8 and 10μM $H_2O_2$, cells preferentially migrated towards IL-8, with 3.6 times greater migration over $H_2O_2$. Finally, when exposed to opposing gradients of 10nM fMLP and 10μM $H_2O_2$, cells preferentially migrated towards fMLP; migration towards fMLP was 9 times greater than towards $H_2O_2$. Interestingly, migration to fMLP was greatly reduced when the cells were co-exposed to $H_2O_2$ compared to when the cells were co-exposed to IL-8.

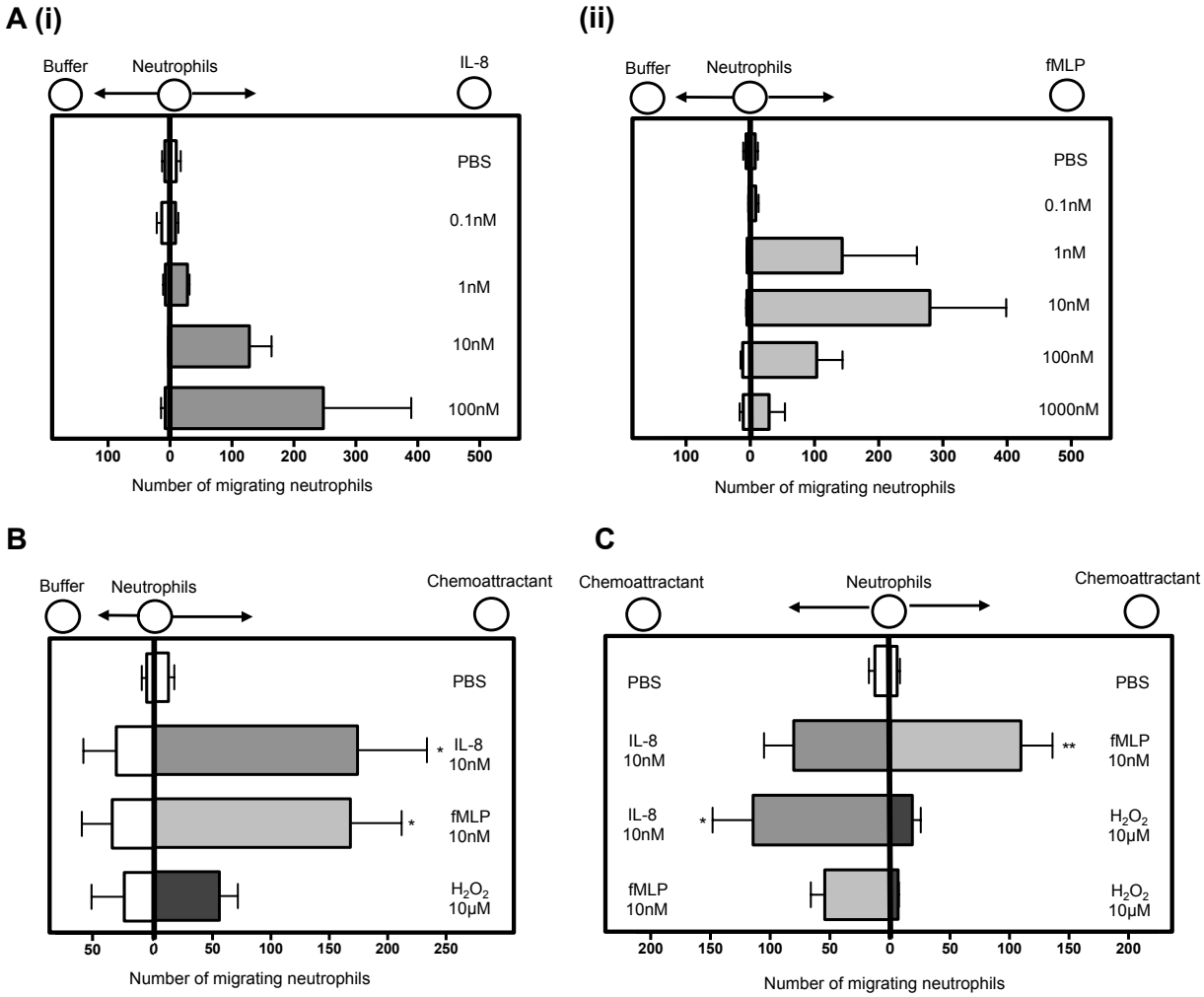


**Figure 4.5: Primary human neutrophils migrate under agarose towards IL-8, fMLP and $H_2O_2$.** Neutrophils were isolated from human blood, resuspended in $Ca^{2+}$-free HBSS at $1x10^6$ cells/ml and rested for 1 hour. $1x10^4$ cells were placed in central wells and 10μl chemoattractant in outer wells of agarose plate prepared as described in Chapter 2. Cells were allowed to migrate for 2 hours at 37°C. Following incubation gels were photographed and the number of cells that had migrated towards the chemoattractant containing well was counted in a defined area. (A) Neutrophil migration towards increasing concentrations of (i) IL-8 or (ii) fMLP or HBSS control. (B) Neutrophil migration towards sub maximal concentrations of IL-8 (10nM) or fMLP (10nM) and 10μM $H_2O_2$. (C) Cells plated between pairs of chemoattractants in different combinations for prioritisation experiment between IL-8, fMLP and $H_2O_2$. Data represents means (±SEM) from at least three separate experiments, samples run in triplicate. Statistical analyses by one way-ANOVA versus PBS control with Dunnett's multiple comparisons post hoc test. *=p<0.05, **=p<0.01.

### 4.6 Neutrophil chemotaxis under agarose is not affected by exogenous $H_2O_2$

Using the ChemoTx migration assay, we demonstrated that exogenous $H_2O_2$ inhibited monocyte and neutrophil migration towards a range of chemoattractants. To investigate whether this observation was reproducible in the under agarose migration assay, neutrophils were pre-treated with increasing concentrations of $H_2O_2$ before being exposed to 10nM IL-8 or 10nM fMLP, with HBSS buffer control in the opposite well for the study of basal migration. Neutrophil migration towards IL-8 or fMLP was not affected when neutrophils were pre-treated with $H_2O_2$ (Figure 4.6a).

The effect of $H_2O_2$ on chemoattractant preference was also studied using the under agarose migration assay. As before, neutrophils were pre-treated with increasing concentrations of $H_2O_2$ before being exposed to opposing gradients of 10nM IL-8 and 10nM fMLP simultaneously. Neutrophils preferentially migrated towards fMLP. Pre-treatment with $H_2O_2$ did not significantly compromise overall neutrophil migration, nor did it affect the cell's preference to migrate to fMLP over IL-8 (Figure 4.6b).

Having examined the effect of exogenous $H_2O_2$ directly on neutrophils in the under agarose assay, we next investigated whether $H_2O_2$ could influence migration if placed in the chemoattractant containing well, together with chemoattractant. Neutrophil migration towards 10nM IL-8 was not affected when cells were pre-treated with 10μM $H_2O_2$ or when $H_2O_2$ was added to the chemoattractant containing well together with IL-8 (Figure 4.7a(i)). Similarly, migration towards 10nM fMLP was not affected if $H_2O_2$ was in the cell or chemoattractant compartment (Figure 4.7a(ii)). Finally, when neutrophils were exposed to both fMLP and IL-8 simultaneously, neither overall migration nor preference for fMLP was compromised when $H_2O_2$ was placed in the cell or chemoattractant compartment (Figure 4.7b).

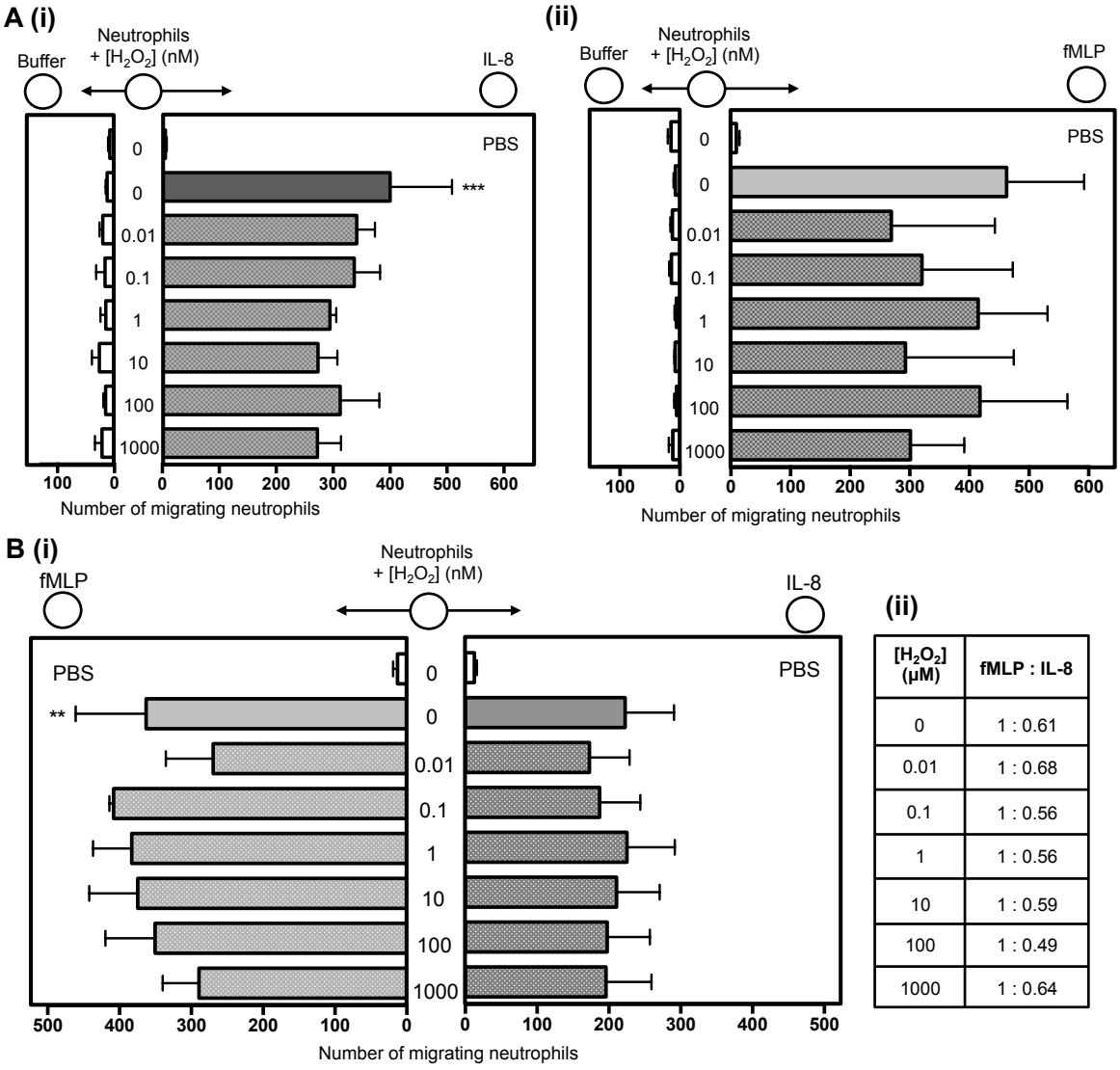


**Figure 4.6: Neutrophil chemotaxis under agarose towards IL-8 or fMLP is not affected by exogenous $H_2O_2$.** Neutrophils were isolated from human blood, resuspended in $Ca^{2+}$-free HBSS at $1x10^6$ cells/ml and rested for 1 hour at 37°C. Cells were treated with increasing concentrations of $H_2O_2$ for 30 minutes. $1x10^4$ cells were placed in central wells and 10µl chemoattractant in outer wells of agarose plate prepared as described in Chapter 2. Cells were allowed to migrate for 2 hours at 37°C. Following incubation gels were photographed and the number of cells that had migrated towards chemoattractant containing well was counted in a defined area. (A) Neutrophil migration towards (i) 10nM IL-8 or (ii) 10nM fMLP or HBSS control following pre-treatment with $H_2O_2$ or PBS. (B) (i) Prioritisation experiment between 10nM IL-8 and 10nM fMLP following pre-treatment with increasing concentrations of $H_2O_2$, (ii) Table showing ratios of IL-8 and fMLP migration responses in prioritisation experiments following pre-treatment with $H_2O_2$. Data represents means (±SEM) from at least three separate experiments, samples run in triplicate. Statistical analyses by one way-ANOVA versus PBS control with Dunnett's multiple comparisons post hoc test. **=p<0.01, ***=p<0.001.

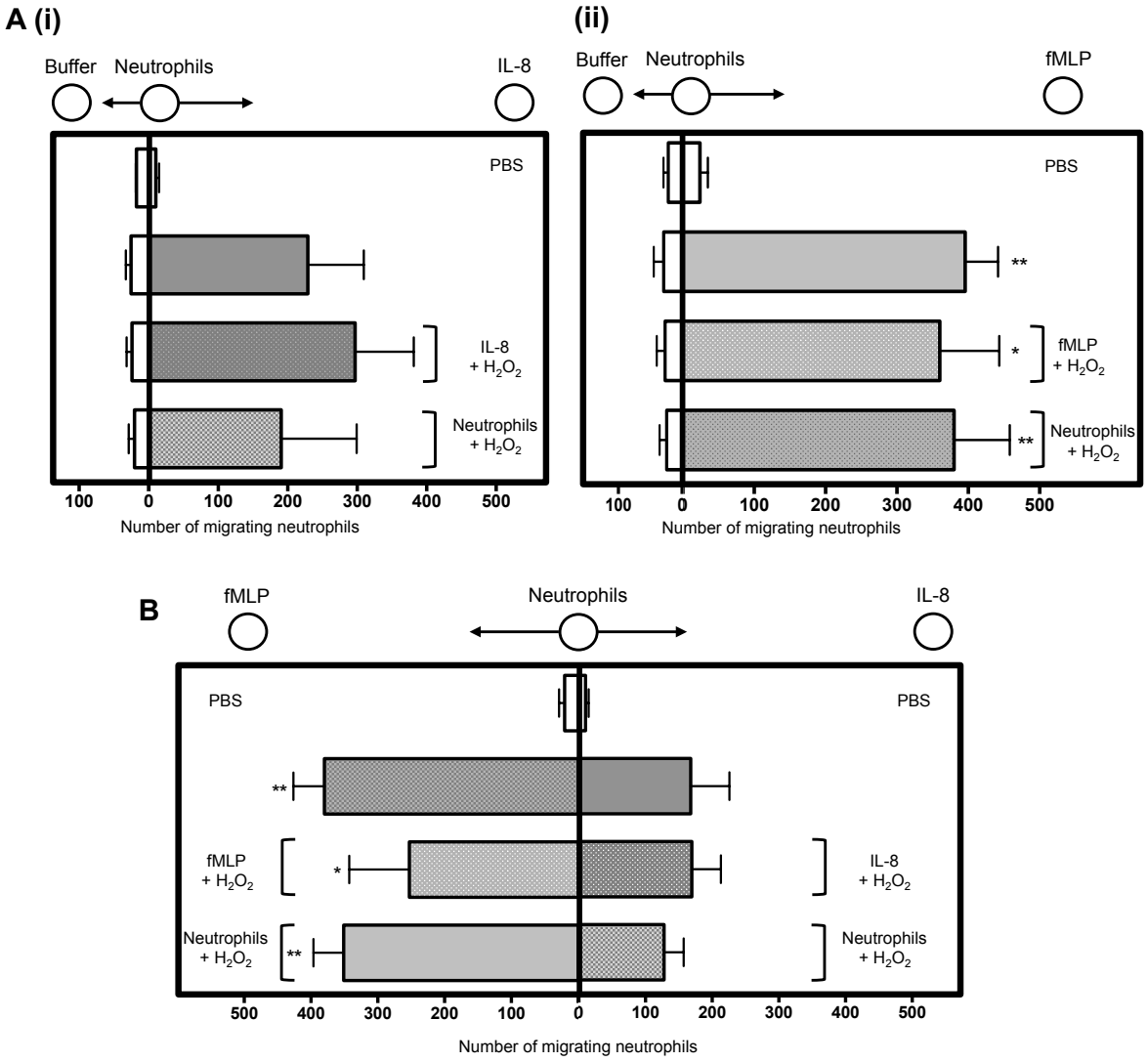


**Figure 4.7: Neutrophil chemotaxis under agarose towards IL-8 or fMLP is not affected by exogenous $H_2O_2$ in either the cell or chemoattractant compartment.** Neutrophils were isolated from human blood, resuspended in $Ca^{2+}$-free HBSS at $1x10^6$ cells/ml and rested for 1 hour at 37°C. Cells were treated with 10μM $H_2O_2$ or PBS for 30 minutes. $1x10^4$ cells were placed in central wells and 10μl chemoattractant in outer wells of agarose plate prepared as described in Chapter 2. Chemoattractant alone, or chemoattractant with 10μM $H_2O_2$ was added to outer wells. Cells were allowed to migrate for 2 hours at 37°C. Following incubation gels were photographed and the number of cells that had migrated towards chemoattractant containing well was counted in a defined area. (A) Neutrophil migration towards (i) 10nM IL-8 or IL-8 with 10μM $H_2O_2$ or (ii) 10nM fMLP or fMLP with 10μM $H_2O_2$ or HBSS control following pre-treatment with 10μM $H_2O_2$ or PBS control. (B) Prioritisation experiment between 10nM IL-8 and 10nM fMLP, or IL-8 with 10μM $H_2O_2$ and fMLP with 10μM $H_2O_2$, or to IL-8 and fMLP following pre-treatment with 10μM $H_2O_2$. Data represents means (±SEM) from at least three separate experiments, samples run in triplicate. Statistical analyses by one way-ANOVA versus PBS control with Dunnett's multiple comparisons post hoc test. *=$p<0.05$, **=$p<0.01$.

### 4.7 $H_2O_2$ does not affect neutrophil chemokinetic velocity

Our *in vitro* migration assays have suggested that $H_2O_2$ is not inducing a chemotactic phenotype in monocytes or neutrophils. To further explore the early migratory responses that occur upon cell stimulation, neutrophil migration on fibronectin coated chambered coverglasses was imaged over 30 minutes using time-lapse confocal microscopy. Migratory responses to different stimulants were recorded and analysed. Individual cell paths were tracked using ImageJ software that also calculates individual cell velocity.

Under basal conditions, neutrophils followed random paths of migration with an average velocity of 36.31μm/min (Figure 4.8). During imaging, cells generally remained round although faster moving cells showed a slightly more elongated form. Cell tracking paths indicate heterogenic motility, with some cells moving across the field of view, while others remain in place throughout imaging.

Stimulation of neutrophils with 10nM IL-8 immediately initiated a change in cell morphology from round and regular at resting to a much more elongated and irregular shape following stimulation. Cells appeared polarised, with a leading face in the direction of migration (Figure 4.8a). Cells were highly motile, with an average velocity of 82.63μm/min, significantly greater than PBS control treated cells (Figure 4.8b). Individual tracking paths indicate how neutrophils also explored a far greater area of the field of view than PBS control treated cells. However, imaging also revealed that approximately 20 minutes after the initial stimulation, the cells appear to return to a more regular rounded shape. Observations with fMLP mirror the responses to IL-8, with similarities in cell elongation and polarisation, exploratory behaviour and significantly increased velocity (89.91μm/min) versus PBS control (Figure 4.8). Neutrophils stimulated with fMLP remain elongated and irregularly shaped 30 minutes after the initial stimulation.

Upon stimulation with 10μM $H_2O_2$, neutrophils did not alter their morphology from the regular, round form pre-stimulation. The cells did not adopt a polarised morphology nor did they exhibit a clear leading edge. $H_2O_2$ stimulated neutrophils showed a reduced exploratory phenotype, although a few cells did migrate some distance while others remained in place throughout imaging. $H_2O_2$ stimulated neutrophils had an average velocity of 31.91μm/min, which is slower, but not significantly so, compared to PBS treated cells (Figure 4.8).

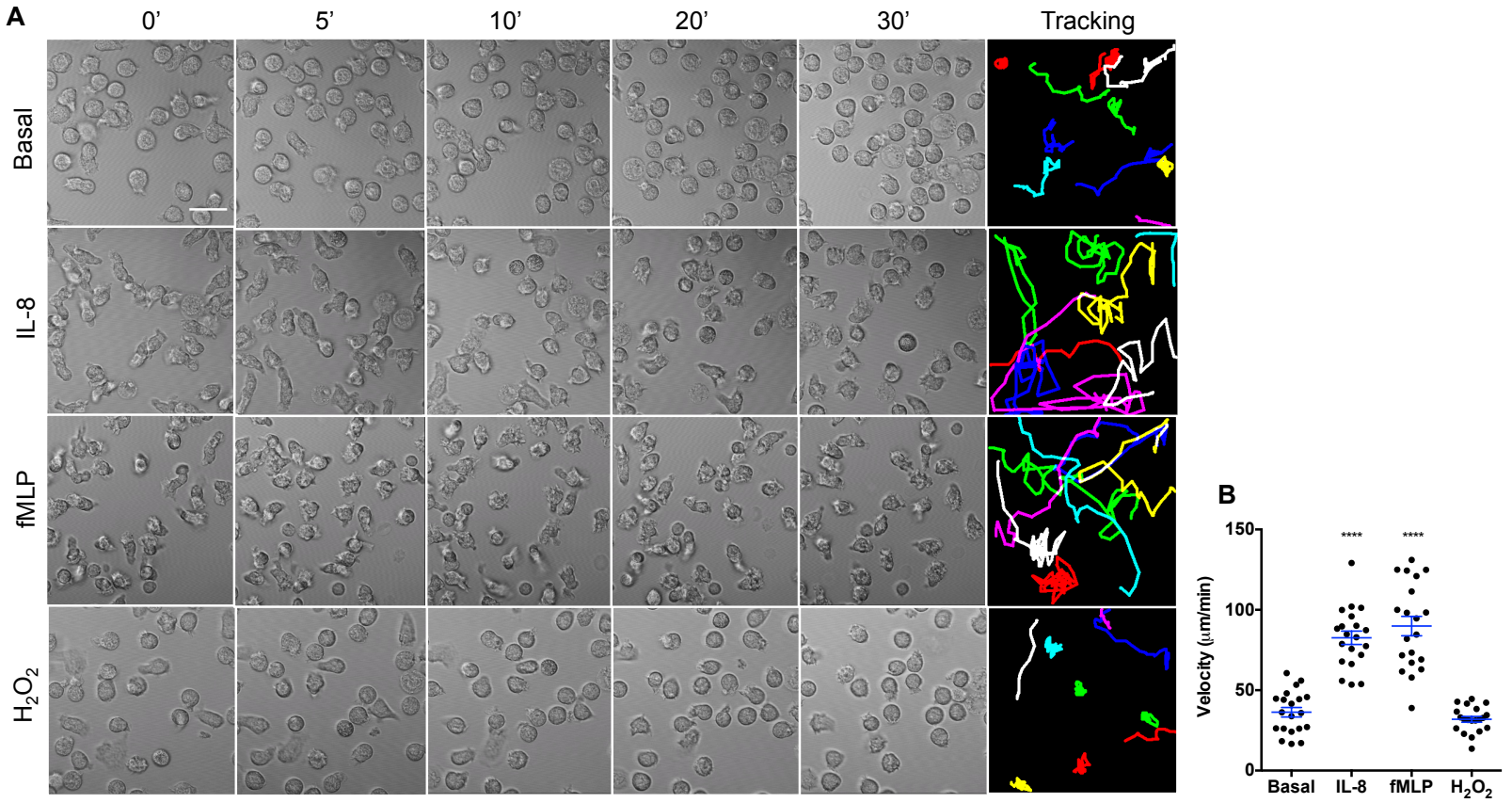


**Figure 4.8: Neutrophil motility is increased by stimulation with IL-8 and fMLP but not with $H_2O_2$.** Primary neutrophils were isolated from human blood, washed and rested. Cells were plated onto chambered coverglasses coated in 10μg/ml fibronectin and allowed to adhere for 20 minutes at 37°C. Cells were imaged using 40x oil objective on confocal microscope. (A) Images were acquired by time-lapse microscopy using the brightfield channel. Cells were stimulated with 10nM IL-8, 10nM fMLP, 10μM $H_2O_2$ or PBS and imaged for 30 minutes. Cell tracking was performed using ImageJ ‘Manual tracking’ plugin. Data shows representative images at time points (0 – 30 minutes) post stimulation, plus representative tracking showing individual cell paths. (B) Quantification of individual cell velocity per treatment group. Data represents means (±SEM) pooled from at least 3 separate experiments. Statistical analysis by one way-ANOVA with Dunnett’s post test, where ****=p<0.0001 versus basal group.

### 4.8 Cell viability is not compromised by sub-milimolar exogenous $H_2O_2$, catalase or DPI

It has been reported that $H_2O_2$ at high concentrations can be cytotoxic to cells [295]. It was therefore prudent to establish if the concentrations of $H_2O_2$ and its modulators selected for these studies were exhibiting such an effect on the cells. Monocytic cell lines and primary human neutrophils were exposed to increasing concentrations of exogenous $H_2O_2$ for up to 4 hours and cell viability was analysed using the MTT assay. Metabolically active, viable cells are able to convert MTT to formazan, giving a colour change detectable by a plate reader.

No significant change in enzymatic activity following up to 4 hours $H_2O_2$ stimulation was observed in THP-1 cells (Figure 4.9a). Enzymatic activity of the U937 monocytic cell line was unaffected by $H_2O_2$ up to 10μM. However, U937 cell viability was significantly decreased by 10mM $H_2O_2$ after 3 or 4 hours exposure compared to PBS treated control cells (Figure 4.9b). The viability of primary human neutrophils was also generally unaffected by increasing concentrations of $H_2O_2$, except 10mM $H_2O_2$ which significantly impaired neutrophil viability after 3 or 4 hours exposure, compared to PBS treated control cells (Figure 4.9c). Cell viability was also analysed in the presence of DPI and catalase. Primary human neutrophils were exposed to increasing concentrations of catalase or DPI for up to 4 hours before being used in the MTT assay. No change in cell viability was observed for all of the concentrations of either DPI or catalase tested (Figure 4.10).

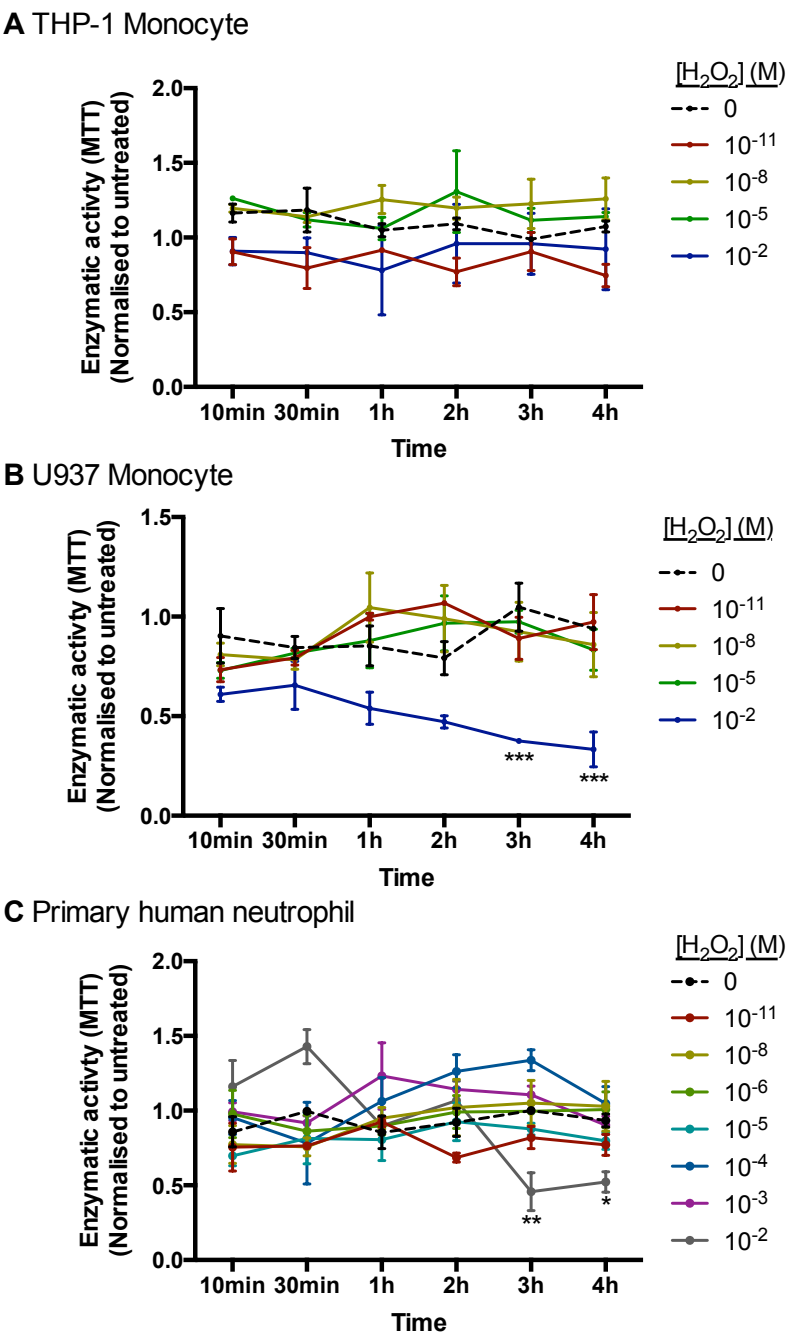


**Figure 4.9: Monocyte and neutrophil viability is unaffected by sub-milimolar concentrations of $H_2O_2$.** (A) THP-1 monocytes (B) U937 monocytes and (C) primary human neutrophils were exposed to increasing concentrations of $H_2O_2$ or PBS for up to 4 hours. Following culture, cells were assessed for viability using the MTT assay. Data presented represent means (± SEM) minus plate background and normalized to untreated control from at least three independent experiments measured in triplicate, n=3. Statistical analysis by two way-ANOVA with Tukey's multiple comparisons post hoc test where *=p<0.05, **=p<0.01, ***=p<0.001, versus time matched PBS control.

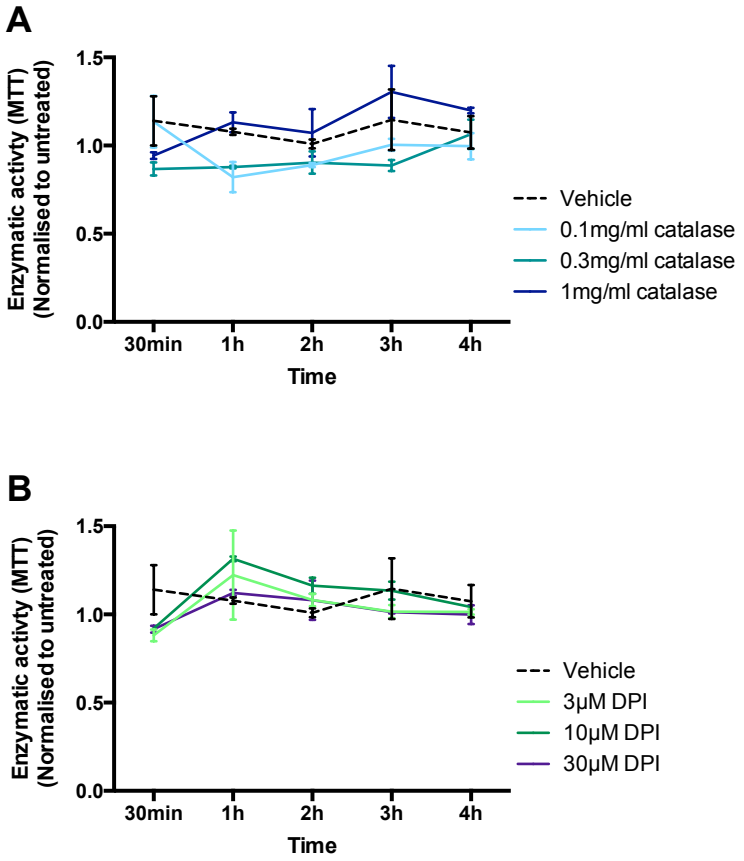


**Figure 4.10: Neutrophil viability is unaffected following exposure to catalase or DPI.** Primary human neutrophils were exposed to increasing concentrations of (A) catalase or (B) DPI or PBS vehicle control for up to 4 hours. Following culture, cells were assessed for viability using MTT assay. Data presented represent means (± SEM) minus plate background and normalized to untreated control from at least three independent experiments measured in triplicate, n=3.

### 4.9 $H_2O_2$ does not induce changes in monocyte actin organisation

Clear changes in cell morphology and motility in response to chemoattractant have so far been demonstrated, however little effect in response to $H_2O_2$ has been observed. To further investigate the effect of exogenous $H_2O_2$, DPI and catalase on cell morphology, THP-1 monocytes were seeded onto fibronectin-coated coverslips. Following treatment, cells were fixed and stained to visualise cellular F-actin by confocal microscopy. Quantitative analysis was carried out using CellProfiler software that calculates the degree of roundness of each individual cell, to give a circularity score that indicates the extent of cell polarisation, where 1 is a perfect circle. This analysis technique also measures the cell surface area.

THP-1 monocytes were treated with increasing concentrations of exogenous $H_2O_2$ for 30 minutes, followed by a 5 minute stimulation with 10nM MCP-1 or PBS. Visualisation of cellular actin revealed that MCP-1 initiates a change in monocyte shape to a more elongated morphology and the cells appear 'polarised' compared to basal cells (Figure 4.11a). $H_2O_2$ alone does not induce a similar phenotype to MCP-1 – cells appear more rounded and mirror the morphology of basal cells. Quantitative analysis indicated that 5 minute MCP-1 stimulation induced significant elongation compared to basal cells (mean circularity: 0.643 versus 0.836), but did not significantly increase cell spreading (Figure 4.11b). The mean circularity scores of cells treated with all concentrations of exogenous $H_2O_2$ did not differ from untreated cells, and were significantly higher than MCP-1-stimulated cells. $H_2O_2$ treatment significantly attenuated MCP-1-induced elongation with all tested concentrations. Furthermore, 10mM $H_2O_2$ alone, and 10nM $H_2O_2$ in combination with MCP-1 stimulation, induced a significant decrease in cell surface area compared to both basal and MCP-1-stimulated cells.

As an alternative approach to studying the action of $H_2O_2$, this assay was repeated using inhibitors of $H_2O_2$ production and signalling. THP-1 monocytes were treated with 1mg/ml catalase or 10μM DPI for 30 minutes before being stimulated with MCP-1 or PBS for 5 minutes, and fixed and stained to visualise F-actin.

Catalase treated monocytes had an elongated, polarised morphology with long, extended protrusions compared to untreated cells (Figure 4.12a), reminiscent of those observed after treatment with MCP-1. Quantitative analysis revealed that catalase alone significantly decreased circularity (mean circularity: 0.703 versus 0.924) and increased surface area (mean area: 249.9μm$^2$ versus 143.1μm$^2$). Catalase treatment did not significantly alter MCP-1-mediated elongation, although MCP-1-mediated increase in cell surface area was significantly decreased (mean area: 356.0μm$^2$ versus 298.0μm$^2$). Monocytes treated with DPI alone were significantly more elongated than control cells (mean circularity: 0.796 versus 0.924), although this was to a lesser extent than MCP-1 alone (Figure 4.12a+c). DPI alone had no effect on cell area compared to basal cells. DPI treatment significantly attenuated MCP-1-mediated elongations (mean circularity: 0.834 versus 0.7034), and significantly reduced the MCP-1-mediated increase in cell surface area (mean area: 114.5μm$^2$ versus 298.0μm$^2$).

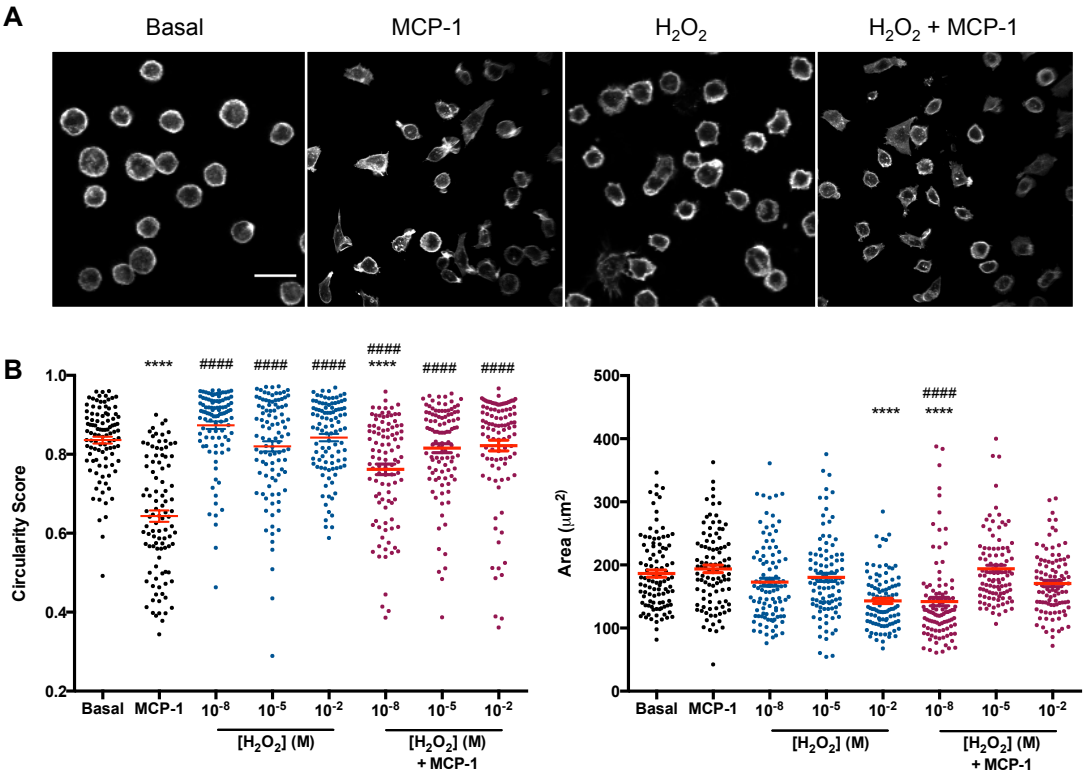


**Figure 4.11: $H_2O_2$ does not induce changes in THP-1 monocyte actin organisation.** THP-1 monocytes were washed in serum free media, rested and plated on coverslips coated with 10µg/ml fibronectin and allowed to adhere for 30 minutes. Cells were treated with increasing concentrations of $H_2O_2$ for 30 minutes, followed by either 10nM MCP-1 or PBS for 5 minutes. Following incubation, cells were fixed in 4% PFA, permeabilised with 0.1% Triton-X and stained with Alexa-Fluor 488 dye (for actin) and DAPI (for nuclei). Samples were imaged using confocal microscopy with 40x oil objective. (A) Representative images showing actin staining, scale bar = 20µm. (B) Circularity score (left) and area (right) were calculated using CellProfiler software, with at least 100 individual cells analysed per sample, from at least 4 pooled experiments. Data presented represents mean (± SEM) with statistical analysis by one way-ANOVA with Tukey's multiple comparisons post hoc test where ****=p<0.0001 versus basal control and ####=p<0.0001 versus MCP-1.

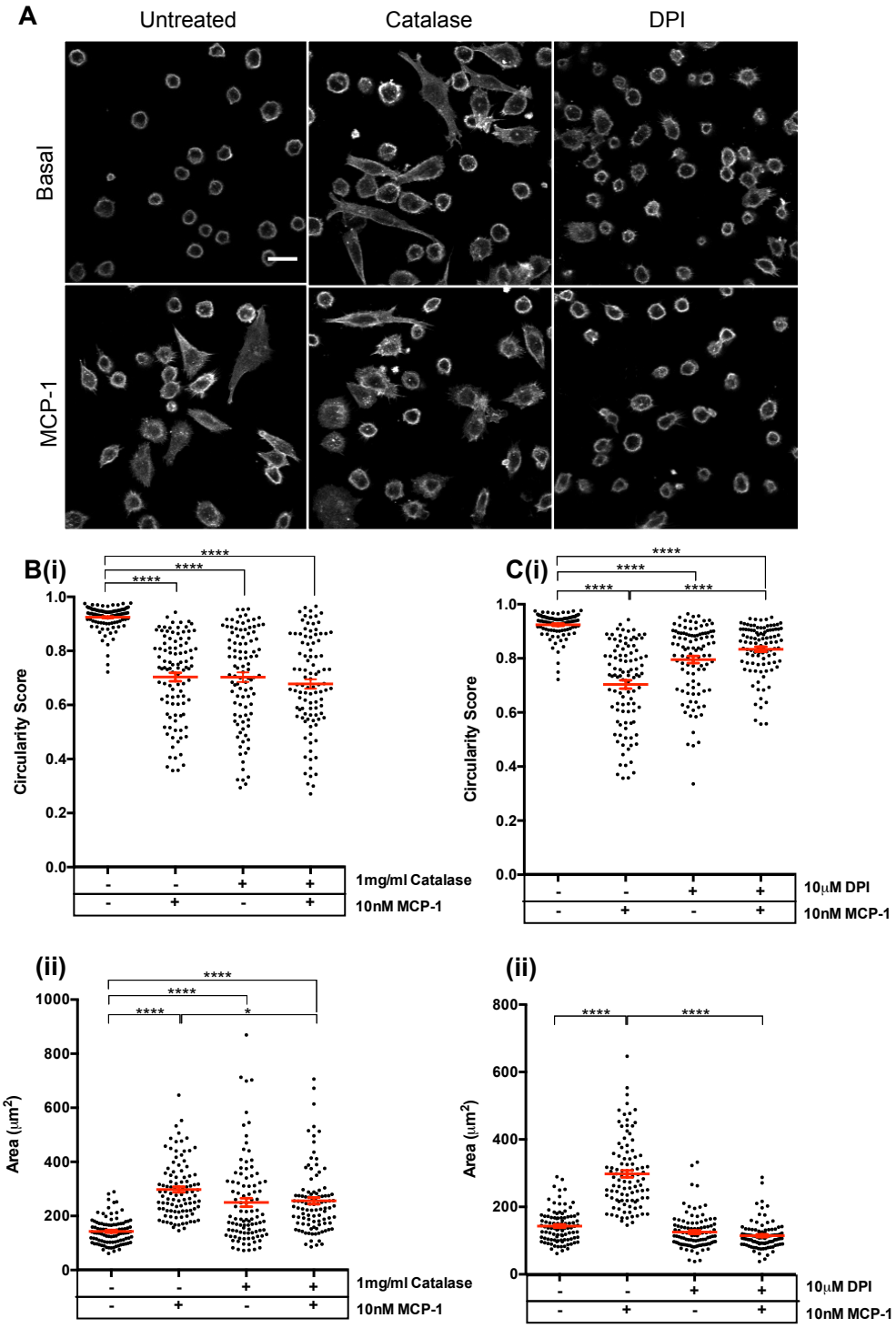


**Figure 4.12: Catalase and DPI induce actin reorganisation in THP-1 monocytes.** THP-1 monocytes were washed, rested and plated on coverslips coated with 10µg/ml fibronectin and allowed to adhere for 30 minutes. Cells were treated with either 1mg/ml catalase or 10µM DPI for 30 minutes, followed by either 10nM MCP-1 or PBS for 5 minutes. Following incubation, cells were fixed in 4% PFA, permeabilised with 0.1% Triton-X and stained with Alexa-Fluor 488 (for actin) and DAPI (for nuclei). Samples were imaged using confocal microscopy with 40x oil objective. (A) Representative images showing actin staining, scale bar = 20µm. (B) Circularity score (i) and area (ii) for catalase treated cells and (C) Circularity score (i) and area (ii) for DPI treated cells were calculated using CellProfiler software, with at least 100 individual cells analysed per sample, from at least 4 pooled experiments. Data presented represents mean (± SEM) with statistical analysis by one way-ANOVA with Tukey's multiple comparisons post hoc test where ***=p<0.001, ****=p<0.0001 versus basal control.

### 4.10 $H_2O_2$ does not affect monocyte receptor expression

Our observations so far have suggested that $H_2O_2$ is negatively affecting chemotaxis and polarisation. These processes are driven by signal detection via receptors expressed on the cell surface. With this in mind, the next approach was to investigate whether $H_2O_2$ could affect monocyte chemokine receptor CCR2 expression, the ligand for which is MCP-1.

THP-1 monocytes were treated with increasing concentrations of $H_2O_2$ for 5 or 30 minutes before being incubated with anti-CCR2 antibody conjugated to fluorophore. CCR2 expression was analysed by flow cytometry. Across all concentrations and times tested, $H_2O_2$ did not significantly affect monocyte CCR2 expression (Figure 4.13a). To extend the investigation, monocytes were treated with increasing concentrations of $H_2O_2$ inhibitors DPI and catalase before CCR2 expression was analysed. Only 30μM DPI significantly inhibited CCR2 expression, while catalase had no significant effect (Figure 4.13b). This suggests that the inhibitory effects of $H_2O_2$, DPI and catalase on monocyte migration are not mediated by altered CCR2 surface expression.

It has been previously reported that MCP-1 stimulation initiates a down regulation of CCR2 expression [408]. However, when monocytes were treated with 10nM MCP-1 for 1, 5 or 10 minutes there was no significant change in CCR2 expression (Figure 4.13c).

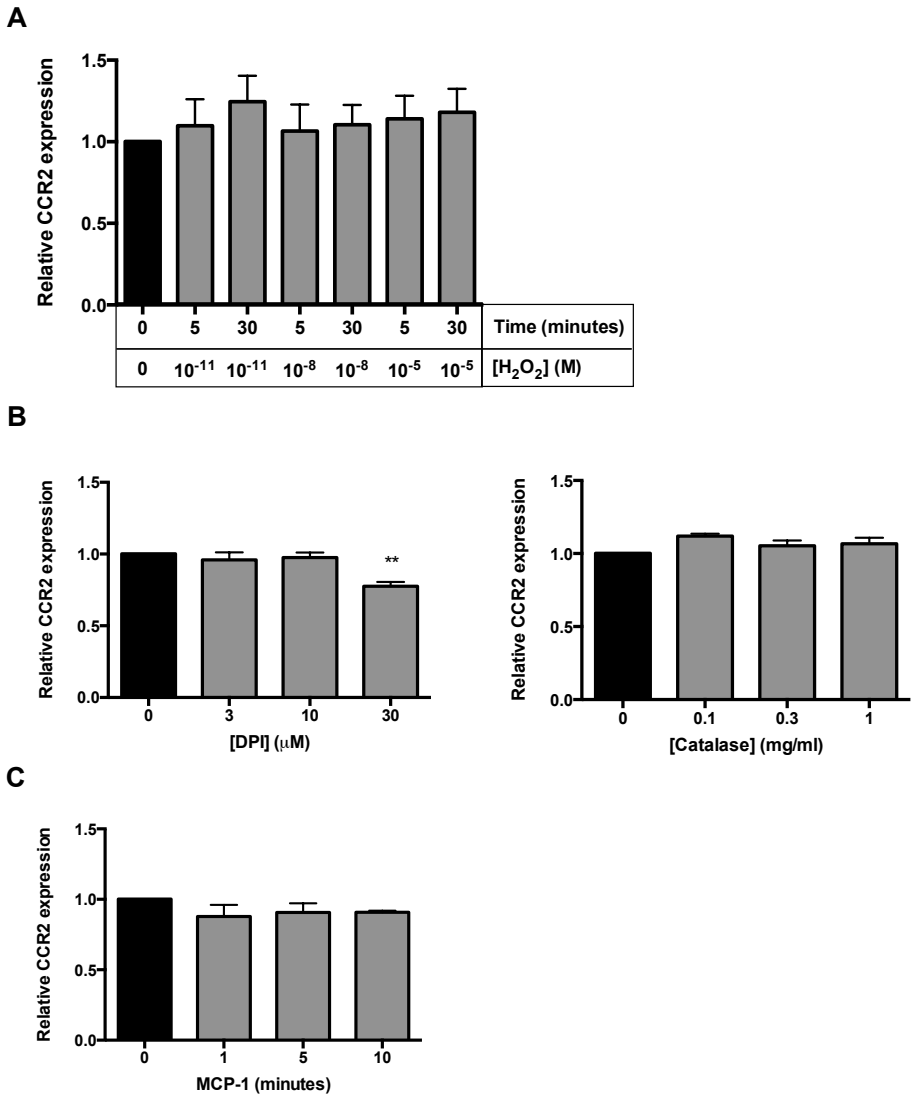


**Figure 4.13: THP-1 monocyte CCR2 surface expression is not affected by $H_2O_2$.** THP-1 monocytes were washed twice in serum free media, rested and treated with (A) increasing concentrations of $H_2O_2$ for 5 or 30 minutes, (B) increasing concentrations of DPI or catalase for 30 minutes, or (C) 10nM MCP-1 for 1, 5 or 10 minutes. Cells were washed twice in ice cold PBS, incubated with Alexa-Fluor 488-conjugated CCR2 antibody or IgG control antibody at room temperature for 30 minutes and washed again in ice cold PBS. Mean fluorescence intensity per 10,000 cells was measured using flow cytometry after gating on live viable population via side and forward scatter. Data presented represents means (± SEM) minus IgG control signal, normalised to untreated control from three separate experiments, with samples run in duplicate. Statistical analysis by one way-ANOVA with Dunnett's post hoc test where **=$p<0.01$ versus control.

### 4.11 Characterisation of THP-1 derived macrophages and primary human neutrophils

Macrophages are considered the 'big eaters' in innate immunology and their ability to engulf debris and microbes is a fundamental process within inflammation. With this in mind, it was important to use macrophages when studying phagocytosis *in vitro*. THP-1 monocyte differentiation has been previously described by Daigneault and colleagues [385]. Briefly, THP-1 monocytes were treated with 80nM PMA for 48 hours in normal culture conditions (i.e. complete RPMI 1640 media). During PMA treatment cells become adherent to the culture flask. Cells are then 'rested' in complete media (minus PMA) for 3-5 days. During the rest period cells become more macrophage-like and present a mature phenotype with a larger surface area and visible cytoplasmic granules.

Figure 4.14a illustrates analysis of monocyte differentiation during the differentiation period. Light phase photographs show rounded monocytes in suspension pre-treatment (Figure 4.14a(i)). Following 48 hours PMA ($PMA_{48}$) cells are adhesive and flattened on the tissue culture flask surface. Following 5 days rest ($PMA_r$), macrophage like cells appear larger, more irregularly shaped and visible granules can be identified within the cell body.

Generation of intracellular granules is a key physical attribute of macrophages. To examine this more closely, cells were analysed using flow cytometry. In a given viable cell population, forward scatter can be used to measure the cell size, while side scatter measures the cell granularity. Figure 4.14a(ii) shows an increase in side scatter in $PMA_{48}$ treated cells, which further increases following the 5 day rest period, indicating increased granularity.

Another marker of monocyte differentiation is CD14 expression. CD14 is lost upon monocyte differentiation into macrophages [385]. Using flow cytometry to quantify CD14 expression, $PMA_{48}$ and $PMA_r$ cells have significantly lower CD14 expression than untreated THP-1 monocytes (Figure 4.14a(iii)).

Together these results confirm that the differentiation protocol generates a clear population of macrophages with increased surface area, granularity, and decreased CD14 expression.

In addition to characterising monocyte differentiation, imaging techniques were used to demonstrate that the neutrophil isolation protocol was yielding a neutrophil population. Wright-Giemsa staining highlights the distinctive lobed neutrophilic nucleus, recognisably unique compared to other leukocytes within the blood smear (Figure 4.14b). This observation is further supported by nuclear staining using DAPI and visualisation using confocal microscopy (Figure 4.14b).

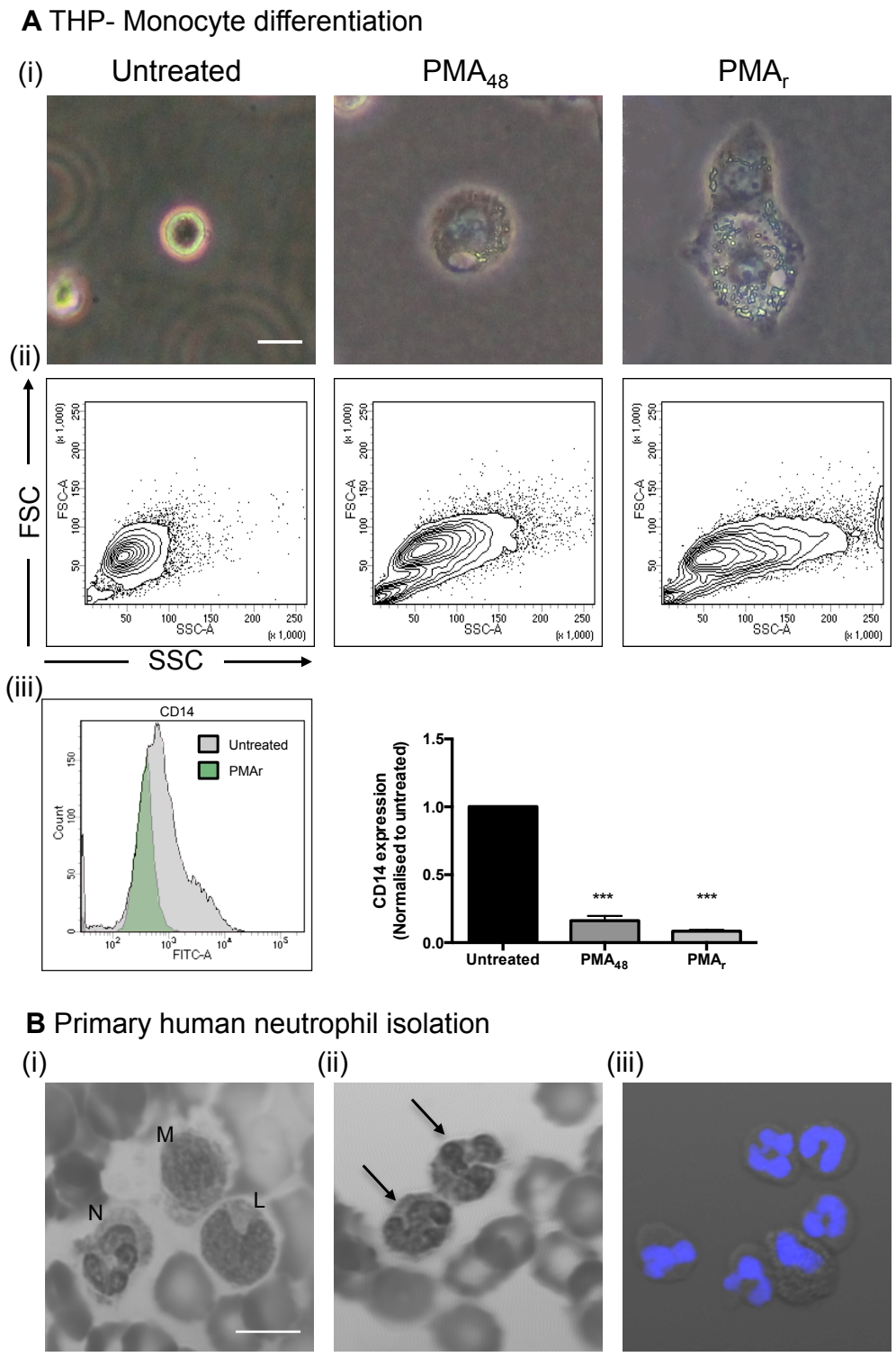


**Figure 4.14: Characterisation and identification of PMA-differentiated macrophages and primary human neutrophils.** (A) THP-1 monocytes were treated with 80nM PMA for 48 hours in culture to induce differentiation into macrophages, scale bar = 10µm. Following treatment, cells were cultured for a further 5 days in PMA-free media (known as rest period). $PMA_{48}$ denotes cells following 48 hours PMA, prior to rest; $PMA_r$ denotes cells that were rested for 5 days following PMA treatment. (i) Photographs showing changes in cell morphology during differentiation period. (ii) Flow cytometry analysis showing forward and side scatter of cells during differentiation. (iii) CD14 expression during differentiation quantified by flow cytometry. (B) Isolation of primary human neutrophils, scale bar = 10µm. (i) Wright-Giemsa staining of whole human blood before neutrophil isolation, (N, neutrophil; M, monocyte; L, Lymphocyte), (i) Wright-Giemsa staining after isolation of neutrophils and before red cell lysis, arrowheads indicate neutrophil, (iii) Lobed neutrophil nuclei as indicated by DAPI staining (blue). Statistical analysis by one way-ANOVA with Dunnett's post test, ***=p<0.001.

### 4.12 Phagocytosis of latex beads and bacteria is inhibited by $H_2O_2$

Clearance of foreign pathogens and dying cells by phagocytes makes a critical contribution to the innate immune response. Similar to previous aspects of innate cell function so far investigated in this thesis, phagocytosis relies on rearrangement of structural components including the actin cytoskeleton. Given the observation that both migration and polarisation are inhibited by $H_2O_2$, we next examined the effects of exogenous $H_2O_2$ on phagocytosis.

*In vitro* studies of phagocytosis have previously been carried out using a variety of experimental particles as targets for engulfment. Here IgG-opsonised latex beads and *E. coli* bacterial cells were to be engulfed by phagocytes. Firstly, primary human neutrophils were treated with chemoattractants, increasing concentrations of $H_2O_2$, or $H_2O_2$ inhibitors catalase and DPI for 30 minutes before being co-incubated with either fluorescent IgG-conjugated latex beads or fluorescently labelled bacteria to allow phagocytosis to occur.

Neutrophils seeded onto fibronectin-coated coverslips were stimulated with chemoattractant or $H_2O_2$, co-incubated with fluorescent latex beads, washed and fixed. Cells were stained to visualise cytoplasm and nuclei. Confocal microscopy was used to visualise the location of beads that were associated with cells. Figure 4.15a provides representative images of a single neutrophil containing a latex bead. Orthogonal projections of stacked image slices indicate that the bead is inside the cell as red fluorescence can be seen throughout the cell body. Neutrophil phagocytosis was inhibited by pre-treatment with increasing concentrations of $H_2O_2$ (Figure 4.15b). The number of cells that contained at least one bead (percent phagocytosis) was significantly inhibited with all $H_2O_2$ concentrations and incubation time points tested. To give an indication of the rate of phagocytosis, the number of phagocytosed latex beads per cell was also measured. Treatment with 10μM $H_2O_2$ for 5 minutes resulted in a significantly reduced number of latex beads per cell.

Furthermore, both percent phagocytosis and the number of beads phagocytosed per cell were not affected by pre-treatment with 10nM IL-8 (Figure 4.15c).

As an alternative approach for quantitatively assessing phagocytosis, flow cytometry was used to analyse the fluorescent signal associated with the viable cell population after phagocytosis had occurred. Neutrophil phagocytosis of latex beads was not affected by pre-treatment with either 10nM IL-8 or 10nM fMLP (Figure 4.16a). Pre-treatment with increasing concentrations of $H_2O_2$ inhibited phagocytosis of beads in a concentration dependent manner, with 10mM $H_2O_2$ significantly inhibiting phagocytosis versus control-treated cells. Neutrophils pre-treated with 10μM DPI showed significant reduction in phagocytosis of latex beads versus control cells. No difference in phagocytosis of latex beads was seen when neutrophils were pre-treated with 1mg/ml catalase (Figure 4.16a).

Neutrophil phagocytosis of bacterial cells was not affected by pre-treatment with 10nM IL-8, however significant inhibition was observed when cells were pre-treated with 10nM fMLP versus control cells (Figure 4.16b). Pre-treatment with increasing concentrations of $H_2O_2$ inhibited phagocytosis of bacteria in a concentration dependent

manner, with 10mM $H_2O_2$ significantly inhibiting phagocytosis versus control-treated cells. Phagocytosis of bacterial cells was not affected when neutrophils were pre-treated with either 10μM DPI or 1mg/ml catalase (Figure 4.16b).

Macrophages are highly phagocytic leukocytes so PMA-differentiated THP-1 monocytes were employed to study macrophage phagocytosis of IgG-conjugated latex beads. Macrophages were pre-treated with either $H_2O_2$ or MCP-1 before being co-incubated with fluorescent beads to allow phagocytosis to occur. Using flow cytometry to measure latex beads fluorescence associated with viable macrophages, we found that $H_2O_2$ inhibited bead uptake in a concentration dependent manner (Figure 4.17a). Significant inhibition was observed with 10μM and 10mM $H_2O_2$.

In addition to flow cytometry analysis, macrophage phagocytosis of latex beads was also assessed using confocal microscopy and manual counting of the number of cells associated with latex beads. In agreement with flow cytometry results, $H_2O_2$ concentration dependently inhibited macrophage phagocytosis of latex beads (Figure 4.17b). The number of macrophages imaged in the field of view that contained at least one bead (percent phagocytosis) was significantly inhibited with all $H_2O_2$ concentrations tested after 30 minutes pre-treatment versus control cells. Additionally, the number of phagocytosed beads per cell was slightly less than untreated controls, although this was not statistically significant.

These results show that macrophage and neutrophil phagocytosis of beads and bacteria is inhibited by pre-treatment with $H_2O_2$.

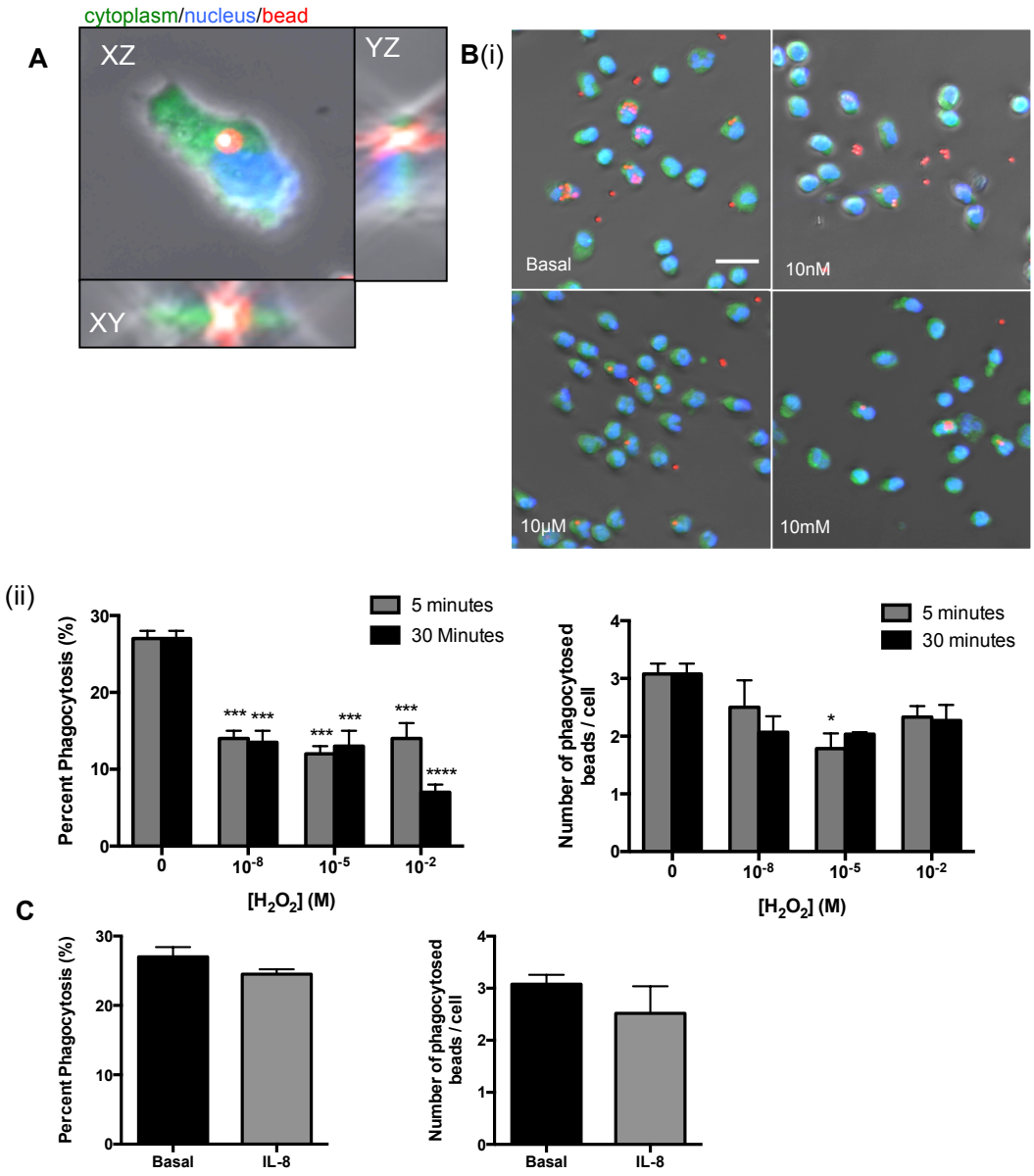


**Figure 4.15: Neutrophil phagocytosis of latex beads is inhibited by $H_2O_2$.** Peripheral human neutrophils were isolated from human blood, loaded with 10μM CFSE, rested and plated on fibronectin (10ng/ml) coated coverglass chambers. (A) Representative images indicating intracellular location of latex bead (red), confirmed by orthogonal projection images. Cells were incubated with (B) increasing concentrations of $H_2O_2$ for 5 or 30 minutes or (C) 10nM IL-8 for 30 minutes at 37°C. Cells were washed in warm HBSS and mixed with IgG-opsonised fluorescent latex beads. Cells were incubated at 37°C for 30 minutes to allow phagocytosis to occur. Cells were fixed in 4% PFA before being stained with DAPI. Samples were immediately imaged using confocal microscopy with 40x oil objective. Images were manually scored for neutrophils containing beads, confirmed by orthogonal projection imaging. Percent phagocytosis is percentage of total cells imaged containing at least one bead. Data presented represents means (± SEM) from at least three separate experiments. Scale bar = 20μm. Statistical analyses (A) by two way-ANOVA versus control with Tukey's multiple comparisons post hoc test. *=p<0.05, **=p<0.01, ***=p<0.001, ****=p<0.0001 and (B) by unpaired t test.

**A** Neutrophil phagocytosis of latex beads

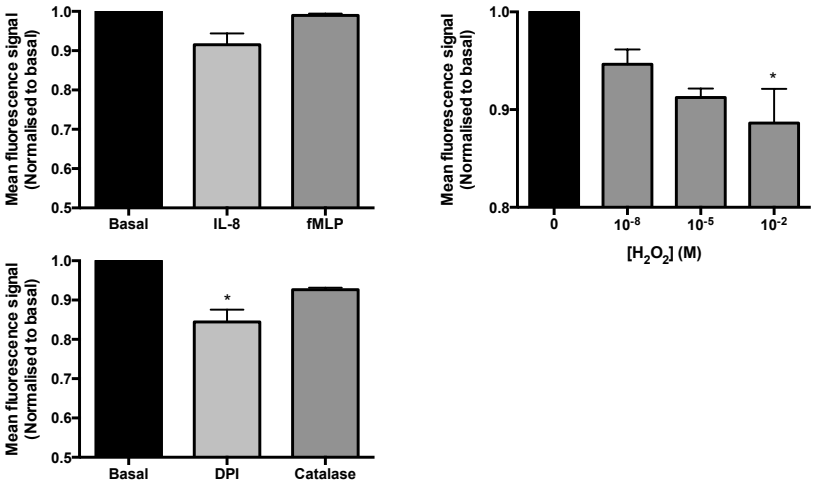


**B** Neutrophil phagocytosis of bacteria

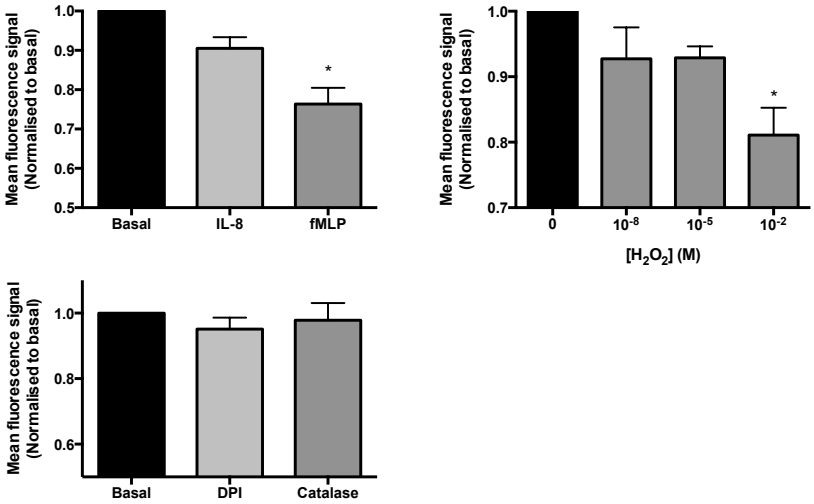


**Figure 4.16: Neutrophil phagocytosis of latex beads and bacteria is inhibited by $H_2O_2$.** Peripheral human neutrophils were isolated from human blood, rested and incubated with 100nM IL-8, 10nM fMLP, 10μM DPI, 1mg/ml catalase, or increasing concentrations of $H_2O_2$ for 30 minutes at 37°C. Cells were washed in warm HBSS and mixed with (A) IgG-opsonised fluorescent latex beads or (B) CFSE (10μM) loaded *E. coli* bacteria. Cells were incubated at 37°C for 30 minutes to allow phagocytosis to occur. Cells were washed 3 times in PBS before fluorescence intensity in viable neutrophil population was measured using flow cytometry. Data represents mean (±SEM) fluorescent signal per 10,000 cells normalised to basal or untreated fluorescence, from at least three separate experiments. Statistical analyses by one way-ANOVA versus control with Dunnett's multiple comparisons post hoc test where *=$p<0.05$.

**A** Macrophage phagocytosis of bacteria (flow cytometry)

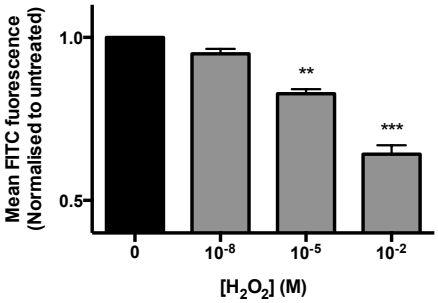


**B** Macrophage phagocytosis of latex beads (microscopy)

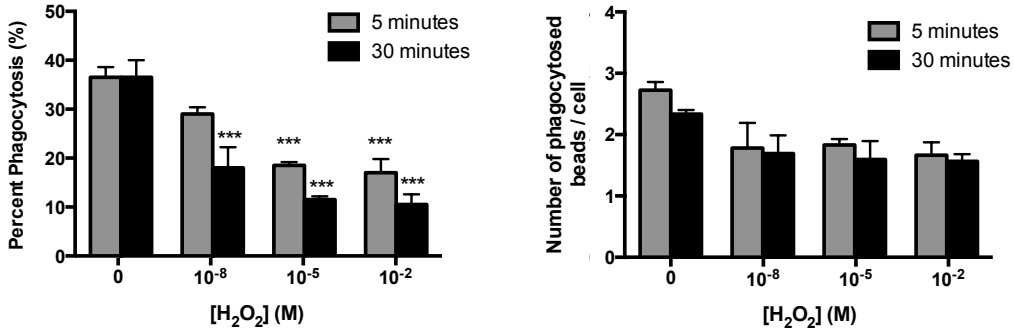


**Figure 4.17: Macrophage phagocytosis of latex beads and bacteria is inhibited by $H_2O_2$.** PMA differentiated THP-1 monocytes were incubated with increasing concentrations of $H_2O_2$ or 10nM MCP-1 for 30 minutes at 37°C. (A) Cells were washed in warm PBS and mixed with CFSE (10μM) loaded E. coli bacteria. Cells were incubated at 37°C for 30 minutes to allow phagocytosis to occur. Cells were washed 3 times in PBS before fluorescence intensity in viable neutrophil population was measured using flow cytometry. Data represents mean (±SEM) fluorescent signal per 10,000 cells normalised to basal or untreated fluorescence, from at least three separate experiments. Statistical analyses by one way-ANOVA versus control with Dunnett's multiple comparisons post hoc test. **=p<0.01, ***=p<0.001. (B) Cells were washed in warm HBSS and mixed with IgG-opsonised fluorescent latex beads. Cells were incubated at 37°C for 30 minutes to allow phagocytosis to occur. Cells were fixed in 4% PFA before being stained with DAPI. Samples were immediately imaged using confocal microscopy with 40x oil objective. Images were manually scored for neutrophils containing beads, confirmed by orthogonal projection imaging. Percent phagocytosis is percentage of total cells imaged containing at least one bead. Data presented represents means ± SEM from at least three separate experiments. Statistical analyses (A) by two way-ANOVA versus control with Tukey's multiple comparisons post hoc test where ***=p<0.001.

### 4.13 Monocyte and neutrophil stimulation induces transient elevation of intracellular calcium

Our results demonstrate that $H_2O_2$ inhibits monocyte and neutrophil motility. It was therefore prudent to investigate whether $H_2O_2$ was targeting the intracellular signalling pathways that drive motility. Elevation of intracellular $Ca^{2+}$ concentration triggered by ligand stimulation is a well-characterised observation in leukocytes and provides an assessment of signalling potential. As a quantitative measurement of intracellular $Ca^{2+}$, Fluo-4 was loaded into cells prior to stimulation. Fluo-4 produces a fluorescent signal upon detection of $Ca^{2+}$ that can be measured over time using a plate reader.

Exposure of cells to increasing concentrations of ligands induced a concentration dependent transient elevation of intracellular calcium ($[Ca^{2+}]_i$) (Figures 4.18+4.19). The responses observed with all ligands were immediate and short lived, typically returning to baseline within 5 minutes. In the THP-1 monocytic cell line, 1-100nM MCP-1 or $LTB_4$ elevated $[Ca^{2+}]_i$ in a concentration dependent manner (Figure 4.18a). A second monocytic cell line, U937, displayed a similar response to $LTB_4$ (Figure 4.18b). For both cell types, stimulation of purinergic receptors with ATP was used as a positive control and indeed prompted a significant increase in detectable $[Ca^{2+}]_i$.

Ligand-stimulated $Ca^{2+}$ mobilisation was also examined in primary human neutrophils with increasing concentrations of chemoattractants IL-8, fMLP and $LTB_4$. All ligands stimulated transient, concentration dependent elevations of $[Ca^{2+}]_i$ that were significantly higher than baseline (Figure 4.19). As a positive control, 1mM ATP elicited a significantly detectable elevation of $[Ca^{2+}]_i$. Furthermore, neutrophils were stimulated with 1μM ionomycin after the chemoattractant-induced response had plateaued. Ionomycin is an ionophore and acts as a mobile ion carrier to transport $Ca^{2+}$ across the plasma membrane. Here it was used as a positive control to indicate maximal potential $[Ca^{2+}]_i$ influx.

To investigate the potential source of $Ca^{2+}$ responsible for the responses observed, monocytic cell lines and primary human neutrophils were stimulated with agonists in the presence of high (1mM) and low extracellular $Ca^{2+}$. MCP-1-mediated $Ca^{2+}$ responses in THP-1 monocytes were attenuated in low extracellular $Ca^{2+}$, although this was not statistically significant. Ionomycin-induced $Ca^{2+}$ influx was significantly attenuated in low extracellular $Ca^{2+}$ in these cells (Figure 4.20a). $LTB_4$- and ionomycin-mediated $Ca^{2+}$ influx in U937 monocytes was significantly attenuated in low extracellular $Ca^{2+}$ (Figure 4.20b). Furthermore, fMLP- and ionomycin-mediated $Ca^{2+}$ influx was significantly attenuated in primary human neutrophils in low extracellular $Ca^{2+}$ (Figure 4.20c). In all three cell types examined, chemoattractant- and ionomycin-mediated $Ca^{2+}$ responses were not completely abolished in low extracellular $Ca^{2+}$, suggesting that an intracellular source of $Ca^{2+}$ contributed to the transient responses.

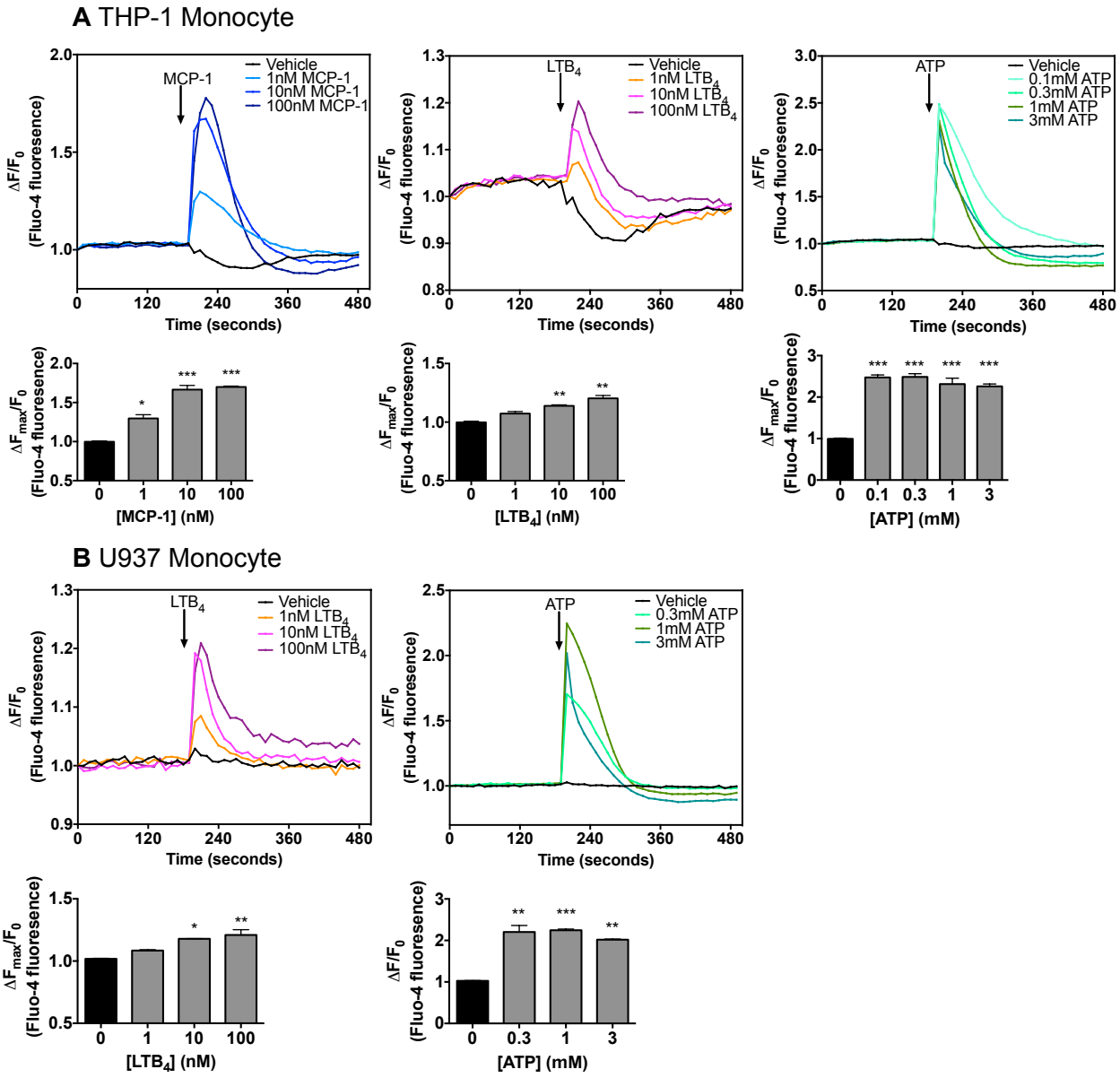


**Figure 4.18: MCP-1, $LTB_4$ and ATP increase intracellular calcium mobilisation in monocytic cell lines. (A)** THP-1 monocytes and **(B)** U937 monocytes were loaded with 10μM Fluo-4 before being washed in $Ca^{2+}$-free HBSS, resuspended in HBSS and extracellular calcium adjusted to 1mM. Cells were plated in black 96 well plates. Fluorescence was measured over time at 37°C using a plate reader (upper panels). Increasing concentrations of MCP-1, $LTB_4$ or ATP were added after baseline established. Peak change in fluorescence signal is plotted against vehicle control (lower panels). Data presented show representative traces from a single experiment and peak change graphs represent mean (± SEM) from three separate experiments, samples run in duplicate. Statistical analysis by one way-ANOVA with Dunnett's post test where *=p<0.05, **=p<0.01, ***=p<0.001.

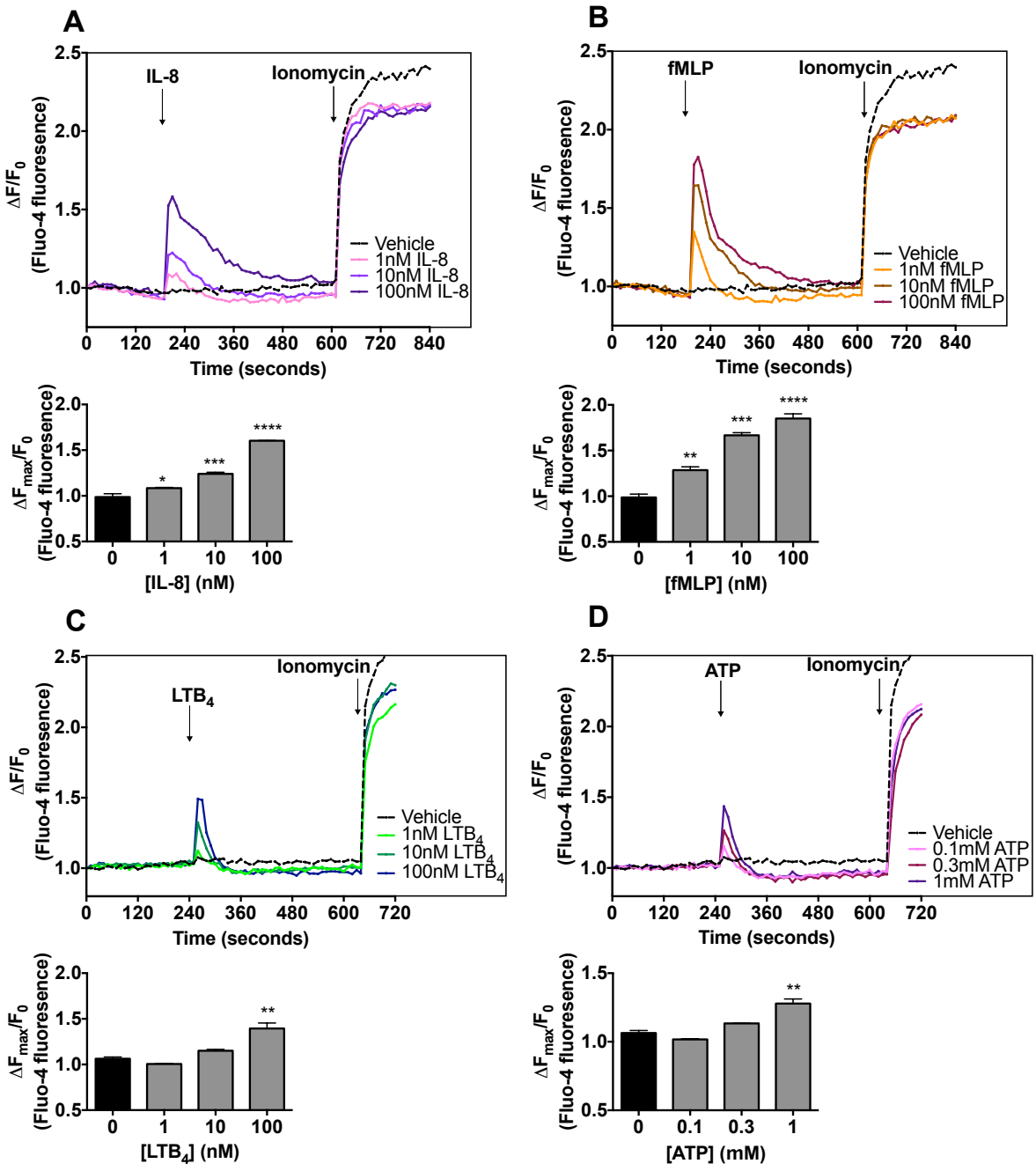


**Figure 4.19: IL-8, fMLP, $LTB_4$ and ATP increase intracellular calcium mobilisation in primary human neutrophils.** Primary human neutrophils were isolated from peripheral human blood and loaded with 10μM Fluo-4 before being washed in $Ca^{2+}$-free HBSS, resuspended in HBSS and extracellular calcium adjusted to 1mM. Cells were plated in black 96 well plates. Fluorescence was measured over time at 37°C using a plate reader (upper panels). Increasing concentrations of (A) IL-8, (B) fMLP, (C) $LTB_4$ or (D) ATP were added after baseline established. 1μM ionomycin was added once response had returned to baseline. Peak change in fluorescence signal plotted against vehicle control (lower panels). Data presented show representative traces from a single experiment and peak change graphs represent mean (± SEM) from three separate experiments, samples run in duplicate. Statistical analysis by one way-ANOVA with Dunnett's post test where *=p<0.05, **=p<0.01, ***=p<0.001.

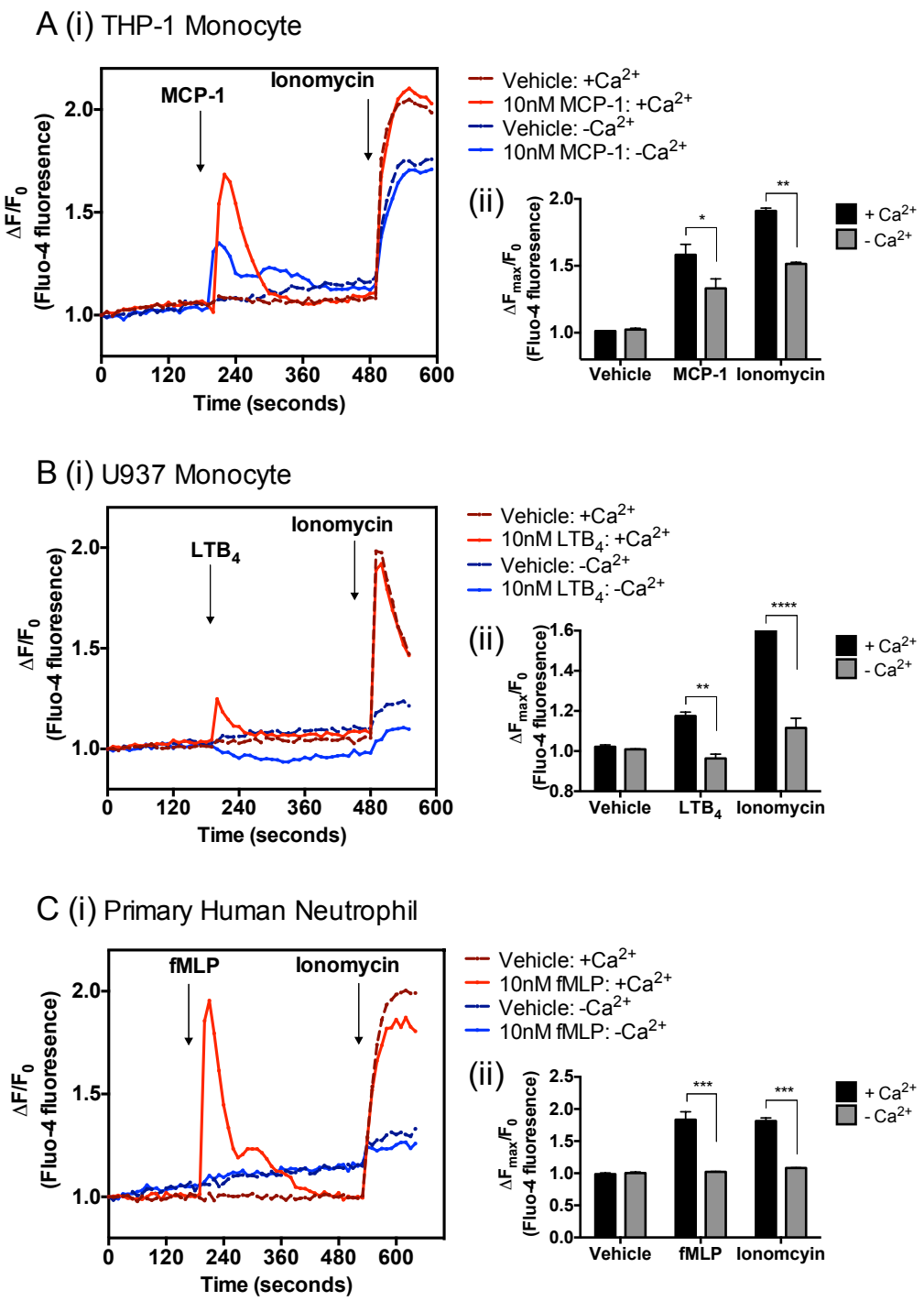


**Figure 4.20: Ligand induced intracellular calcium mobilisation in monocytes and neutrophils is reduced in low extracellular calcium.** (A) THP-1 monocytes, (B) U937 monocytes and (C) Primary human neutrophils were loaded with 10μM Fluo-4 before being washed in $Ca^{2+}$-free HBSS, resuspended in HBSS. Half the populations had extracellular calcium adjusted to 1mM, the other half remained in $Ca^{2+}$-free HBSS. Cells were plated in black 96 well plates. Fluorescence was measured over time at 37°C using a plate reader (i). 10nM MCP-1, 10nM $LTB_4$ or 10nM fMLP were added after baseline established. Finally, 1μM ionomycin was added to all samples. Peak change in ligand- and ionomycin-induced fluorescence signal is plotted against vehicle control in the presence and absence of extracellular $Ca^{2+}$ (ii). Data presented show representative traces from a single experiment and peak change graphs represent mean (± SEM) from three separate experiments, samples run in duplicate. Statistical analyses by two way-ANOVA with Sidak's multiple comparisons post hoc test where *=p<0.05, **=p<0.01, ***=p<0.001, ****=p<0.0001.

After validating the assay with known chemoattractants, the next step aimed to examine whether $H_2O_2$ could induce a similar elevation of $[Ca^{2+}]_i$. THP-1 and U937 monocytes, and primary human neutrophils were stimulated with increasing concentrations of $H_2O_2$ and changes in $[Ca^{2+}]_i$ measured over time. In THP-1 cells, $H_2O_2$ had no significant effect upon $[Ca^{2+}]_i$ although a decrease in $Ca^{2+}$ signal was observed with 10mM $H_2O_2$ (Figure 4.21a). THP-1 cells were still able to respond to ionomycin following $H_2O_2$ stimulation. $H_2O_2$ did not cause a transient response in U937 monocytes (Figure 4.21b). Interestingly, only 10mM $H_2O_2$ provoked a gradual and steep rise in $[Ca^{2+}]_i$ in U937 cells that did not plateau over time, although ionomycin was still able to further increase the response. Out of all the concentrations tested, only 10mM $H_2O_2$ provoked an increase in $[Ca^{2+}]_i$ in primary human neutrophils (Figure 4.21c). Whilst transient, this response was longer-lived that those observed with neutrophil chemoattractants, however the response had returned to baseline within 5 minutes. Ionomycin triggered a large and rapid increase in detectable $[Ca^{2+}]_i$ in neutrophils, regardless of any previous treatment.

It has previously been reported that $H_2O_2$ can provoke a biphasic elevation of $[Ca^{2+}]_i$ in rat pancreatic cells [335]. To see if this response could be replicated in primary human neutrophils, cells were stimulated with 10mM $H_2O_2$ for 30 minutes and $[Ca^{2+}]_i$ levels continuously detected using a Fluo-4 probe (Figure 4.22a). Indeed, an initial, short, transient peak that returned to baseline after approximately 5 minutes was observed, followed by a gradual, sustained increase in $[Ca^{2+}]_i$ that plateaued during the 30 minute incubation. Addition of ionomycin after $H_2O_2$ further increased the $Ca^{2+}$ elevation. To elucidate the possible mechanisms of $Ca^{2+}$ influx responsible for the biphasic response seen with $H_2O_2$ stimulation, the experiment was repeated in low extracellular $Ca^{2+}$. 10mM $H_2O_2$ elicited an initial increase in $[Ca^{2+}]_i$ signal, which peaked approximately 5 minutes after stimulation at which point it plateaued (Figure 4.22b). Over the next 25 minutes the elevated signal did not return to baseline, nor did it increase further. Responses to ionomycin were attenuated in cells in the absence of extracellular $Ca^{2+}$.

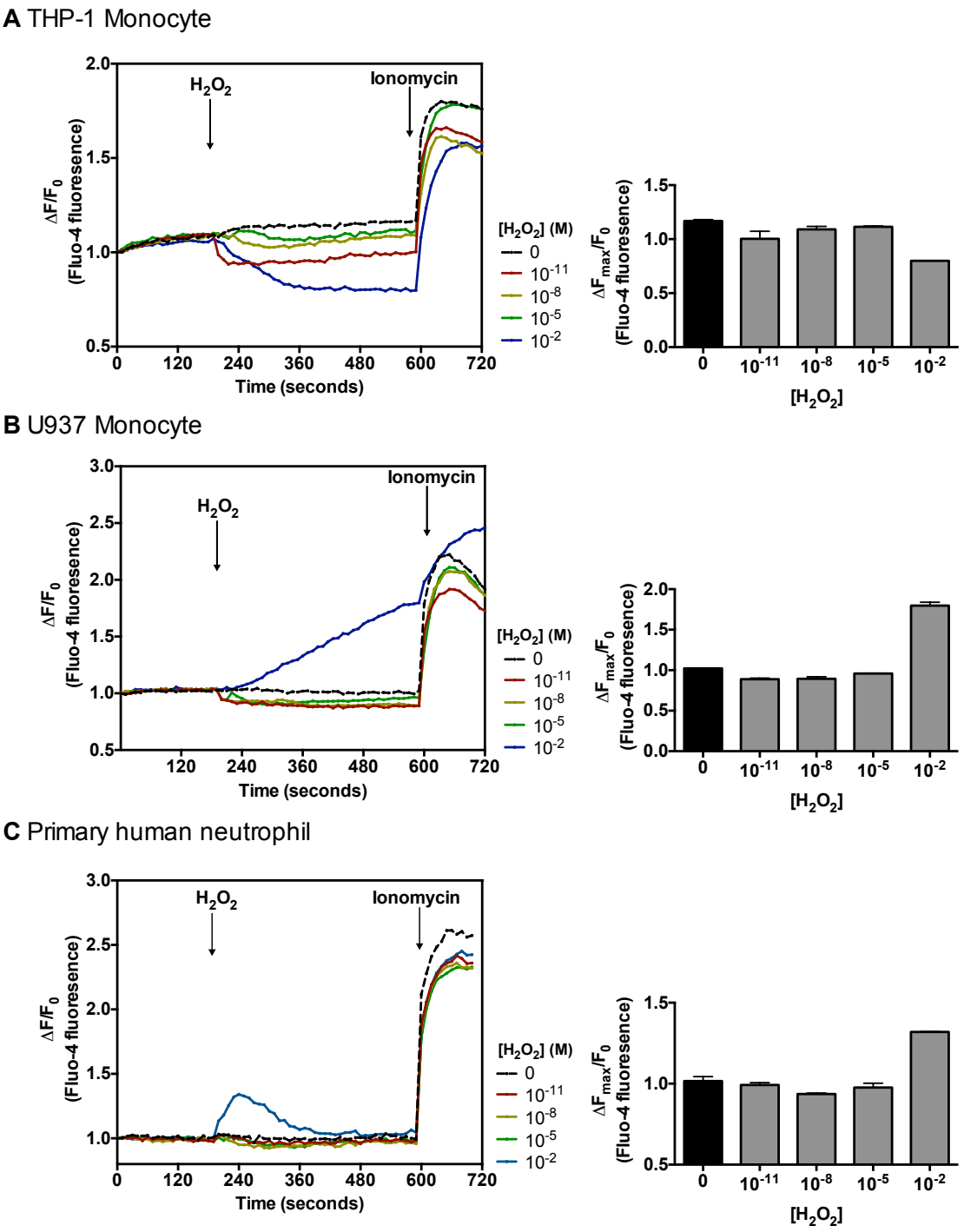


**Figure 4.21: The effect of exogenous $H_2O_2$ upon intracellular calcium mobilisation in human monocytes and neutrophil.** THP-1 monocytes, U937 monocytes or primary human neutrophils were loaded with 10μM Fluo-4 before being washed in $Ca^{2+}$-free HBSS, resuspended in HBSS and extracellular calcium adjusted to 1mM. Cells were plated in black 96 well plates. Fluorescence was measured over time at 37°C using a plate reader (left panels). Increasing concentrations of $H_2O_2$ were added after baseline established. 1μM ionomycin was added once response had returned to baseline. Peak change in fluorescence signal plotted against vehicle control (right panels). Data presented show representative traces from a single experiment and peak change graphs represent mean (± SEM) from three separate experiments, samples run in duplicate.

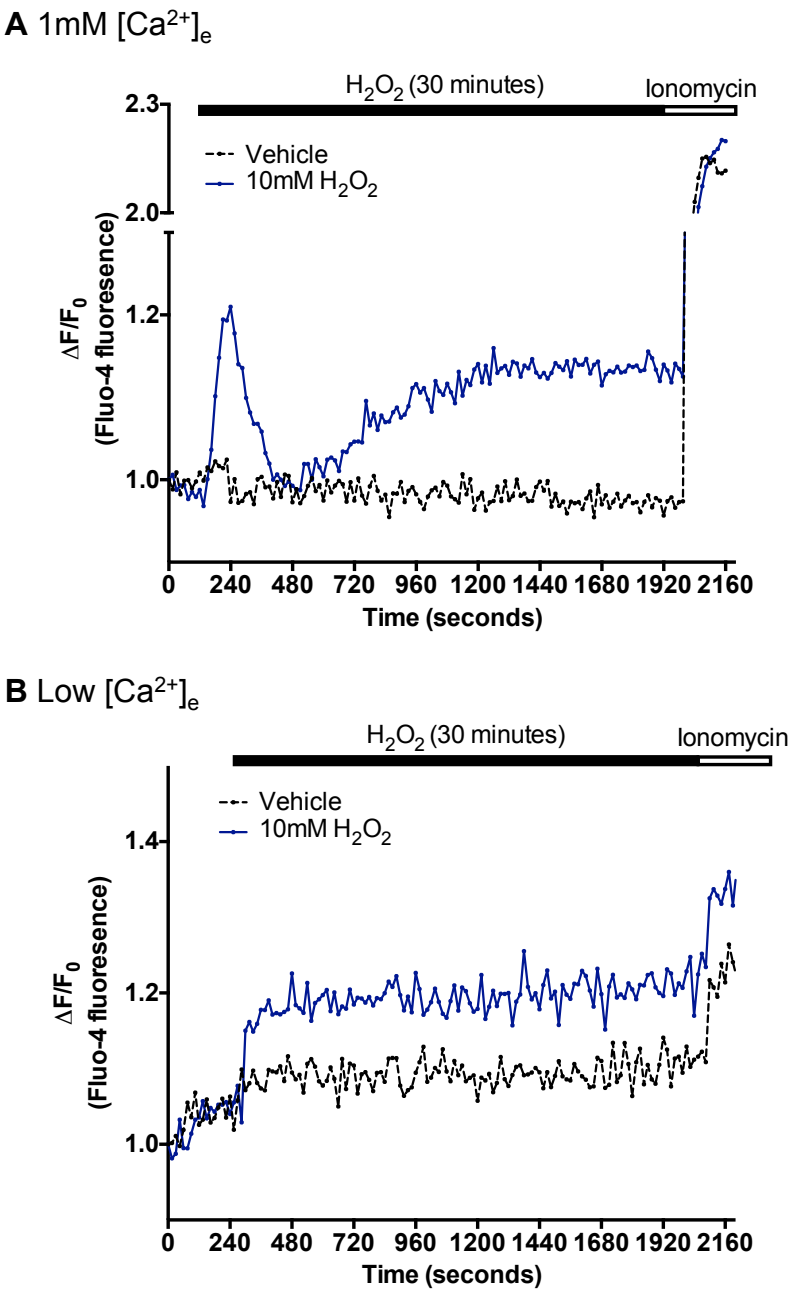


**Figure 4.22: $H_2O_2$ induces a biphasic increase in intracellular calcium in primary human neutrophils**. Primary human neutrophils were isolated from peripheral human blood and loaded with 10μM Fluo-4 before being washed in $Ca^{2+}$-free HBSS, resuspended in HBSS and extracellular calcium adjusted to (A) 1mM, or (B) left calcium free. Cells were plated in black 96 well plates. Fluorescence was measured over time at 37°C using a plate reader. 10μM $H_2O_2$ was added after baseline established and fluorescence signal captured for 30 minutes before 1μM ionomycin was added. Peak change in fluorescence signal plotted against vehicle. Data presented show representative traces from two experiments.

### 4.14 $H_2O_2$ does not affect ligand-stimulated calcium mobilisation in monocytes or neutrophils

To test whether $H_2O_2$ could influence the immediate $Ca^{2+}$ signal observed in ligand-stimulated cells, monocytic cell lines and primary human neutrophils were pre-treated with 10μM $H_2O_2$ for 10 minutes before stimulation with a known chemoattractant, and levels of $[Ca^{2+}]_i$ analysed using Fluo-4 loaded cells and a plate reader.

THP-1 monocyte stimulation with increasing concentrations of MCP-1 induced a concentration dependent increase in $[Ca^{2+}]_i$. This was not affected when cells were pre-treated with $H_2O_2$ (Figure 4.23a). Similarly, U937 monocyte stimulation with increasing concentrations of $LTB_4$ induced a concentration dependent increase in $[Ca^{2+}]_i$ signal. Again, pre-treatment with $H_2O_2$ did not alter the chemoattractant-induced response (Figure 4.23b).

Furthermore, primary human neutrophil $Ca^{2+}$ mobilisation with a range of known chemoattractants was investigated. 10nM IL-8, 10nM fMLP and 10nM $LTB_4$ increase $[Ca^{2+}]_i$ influx compared to PBS control. The chemoattractant-mediated rise in $[Ca^{2+}]_i$ was not affected when neutrophils were pre-treated with $H_2O_2$ prior to stimulation with chemoattractant (Figure 4.24).

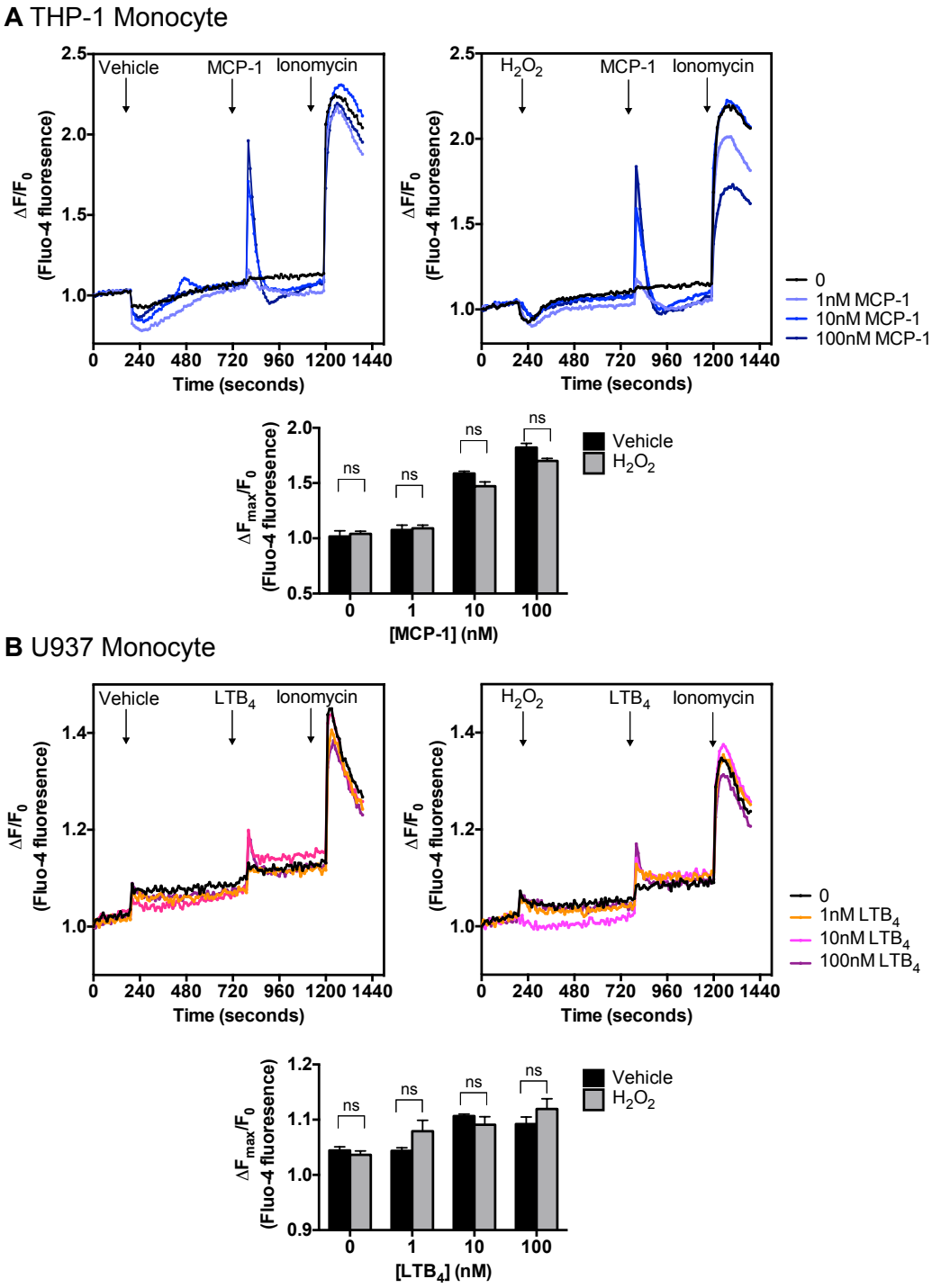


**Figure 4.23: $H_2O_2$ does not affect chemoattractant-induced intracellular calcium mobilisation in monocytic cell lines. (A)** THP-1 monocytes and **(B)** U937 monocytes were loaded with 10μM Fluo-4 before being washed in $Ca^{2+}$-free HBSS, resuspended in HBSS and extracellular calcium adjusted to 1mM. Cells were plated in black 96 well plates. Fluorescence was measured over time at 37°C using a plate reader (upper panels). Cells were treated with either 10μM $H_2O_2$ or vehicle for 10 minutes before increasing concentrations of MCP-1 or $LTB_4$ were added. Finally, 1μM ionomycin was added to each well. Peak change in fluorescence signal is plotted against vehicle control (lower panels). Data presented show representative traces from a single experiment and peak change graphs represent mean (± SEM) from three separate experiments, samples run in duplicate. Statistical analyses by two way-ANOVA with Sidak's multiple comparisons post hoc test where ns=no significant difference.

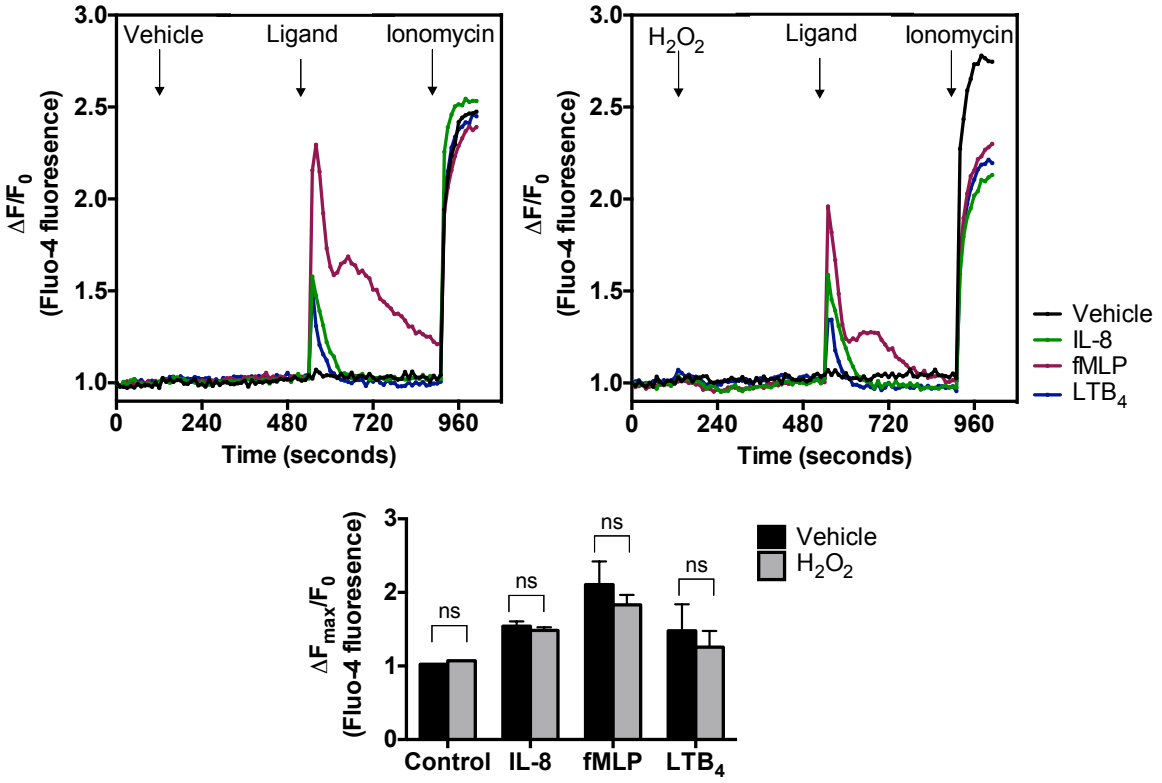


**Figure 4.24: Ligand induced intracellular calcium mobilisation in neutrophils is not affected by pre-treatment with $H_2O_2$.** Primary human neutrophils were isolated from peripheral human blood, loaded with 10μM Fluo-4, washed in $Ca^{2+}$-free HBSS, resuspended and extracellular calcium adjusted to 1mM. Cells were plated in black 96 well plates. Fluorescence was measured over time at 37°C using a plate reader (upper panels). 10μM $H_2O_2$ or vehicle was added after baseline established and fluorescence signal captured for 10 minutes before 10nM IL-8, 10nM fMLP or 10nM $LTB_4$ was added. Once responses had returned to baseline, 1μM ionomycin was added to each well. Peak change in fluorescence signal is plotted against vehicle control (lower panels). Data presented show representative traces from a single experiment and peak change graphs with mean (± SEM) from three separate experiments, samples run in duplicate. Statistical analyses by two way-ANOVA with Sidak's multiple comparisons post hoc test where ns=no significant difference.

### 4.15 $H_2O_2$ activates PI3K and MAPK signalling pathways in monocytes

There are many reports implying $H_2O_2$ as an important signalling component in many signalling pathways, including PI3K and SFK signalling cascades, as reviewed by Truong and Carroll (2013) [313]. Given our observations that $H_2O_2$ appears to inhibit cell chemotaxis and polarisation, but does not affect receptor expression or calcium mobilisation, we next sought to examine whether $H_2O_2$ could activate other signalling pathways. The monocytic cell line U937 was employed for these experiments due to its robustness and sensitivity.

U937 monocytic cells were stimulated with increasing concentrations of fMLP or $H_2O_2$ before being lysed and protein extracted. Lysates were run on SDS-PAGE gels to separate proteins by electrophoresis, transferred to membranes and probed for pAkt(S473) as an indicator of PI3K activation, and pERK(Y204) as an indicator of MAPK signalling. Membranes were also probed for total ERK as a loading control.

Stimulation with increasing concentrations of fMLP increased pAkt levels in a concentration dependent manner. fMLP also increased pERK compared to untreated samples, which peaked with 10nM fMLP (Figure 4.25a). Stimulation with increasing concentrations of $H_2O_2$ increased pAkt above basal levels. $H_2O_2$ did prompt a small increase in pERK versus untreated controls, although this did not appear to be concentration dependent and fluctuated over the concentration range tested (Figure 4.25a).

To investigate the combined effect of $H_2O_2$ and fMLP and to examine whether $H_2O_2$ was able to affect fMLP mediated increases in pAkt and pERK, U937 cells were treated with 10μM $H_2O_2$ for 30 minutes either alone or followed by 5 minutes with 10nM fMLP. While both fMLP and $H_2O_2$ alone increased pAkt levels, the extent of this increase was not affected when $H_2O_2$ and fMLP stimulation was combined (Figure 4.25b). Interestingly, while fMLP alone increased pERK, $H_2O_2$ alone had only a very modest effect on pERK levels. Pre-treating cells with $H_2O_2$ before fMLP stimulation appeared to enhance the fMLP mediated increase in pERK in an additive manner (Figure 4.25b).

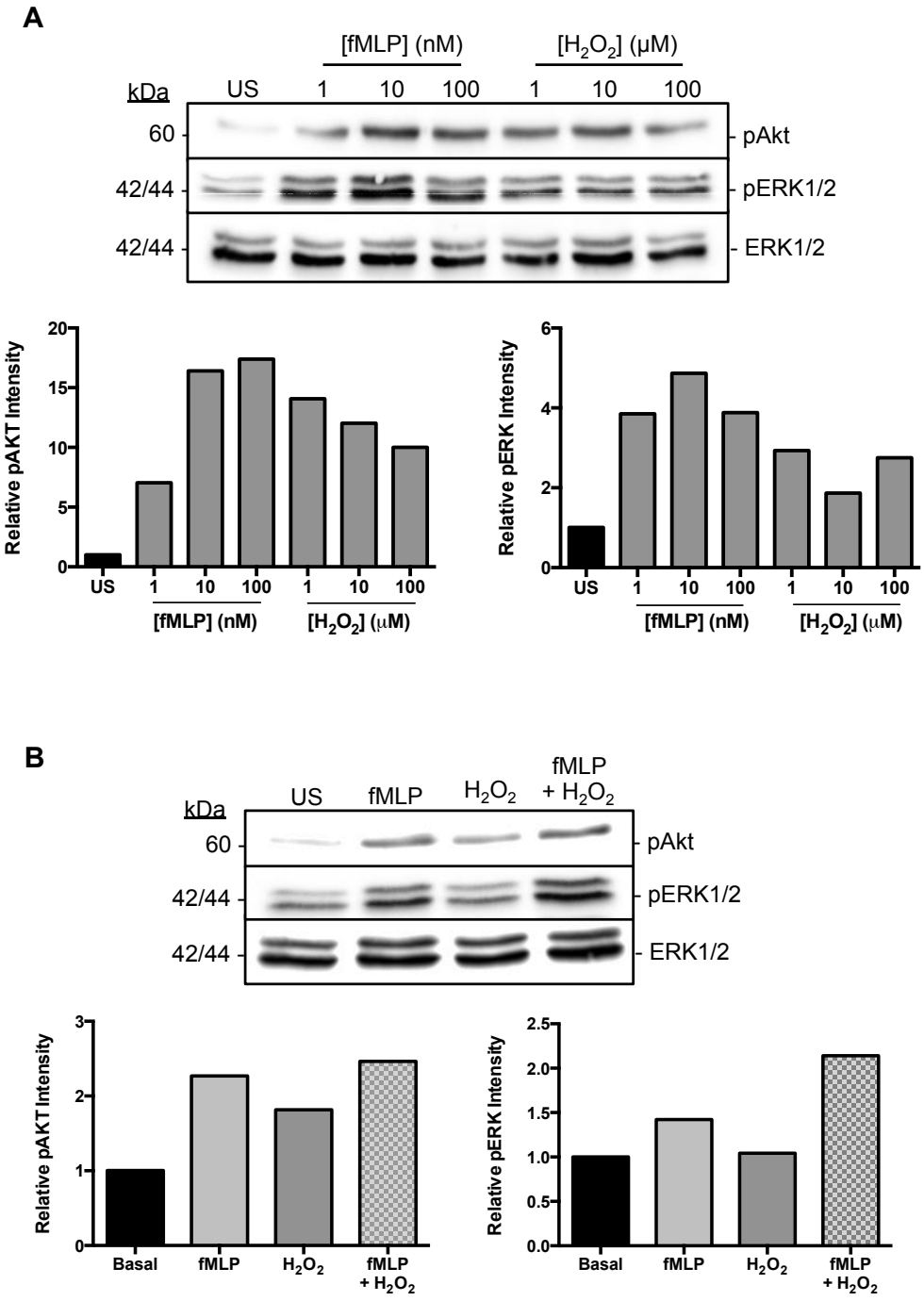


**Figure 4.25: fMLP and $H_2O_2$ induce activation of PI3K and ERK signalling pathways in monocytes.** Western blot analysis of pAKT, pERK and ERK expression in U937 cells cultured (A) for 5 minutes with increasing concentrations of fMLP or for 30 minutes with increasing concentrations of $H_2O_2$ or (B) for 5 minutes with 10nM fMLP alone, for 30 minutes with10μM $H_2O_2$ alone, or fMLP and $H_2O_2$ in combination (upper panels). Band intensity was quantified using ImageJ (lower panels). Immunoblots from a single experiment.

### 4.16 $H_2O_2$ does not affect ICAM-1 expression in endothelial cells

Following tissue damage or infection, inflammatory mediators stimulate the expression of adhesion molecules on the vasculature in the affected tissue. Circulating leukocytes interact with these adhesion molecules and this leads to their extravasation from vessels into tissue. TNFα is a pro-inflammatory mediator that is known to upregulate ICAM-1 expression on endothelial cells [409]. $H_2O_2$ has previously been reported to increase adhesion of neutrophils to human endothelial cells [324]. In order to examine the effect of $H_2O_2$ on vasculature adhesiveness, the next objective sought to investigate whether $H_2O_2$ could influence adhesion molecule expression on the endothelial surface.

Firstly, to create pro-inflammatory conditions, monolayers of EA.hy926 endothelial cells were stimulated with 10ng/ml TNFα for up to 6 hours to induce ICAM-1 expression. Confocal microscopy (Figure 4.26a(i)) and Western blot analysis (Figure 4.26(ii,iii)) show an increase in ICAM-1 expression following 6 hours TNFα stimulation. (Positive control for ICAM-1 expression is presented in Appendix 1). ICAM-1 protein expression indicates this occurs in a time dependent manner.

To investigate the effects of $H_2O_2$ on TNFα stimulated endothelial cells, confluent monolayers were treated with 10μM $H_2O_2$ for up to 6 hours before cells were lysed and assayed for ICAM-1 expression, and total ERK, as a loading control. Western blot analysis indicated that $H_2O_2$ alone only induced very modest expression of ICAM-1 compared to TNFα treated cells (Figure 4.26b(i)). Furthermore, $H_2O_2$ did not affect TNFα-induced ICAM-1 expression over a 6 hour period (Figure 4.26b(ii)).

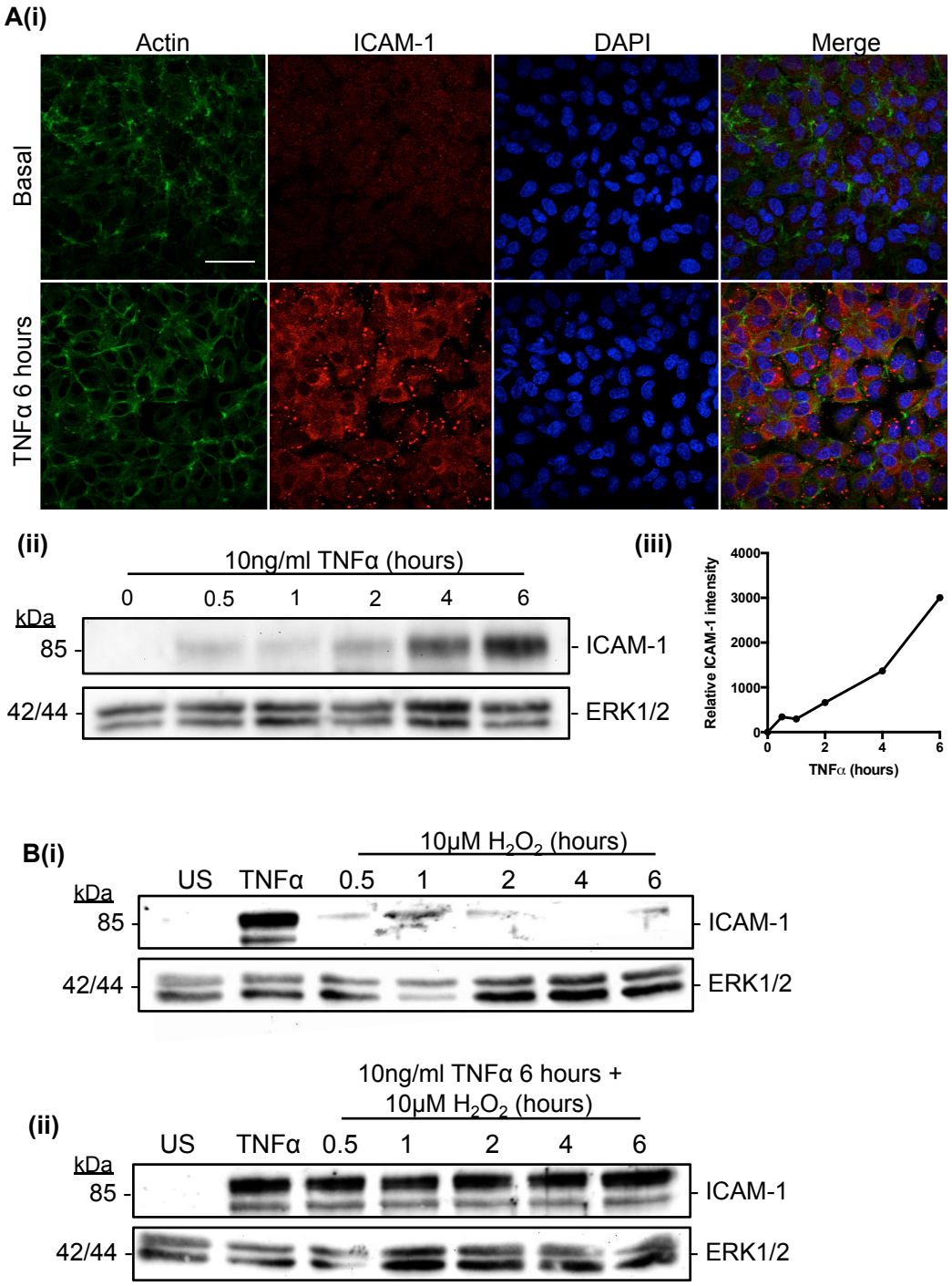


**Figure 4.26: $H_2O_2$ alone does not induce ICAM-1 expression or affect TNFα induced ICAM-1 expression in endothelial monolayers.** (A) Confluent monolayers of EA.hy926 endothelial cells were treated with 10ng/ml TNFα for up to 6 hours. ICAM-1 expression was assessed by (i) confocal microscopy, scale bar = 50μm, or (i,ii) Western blot. (B(i)) ICAM-1 and ERK expression in endothelial monolayers following 6 hours 10ng/ml TNFα or up to 6 hours 10μM $H_2O_2$ alone. (B(ii)) ICAM-1 and ERK expression following 6 hours 10ng/ml TNFα or up to 6 hours 10μM $H_2O_2$ with 10ng/ml TNFα for 6 hours. Representative immunoblots from two separate experiments.

### 4.17 fMLP and exogenous $H_2O_2$ increase intracellular ROS in primary human neutrophils

Phagocytes produce ROS following activation, either as part of respiratory burst or inside a phagolysosome. Using an intracellular ROS detector, DCFDA, the effect of chemoattractant stimulation upon intracellular ROS formation was measured. Moreover, to validate the use of DPI in other experimental settings, we tested whether DPI could reduce intracellular ROS concentrations. It must be noted that DCFDA is a general ROS detector and therefore it cannot be assumed that it specifically reflects true $H_2O_2$ levels. A cell permeable SOD mimetic, MnTBAP, was also employed to generate intracellular $H_2O_2$. Here, MnTBAP acted as a validation tool to confirm that DCFDA was functioning correctly.

Firstly, primary human neutrophils were loaded with 10μM DCFDA and treated with increasing concentrations of DPI for 30 minutes. Following incubation we observed significantly lower intracellular ROS in cells treated with 10μM DCFDA versus untreated controls (Figure 4.27a). To further validate the ROS detector, neutrophils were treated with SOD mimetic MnTBAP for 30 minutes. Following incubation, MnTBAP-treated cells showed a modest increase in intracellular ROS versus untreated cells, although this was not significant (Figure 4.27a). Next, neutrophils were treated with 10nM fMLP, a concentration determined to be optimal in chemotaxis assays. Intracellular ROS was sampled at time points over 30 minutes and a gradual increase in intracellular ROS following initial stimulation with fMLP was observed (Figure 4.27b). This was significantly higher than untreated cells after 15 minutes fMLP exposure. Finally, neutrophils were treated with increasing concentrations of exogenous $H_2O_2$ and intracellular ROS was detected after 5 or 30 minutes. A significant concentration dependent increase in intracellular ROS was seen after just 5 minutes with $H_2O_2$ concentrations greater than 10μM. This response was further amplified following the same trend after 30 minutes (Figure 4.27c).

Analysis of intracellular ROS was also carried out in monocytic cell lines. In both THP-1 and U937 cells (Figure 4.28), DPI evoked a concentration dependent reduction in intracellular ROS. SOD mimetic MnTBAP induced no increase in intracellular ROS in THP-1 monocytes and only a modest increase in U937 cells. Interestingly, in both monocytic cell lines, chemoattractant stimulation over 5 or 30 minutes (MCP-1 and $LTB_4$) did not provoke any observable change in intracellular ROS. Finally, exogenous $H_2O_2$ significantly increased detectable ROS in both monocytic cell lines.

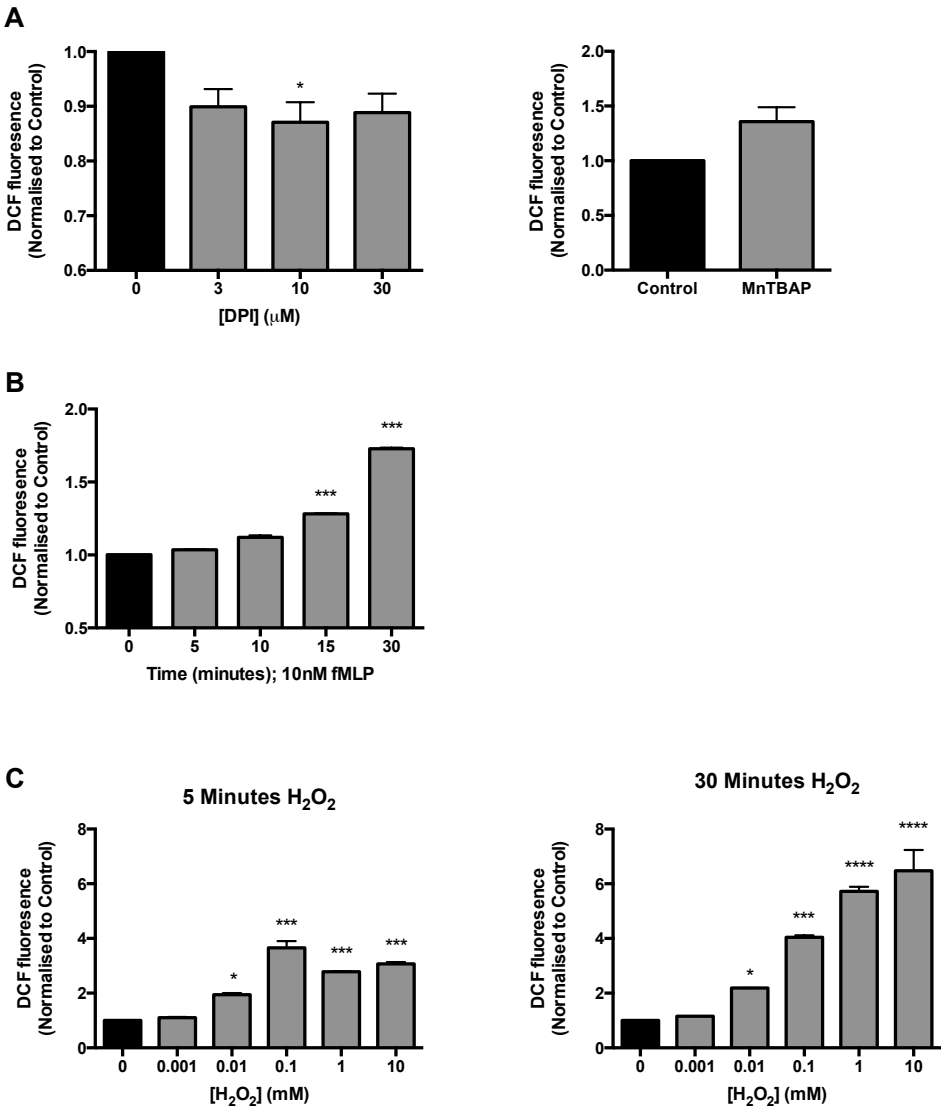


**Figure 4.27: Intracellular ROS detection in primary human neutrophils.** Neutrophils were isolated from peripheral human blood, rested in $Ca^{2+}$ free HBSS and loaded with 10μM DCFDA for 30 minutes. Cells were washed in HBSS and treated with (A) increasing concentrations of DPI (NADPH oxidase inhibitor) or 1μM MnTBAP (SOD mimetic) for 30 minutes, (B) 10nM fMLP for 5 to 30 minutes, or (C) increasing concentrations of $H_2O_2$ for 5 or 30 minutes. Fluorescence was analysed immediately using a FluoStar Optima plate reader. Data presented represent mean (±SEM) fluorescence minus plate background, normalized to untreated control from at least three separate experiments. Statistical analysis via one way-ANOVA with Dunnett's post hoc test where *=p<0.05, **=p<0.01, ***=p<0.001, ****=p<0.0001 versus control.

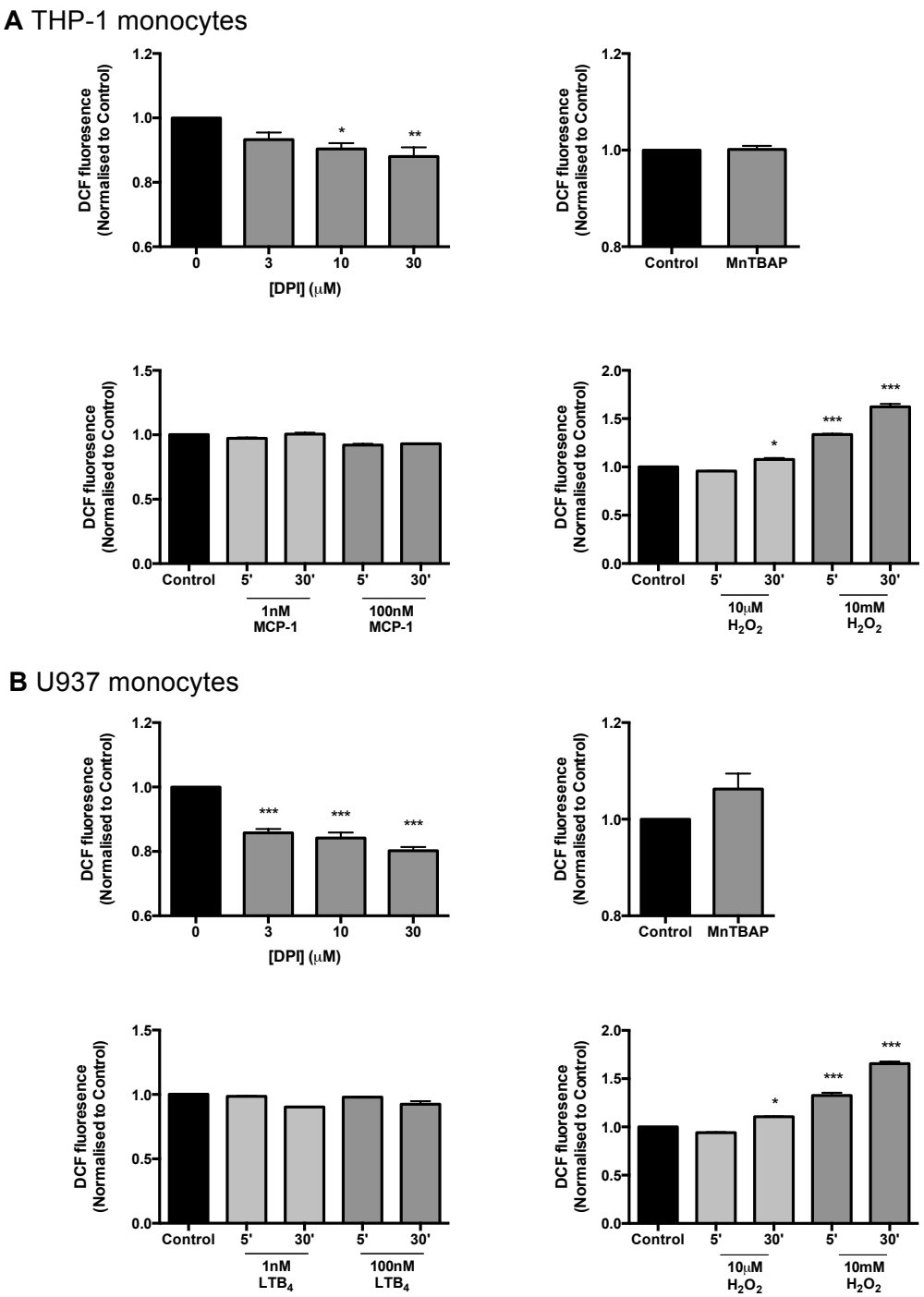


**Figure 4.28: Intracellular ROS detection in monocytic cell lines.** THP-1 monocytes (A) or U937 monocytes (B) were washed twice in plain media and loaded with 10μM DCFDA for 30 minutes. Cells were washed again and treated with increasing concentrations of DPI (NADPH oxidase inhibitor), 1μM MnTBAP (SOD mimetic) for 30 minutes, or increasing concentrations of MCP-1 or $LTB_4$ or $H_2O_2$ for 5 or 30 minutes. Fluorescence was analysed immediately using a FluoStar Optima plate reader. Data presented represent mean (±SEM) fluorescence minus plate background, normalized to untreated control from at least three separate experiments. Statistical analysis via one way-ANOVA with Dunnett's post hoc test where *=p<0.05, **=p<0.01, ***=p<0.001, ****=p<0.0001 versus control.

### 4.18 ATP induces migration of monocytes and neutrophils

As well as its known function in signalling and energy transfer, at high concentrations ATP acts as a damage-associated molecular signal. ATP is released by activated cells at sites of inflammation and therefore has key autocrine and paracrine signalling functions. The effect of exogenous ATP on innate cell chemotaxis, polarisation and morphology was investigated to complement the analysis of damage-associated signal $H_2O_2$ in innate cell function.

In the ChemoTx migration assay, THP-1 monocytes and primary human neutrophils migrated in a concentration dependent manner towards sub-milimolar concentrations of ATP (Figure 4.29a+b). This migration response showed a characteristic bell shaped trend, as seen previously with known chemoattractants in Figure 4.1. In order to investigate whether ATP-mediated migration was acting via G-protein related mechanisms, THP-1 monocytes were incubated with pertussis toxin (PTX) for 16 hours, before being plated in the ChemoTx assay above ATP. 1-100ng/ml PTX inhibited monocyte migration towards all concentrations of ATP (Figure 4.29a(ii)).

To test whether ATP was stimulating chemokinesis, or whether exogenous ATP could affect chemotaxis to known chemoattractants, cells were treated with increasing concentrations of exogenous ATP before being plated in the ChemoTx migration assay above 10nM MCP-1 (monocytes) or 10nM IL-8 (neutrophils), or plain media. ATP pre-treatment increased both MCP-1-mediated and basal migration of THP-1 monocytes to a comparable extent (Figure 4.30a(i)). However, the lowest ATP concentration tested (0.01mM) potentiated MCP-1-mediated chemotaxis but did not affect basal migration. Pre-treatment of neutrophils with increasing concentrations of ATP inhibited IL-8 mediated chemotaxis, to a significant extent with 1mM ATP (Figure 4.30b(i)). Basal migration appeared to be increased by ATP pre-treatment, in a bell shaped concentration dependent manner.

We have previously demonstrated that treatment with exogenous $H_2O_2$ inhibits both monocyte and neutrophil chemotaxis to known chemoattractants. The next approach tested whether this was also the case with ATP-stimulated chemotaxis. Both monocyte and neutrophil chemotaxis to 0.1mM ATP was significantly and concentration dependently inhibited by exogenous $H_2O_2$. Basal migration was also inhibited, but to a lesser extent (Figure 4.29a+b(ii)).

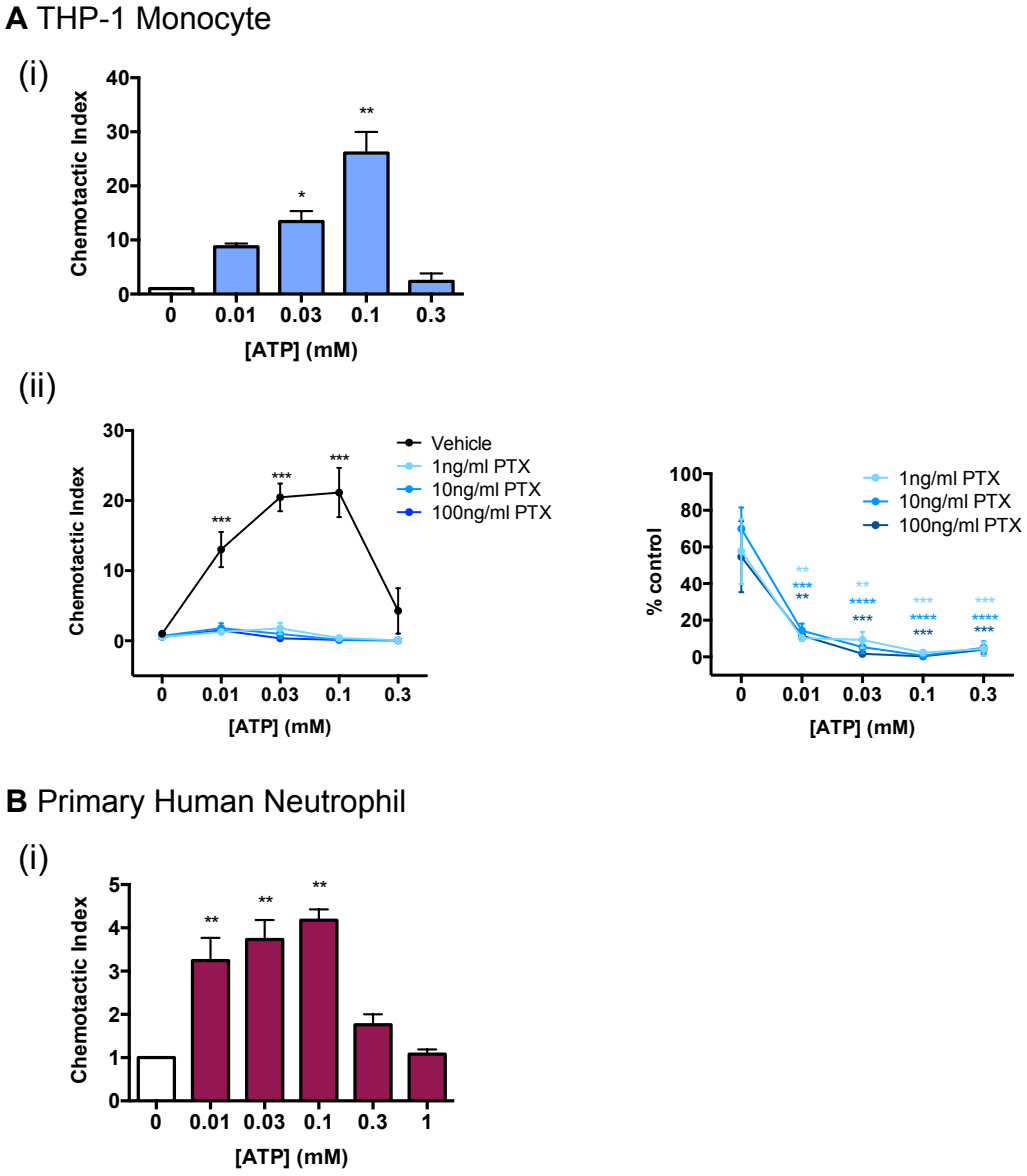


**Figure 4.29: ATP induces migration of monocytes and neutrophils.** (A) THP-1 monocytes or (B) primary human neutrophils were washed in serum free media, resuspended to $3.2x10^6$ cells/ml and rested. (i) Cells were plated on top of filter membranes above lower chambers containing increasing concentrations of ATP. (ii) Cells were stimulated with increasing concentrations of pertussis toxin (PTX) or vehicle for 16 hours at 37°C before being plated on top of filter membrane above lower chambers containing increasing concentrations of ATP or plain media. Chemotaxis across 5µm pore size membrane was determined after a 3 hour incubation at 37°C in 5% $CO_2$ as previously described. Data presented represents means ± SEM from at least three separate experiments. Statistical analyses (i) by one way-ANOVA versus untreated control with Dunnett's post and (ii) by two way-ANOVA versus untreated control with Tukey's multiple comparisons post test, where *=p<0.05, **=p<0.01, ***=p<0.001 and ****=p<0.0001.

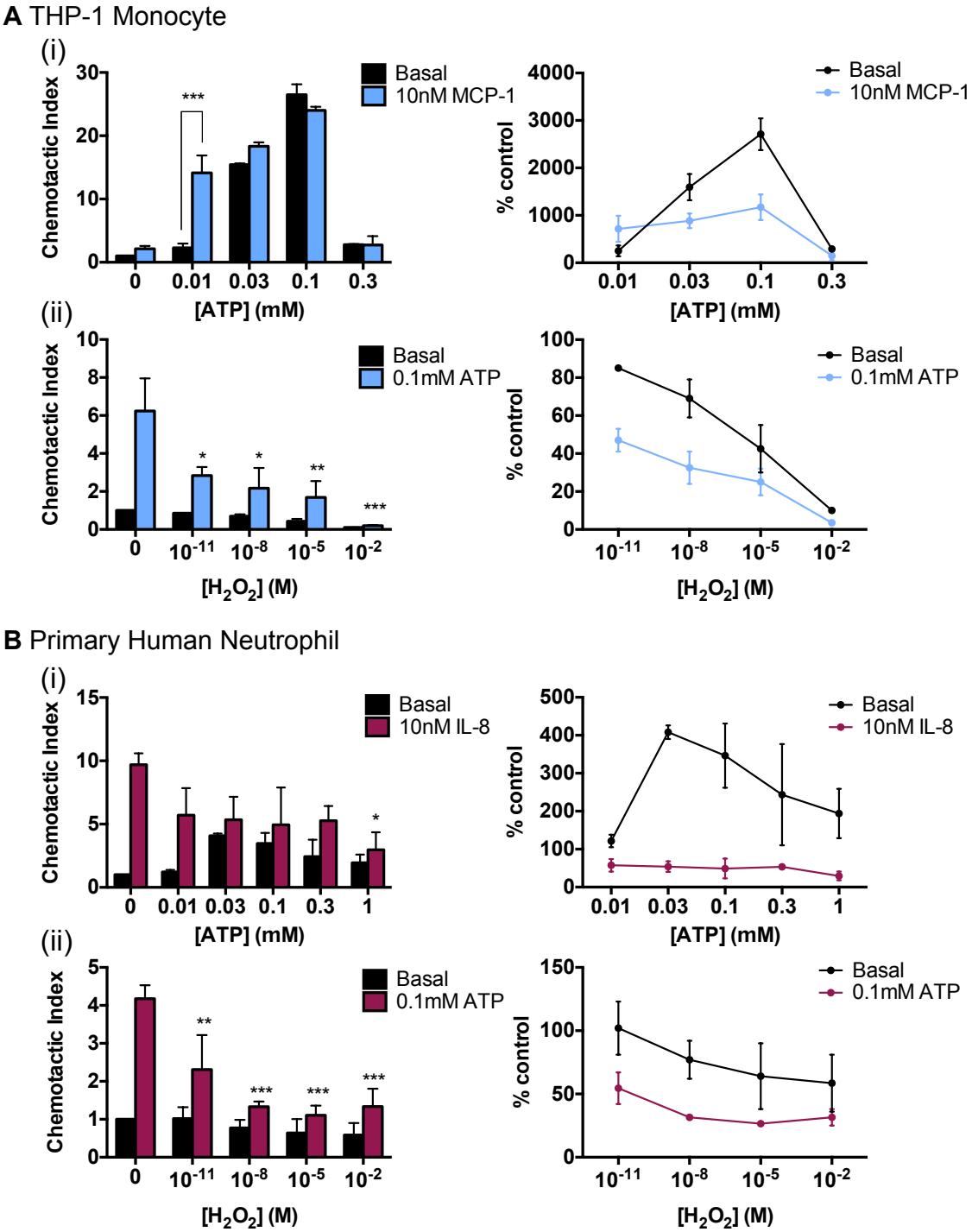


**Figure 4.30: ATP-mediated chemotaxis is inhibited by exogenous $H_2O_2$.** (A) THP-1 monocytes or (B) primary human neutrophils were washed in serum free media, resuspended to $3.2x10^6$ cells/ml and rested. (i) Cells were stimulated with increasing concentrations of ATP for 5 minutes at 37°C before being plated on top of filter membrane above lower chambers containing (A) 10nM MCP-1 or (B) 10nM IL-8 or plain media. (ii) Cells were stimulated with increasing concentrations of $H_2O_2$ for 30 minutes at 37°C before being plated on top of filter membrane above lower chambers containing 0.1mM ATP or plain media. Chemotaxis across 5µm pore size membrane was determined after a 3 hour incubation at 37°C in 5% $CO_2$ as previously described. Data presented represents means ± SEM from at least three separate experiments. Statistical analyses by two way-ANOVA versus untreated control with Tukey's multiple comparisons post hoc test. *=p<0.05, **=p<0.01, ***=p<0.001.

### 4.19 ATP stimulates actin reorganisation and spreading of THP-1 monocytes

We have seen that ATP induces a strong migratory effect in monocytes. To further explore the effect of ATP upon monocyte morphology *in vitro*, cell roundness and area in ATP treated cells was compared to untreated control cells. THP-1 monocytes were allowed to adhere to fibronectin-coated coverslips, treated with increasing concentrations of ATP for 5 minutes, fixed and stained to reveal F-actin. Confocal microscopy images reveal an elongated, irregular morphology of ATP treated monocytes compared to untreated cells (Figure 4.31a). Quantitative analysis revealed that ATP induced a significant concentration dependent reduction in cell circularity and increase in cell area compared to untreated cells (Figure 4.31b).

Studying immediate morphological responses to ligands can give us an insight into dynamic cell activation and the nature of their next actions, i.e. if they will migrate. THP-1 monocytes seeded onto fibronectin-coated coverglasses, stimulated with MCP-1, ATP or $H_2O_2$ and their immediate responses were imaged using phase contrast time-lapse microscopy. Following stimulation with 10nM MCP-1, cells appeared irregularly shaped and after 3 minutes they were elongated with a leading protrusive 'arm' (Figure 4.32a). Stimulation with 0.3mM ATP provoked a rapid change in monocyte morphology: many large protrusions around the cells extending into the surrounding space appeared within two minutes, which appeared to have collapsed and moved closer to the cell body by three minutes post stimulation (Figure 4.32b). 10μM $H_2O_2$ did not elicit any marked changes in monocyte morphology within 6 minutes post stimulation (Figure 4.32c). To provide a quantitative assessment of morphology, cell circularity was analysed over time and reveals a prominent shape change in ATP treated cells, with very little variation of morphology in $H_2O_2$-treated cells (Figure 4.32d).

### 4.20 ATP does not affect cell viability

As ATP is a known marker of damage and a strong damaging molecule, the effect of ATP on cell viability was assessed. Using the MTT viability assay, increasing concentrations of exogenous ATP did not have any significant effect on neutrophil viability over 4 hours (Figure 4.33).

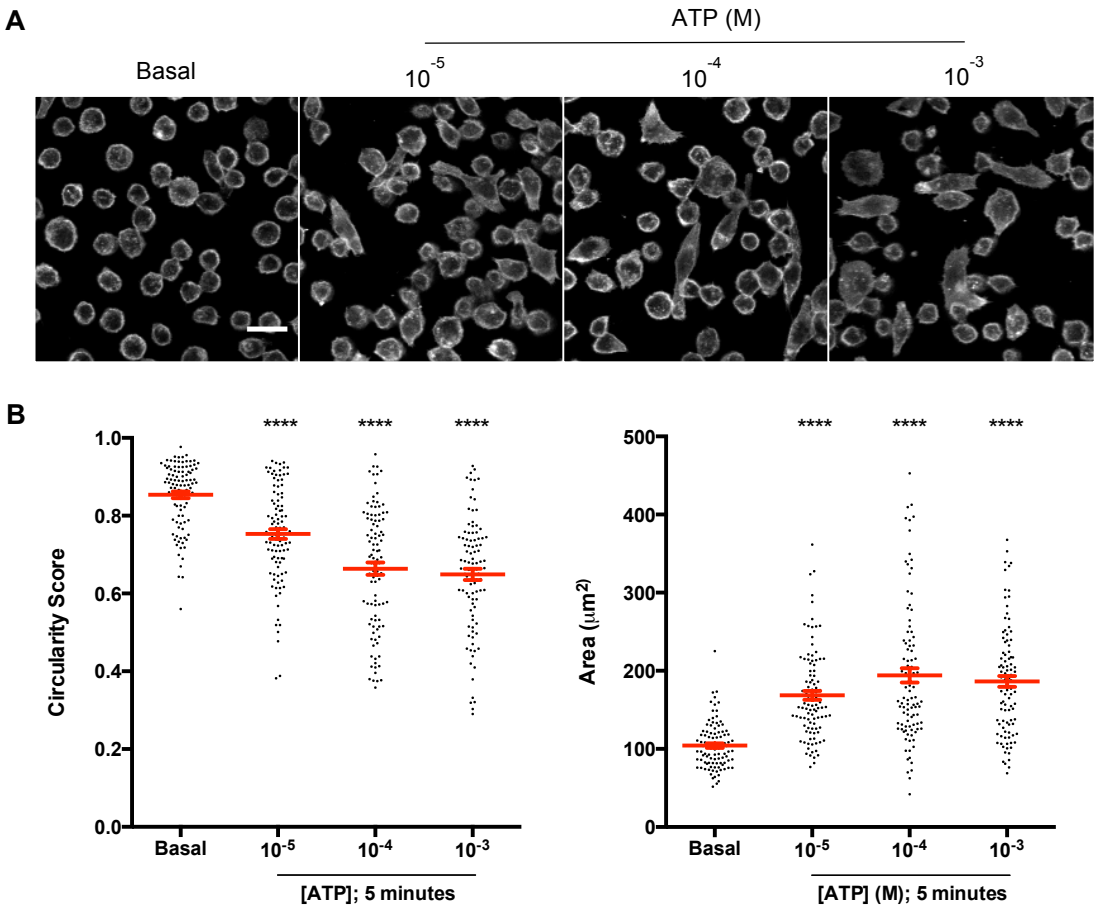


**Figure 4.31: ATP increases THP-1 actin reorganisation and spreading.** THP-1 monocytes washed, rested and plated on coverslips coated with 10μg/ml fibronectin and allowed to adhere for 30 minutes. Cells were treated with increasing concentrations of ATP for 5 minutes. Following incubation, cells were fixed in 4% PFA, permeabilised with 0.1% Triton-X and stained with Alexa-Fluor 488 conjugated Phalloidin and DAPI. (A) Representative images showing actin staining, scale bar = 20μm. (B) Circularity score (left) and area (right) were calculated using CellProfiler software, with at least 100 individual cells analysed per sample, from at least 4 pooled experiments. Data presented represents mean (± SEM) with statistical analysis by one way-ANOVA with Dunnett's post hoc test where ****=p<0.0001 versus basal control.

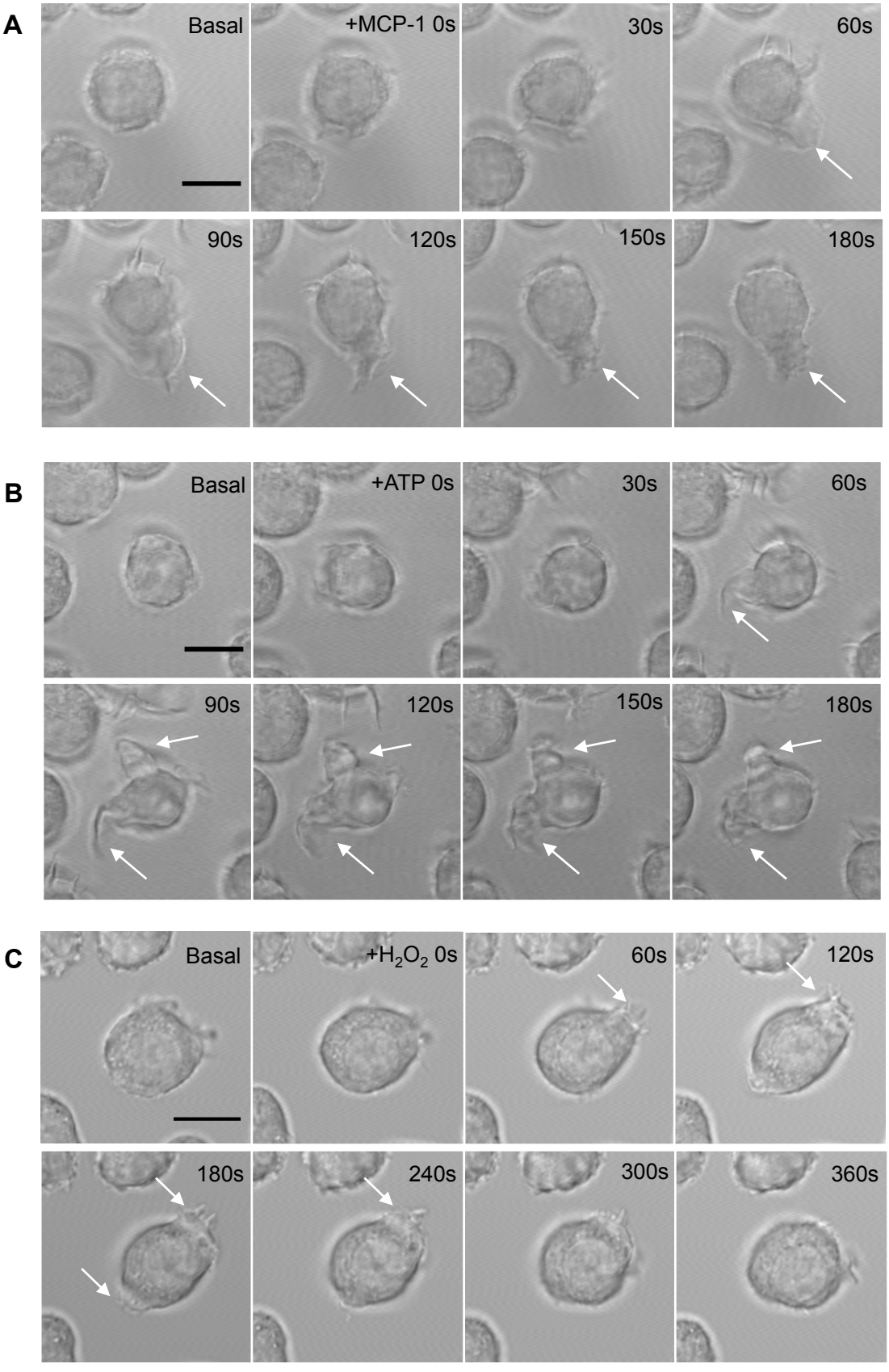
A
Basal
+MCP-1 0s
30s
60s
90s
120s
150s
180s
B
Basal
+ATP 0s
30s
60s
90s
120s
150s
180s
C
Basal
+H2O2 0s
60s
120s
180s
240s
300s
360s

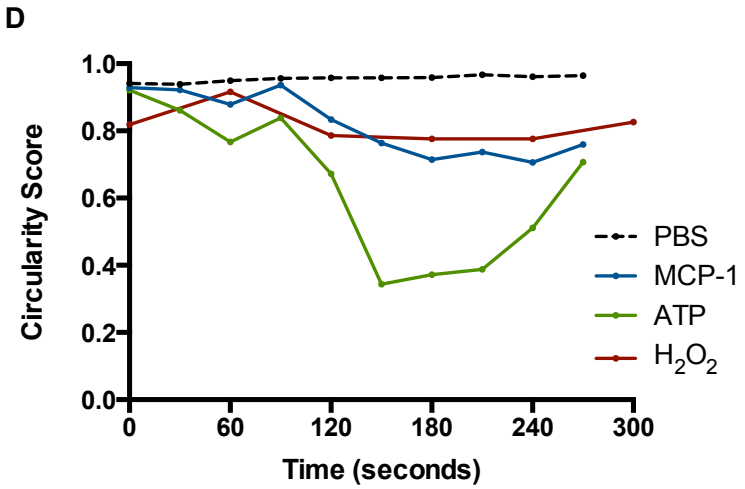


**Figure 4.32: Time lapse imaging of THP-1 monocytes seeded on fibronectin reveals changes in shape following stimulation with different agonists.** $10^6$ cells/ml were seeded on a chambered coverglass coated with 10µg/ml fibronectin and allowed to adhere for 30 minutes. Time-lapse recording began before cells were stimulated with (A) 10nM MCP-1, (B) 0.3mM ATP or (C) 10µM $H_2O_2$. Cells were imaged using confocal microscope with 63x oil objective under brightfield light. White arrows indicate membrane protrusions. Scale bar = 10µm. (D) Quantification of circularity over time as analysed by CellProfiler software with the FormFactor tool. Data presented represents a single experiment.

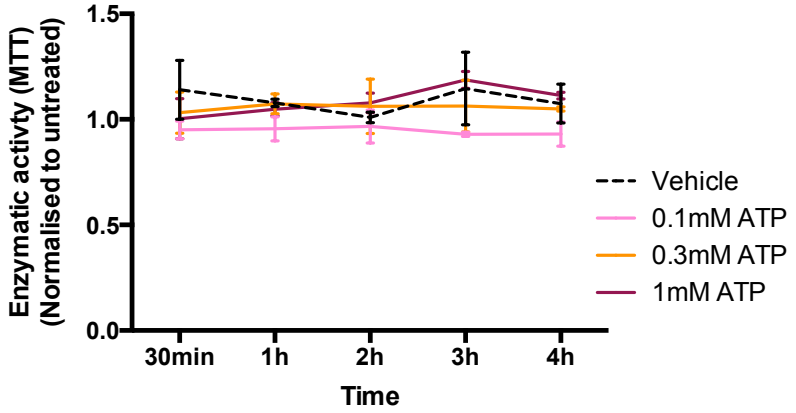


**Figure 4.33: Neutrophil viability is unaffected following exposure to ATP.** Primary human neutrophils were exposed to increasing concentrations of ATP or PBS vehicle control for up to 4 hours. Following culture, cells were assessed for viability using MTT assay. Data presented represent means (± SEM) minus plate background and normalized to untreated control from at least three independent experiments measured in triplicate, n=3.

## 4.21 Chapter 4 – Summary of Results

**Exogenous $H_2O_2$:**

- Inhibits basal and chemoattractant-mediated migration in neutrophils and monocytes in the ChemoTx migration model.
- Does not affect neutrophil chemotaxis to IL-8 or fMLP in the under agarose migration assay, nor does it affect neutrophil prioritisation in opposing gradients of IL-8 and fMLP.
- Does not induce monocyte actin reorganisation on fibronectin, nor does it affect chemokinesis or exploratory motility.
- Does not affect monocyte CCR2 expression or endothelial cell ICAM-1 expression.
- Inhibits macrophage and neutrophil phagocytosis of latex beads and bacteria.
- Induces a transient, biphasic rise in intracellular calcium in neutrophils but does not affect ligand-stimulated transient elevation of intracellular calcium in monocytes or neutrophils.
- Activates PI3K and MAPK signalling pathways in monocytes.
- Has no effect on neutrophil or monocyte viability at concentrations below 10mM.
- Increases intracellular ROS in monocytes and neutrophils.

**DPI:**

- Reduces intracellular ROS formation and inhibits monocyte and neutrophil chemotaxis, polarisation and spreading on fibronectin.
- Does not affect monocyte CCR2 expression

**Catalase:**

- Inhibits neutrophil chemotaxis, but enhances monocyte chemotaxis, polarisation and spreading in response to MCP-1.
- Does not affect monocyte CCR2 expression

**ATP:**

- Stimulates chemokinesis in monocytes and neutrophils, polarisation and spreading of monocytes on fibronectin, and does not affect viability.
- ATP-mediated monocyte migration is sensitive to pertussis toxin.
- Potentiates monocyte chemotaxis to MCP-1 but inhibits neutrophil chemotaxis to IL-8.
- Monocyte and neutrophil chemotaxis to ATP is inhibited by exogenous $H_2O_2$.

## 4.22 Chapter 4 – Discussion

### $H_2O_2$ does not act as a chemoattractant for human innate immune cells *in vitro*

In the ChemoTx migration assay, monocytes and neutrophils did not migrate towards $H_2O_2$. In fact, increasing concentrations of $H_2O_2$ inhibited basal migration. These results were unexpected given that $H_2O_2$ triggers immune cell recruitment to sites of injury in model organisms [233], [270]. To assess whether our results were consistent *in vitro*, an additional, alternative model of migration was used. In the under agarose migration assay, neutrophil migration towards a source of $H_2O_2$ was greater than migration towards an opposing gradient of plain control media. This has been demonstrated by other groups using zebrafish [282] and mouse neutrophils [325]. However, the extent of chemotaxis observed was considerably smaller than similar reported results. Furthermore, when compared to chemotaxis induced by IL-8 or fMLP, chemotaxis to $H_2O_2$ was noticeably smaller. Our observations suggest that $H_2O_2$ is not acting as a chemoattractant for human innate immune cells on a comparable level to known chemoattractants in an *in vitro* setting. The $H_2O_2$ concentration in these assays was not monitored over time, and therefore it cannot be assumed that a stable gradient of $H_2O_2$ was formed. In the ChemoTx migration assay, where the liquid-phase compartments are less likely to maintain a gradient of $H_2O_2$ for very long, cells in the top compartment are unlikely to sense a gradient of $H_2O_2$, and therefore may not migrate. This could be a contributing factor to the unexpected and inconsistent results observed in these assays.

### Exogenous $H_2O_2$ does not induce human innate cell migration and polarisation

At a site of tissue damage, activation of inflammatory cells will lead to the generation of multiple signals in addition to wound-generated cues. We sought to investigate whether $H_2O_2$ could influence the ability of known chemoattractants to stimulate migration. Cells were treated with exogenous $H_2O_2$ before being placed in either *in vitro* migration assay. In the ChemoTx migration assay, both monocyte and neutrophil migration to a range of chemoattractants was inhibited in $H_2O_2$-treated cells compared to untreated cells. In the under agarose migration assay, neutrophil migration to either IL-8 or fMLP was not affected by exogenous $H_2O_2$. This result highlights the differences in our *in* vitro assays, and suggests that exposure to short-lived gradients and subsequent saturated concentrations of $H_2O_2$ in the ChemoTx migration model is sufficient to induce arrest of motility. This response is less pronounced in the under agarose migration assay, possibly because gradients of $H_2O_2$ are longer lived.

Interestingly, another group have demonstrated that incubation of isolated human neutrophils with 10mM $H_2O_2$ caused a significant decrease in both chemotaxis and random migration of cells in agarose gel [410]. This was suggested to be due to a loss of deformability following exposure to $H_2O_2$. Exogenous $H_2O_2$ also inhibits induced pluripotent stem cell migration through fibronectin-coated porous filters and transendothelial migration [411]. Other groups have demonstrated that inflammatory mediators LPS and TNFα inhibit monocyte chemotaxis. This has been suggested to be due to transcription of MAPK phosphatase 1 (MKP1) which arrests MAPK-mediated chemotaxis [412]. Since phosphorylation of MAPK is required for monocyte and

macrophage chemotaxis towards MCP-1, $H_2O_2$ may be acting in a similar manner to inflammatory mediators to inhibit chemotaxis.

The effect of exogenous $H_2O_2$ on neutrophil random exploratory motility on fibronectin was also examined. This experiment mirrored the exogenous $H_2O_2$ experiment carried out in *Drosophila* embryos, where exogenous $H_2O_2$ reduced immune cell velocity *in vivo*. *In vitro*, when placed in exogenous $H_2O_2$, neutrophils did not polarise, move or explore the sample area to the same extent as when they were activated with IL-8 or fMLP, indicating that these defects could account for loss of migration. To investigate this further, monocytes were stimulated and fixed on fibronectin coated coverslips. Actin fibres were visualised to indicate cytoskeletal organisation in response to $H_2O_2$ or MCP-1. We found that monocytes adopt an irregular, 'polarised' morphology and increased area in response to stable concentrations of MCP-1, indicative of an activated adhesive cell that is ready to migrate. $H_2O_2$-treated cells remained round and regular in shape. Furthermore, $H_2O_2$ inhibited MCP-1-mediated changes in morphology when monocytes were first treated with $H_2O_2$. These data suggest that $H_2O_2$ may be modulating adhesive responses, and that $H_2O_2$ may be a negative regulator that limits lamellipodia formation.

We hypothesised that loss of surface expression or inactivation of the monocyte chemokine receptor CCR2 could account for the inhibition of monocyte chemotactic migration by $H_2O_2$. Certain inflammatory signals (e.g. LPS and TNFα) rapidly inhibit chemokine-receptor expression by targeting transcript stability. In a study of human monocytes, CCR2 mRNA was down-regulated 4 hours after the addition of LPS, although migration was inhibited before this [413]. Others have found that LPS induced a marked reduction in CCR2 cell surface protein levels within 2 hours [414]. However, studies using cultured human monocytes have shown that mRNA expression levels of the major chemokine receptors, CCR2, CCR5, and CXCR4 are upregulated by treatment with $H_2O_2$, and are downregulated by treatment with antioxidant reagents [415]. In contrast to these reports, we found no change in monocyte surface CCR2 by flow cytometry after 30 minutes exposure to exogenous $H_2O_2$. However, a significant loss of CCR2 following treatment with 30μM DPI was demonstrated, indicating that CCR2 expression may be redox sensitive. The detection method in our study could account for these contrasting results. It is possible that CCR2 mRNA, intracellular localisation and degradation could each be influenced by redox stimulation, but is unlikely that changes in transcription would occur within the 30 minute stimulation period. Therefore it is more likely that early changes in receptor expression may be due to receptor trafficking, which cannot be determined by flow cytometry alone.

**Alternative approaches to modulate ROS signalling**

Innate immune cells continuously produce ROS, even more so during activation following detection of inflammation [416]. NOX-generated $H_2O_2$ is produced at the plasma membrane, moves into the extracellular space and feeds back into cells to drive many important processes. For example, $H_2O_2$ influx via aquaporins is essential for T cell migration in response to a chemoattractant [327]. In light of this, we chose to investigate the effect of blocking the intracellular or extracellular compartments of $H_2O_2$

in order to dissect the contribution of intrinsic $H_2O_2$ generation and feedback upon immune cell processes *in vitro*.

Catalase is a naturally produced catalyst of $H_2O_2$ breakdown and was used to remove extracellular $H_2O_2$. Catalase inhibited monocyte migration towards MCP-1 in the ChemoTx migration assay, suggesting that ROS generation and subsequent autocrine or paracrine signalling in monocytes is an important regulatory mechanism in migration towards MCP-1. Interestingly, the opposite effect was observed in neutrophils; catalase induced a potentiation of IL-8-mediated migration. This observation suggests that $H_2O_2$ feedback may be important in promoting controlled migratory responses or immunosuppression. Monocytes plated on fibronectin and stimulated with catalase adopted an irregular, flattened morphology, and excessive lamellipodia. This indicates that extracellular $H_2O_2$ and feedback into monocytes is involved in regulating cell shape and substrate-integrin interactions and signalling. The morphology of catalase-treated monocytes is indicative of a cell with reduced motility, as lamellipodia are not focussed in one particular direction.

The effect of inhibiting NADPH oxidase with DPI to block ROS generation was also investigated. DPI-treated monocytes and neutrophils both displayed significantly reduced migration to chemoattractants. In the presence of DPI, monocyte morphology is more irregular than untreated cells, but not to the same extent as with MCP-1 alone. When co-treated with DPI and MCP-1, cells are more round and have fewer lamellipodia than with MCP-1 alone. These results suggest that intracellular NADPH oxidase signalling is vital in regulating cell migration and polarisation and is consistent with previously published reports. NOX4, an NADPH oxidase in monocytes and macrophages, has been shown to localise to focal adhesions and the actin cytoskeleton, and was associated with phospho-FAK, paxillin and actin, implicating it in the regulation of human monocyte adhesion and migration [417].

### The influence of $H_2O_2$ in opposing chemoattractant gradients

During an inflammatory event, leukocytes must follow endogenous and bacterial chemoattractant cues, as well as wound-generated cues if present. When faced with multiple cues, leukocytes must be able to distinguish and prioritise end target signals emanating from the source of damage or infection over intermediary chemoattractants encountered en route. Heit *et al* (2002) have reported that an intracellular signalling hierarchy determines the direction of neutrophil migration in opposing chemotactic gradients of end-target fMLP and intermediary IL-8, using the under agarose migration assay [189]. Other *in vitro* experiments have studied how neutrophils respond to stepwise and competing gradients of IL-8 and $LTB_4$, and have highlighted the ability of neutrophils to carry out serial responses to agonists presented in a defined spatial array [23]. We were interested to investigate whether $H_2O_2$ could be placed within this hierarchy, and to discover if $H_2O_2$ could be influencing signal prioritisation at sites of tissue damage.

In the under agarose migration assay, neutrophils migrated preferentially towards fMLP over IL-8, and this response was not affected by exogenous $H_2O_2$ in the cell or chemoattractant compartments. Neutrophils placed in opposing gradients of $H_2O_2$ and

IL-8 or fMLP, preferentially migrated towards IL-8 or fMLP over $H_2O_2$. Our results indicate that in the under agarose migration assay, $H_2O_2$ does not disrupt the ability of neutrophils to detect and distinguish competing cues. Exogenous $H_2O_2$ does not impair migration to IL-8 or fMLP alone or in opposing gradients, and is therefore is not prioritised over either intermediary or end-target cues.

### ChemoTx versus under agarose migration assays

Our *in vitro* migration assays have revealed considerable differences in responses of innate cells to $H_2O_2$. The nature of these models could influence experimental outcomes and could be responsible for discrepancies observed between the models. Several important differences are summarised in table 4.1.

| ChemoTx migration assay | Under agarose migration assay |
|---|---|
| • Vertical migration – influence of gravity | • Horizontal migration |
| • Liquid phase | • Agarose is semi-solid |
| • Fast diffusion rate | • Slower diffusion rate |
| • Uncoated polycarbonate filter | • Plates coated with FBS-enriched media |
| • Movement restricted by 5μm pores | • Un-restricted movement in all directions |
| • Only one gradient at a time | • Multiple gradients possible |
| • High throughput | • Low throughput |

**Table 4.1: Differences between *in vitro* migration assays.**

The most prominent experimental difference we have noticed between the models is that in the ChemoTx model, basal and chemoattractant-mediated cell migration is inhibited by $H_2O_2$, whereas in the under agarose model chemoattractant-mediated migration is not affected by $H_2O_2$. While the ChemoTx migration assay is a simplistic, high-throughput model of migration, it lacks physiological characteristics such as a substrate or forces exerted onto cells that the under agarose assay provides. Neutrophils migrating under agar will do so along serum coated plastic and will therefore engage adhesion receptors that will influence intracellular signalling. Neutrophils migrating through a vertical porous filter with no substrate are unlikely to be engaging the same adhesive processes. Additionally, the rate of diffusion between each molecule will vary greatly. The liquid-phase ChemoTx assay will facilitate very fast diffusion rates and sharp, short-lived gradients. In the under agarose model, the agar is likely to slow the rate of diffusion, but also provides a medium with which $H_2O_2$ can interact and breakdown. It is likely that all of these factors will influence experimental outcome and this highlights the limitations of simplistic *in vitro* models. In light of this, the pipette-tip chemotaxis assay [418], whereby a continuous source of $H_2O_2$ is perfused into an environment, may provide a better model for the gradients of $H_2O_2$ likely to be produced at a site of tissue damage.

**The effect of $H_2O_2$ on particle engulfment**

Our results demonstrate that $H_2O_2$ inhibits actin reorganisation and actin-mediated motility. We were therefore interested to see if this was also the case for phagocytosis, another actin-driven process. $H_2O_2$ is a secreted mediator during phagocytosis and contributes to bactericidal activity [419], so it was possible that $H_2O_2$ may have a regulatory role in this process. The effect of exogenous $H_2O_2$ on phagocyte engulfment of IgG-coated latex beads and bacteria was studied. One mechanism triggering phagocytosis is recognition of the Fc portion of immunoglobulins. Engagement of FcγRs by IgG-coated particles leads to the induction of signalling events involving actin reorganisation and membrane restructuring [420]. Alternatively, phagocytosis may be stimulated by activation of pathogen recognition receptors by bacteria [25]. Two phagocytes were used, macrophages and neutrophils, to study the engulfment of both IgG-coated beads and bacteria. Our results indicated that phagocytosis of both particles was significantly inhibited when phagocytes were pre-exposed to exogenous $H_2O_2$. This was an interesting result because it confirmed that another actin-regulated process was inhibited by exogenous $H_2O_2$ and suggests that $H_2O_2$ is indeed important in regulating phagocytosis. Our data was also in contrast to similar reports showing that high micromolar concentrations of $H_2O_2$ increased phagocytic function of human neutrophils [323]. In this case, $H_2O_2$-mediated calcium mobilisation was proposed as a mechanism for inducing subsequent phagocytosis of beads, and was reduced in the presence of catalase. No significant effect of catalase on neutrophil engulfment of beads or bacteria was observed, although we did find slight but significant inhibition of neutrophil phagocytosis of beads in the presence of DPI.

It is likely that a global effect of $H_2O_2$ is to account for the reduced phagocytosis, as we observed the same trends regardless of the particle type being engulfed and subsequent signalling pathways that would be activated.

During phagocytosis, phagocytes release $H_2O_2$ into the phagosomes and into the extracellular space. Because $H_2O_2$ can diffuse back into phagocytes, the intracellular environment is protected against peroxidation by catalase. Studies have shown that human phagocytes are damaged by extracellularly-generated $H_2O_2$ when intracellular catalase is inhibited [421]. When $H_2O_2$, generated during phagocytosis or adherence, is scavenged with catalase, the phagocytosis and chemotactic responsiveness of neutrophils is enhanced [422]. Furthermore, incubation of human neutrophils with $H_2O_2$ resulted in impairment of these functions [422]. This mechanism could also be accounting for the observation we have made – intracellular peroxidation by high concentrations of exogenous $H_2O_2$ may promote cell damage.

**Redox regulation of intracellular signalling – *calcium***

Our results demonstrate that monocyte and neutrophil ligand-stimulated activation results in a rapid and transient rise in intracellular calcium. This signal was only partially reduced in the absence of extracellular calcium, indicating that the responses were, in part, due to mobilisation of intracellular stores. These results are in line with published reports investigating agonist-mediated calcium mobilisation in innate cells [423]. In both monocytic cell lines and primary neutrophils tested, ATP induced a very

strong rise in intracellular calcium, consistent with other reported studies [360]. Our previous observations of immune cell function have revealed that in our hands many processes are impaired in the presence of exogenous $H_2O_2$. It was important to next investigate whether intracellular signalling pathways were also being inhibited by $H_2O_2$. Many published reports have suggested that $H_2O_2$ can induce mobilisation of intracellular calcium. However, the mechanism of how this occurs remains an issue of conflict, as discussed below.

Whilst $H_2O_2$ did not appear to induce transient calcium mobilisation in either of our monocytic cell lines, in THP-1 monocytes calcium levels decreased slightly and stably. In U937 monocytic cells, however, 10mM $H_2O_2$ induced a steady and linear rise in cytosolic calcium. These abnormal responses indicate that these concentrations of $H_2O_2$ could negatively affect the integrity of cell membranes. In primary neutrophils, however, 10mM $H_2O_2$ induced a transient and relatively short-lived increase in cytosolic calcium, although the kinetics appeared to be slower than responses induced by fMLP or IL-8 in these cells. Previous studies utilising neutrophils have observed a biphasic response to $H_2O_2$ in smooth muscle cells and cell lines [323], [333] so we were interested to see if this occurred in human neutrophils. 10mM $H_2O_2$ induced an initial transient and short-lived peak that returned to baseline. When recording was continued for a further 25 minutes, the initial peak was followed by a slower, sustained rise in cytosolic calcium that plateaued after approximately 10 minutes.

To dissect the possible mechanism driving this response, the experiment was repeated in the absence of extracellular calcium. Here, we observed an initial peak that was considerably smaller in intensity to that observed in the presence of extracellular calcium. This response plateaued and did not return to baseline and the response did not appear to be biphasic. Our results suggest that the initial transient increase in calcium could be due, in part, to mobilisation from intracellular stores because it was still apparent in the absence of extracellular calcium. However, the reuptake, or descending phase, of the initial transient response was lost following $H_2O_2$ stimulation in the absence of extracellular calcium. This suggests that reuptake of calcium into internal stores following stimulation by $H_2O_2$ is dependent upon the extracellular calcium concentration. This is distinct from our responses to other agonists, where reuptake appeared to occur in the absence of extracellular calcium.

Many reports have attempted to establish the mechanism of $H_2O_2$-evoked calcium responses, but these vary widely between cell types. Most relevantly, Korzets *et al* (1999) used PBMCs to show that the $H_2O_2$-induced rise in intracellular calcium was mostly due to influx via RTK-mediated mechanisms because of sensitivity to the tyrosine kinase inhibitor genistein. However, part of the response was due to the translocation from internal stores [334]. An alternative and less commonly discussed source of intracellular calcium mobilisation can occur through the membrane dissociation and cytoplasmic mobilisation of the phospholipid and calcium bound protein annexin VI. This potential source of oxidant-induced calcium flux has been characterised by Cuscheiri *et al* (2005). Using THP-1 monocytic cells, they identified that exposure to $H_2O_2$ results in lipid raft-regulated changes in annexin VI that results in cytosolic calcium flux, caMKII activation, and the formation of focal adhesion-like complexes [424]. Additionally, ROS-induced calcium influx could be via regulation of neutrophil death. After phagocytosis, where vast amounts of $H_2O_2$ are produced,

neutrophils eventually undergo apoptosis to prevent excessive inflammation. In a monocytic cell line $H_2O_2$ treatment of cells expressing the calcium channel TRPM2 resulted in calcium influx and onset of apoptosis [425]. What is noticeable in our calcium experiments is the very high $H_2O_2$ concentration (milimolar) required to initiate a response. The high threshold of $H_2O_2$ activation might serve to hold off activation in circulating neutrophils that, after transmigration and degranulation in the site of infection, would activate the calcium influx to reinforce the neutrophil activity. Alternatively, the calcium influx could be an apoptotic signal when ambient oxidant levels reach a level dangerous for the surrounding cells.

In light of a response being induced by $H_2O_2$ in neutrophils, we briefly explored the possibility of $H_2O_2$ being able to influence calcium signalling driven by other chemoattractants. Pre-exposure of cells to $H_2O_2$ before stimulation by chemoattractants did not affect calcium mobilisation, suggesting that the $H_2O_2$-mediated inhibition of leukocyte migration and polarisation is probably not due to $H_2O_2$ disrupting calcium signalling.

**Redox regulation of intracellular signalling – *protein kinases***

The direct targeting of protein kinases by $H_2O_2$ is considered to be a likely mechanism by which $H_2O_2$ modulates intracellular signalling as redox regulation of protein kinases contributes to their activity in a number of settings [305]. The effect of exogenous $H_2O_2$ on kinase phosphorylation in a monocytic cell line was briefly investigated. U937 monocytic cell lysates were probed for levels of pAkt and pERK following stimulation with $H_2O_2$ and compared to responses induced by fMLP, which increases PI3K and MAPK signalling in leukocytes [426]. $H_2O_2$-mediated ERK activation has been previously reported in human monocytes [427].

Our initial data indicate that micromolar concentrations of exogenous $H_2O_2$ can increase pAkt and pERK levels in a monocytic cell line compared to untreated control cells. However, this was not a concentration dependent response although levels were similar to those induced by fMLP. This suggests that PI3K/Akt and MAPK signalling pathways are being activated by the presence of exogenous $H_2O_2$. When treated in combination with $H_2O_2$ and fMLP, pAkt levels did not alter from fMLP-alone treated cells, while pERK levels increased almost 1.5 fold from fMLP-alone. Taken together, these preliminary results suggest that both bacterial and wound-derived cues can activate PI3K/Akt and MAPK signalling pathways. However, increased pAkt and pERK could be indicative of general cell stress or damage.

**Redox regulation of intracellular signalling - *ROS generation***

Dichlorofluorescein was used to detect intracellular ROS and show that fMLP stimulated an increase in intracellular ROS in neutrophils, but this was not apparent in MCP-1- or $LTB_4$-stimulated monocytic cells, even with concentrations optimal for migration. This indicates that production of ROS and feedback into cells may be more tightly controlled in monocytes than in neutrophils. It has previously been reported that THP-1 cells undergo mild redox remodelling in response to PAMPs, a process that is

absent in primary monocytes. Upon challenge with several TLR ligands, including pro-inflammatory mediator LPS, intracellular ROS did not change in THP-1 cells [428]. This was found to be because THP-1 cells have upregulated antioxidant systems that buffer the oxidative hit provided by TLR triggering and suppress the consequent redox response. Only very high (5mM) concentrations of $H_2O_2$ overcame the high antioxidant capacity of THP-1 cells to restore a redox response [428]. It is likely that a similar process is occurring upon exposure of THP-1 monocytes to chemoattractants such as MCP-1.

Exogenous $H_2O_2$ lead to significant increases in intracellular ROS most notably in neutrophils with micromolar concentrations, although monocytic cell lines required higher concentrations to have similar effects. This does not, however, indicate whether the exogenous $H_2O_2$ is entering the cells, possibly via aquaporins, or whether stimulation with $H_2O_2$ leads to upregulated NOX activity. Either way it confirms that in our experiments exogenous $H_2O_2$ gives rise to an oxidative intracellular environment. Treatment of unstimulated cells with DPI resulted in reduced detectable levels of ROS, and indicates the ROS generation occurs in the absence of cell activation. This observation concurs with many reports on the mechanism of action of DPI [429].

**Redox regulation of adhesion receptor expression**

Endothelial activation by inflammatory mediators, including TNFα, is associated with specific increases in surface expression of leukocyte receptors including ICAM-1. Using the EA.hy926 endothelial cell line, we were able to recapitulate TNFα-induced ICAM-1 expression, as confirmed by microscopy and analysis of protein expression. The human umbilical vein cell line, EA.hy926, was established by fusing primary human umbilical vein cells with a permanent human cell line A549 [384]. At a site of tissue damage, there is potential for wound-generated signals to diffuse into an area of tissue containing vasculature. Like other inflammatory mediators, several studies have indicated that $H_2O_2$ can affect endothelial cell properties including permeability [430], and adhesiveness [431]. $H_2O_2$-induced increases in neutrophil adhesion are inhibited *in vivo* by antibodies against ICAM-1 and CD18 [432], highlighting the relevance of $H_2O_2$ in regulating adhesion molecules. We next sought to determine whether $H_2O_2$ could influence endothelial cell ICAM-1 expression in a similar manner to that induced by TNFα.

Our results demonstrate that 10μM $H_2O_2$ alone does not induce ICAM-1 expression to levels similar to those induced by TNFα over a six hour time period. Furthermore, co-treatment with $H_2O_2$ did not affect TNFα-mediated ICAM-1 expression. These results are in direct contrast to those of a group that studied the action of $H_2O_2$ in human umbilical endothelial cells. Bradley *et al* (1993) used 'subinjurious' concentrations of $H_2O_2$ to modulate ICAM-1 expression. Here, 50-100μM $H_2O_2$ selectively increased surface expression of ICAM-1 after 24 hours [433]. They also found increased ICAM-1 mRNA after 4 hours. Interestingly, co-treatment with $H_2O_2$ inhibited TNF-induced gene expression at 4 hours – they attribute this to reversible inhibition of TNF binding to endothelial surface receptors. A key difference between our study and that of Bradley *et al* is the timing of measurement. The 6 hour time frame in this investigation may have been too early to allow for any transcriptional changes in ICAM-1 to be measured.

However, another group have observed changes at earlier time points. In a study of the effect of $H_2O_2$ on endothelial cell adhesiveness, expression of steady state ICAM-1 mRNA and protein was determined in human umbilical cord vein endothelial cells [324]. It was reported that adhesion of human leukocytes to the endothelium, ICAM-1 protein and ICAM-1 mRNA were all increased following stimulation with $H_2O_2$ within two hours. Furthermore, the addition of catalase inhibited $H_2O_2$-induced adhesion. Differences between our investigations and those of others could arise due to factors such as use of a hybrid cell line instead of primary endothelial cells; the timing of measurement to allow for transcription, trafficking, or degradation; and the stability of the initial $H_2O_2$ signal and how long it is maintained for. In a similar manner to experiments analysing CCR2 expression, protein levels alone do not provide a dynamic assessment of ICAM-1 localisation, trafficking or activation, which are likely to be essential features of adhesion receptor expression in response to damage associated signals.

### $H_2O_2$ and cell viability

The MTT cell viability assay was employed to assess the toxicity of $H_2O_2$ in our cell populations. Our results indicate that sub-milimolar concentrations of exogenous $H_2O_2$, catalase or DPI, did not affect mitochondrial enzymatic activity. In experimental models exploring the physiological functions and toxic effects of $H_2O_2$, cultured cells are often exposed to $H_2O_2$ added as a bolus into the culture medium, as was the case in our experiments. In these settings, considerable variations in the concentrations of $H_2O_2$ determined to be cytotoxic can be found ranging from less than 10μM to 1000μM [434]. In a study of mammalian cell viability, Nakamura *et al* (2003) reported that micromolar concentrations of $H_2O_2$ induce oxidative DNA lesions more efficiently than milimolar concentrations [435]. Because of the variability and inconsistency between reported effects of $H_2O_2$, Gulden *et al* (2010) demonstrated that experimental conditions such as exposure time and cell concentration can affect the variability of extracellular cytotoxic concentrations [434].

### Extracellular ATP promotes chemokinesis

Extracellular ATP is a damage-associated signal, which, like $H_2O_2$, can have distinct effects at different concentrations. Elevated and sustained concentrations of ATP cause cell death through $P2X_7R$ signalling [363] while lower concentrations have been linked with regulatory processes such as cell proliferation [436]. We were interested to investigate the effects of sub-toxic concentrations of ATP on immune cell function *in vitro*. Importantly, no loss of cell viability was observed with any of the ATP concentrations used in these studies.

In the ChemoTx migration assay, monocytes and neutrophils migrated towards increasing sub-milimolar concentrations of ATP with a bell shaped response curve. These observations were similar to published studies showing migration of human blood-derived monocytes and macrophages to ATP in the ChemoTx migration assay [437]. ATP-mediated chemotaxis of THP-1 monocytes was pertussis toxin sensitive, indicating that migratory processes are likely to be activated by the action of G

proteins, possibly downstream of the ATP-sensitive P2Y receptors. Indeed, Chen *et al* (2006) report that ATP release by human neutrophils at their leading edge directly feeds back through $P2Y_2Rs$ to amplify chemotactic signals and direct cell orientation [438].

To determine whether the ATP-induced migration of monocytes and neutrophils was dependent on gradient formation, studies were conducted in which ATP was added to the upper compartment of the chemotaxis chamber, together with the cell population. Migration of cells with ATP in the cell compartment was increased in the absence of an additional chemoattractant cue in the bottom chamber, indicating ATP was stimulating chemokinesis. This result echoes previous observations by Lambert *et al* (2010), where ATP-mediated migration of microglia was found to be due to ATP-mediated chemokinesis [437].

When monocytes were plated with ATP in the upper compartment, migration to MCP-1 was also considerably increased, even at lower concentrations of ATP. This suggests that the chemokinetic effect of ATP was potentiating MCP-1/CCR2-mediated migration. However, when neutrophils were plated with ATP in the upper compartment, their migration to IL-8 was inhibited, while migration to plain media was increased. This result is conflicting with other reports that show ATP synergises with IL-8 to activate neutrophil migration [439]. However, it is important to consider that IL-8-induced neutrophil chemotaxis requires concurrent activation of $P2Y_2R$ by ATP [439], and this may be gradient sensitive. Additionally, cell activation by IL-8 is likely to induce ATP release [440], which, together with exogenously added ATP, may push the extracellular concentration towards excessive levels and thus inhibit migration, as observed with our earlier bell-shaped concentration response curve.

Our results indicate that ATP might regulate distinct responses in monocytes and neutrophils. It was therefore important to test whether $H_2O_2$ could also influence ATP-mediated chemokinesis. Consistent with earlier results, plating monocytes or neutrophils with $H_2O_2$ in the top compartment of the chemotaxis chamber resulted in the inhibition of migration towards ATP. This suggests that $H_2O_2$ may be inhibiting ATP-induced chemokinesis and provides additional evidence to support the hypothesis that $H_2O_2$ is acting to inhibit global motility and not directed chemotaxis in the ChemoTx migration assay.

To further explore the effect of ATP on cell activation, we also studied the ability of ATP to induce cell polarisation and spreading on fibronectin. Staining of F-actin in fixed ATP-treated THP-1 monocytes revealed a concentration dependent decrease in circularity, and a concurrent increase in cell area, indicative of an activated phenotype. This response is in agreement with early studies that revealed extracellular ATP promotes the formation of microglial processes that are characteristic of the surveillance state [441]. To extend this investigation we compared the immediate morphological responses of monocytes to bolus additions of ATP, $H_2O_2$ or MCP-1 using time-lapse imaging. Within seconds of ATP stimulation, membrane extensions are visible on all sides of the cell and are indicative of rapid activation capable of driving motility. This was not observed with $H_2O_2$, where only small and broader lamellipodial extensions were formed more slowly, although not in one particular direction or with any comparable intensity to ATP. In contrast to both damage

associated cues, MCP-1 induced the formation of what appeared to be one leading broad projection, promoting its role as a chemoattractant even in the absence of a gradient. Taken together, these morphological studies support the idea that $H_2O_2$ and ATP are distinct in their abilities to induce cell activation or promote motility.

**Proposed model for redox and ATP-mediated regulation of cell motility**

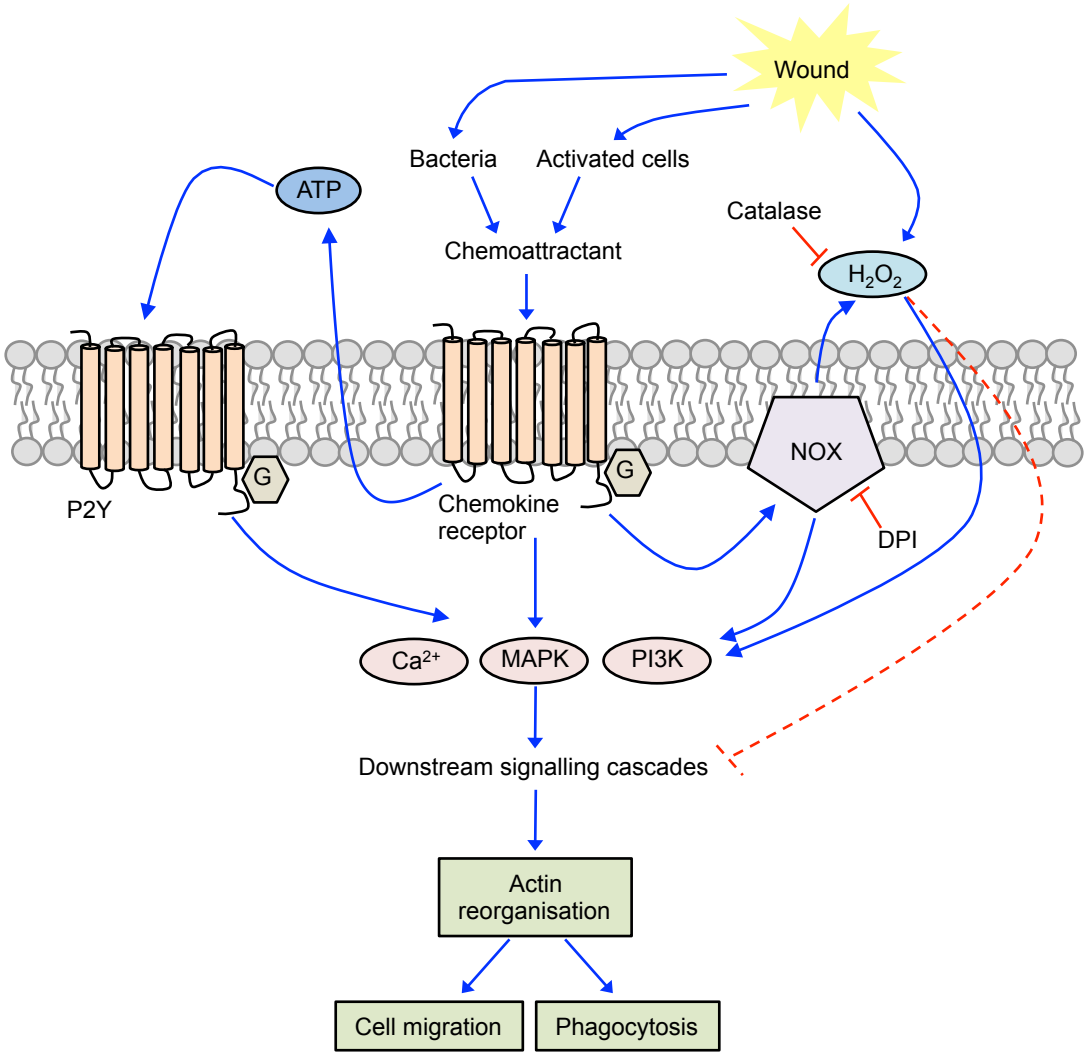


**Figure 4.34: Proposed model for redox and ATP-mediated control of cell polarisation and phagocytosis.** Bacterial and intermediate chemoattractant cues activate GPCRs, which in turn activate NOX enzymes to generate $H_2O_2$. Extracellular $H_2O_2$ can feedback into cells and activates signalling pathways including MAPK and PI3K cascades. $H_2O_2$ may be acting on downstream signalling mediators to inhibit actin-driven processes such as migration and phagocytosis. Chemokine receptor activation also leads to production of ATP, which feedback through P2YRs to engage similar pathways involved in actin reorganisation. Addition of exogenous $H_2O_2$ or ATP exacerbates the signalling pathways shown. Catalase can break down extracellular $H_2O_2$ and DPI can inhibit NOX enzymes.

# CHAPTER 5: SFK AND PI3K SIGNALLING AND FUNCTION IN HUMAN INNATE IMMUNE CELLS

## 5.1 Rationale

Src family kinases (SFKs) are a conserved group of enzymes known for their widespread cellular functions across many signalling pathways in multiple species. In human cells, multiple SFK family members play overlapping roles, particularly during activation of the immune system. They signal downstream of various receptor types by phosphorylating tyrosine residues and enable recruitment of key adaptor molecules, including Syk kinase. Importantly, SFKs have been shown to act as redox sensors *in vivo* and are involved in driving immune cell recruitment to a wound [282].

Earlier in this thesis, using an embryonic *Drosophila* model of tissue damage, we have observed a significant role of SFK member Src42A in hemocyte recruitment to a wound. Furthermore, we have detected compromised motility and directed migration of hemocytes in flies lacking functional Src42A. These results agree with external reports suggesting a role for zebrafish Src42A homologue Lyn in neutrophil recruitment in a similar tissue damage model [282]. We have also shown that the adaptor molecule Syk (*Drosophila* Shark) is also involved in mediating immune cell migration to a wound in *Drosophila* (see section 3.3). In light of these findings, a natural progression for this study is to next examine the role of SFKs and Syk in human innate immune cell function, to identify possible conservation or divergence in responses between species. To achieve this, pharmacological modulators of SFK and Syk can be used in *in vitro* models of innate cell activation and function.

Hanke *et al* (1996) first reported of PP1, a pyrazolopyrimidine, and its close relative PP2, both discovered in tyrosine kinase inhibitor screens [442]. PP1 and PP2 display considerable selectivity for SFKs, although they do not discriminate between family members. Hanke's group used an *in vitro* kinase assay with human peripheral blood lymphocytes to indicate PP2 $IC_{50}$ values against Lck (4nM), Hck (5nM), Fyn (5nM), JAK2 (>50μM), and EGF-R (480nM) [442]. In a later, more comprehensive screen, PP1 and PP2 inhibited Src and Lck with $IC_{50}$ values of 50nM, whereas Csk, p38a MAPK and CK1d were inhibited with 3-10 fold lower potency. Interestingly, RIP2 was inhibited more potently than either Src or Lck [443]. A recent kinome profile using a panel of over 200 kinases deemed PP2 to be non-selective [444].

One report has questioned the mechanism of action of PP2 as a competitor for the ATP binding pocket of SFKs. Karni *et al* (2003) report that PP1 and PP2 are not ATP competitors and are 'mixed-competitive' regarding the substrate [445]. The relative selectivity of PP1/PP2 towards active Src may be accounted for by their binding to a unique domain close to the substrate site but removed from the ATP binding domain. The sequences of Src, Lck and Hck at domains adjacent to the ATP binding site show significant differences. PP2 may therefore bind to the ATP-adjacent domain, and this would account for the significant differences in the $IC_{50}$ values for PP2 for Hck, Lck, Fyn and Src demonstrated by Hanke *et al* (1996) [445].

The small molecule protein kinase inhibitor piceatannol can be used to study the contribution of Syk in the responses of monocytes and neutrophils to chemoattractants. Piceatannol is a resveratrol analogue that exhibits anti-proliferative and anti-inflammatory effects. It inhibits protein tyrosine kinases by competing for the tyrosine-containing substrate binding site [446]. In a cell-free kinase activity assay, piceatannol

was shown to inhibit p40 kinase, a proteolytic fragment of Syk, with $K_i$ = 15μM. This concentration was lower than that required in inhibit Lck [446]. Another study showed that piceatannol is also more selective for Syk ($IC_{50}$ = 10μM, cell-free kinase assay) than another SFK, Lyn ($IC_{50}$ = 100μM) [447].

The role of PI3K enzymes in leukocyte biology has been extensively studied and it is clear that PI3K signalling contributes to many cellular processes, especially those involved in immune responses. PI3K signalling has been reported to regulate neutrophil protrusion and polarity in an *in vivo* zebrafish model by activation of Rac in a spatial manner within cells [190]. Additionally, PI3K has been shown to be essential for hemocyte chemotaxis towards a wound in a *Drosophila* embryonic wound model [269]. To complement our investigations into SFK signalling in innate cells, we also sought to examine the role of PI3K in models of human innate immune cell chemotaxis using pharmacological tools.

Pan-isoform inhibitors such as LY294002 and ZSTK474 have been well studied and widely used to elucidate the function of PI3K. LY294002 is a first generation, non-selective and reversible inhibitor of PI3K [448], with some activity against mTOR signalling at concentrations above 5μM [196]. ZSTK474 is an ATP-competitive inhibitor of class I PI3K isoforms with weak activity against mTOR even at high micromolar concentrations [197]. *In vivo* models have revealed that ZSTK474 inhibits the growth of solid tumours in mice xenograft models [449], and is currently in Phase I clinical trials in patients with solid tumours. ZSTK474 also has anti-inflammatory effects. A recent study demonstrated that ZSTK474 protected mice from collagen-induced arthritis [450], and another showed that ZSTK474 ameliorates the progression of adjuvant-induced arthritis in rats [451].

As PI3K family members are involved in many different processes, therapeutic targeting of PI3K with pan-isoform inhibitors is likely to provoke strong side effects. Therefore, endogenous and leukocyte-specific negative regulators of PI3K have emerged as potential therapeutic candidates through which PI3K signalling can be modulated. SHIP-1 and PTEN control local spatial localisation of $PI(3,4,5)P_3$ and thus regulate cell polarisation, as described in section 1.2.2.

SHIP-1 dephosphorylates the PI3K product $PI(3,4,5)P_3$, yielding $PI(3,4)P_2$. SHIP-1 activators should therefore mimic the actions of PI3K inhibitors and provide an alternative way of targeting the PI3K pathway. Aquinox pharmaceuticals have developed SHIP-1 activating compounds for application in inflammatory disorders. AQX-1 (AQX-1125) is the most advanced and displayed positive effects in a recent Phase I clinical trial for asthma [452]. AQX-1 directly binds to SHIP-1 and requires an intact SHIP-1 C2 domain to function [201]. 260nM AQX-1 was demonstrated to inhibit monocyte migration by 50% in a modified Boyden chamber chemotaxis assay [201]. This compound has now entered Phase II trials for the treatment of COPD and interstitial cystitis.

In addition to mimicking PI3K inhibition using a SHIP-1 activator, we also tested a SHIP-1 inhibitor to demonstrate whether relieving the negative regulation of PI3K could affect functional responses. 3 α-aminocholestane (3AC) is a selective, small molecule inhibitor of SHIP-1, although the site of drug-protein interaction is unclear [202]. 3AC

inhibits SHIP-1 with an $IC_{50}$ value of 10μM, compared to >1mM against SHIP-1 or PTEN, as determined using an *in vitro* phosphatase assay [202]. SHIP-1 inhibition by 3AC triggers apoptosis of human acute myeloid leukaemia cell line, and may serve to increase immunoregulatory capacity [202].

PTEN is another PI3K negative regulator that converts $PI(3,4,5)P_3$ to $PI(4,5)P_2$. We tested an inhibitor of PTEN, dipotassium bisperoxo (5-hydroxypyridine-2-carboxyl) oxovanadate (BpV(HOpic)). BpV(HOpic) has a reported $IC_{50}$ value of 14nM in an *in vitro* phosphatase assay [453]. Other groups have reported that *Dictyostelium* cells lacking PTEN fail to migrate efficiently and show increased frequency of spontaneous protrusion and multiple, broad pseudopodia pointing generally but not directly at a chemoattractant source [454], [455]. Therefore, it is important to investigate whether pharmacological inhibition of PTEN could also affect leukocyte migration *in vitro*.

Additionally, a focussed study of specific class I PI3K isoforms in cell polarisation and spreading will be undertaken to study the roles of individual PI3K isoforms in more detail. Isoform-selective inhibitors against p110α (A66), p110β (GSK2636771) and p110δ (IC87114) are described with $IC_{50}$ values in more detail in section 1.2.2 and table 1.3.

In summary, this chapter aims to examine the contribution of SFK and PI3K signalling to monocyte and neutrophil motility, chemotaxis and actin organisation. We also aim to investigate whether the wound cue $H_2O_2$ can influence SFK signalling in human innate cells *in vitro*.

## 5.2 Distinct roles for SFK and Syk during innate cell chemotaxis

Our first objective was to identify the contributions of SFK signalling mediators in innate cell chemotaxis using the ChemoTx migration assay. Using pharmacological inhibitors of SFKs and Syk, we hoped to identify an effect upon migration to known chemoattractants. THP-1 monocytes and primary human neutrophils were pre-treated with the pan-SFK inhibitor PP2, or the Syk kinase inhibitor piceatannol, for 30 minutes before chemotaxis to known chemoattractants was measured using the ChemoTx migration assay.

PP2 inhibited both THP-1 monocyte migration to 10nM MCP-1, and primary neutrophil migration to 10nM IL-8 (Figure 5.1a+b). PP2 inhibited monocyte migration to MCP-1 with an $IC_{50}$ value of approximately 100nM, greater than previously reported values in alternative kinase assays [442]. In both cell types, basal migration to plain media was also inhibited by pre-treatment with PP2.

Interestingly, MCP-1-mediated THP-1 monocyte migration was significantly enhanced following treatment with Syk inhibitor piceatannol, in a concentration dependent and bell-shaped manner (Figure 5.1a). Piceatannol increased MCP-1-mediated chemotaxis with an $EC_{50}$ value of approximately 100nM. Pre-treatment with piceatannol had no significant effect on basal THP-1 monocyte migration. Conversely, pre-treatment of primary human neutrophils with 1μM piceatannol significantly inhibited chemotaxis towards 10nM IL-8 (Figure 5.1b).

## 5.3 SFK and $H_2O_2$ may signal through a common pathway

We have observed that both exogenous $H_2O_2$ and SFK inhibition induce similar inhibition of both monocyte and neutrophil chemotaxis to known chemoattractants. SFK and $H_2O_2$ signalling has previously been linked in studies with zebrafish models of inflammation [282], where it was proposed that $H_2O_2$ oxidises zebrafish SFK Lyn in neutrophils, leading to migration. We have taken a simplistic *in vitro* approach to identify whether SFK and $H_2O_2$ could signal via the same pathway in human cells. We compared the effect of inhibiting SFKs, or treating cells with exogenous $H_2O_2$, alone and in combination.

THP-1 monocytes and primary neutrophils were treated with 0.1μM PP2 alone, 10μM $H_2O_2$ alone, or both 0.1μM PP2 and 10μM $H_2O_2$ in combination for 30 minutes before being exposed to a chemoattractant in the ChemoTx migration assay. In both cell types, all treatment combinations induced very similar inhibition in chemoattractant-mediated migration to approximately 50% of chemoattractant-induced and basal responses. There were no significant differences observed when cells were treated with PP2 or $H_2O_2$ alone compared to treatments given in combination (Figure 5.2).

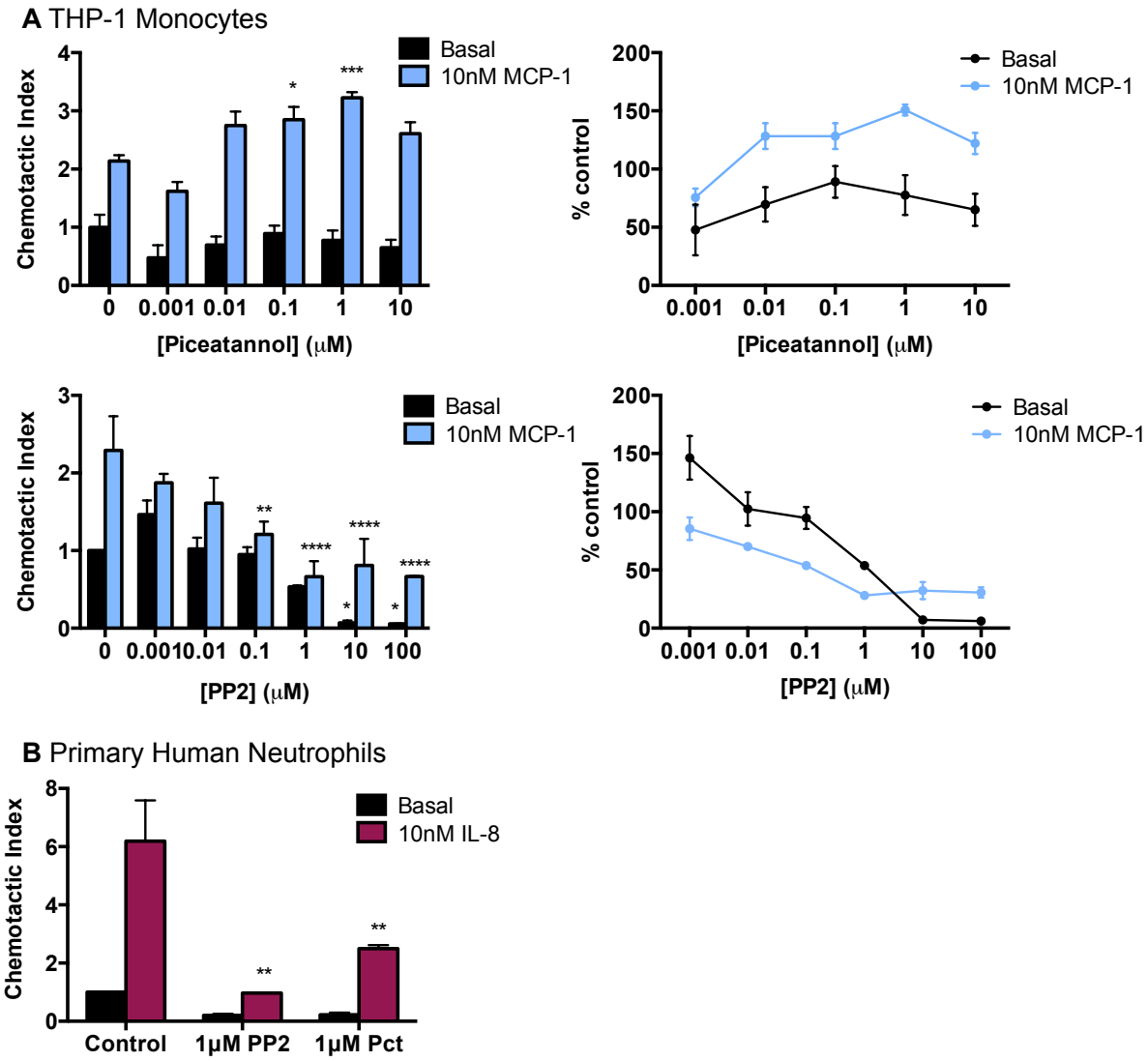


**Figure 5.1: Syk inhibition increases THP-1 monocyte chemotaxis but inhibits neutrophil chemotaxis, SFK inhibition inhibits both monocyte and neutrophil chemotaxis.** (A) THP-1 monocytes or (B) primary human neutrophils were washed in serum-free media, resuspended to $3.2x10^6$ cells/ml and incubated with piceatannol (Syk inhibitor) or PP2 (SFK inhibitor) for 30 minutes at 37°C before being plated on top of filter membrane above lower chambers containing (A) 10nM MCP-1 or (B) 10nM IL-8 or plain media. Migration is expressed as chemotactic index (left panels), and as a percentage of control cells (right panels). Chemotaxis across 5μm pore size membrane was determined after a 3 hour incubation at 37°C in 5% $CO_2$ as previously described. Data presented represents means ± SEM from at least three separate experiments. Statistical analyses by two way-ANOVA versus untreated control with Dunnett's multiple comparisons post hoc test. *=p<0.05, **=p<0.01, ***=p<0.001, ****=p<0.0001.

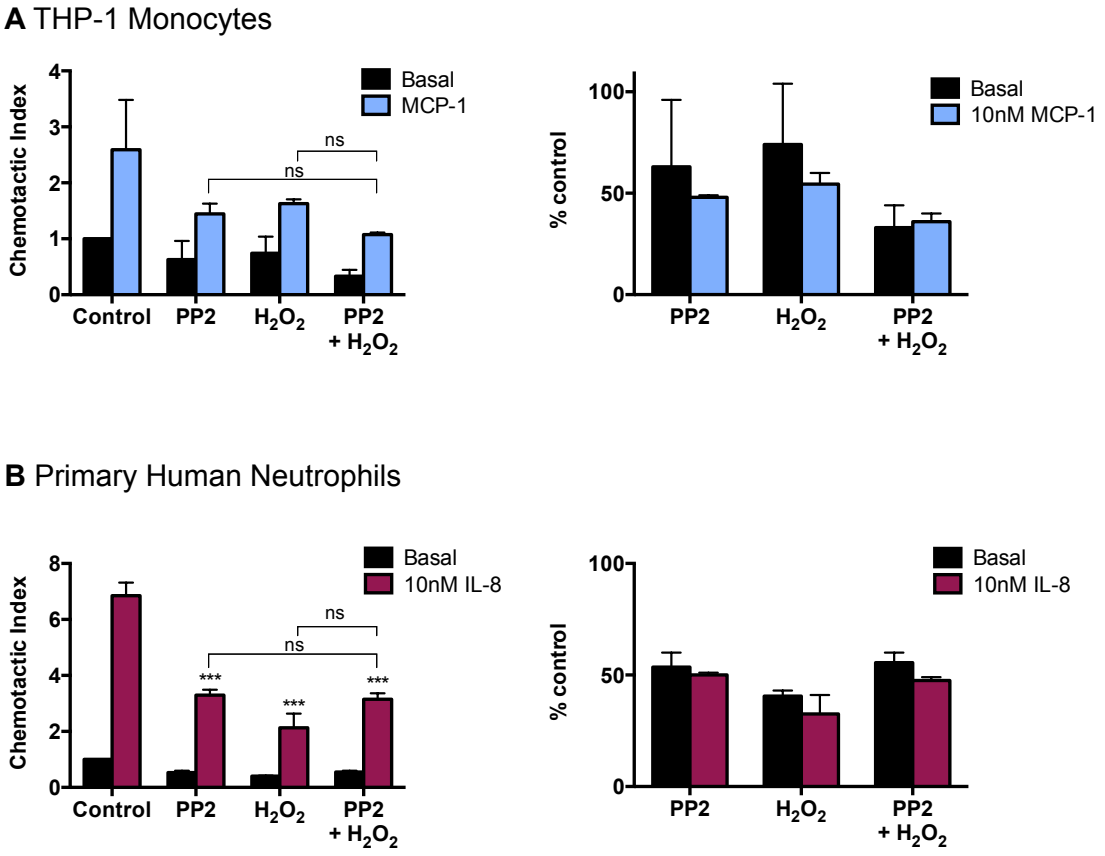


**Figure 5.2: Simultaneous SFK inhibition and exogenous $H_2O_2$ stimulation does not rescue or exacerbate migration in monocytes or neutrophils.** A) THP-1 monocytes or (B) primary human neutrophils were washed in serum free media, resuspended to $3.2x10^6$ cells/ml and incubated with 0.1μM PP2, 10μM $H_2O_2$ or both 0.1μM PP2 and 10μM $H_2O_2$ together for 30 minutes at 37°C before being plated on top of filter membrane above lower chambers containing (A) 10nM MCP-1 or (B) 10nM IL-8 or plain media. Chemotaxis across 5μm pore size membrane was determined after a 3 hour incubation at 37°C in 5% $CO_2$ as previously described. Data presented represents means ± SEM from at least three separate experiments. Statistical analyses by two way-ANOVA with Tukey's multiple comparisons post hoc test where ns = no significant difference, ***=p<0.001 versus control.

### 5.4 Neutrophil viability is not affected by PP2 and piceatannol

Pharmacological inhibitors of signalling cascades can have non-specific targeting effects, and may cause cytotoxicity. It was therefore sensible to establish if the concentrations of PP2 and piceatannol selected for these studies were exhibiting such an effect on the cells. In the assays described in this chapter, cells could be exposed to compounds for times ranging from 30 minutes to 4 hours. Therefore, we chose to assay viability over a 4-hour time course.

Using the MTT viability assay, neither PP2 nor piceatannol had any significant effect upon neutrophil viability over a 4-hour time course (Figure 5.3).

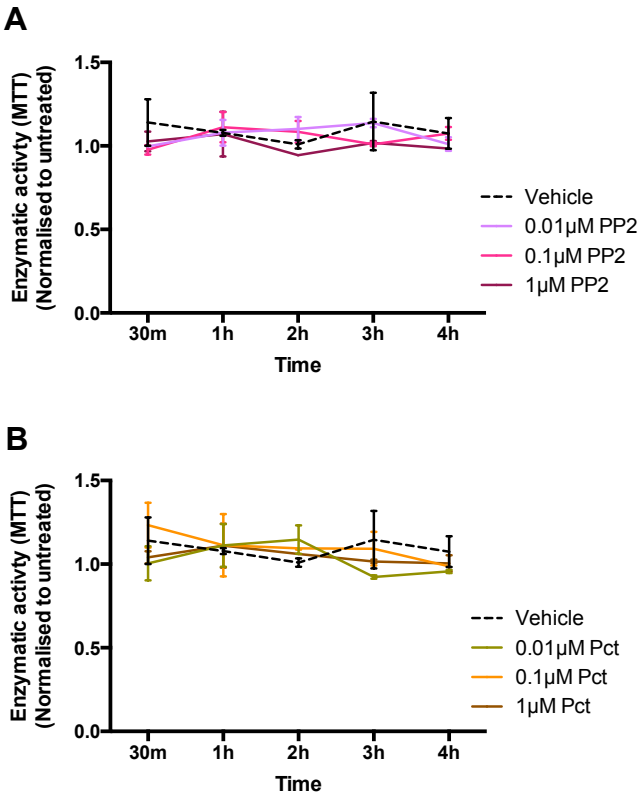


**Figure 5.3: Neutrophil viability is unaffected following exposure to PP2 or piceatannol.** Primary human neutrophils were exposed to increasing concentrations of PP2 (A) or piceatannol (Pct) (B) or PBS vehicle control for up to 4 hours. Following culture, cells were assessed for viability using MTT assay. Data presented represent means (± SEM) minus plate background and normalized to untreated control from at least three independent experiments each measured in triplicate.

### 5.5 Syk inhibition, but not SFK inhibition, potentiates MCP-1-induced THP-1 monocyte actin organisation

In the ChemoTx migration assay, THP-1 monocytes exhibited contrasting responses following SFK inhibition or Syk inhibition. Notably, inhibition of Syk by piceatannol resulted in enhanced MCP-1-mediated migration. To investigate the effect of these pharmacological inhibitors in more detail, THP-1 monocytes were seeded onto fibronectin-coated coverslips. Following treatment, cells were fixed and stained to visualise cellular F-actin by confocal microscopy. Quantitative analysis was carried out using software that calculates the degree of roundness of each individual cell, to give a circularity score that indicates the extent of cell polarisation and elongation, and cell surface area, to indicate the degree of cell spreading and flattening.

Confocal microscopy of cellular F-actin revealed that MCP-1-stimulated cells had an irregular, elongated morphology, and appeared to be 'polarised' compared to untreated cells that were much rounder and regularly shaped (Figure 5.4a). This phenotype was previously demonstrated in section 4.9. Quantitative analysis revealed that MCP-1-stimulated cells were significantly less circular (mean circularity: 0.778 versus 0.918) and were significantly larger (mean area: 148.4μm$^2$ versus 123.5μm$^2$), compared to untreated cells.

Cells treated with 0.1μM PP2 were regular, round and without any visible lamellipodial projections. Quantitative analysis revealed no significant difference in circularity between PP2-treated and untreated cells (Figure 5.4b). However, PP2-treated cells were significantly smaller than untreated cells (mean area: 105.2μm$^2$ versus 123.5μm$^2$). Treatment of cells with PP2 reversed the MCP-1-mediated decrease in circularity (mean circularity: 0.903 versus 0.778) and reversed the MCP-1-mediated increase in surface area (mean area: 102.0μm$^2$ versus 148.4μm$^2$) (Figure 5.4b).

Cells treated with 0.1μM piceatannol were also regularly shaped with no clear membrane extension or protrusions (Figure 5.4a). Quantitative analysis revealed no significant difference in circularity or cell surface area between piceatannol-treated and untreated cells (Figure 5.4c). However, piceatannol further potentiated MCP-1-mediated polarity (mean circularity: 0.698 versus 0.778) but did not affect the MCP-1 mediated increase in mean cell surface area.

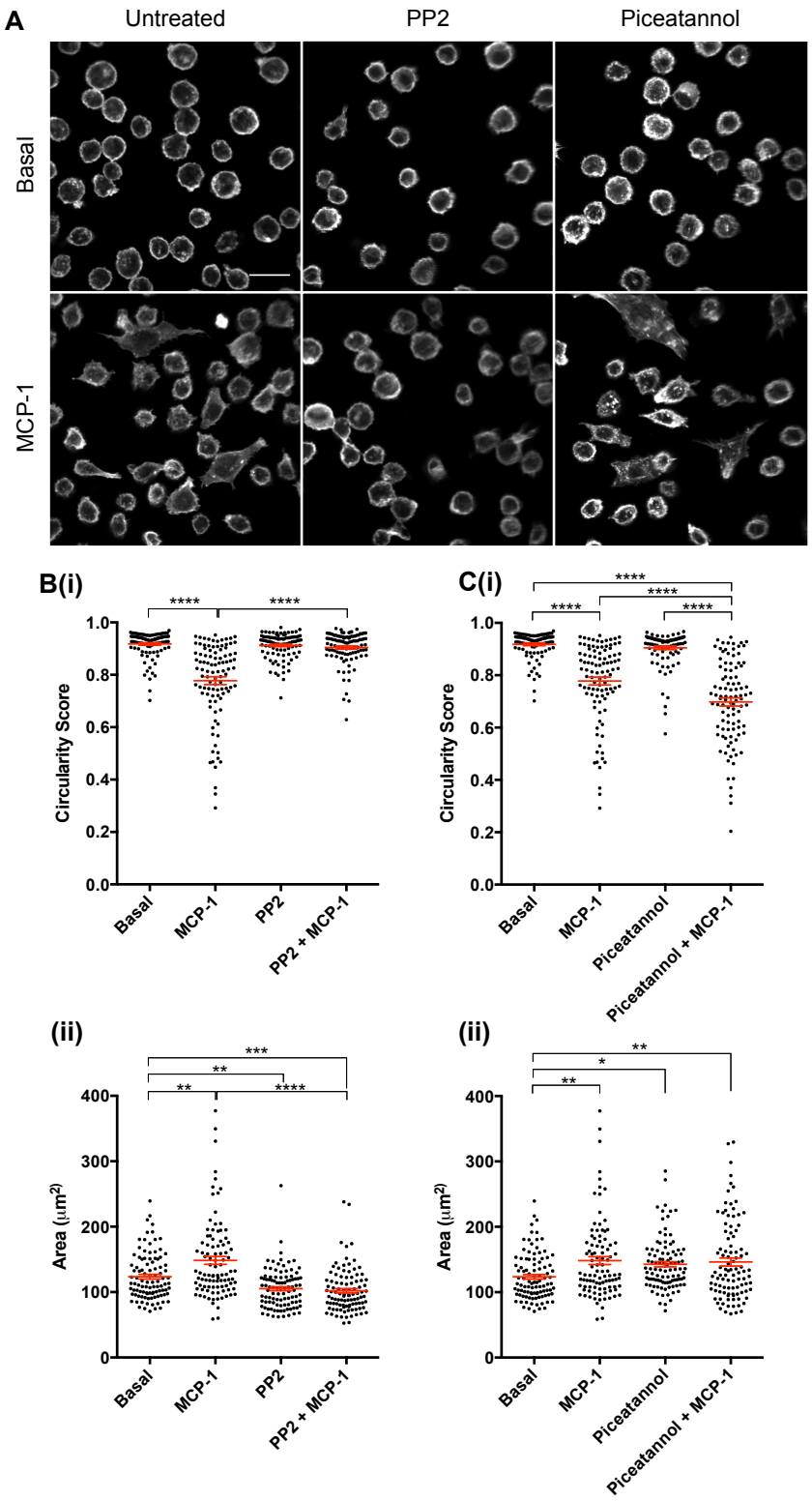


**Figure 5.4: Piceatannol, but not PP2, potentiates MCP-1 induced THP-1 monocyte polarisation and spreading.** THP-1 monocytes washed, rested and plated on coverslips coated with 10μg/ml fibronectin and allowed to adhere for 30 minutes. Cells were treated with either 0.1μM piceatannol or 0.1μM PP2 for 30 minutes, followed by either 10nM MCP-1 or PBS for 5 minutes. Following incubation, cells were fixed in 4% PFA, permeabilised with 0.1% Triton-X and stained with Alexa-Fluor 488 conjugated Phalloidin and DAPI. (A) Representative images showing F-actin, scale bar = 20μm. (B) Circularity score (i) and area (ii) for PP2 treated cells and (C) circularity score (i) and area (ii) for piceatannol treated cells were calculated using CellProfiler software, with at least 100 individual cells analysed per sample, from at least 4 pooled experiments. Data presented represents mean (± SEM) with statistical analysis by one way-ANOVA with Tukey's multiple comparisons post hoc test where *=p<0.05, **=p<0.01, ***=p<0.001, ****=p<0.0001.

### 5.6 Phagocytosis of latex beads and bacteria is inhibited by SFK inhibition

Phagocytosis is a very complex process involving numerous recognition and signalling cascades, motility mechanisms, and degradation systems. SFK and Syk kinases have been shown to mediate phagocytic activity of glial cells in *Drosophila* models [287]. Here we sought to establish if this was also the case in human innate immune cells, by using IgG-opsonised fluorescent latex beads and CFSE-loaded bacteria as fluorescent particles for engulfment, and neutrophils and macrophages as phagocytes.

Pre-treatment of primary neutrophils with 0.1μM PP2 significantly inhibited phagocytosis of IgG-opsonised latex beads and bacteria (Figure 5.5a+b). This was analysed by both flow cytometry, to measure mean fluorescence intensity of viable phagocytes, and confocal microscopy, with manual counting of the percentage of cells containing at least one particle. PP2 treatment resulted in an approximately 60% reduction in the phagocytosis of beads, and an 80% reduction in the phagocytosis of bacteria. Similarly, phagocytosis of IgG-opsonised latex beads by macrophages was inhibited by pre-treatment with 0.1μM PP2 (Figure 5.5c). PP2 inhibited both the proportion of cells engulfing beads and the average number of beads engulfed per cell, by approximately 50%. This was determined by confocal microscopy and manual counting of phagocytosed beads.

### 5.7 SFK inhibition does not affect ligand-stimulated elevation of intracellular calcium

SFK signalling operates in many cellular processes. We have previously observed an inhibitory effect of SFK inhibition upon innate cell chemotaxis, polarisation and phagocytosis. We next sought to examine whether intracellular $Ca^{2+}$ ($[Ca^{2+}]_i$) signalling was compromised in these cells following similar treatment with the pharmacological inhibitor PP2. Elevation of $[Ca^{2+}]_i$ triggered by ligand stimulation is a well characterised observation in leukocytes and provides an assessment of signalling potential. To measure the responses of ligands in leukocytes pre-treated with PP2 or vehicle, cells were loaded with $Ca^{2+}$ sensor Fluo-4 that produces a fluorescent signal relative to the amount of available $Ca^{2+}$ in the cell.

Primary human neutrophils were loaded with 10μM Fluo-4 and the fluorescence signal that reports $[Ca^{2+}]_i$ was recorded continuously. After a baseline was established, cells were treated with 0.1μM PP2 for 10 minutes. Following incubation, cells were stimulated with 10nM IL-8, 10nM fMLP or 10μM $H_2O_2$ to induce a transient ligand-stimulated elevation in $[Ca^{2+}]_i$. In this assay, fMLP induced a significant increase in detectable $[Ca^{2+}]_i$, as quantitatively measured by $F_{max}/F_0$ (Figure 5.6c). While both IL-8 and $H_2O_2$ also induced an elevation of $[Ca^{2+}]_i$, this was not significantly greater than vehicle treated cells (Figure 5.6c). Importantly, pre-treatment with PP2 had no significant effect on the extent of $[Ca^{2+}]_i$ elevation induced by any of the ligands tested (Figure 5.6b), versus vehicle treated cells (Figure 5.6a). Additionally, PP2 did not affect the neutrophil response to ionomycin.

To summarise, the defect in chemotaxis in PP2-treated cells is not due to a defective calcium response.

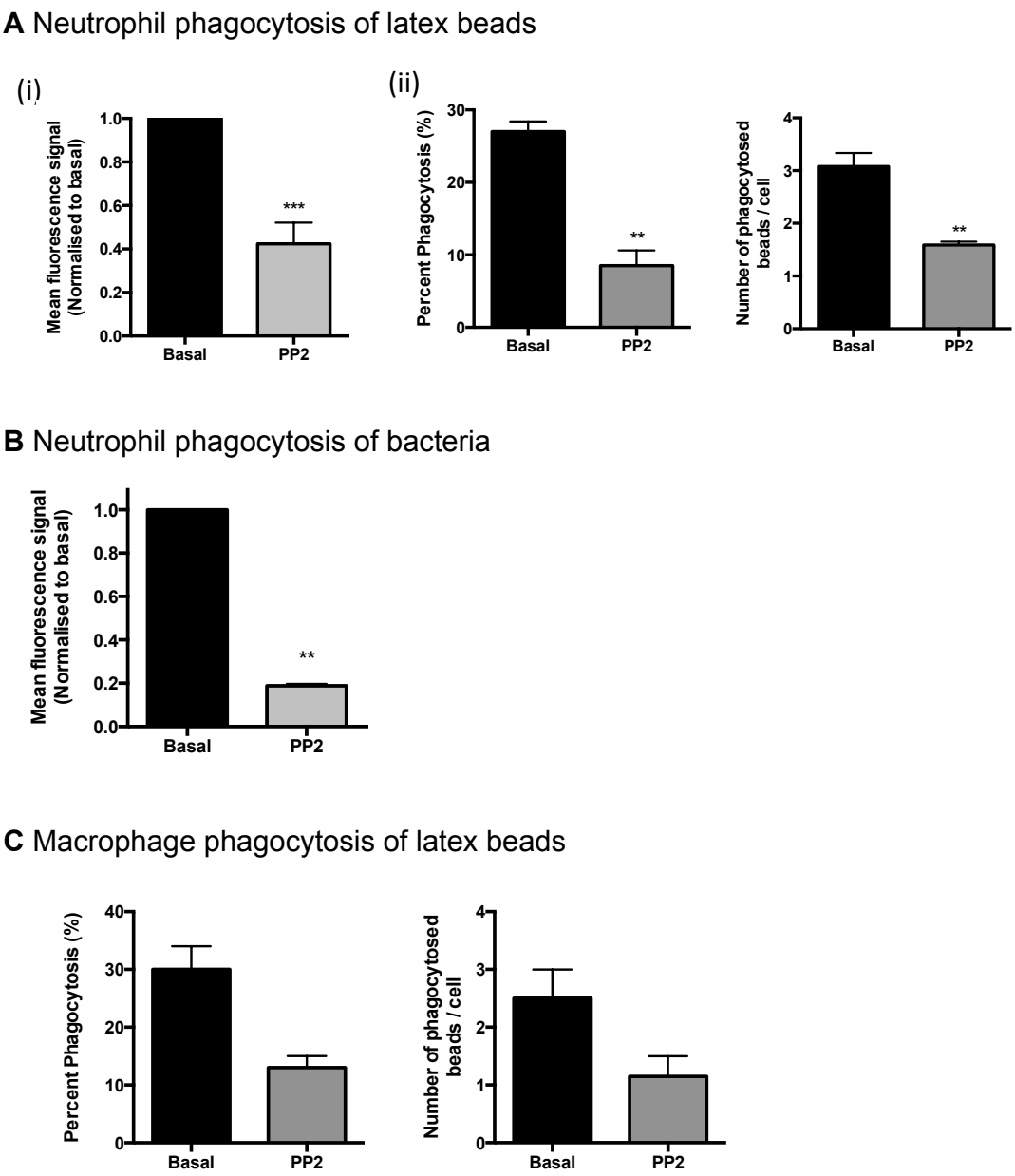


**Figure 5.5: Macrophage and neutrophil phagocytosis of latex beads and bacteria is inhibited by SFK inhibitor PP2.** PMA differentiated THP-1 monocytes or peripheral human neutrophils were incubated with 0.1μM PP2 for 30 minutes at 37°C. Cells were washed in warm HBSS, mixed with (A) and (C) IgG-opsonised fluorescent latex beads or (B) CFSE (10μM) loaded E. coli bacteria, and incubated at 37°C for 30 minutes to allow phagocytosis to occur. (A(i)) and (B) Cells were washed 3 times in PBS before fluorescence intensity in the viable neutrophil population was measured using flow cytometry. Data represents mean (±SEM) fluorescent signal per 10,000 cells normalised to basal or untreated fluorescence, from at least three separate experiments. (A(ii)) and (C) Cells were fixed in 4% PFA before being stained with DAPI. Samples were immediately imaged using confocal microscopy with 40x oil objective. Images were manually scored for neutrophils containing beads, confirmed by orthogonal projection imaging. Percent phagocytosis is percentage of total cells imaged containing at least one bead. Data presented represents means ± SEM from at least three separate experiments. Statistical analyses by unpaired t test where **=p<0.01 and ***=p<0.001.

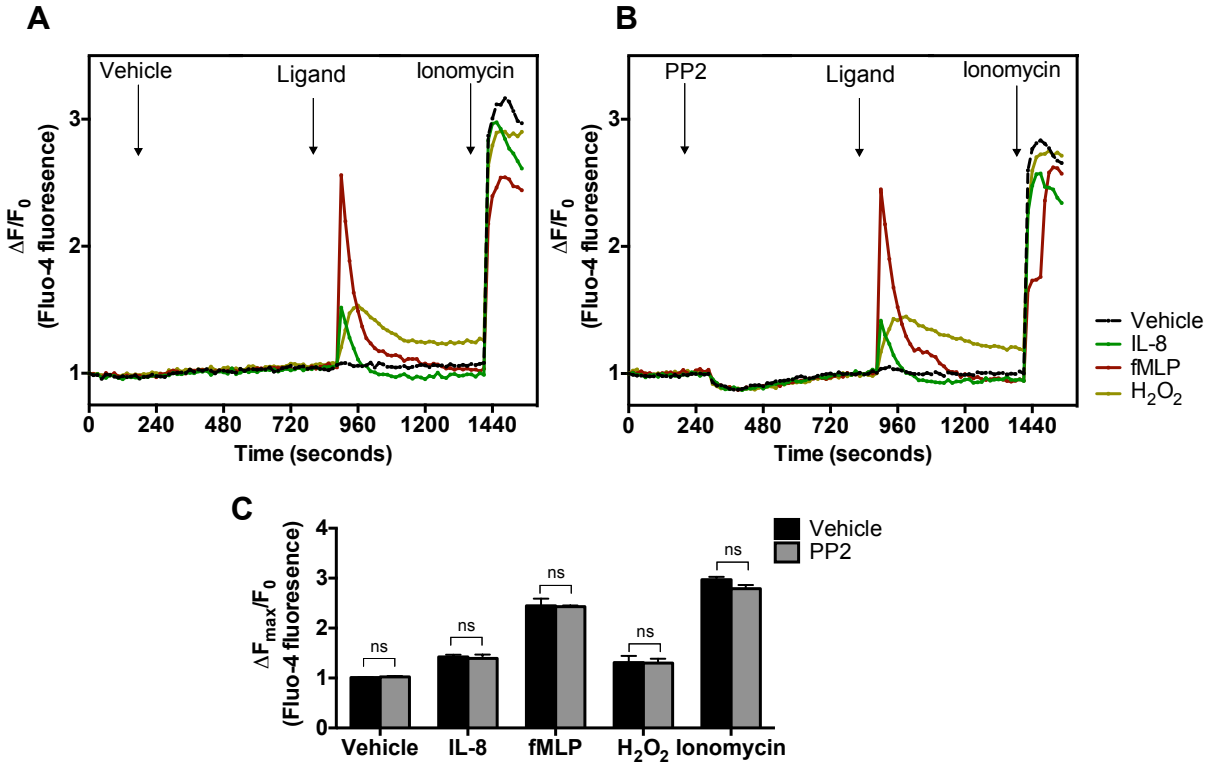


**Figure 5.6: Ligand or $H_2O_2$ induced intracellular calcium mobilisation in primary human neutrophils is not affected by inhibition of SFKs.** Primary human neutrophils were isolated from peripheral human blood and loaded with 10μM Fluo-4 before being washed in $Ca^{2+}$-free HBSS, resuspended in HBSS and extracellular calcium adjusted to 1mM. Cells were plated in black 96 well plates. Fluorescence was measured over time at 37°C using a plate reader (upper panels). 0.1μM PP2 (SFK inhibitor) or vehicle was added after baseline established and fluorescence signal captured for 10 minutes before 10nM IL-8, 10nM fMLP or 10mM $H_2O_2$ was added. For all samples, once the response had returned to baseline, 1μM ionomycin was added to induce a positive response. Peak change in fluorescence signal is plotted against vehicle control (lower panels). Data presented show representative traces from a single experiment and peak change graphs represent mean (± SEM) from three separate experiments, samples run in duplicate. Statistical analyses by two way-ANOVA with Sidak's multiple comparisons post hoc test, where, ns=no significant difference.

### 5.8 PI3K signalling is required for monocyte and neutrophil chemotaxis

The PI3K signalling cascade is essential for a wide array of cellular functions and has been implicated in many inflammatory disease settings. Downstream effects of PI3K signalling include activation of migration pathways in response to chemoattractants. We next studied the effect of PI3K inhibition on innate cell chemotaxis in the transwell migration assay, in order to examine the contribution of PI3K to monocyte and neutrophil chemotaxis to known chemoattractants.

Cells were pre-treated with increasing concentrations of pan-isoform PI3K inhibitor ZSTK474 for 30 minutes before being plated on porous filters above chemoattractants. MCP-1-mediated migration of THP-1 monocytes was significantly inhibited by nanomolar concentrations of ZSTK474, to approximately 50% of the untreated control cell response (Figure 5.7a). Basal THP-1 migration was also inhibited by ZSTK474. Neutrophil migration towards IL-8 was significantly inhibited by pre-treatment with ZSTK474 by approximately 60% (Figure 5.7b). Basal neutrophil migration was also inhibited by ZSTK474.

Specific pharmacological modulators of other PI3K signalling components have recently been developed and offer researchers an alternative approach to manipulate PI3K signalling. Such compounds include those targeting the action of endogenous PI3K negative regulators, the phosphatases SHIP-1 and PTEN. Here we have employed two SHIP-1 modulators: AQX-1, a SHIP-1 activator (hypothesised to mimic a PI3K inhibitor), and 3AC, a SHIP-1 inhibitor. A PTEN inhibitor, BpV, was also used to study PI3K signalling in monocyte chemotaxis in the transwell migration assay. These compounds are described in section 5.1.

THP-1 monocytes were pre-treated with increasing concentrations of AQX-1, 3AC or BpV for 30 minutes before being plated on porous filters above 10nM MCP-1. SHIP-1 activation by AQX-1 resulted in concentration dependent inhibition of MCP-1-mediated monocyte migration, which was significant with 30μM AQX-1 (Figure 5.8a). Basal migration was also inhibited by AQX-1, although not significantly. Increasing concentrations of SHIP-1 inhibitor 3AC induced significant and concentration dependent inhibition of MCP-1 mediated monocyte migration with an approximate $IC_{50}$ value of 3μM; basal migration was also significantly inhibited by 30μM 3AC (Figure 5.8b). Finally, increasing concentrations of PTEN inhibitor BpV significantly and concentration dependently inhibited monocyte migration towards MCP-1, and also inhibited basal migration, significantly with 30nM BpV (Figure 5.8c).

In summary, pan-isoform PI3K inhibition, PTEN inhibition and both SHIP-1 activators and SHIP-1 inhibitors, reduce chemotaxis.

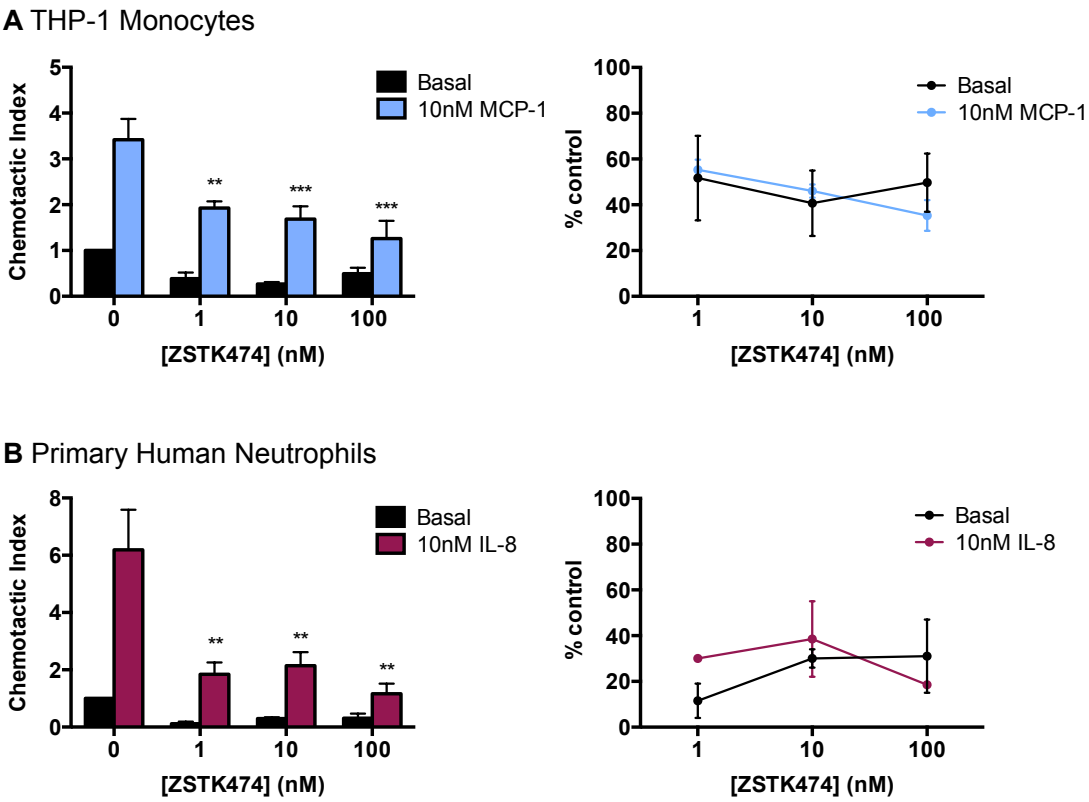


**Figure 5.7: PI3K inhibition inhibits monocyte and neutrophil chemotaxis.** (A) THP-1 monocytes or (B) primary human neutrophils were washed in serum free media, resuspended to $3.2x10^6$ cells/ml and incubated with increasing concentrations of ZSTK474 (pan-isoform PI3K inhibitor) for 30 minutes at 37°C before being plated on top of filter membrane above lower chambers containing (A) 10nM MCP-1 or (B) 10nM IL-8 or plain media. Migration is expressed as chemotactic index (left panels), and as a percentage of control cells (right panels). Chemotaxis across 5µm pore size membrane was determined after a 3 hour incubation at 37°C in 5% $CO_2$ as previously described. Data presented represents means ± SEM from at least three separate experiments. Statistical analyses by two way-ANOVA versus untreated control with Dunnett's multiple comparisons post hoc test. **=p<0.01, ***=p<0.001, ****=p<0.0001.

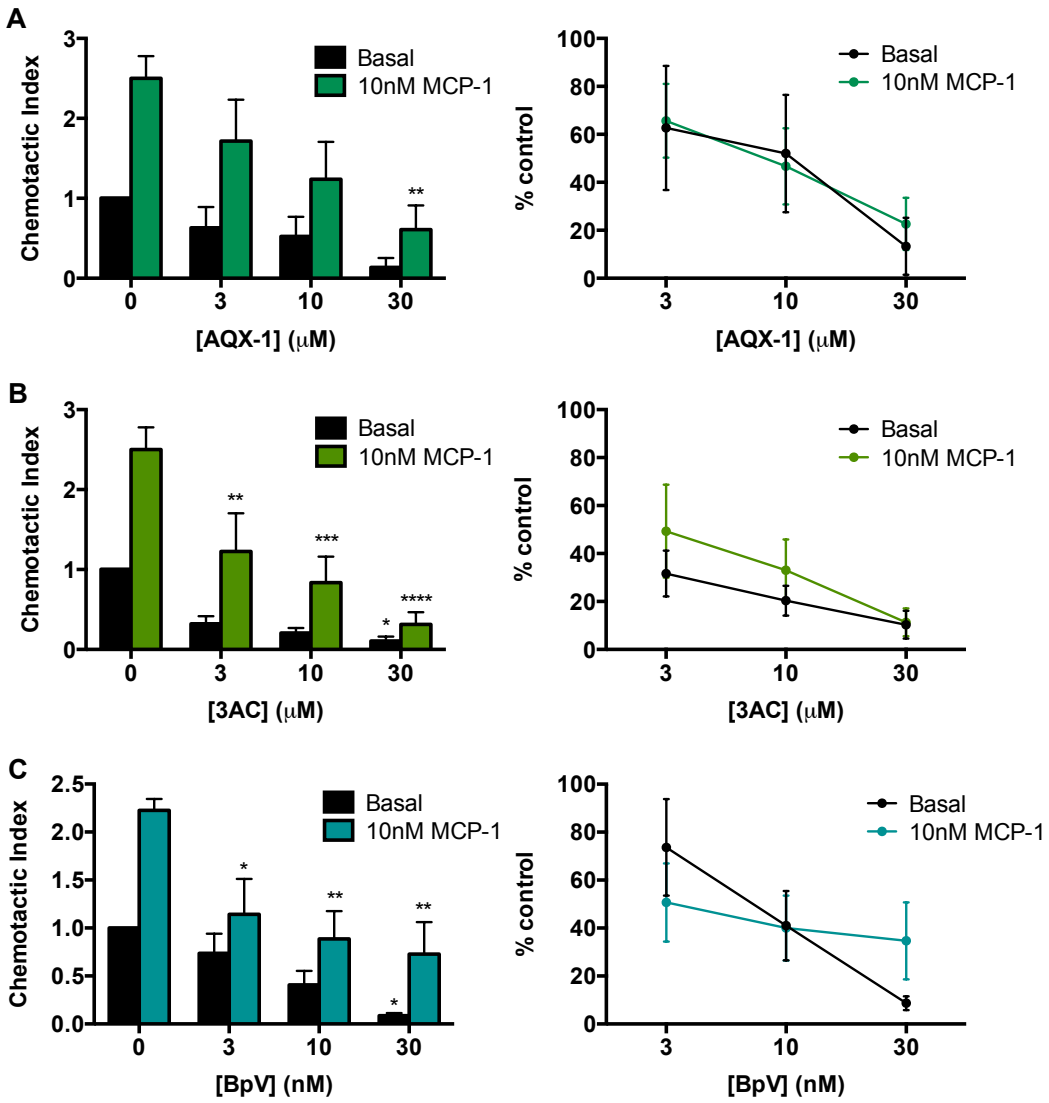


**Figure 5.8: SHIP-1 inhibition and activation, and PTEN inhibition inhibits THP-1 monocyte chemotaxis.** THP-1 monocytes were washed in serum free media, resuspended to $3.2x10^6$ cells/ml and incubated with increasing concentrations of (A) AQX-1 (SHIP-1 activator), (B) 3AC (SHIP-1 inhibitor) or (C) BpV (PTEN inhibitor) for 30 minutes at 37°C before being plated on top of filter membrane above lower chambers containing 10nM MCP-1 or plain media. Migration is expressed as chemotactic index (left panels), and as a percentage of control cells (right panels). Chemotaxis across 5μm pore size membrane was determined after a 3 hour incubation at 37°C in 5% $CO_2$ as previously described. Data presented represents means ± SEM from at least three separate experiments. Statistical analyses by two way-ANOVA versus untreated control with Dunnett's multiple comparisons post hoc test. *=p<0.05, **=p<0.01, ***=p<0.001, ****=p<0.0001.

### 5.9 Contributions of negative regulators of PI3K on actin organisation in monocytes

Since both inhibition and activation of the endogenous negative regulators of PI3K leads to inhibition of THP-1 monocyte migration, we next extended this investigation to examine the effects of these inhibitors on actin organisation and cell spreading. THP-1 monocytes were plated onto fibronectin-coated coverslips and treated with 10nM BpV (PTEN inhibitor), 10μM 3AC (SHIP-1 inhibitor) or 10μM AQX-1 (SHIP-1 activator), or vehicle control for 30 minutes before being stimulated with MCP-1 or vehicle. In general, 3AC induced the most severe decrease in circularity and increase in cell surface area compared to BpV and AQX-1.

BpV alone induced an elongated, irregular morphology with multiple lamellipodia, similar to that observed with MCP-1 alone (Figure 5.9a). Compared to untreated cells, BpV-treated cells were significantly less circular (mean circularity: 0.566 versus 0.654) and had a significantly larger surface area (mean area: 520.8μm$^2$ versus 455.6μm$^2$) (Figure 5.9b). Compared to MCP-1-stimulated, untreated cells, THP-1 monocytes that were treated with BpV followed by MCP-1 stimulation were smaller (mean area: 429.6μm$^2$ versus 477.9μm$^2$) and more circular (mean circularity: 0.604 versus 0.551).

3AC-treated cells had a large surface area and an irregular, extended morphology with multiple visible projections, similar to the phenotype of MCP-1-stimulated cells (Figure 5.9a). Compared to untreated cells, 3AC-treated cells were significantly less circular (mean circularity: 0.506 versus 0.654) and had a significantly larger surface area (mean area: 555.5μm$^2$ versus 455.6μm$^2$) (Figure 5.9b). Cell circularity and mean surface area of 3AC-treated, MCP-1-stimulated cells were not significantly different to cells stimulated with MCP-1 in the absence of 3AC.

AQX-1-treated cells were irregularly shaped and elongated, but not to the same extent as cells treated with MCP-1 alone (Figure 5.9a). Compared to untreated cells, AQX-1-treated cells were significantly less circular (mean circularity: 0.604 versus 0.654) and had a significantly larger surface area (mean area: 517.5μm$^2$ versus 455.6μm$^2$) (Figure 5.9c). AQX-1 treated monocytes showed a modest but significant inhibition of MCP-1-mediated elongation (mean circularity: 0.597 versus 0.550), but there was no difference in mean cell surface area.

To summarise, all treatments alone increase monocyte polarisation and spreading, which is roughly comparable to MCP-1-induced responses. However, BpV and AQX-1 induce modest but significant reversal of MCP-1 mediated polarisation.

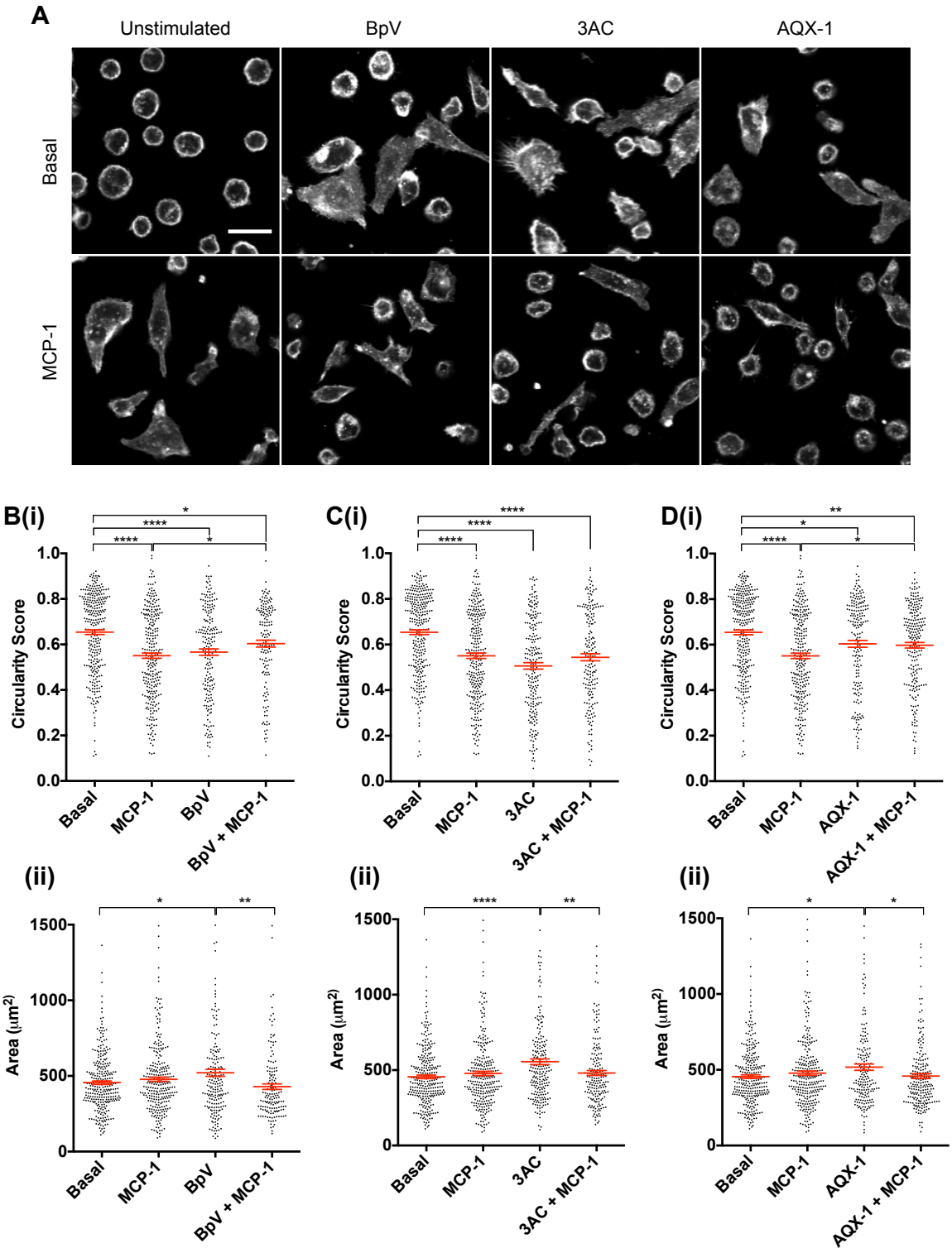


**Figure 5.9: The effect of modulating PI3K signalling on THP-1 monocyte polarisation and spreading.** THP-1 monocytes were plated on coverslips coated with 10ug/ml fibronectin and treated with 10nM BpV (PTEN inhibitor), 10μM 3AC (SHIP-1 inhibitor) or 10μM AQX-1 (SHIP-1 activator), or vehicle control. After 30 minutes cells were stimulated with 10nM MCP-1 or vehicle control. After 5 minutes cells were fixed in 4% PFA, permeabilised with 0.1% Triton-X and stained with Alexa-Fluor 488 conjugated phalloidin and DAPI. Samples were imaged by confocal microscopy. (A) Representative images showing F-actin, scale bar = 20μm. (B,C&D) circularity score (i) and area (ii) for each treatment group were calculated using CellProfiler software, with at least 100 individual cells analysed per sample, from at least 4 pooled experiments. Data presented represents mean (± SEM) with statistical analysis by one way-ANOVA with Tukey's multiple comparisons post hoc test where *=p<0.05, **=p<0.01, ***=p<0.001 and ****=p<0.0001.

### 5.10 Contributions of individual class IA PI3K isoforms to actin organisation in monocytes

The generation of isoform specific knock-out mouse lines and isoform-specific pharmacological compounds has increased our knowledge of PI3K signalling. These tools have enabled researchers to investigate the contribution of specific PI3K isoforms in disease settings, and have highlighted that p110γ and p110δ isoforms have important non-redundant functions in multiple cells of the immune system [193]. Here, our aim was to investigate the effect of inhibiting individual class IA PI3K isoforms on the ability of human monocytes to organise actin and spread on a substrate in the presence and absence of MCP-1.

THP-1 cells were seeded onto fibronectin-coated coverslips and treated with compounds or vehicle for 30 minutes followed by 10nM MCP-1 or vehicle for 5 minutes. Cells were then fixed and stained to visualise cellular F-actin by confocal microscopy. Concentrations of inhibitors were chosen based on published data, as described in section 1.2.2. Consistent with our previous experiments, MCP-1-stimulation induced an elongated, irregular cell shape, with visible lamellipodia formations (Figures 5.10-11).

Treatment with pan-isoform PI3K inhibitor LY294002 alone did not affect circularity, although cells did have significantly smaller surface area compared to untreated cells (mean area: 487.2μm$^2$ versus 612.6μm$^2$) (Figure 5.10b). LY294002 treatment significantly attenuated MCP-1-mediated elongation (mean circularity: 0.430 versus 0.381) and significantly decreased the MCP-1-mediated increase in cell surface area (mean area: 523.5μm$^2$ versus 690.5μm$^2$). Similarly, treatment with pan-isoform PI3K inhibitor ZSTK474 alone did not affect circularity, but cells were smaller than untreated cells (mean area: 466.7μm$^2$ versus 612.6μm$^2$) (Figure 5.10c). ZSTK474 treatment significantly attenuated MCP-1-mediated elongation (mean circularity: 0.450 versus 0.381) and significantly decreased the MCP-1-mediated increase in cell surface area (mean area: 507.2μm$^2$ versus 690.5μm$^2$).

Monocytes that were treated with PI3K p110α-selective inhibitor A66 did not differ in mean circularity or area compared to untreated, unstimulated cells (Figure 5.11b). A66 treatment significantly increased MCP-1-mediated elongation (mean circularity: 0.453 versus 0.525), but did not affect the MCP-1-mediated increase in cell surface area. Treatment with PI3K p110β-selective inhibitor GSK2636771 did not affect mean circularity or surface area compared to basal cells (Figure 5.11c). However, GSK2636771 treatment significantly attenuated MCP-1-mediated elongation (mean circularity: 0.654 versus 0.525) and attenuated the MCP-1-mediated increase in cell surface area (mean area: 364.2μm$^2$ versus 491.3μm$^2$). Monocytes that were treated with PI3K p110δ-selective inhibitor IC87114 were significantly more round compared to untreated, unstimulated cells (mean circularity: 0.501 versus 0.437) (Figure 5.11d). IC87114 treatment significantly attenuated MCP-1-mediated elongation (mean circularity: 0.438 versus 0.381) and significantly decreased the MCP-1-mediated increase in cell surface area (mean area: 492.8μm$^2$ versus 690.5μm$^2$).

To summarise, pan-isoform, p110δ and p110β, but not p110α, PI3K inhibitors abrogate MCP-1-mediated monocyte polarisation and spreading on fibronectin (see summary table 5.1).

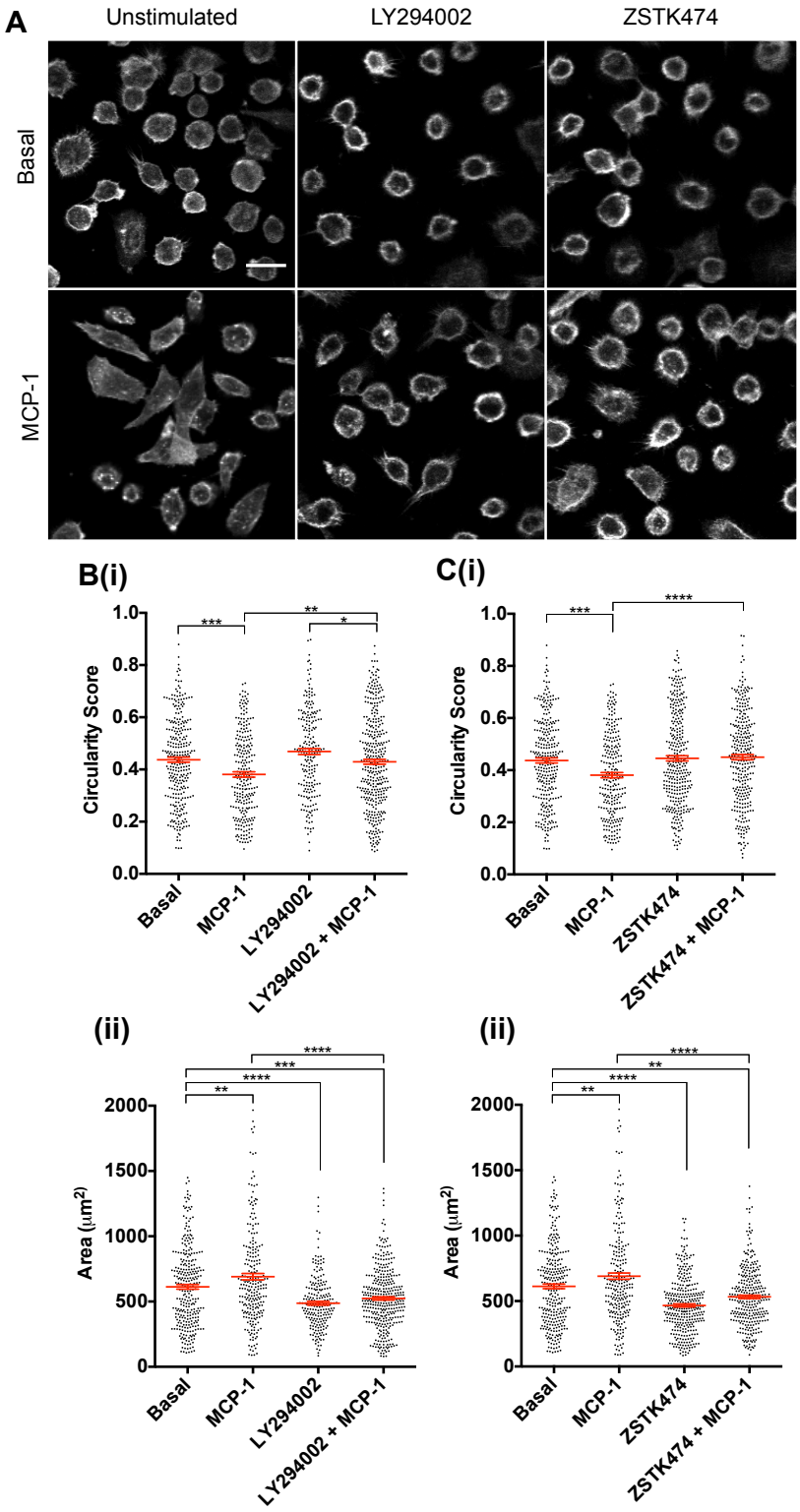


**Figure 5.10: The effect of pan-isoform PI3K inhibitors on THP-1 monocyte actin organisation.** THP-1 monocytes were plated on coverslips coated with 10ug/ml fibronectin and treated with 1μM LY294002 (pan-isoform p110 inhibitor), 40nM ZSTK474 (pan-isoform p110 inhibitor) or vehicle control. After 30 minutes cells were stimulated with 10nM MCP-1 or vehicle control. After 5 minutes cells were fixed in 4% PFA, permeabilised with 0.1% Triton-X and stained with Alexa-Fluor 488 conjugated phalloidin and DAPI. Samples were imaged by confocal microscopy. (A) Representative images showing actin staining (green), scale bar = 20μm. (B,C&D) circularity score (i) and area (ii) for each treatment group were calculated using CellProfiler software, with at least 100 individual cells analysed per sample, from at least 4 pooled experiments. Data presented represents mean (± SEM) with statistical analysis by one way-ANOVA with Tukey's multiple comparisons post hoc test where *=p<0.05, **=p<0.01, ***=p<0.001 and ****=p<0.0001.

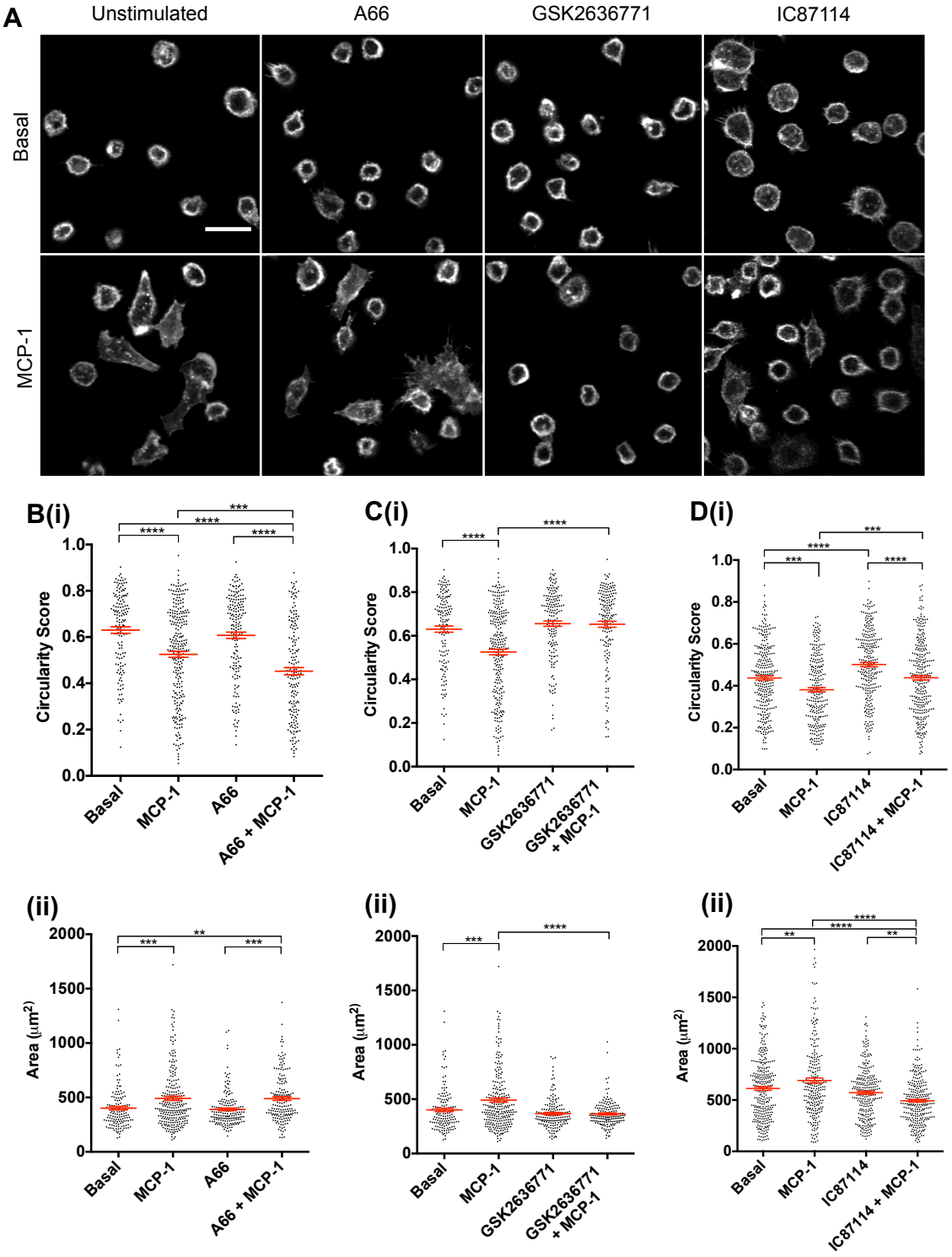


**Figure 5.11: The effect of p110α, β and δ-selective PI3K inhibitors on THP-1 monocyte actin organisation.** THP-1 monocytes were plated on coverslips coated with 10ug/ml fibronectin and treated with 30nM A66 (p110α inhibitor), 20nM GSK2636771 (p110β inhibitor), 70nM IC87114 (p110δ inhibitor) or vehicle control. After 30 minutes cells were stimulated with 10nM MCP-1 or vehicle control. After 5 minutes cells were fixed in 4% PFA, permeabilised with 0.1% Triton-X and stained with Alexa-Fluor 488 conjugated phalloidin and DAPI. Samples were imaged by confocal microscopy. (A) Representative images showing F-actin, scale bar = 20μm. (B,C&D) circularity score (i) and area (ii) for each treatment group were calculated using CellProfiler software, with at least 100 individual cells analysed per sample, from at least 4 pooled experiments. Data presented represents mean (± SEM) with statistical analysis by one way-ANOVA with Tukey's multiple comparisons post hoc test where *=p<0.05, **=p<0.01, ***=p<0.001 and ****=p<0.0001.

| | | Effect on THP-1 circularity | | Effect on THP-1 spreading (area) | |
|---|---|---|---|---|---|
| **Compound** | **Mechanism** | **- MCP-1** | **+ MCP-1** | **- MCP-1** | **+ MCP-1** |
| **LY294002** | Pan-isoform PI3k Inhibitor | - | ↑ | ↓ | ↓ |
| **ZSTK474** | Pan-isoform PI3k Inhibitor | - | ↑ | ↓ | ↓ |
| | | | | | |
| **A66** | p110α inhibitor | - | - | - | - |
| **GSK2636771** | p110β inhibitor | - | ↑ | - | ↓ |
| **IC87114** | p110δ inhibitor | ↑ | ↑ | - | ↓ |
| | | | | | |
| **BpV** | PTEN inhibitor | ↓ | ↑ | ↑ | - |
| **3AC** | SHIP-1 inhibitor | ↓ | - | ↑ | - |
| **AQX-1** | SHIP-1 activator | ↓ | ↑ | ↑ | - |

**Table 5.1: Summary of the actions of PI3K inhibitors and modulators upon THP-1 monocyte polarisation and spreading on fibronectin.** Summary of results from Figure 5.9-5.11. ↓= response inhibited, ↑= response potentiated, - = no effect.

## 5.11 Chapter 5 – Summary of Results

- Inhibition of SFKs blocked monocyte and neutrophil chemotaxis, chemoattractant-mediated polarisation and spreading, and phagocytosis of beads and bacteria.
- Ligand-stimulated transient intracellular $Ca^{2+}$ responses in neutrophils are not PP2-sensitive.
- Inhibition of Syk kinase inhibits neutrophil chemotaxis to IL-8 but promotes monocyte chemotaxis to MCP-1.
- Inhibition of Syk kinase potentiated MCP-1-mediated monocyte polarisation.
- Pharmacological inhibitors of SFK and Syk kinases do not affect neutrophil viability.

- Inhibition of PI3Ks blocked monocyte and neutrophil chemotaxis.
- Activation and inhibition of SHIP-1, and inhibition of PTEN, blocked monocyte chemotaxis.
- p110β and p110δ, but not p110α, PI3K isoforms are involved in monocyte polarisation and spreading.

## 5.12 Chapter 5 – Discussion

### SFKs mediate innate cell migration, polarisation and phagocytosis

Studies with rodent SFK knock-out strains first highlighted the importance of SFK signalling in immune cell function. However, the need for a simplistic *in vitro* model led to the design of novel, potent, SFK-selective small molecule inhibitors. Generating selective inhibitors for kinases remains a considerable challenge because essentially most kinase inhibitors function through competitive binding in a highly conserved ATP pocket. Genetic techniques (e.g. RNAi) can inactivate specific genes, but most kinases are multi-domain proteins and each domain has an independent function. Small molecules have the potential to inhibit kinase catalytic activity without affecting the other domains.

The SFK inhibitor PP2 was used to study the role of SFKs in innate cell function. PP2-treated monocytes and neutrophils displayed significantly impaired chemotaxis towards MCP-1 or IL-8 in the ChemoTx migration assay. Furthermore, basal migration of both cell types was also inhibited. While considering the previously discussed caveats of PP2 (see section 5.1), this would suggest that SFKs contribute to chemoattractant-mediated and basal migration in these cell types. Our results agree with previously published reports demonstrating PP2-mediated inhibition of MCP-1-mediated THP-1 chemotaxis [140] and IL-8- and fMLP-mediated human neutrophil chemotaxis [142], [456] in similar transwell migration models. Notably, Yoo *et al* (2011) showed that micromolar concentrations of PP2 inhibited $H_2O_2$-mediated neutrophil chemotaxis in the under agarose migration assay [282]. Our observed $IC_{50}$ value for PP2 (100nM) is higher than previously published values for PP2 activity against SFK members [442], however these were carried out in cell-free kinase assays. In spite of this, our observed

inhibition of chemotaxis at high nanomolar concentrations of PP2 may be due to off-target inhibition of other kinases.

The effect of SFK inhibition by PP2 on THP-1 monocyte morphology and spreading on fibronectin was also studied. Fibronectin is an important ligand for integrins, and will induce integrin signalling. MCP-1 triggers the rearrangement of F-actin leading to increased adhesion and spreading. This is likely to be mediated by an SFK-dependent pathway because pre-treatment with 0.1μM PP2 blocked MCP-1-induced spreading and polarisation. Consistent with its actions on actin-mediated processes, PP2 inhibited neutrophil phagocytosis of IgG-opsonised beads and bacteria, and inhibited macrophage phagocytosis of IgG-opsonised beads. IgG-opsonised bead recognition will activate FcγR signalling. Hck and Lyn phosphorylate ITAMs in the signalling chains of the FcγR complex, which then serve as docking sites for other tyrosine kinases, such as Syk [457]. The global inhibitory effect of PP2 on phagocytosis indicates that SFKs do not discriminate between the type of particle being detected and engulfed, and are therefore likely to be involved in regulating processes downstream of various receptors.

We briefly investigated the effect of SFK inhibition on chemoattractant-induced intracellular signalling processes. Neutrophil pre-treatment with PP2 did not affect ligand- or ionomycin-mediated mobilisation of intracellular calcium, suggesting that this is an SFK-independent process. Similarly, PP2 did not affect cell viability with the concentrations tested in these experiments, so it is unlikely that potential toxicity is influencing our results.

Taken together, our results are consistent with the finding of many others. SFKs regulate several actin-dependent processes, for example, Hck has been shown to regulate F-actin based membrane protrusions [458], monocyte chemotaxis [149], [459], phagocytosis [460], [461] and cellular adhesion [462]. Recently, Sanjuan *et al* (2006) discovered that SFK activation downstream of TLR9 resulted in cytoskeletal changes and transcription of effector genes. Upon TLR9 activation by CpG, Pyk2, Vav, Cbl, talin, paxillin and vinculin (and PI3K) were all phosphorylated, and they have all been described as mediators of actin cytoskeleton rearrangement that promote spreading, adhesion and motility. Furthermore, PP2 blocked the phosphorylation of Pyk2 and Vav1, and inhibited cellular adhesion [463].

**Do SFKs and $H_2O_2$ act through a common pathway?**

$H_2O_2$ has been suggested to act directly on SFKs. This has been demonstrated *in vivo* where wound-generated $H_2O_2$ directly oxidises and activates Lyn [282]. However, contrary to these reports, our results suggest that exogenous $H_2O_2$ is acting in an inhibitory manner upon human cell motility. We briefly explored the possibility that SFK- and $H_2O_2$-mediated signalling occurred in the same pathways using the *in vitro* ChemoTx migration assay. Treatment of monocytes or neutrophils with either PP2 or $H_2O_2$ alone inhibits migration towards MCP-1 or IL-8 by approximately 50%, thus providing a potential window to observe exacerbation or rescue of the phenotype. We next treated the cells with PP2 and $H_2O_2$ simultaneously and observed the effect on chemotaxis. Co-treatment was not significantly different to either treatment alone. If

PP2 and $H_2O_2$ were acting via different pathways, we would predict the inhibitory effects to be additive.

Together, these results confirm that SFK activity is necessary for migration towards a chemoattractant. They also support our earlier results indicating that in this assay, exogenous $H_2O_2$ inhibits migration towards a chemoattractant, in a similar manner to inhibition induced by PP2. Observing no change to the phenotype seen when SFK inhibition and $H_2O_2$ are applied simultaneously suggests that both PP2 and $H_2O_2$ could be inhibiting migration through a common mechanism. This could be by directly targeting SFKs or by targeting downstream mediators of SFK signalling that contribute to motility; this cannot be confirmed from this experiment alone. Additionally, the non-specific nature of PP2 could lead to inhibition of other kinases that are also targets for oxidation by $H_2O_2$.

Candidate proteins downstream of SFKs that are involved in actin-mediated processes and could be targets for inhibitory oxidation by $H_2O_2$ identified *in vitro* include Pyk2, Cbl and Vav. SFK-mediated phosphorylation of Pyk2 promotes actin cytoskeletal rearrangements that induce adhesion, spreading and lamellipodial formation [146]. Cbl interacts with SFKs, Pyk2 and Vav and has been associated with increased macrophage motility [147]. Vav is a multi-domain signal integrator and transduces signals to cytoskeleton-dependent pathways, including PI3K [464].

**Syk kinase in migration and spreading**

The role of Syk kinase in chemoattractant-mediated migration has not yet been fully elucidated. It has been demonstrated that Syk does not play a major functional role in chemoattractant signalling in neutrophils or mast cells [167]. Migration of neutrophils towards fMLP was not affected in Syk deficient cells, and fMLP initiated normal polymerization of cellular actin in the absence of Syk [167]. Another report suggests that Syk makes a limited contribution to $\beta_2$ integrin-mediated migration of neutrophils [465]. However, *in vivo* studies showed that Syk is necessary for firm leukocyte adhesion to inflamed endothelia [466]. Gevrey *et al* (2005) report that Syk is required for chemotaxis of a monocyte/macrophage cell line to $CX_3CL1$ [157]. $CX_3CL1$ triggers an increase in F-actin and the formation of actin-rich cell protrusions, in addition to Syk activation. Syk inhibition by small molecule inhibitors and RNAi impairs the migration of a mouse macrophage cell line to $CX_3CL1$ and F-actin reorganisation [157].

When THP-1 monocytes were pre-treated with Syk inhibitor piceatannol and placed in the upper compartment of the ChemoTx migration assay above MCP-1, we found that chemotaxis was significantly enhanced compared to untreated control cells. Basal THP-1 monocyte migration was not significantly affected by piceatannol. These results suggest that Syk may be acting in a regulatory manner downstream of MCP-1/CCR2 activation. This result was unexpected, given that others have demonstrated a role for Syk in leukocyte migration and have shown piceatannol activity against Syk with $IC_{50}$=10-15μM [447]. In contrast, both basal and IL-8-mediated primary human neutrophil migration was inhibited by ~60-80% when pre-treated with piceatannol, compared to untreated cells. This suggests that in neutrophils, Syk is necessary for IL-8/CXCR1/2 signalling driving migration, and that these receptors may link to ITAM-

containing motifs, which subsequently recruit Syk. Integrin receptors associated with ITAM-containing motifs, for example, may associate with CXCR1/2.

We next studied the effects of piceatannol pre-treatment on THP-1 monocyte actin organisation and spreading on fibronectin. We found that while piceatannol did not alter monocyte circularity, monocyte area was increased. When monocytes were stimulated with MCP-1 in addition to piceatannol pre-treatment, polarisation and spreading was not significantly affected. This suggests that Syk may be involved in monocyte spreading but is not involved in MCP-1-mediated polarisation and elongation on fibronectin.

**PI3K and its modulation by negative regulators – effects on migration and actin organisation**

Our results show that in an *in vitro* model of chemotaxis, both basal and chemoattractant-mediated monocyte and neutrophil migration required PI3K signalling and was inhibited by pan-isoform selective inhibitor ZSTK474. These results provide more evidence to support the function of ZSTK474 as an anti-inflammatory compound. Leukocyte migration was inhibited by 50% with nanomolar range concentrations of ZSTK474, which is consistent with other reported $IC_{50}$ values for ZSTK474 against all p110 isoforms [197], as shown in table 1.3.

In order to provide alternative ways to target the PI3K pathway, a SHIP-1 activator compound was used to mimic the effects of PI3K inhibition. Using *in vitro* models, others have demonstrated that the SHIP-1 specific activator AQX-1 inhibits monocyte chemotaxis to MCP-1 [201]. Our results confirm this – migration of AQX-1-treated THP-1 monocytes to MCP-1 was significantly impaired compared to untreated cells. Basal migration was also inhibited, although this was not statistically significant. This result does indeed mimic the response we have demonstrated with the PI3K inhibitor ZSTK474.

We also tested the SHIP-1 inhibitor 3 α-aminocholestane (3AC) in this assay, and hypothesised that SHIP-1 inhibition would potentially lead to enhanced migration, due to relief of negative regulation of PI3K signalling by SHIP-1 in these cells. Interestingly, we found that 3AC actually inhibited monocyte basal and MCP-1-mediated migration in a similar fashion to AQX-1. Our $IC_{50}$ value for 3AC (3μM) mirrored those previously demonstrated in phosphatase assays [202].

Inhibition of a second negative regulator of PI3K, PTEN, was hypothesised to again induce a migratory phenotype. Our results indicate that, similar to SHIP-1 inhibition, basal and MCP-1-mediated migration of BpV-treated monocytes was significantly impaired compared to control cells. Interestingly, others have shown that loss of PTEN in neutrophils has no impact on neutrophil chemotaxis [467], indicating that the role of PTEN in neutrophils and monocytes may be distinct.

As morphological polarisation is a pre-requisite for cell motility, we investigated the effects of SHIP-1 and PTEN inhibition/activation on actin organisation and spreading of THP-1 monocytes on fibronectin. We found that both the SHIP-1 inhibitor 3AC and the

SHIP-1 activator AQX-1 increase basal cell surface area and irregularity, and decrease circularity. In response to MCP-1, 3AC and AQX-1-treated monocytes remain broad and poorly polarised. This dysregulation of actin organisation may underlie the impaired motility of 3AC- and AQX-1-treated THP-1 monocytes. Our results are consistent with the findings of a similar study, where resting SHIP-$1^{-/-}$ neutrophils were broad, flattened and surrounded by well-developed lamellipodia when seeded on glass coverslips [467]. In response to fMLP, SHIP-$1^{-/-}$ neutrophils remained poorly polarised with irregular lamellae present on all sides of the cell, and their chemotaxis was impaired.

The results discussed here imply that both inhibition and activation of SHIP-1 leads to the same functional outcome – impaired migration and polarisation. Several groups have also reported opposing phenotypes in SHIP-1 deficient cells [467], [468]. In light of these findings, it is apparent that there exists a critical balance between $PI(3,4,5)P_3$ and $PI(3,4)P_2$, which can be disrupted by SHIP-1 activation or inhibition, or PTEN inhibition. Indeed, both substrate ($PI(3,4,5)P_3$) and product ($PI(3,4)P_2$) of SHIP-1 have been shown to influence Akt activation and cell survival [175]. Additionally, down- or up-regulation of $PI(3,4,5)P_3$ by deletion of PI3Ks or PTEN, respectively, results in severely reduced efficiency of chemotaxis in *Dictyostelium* [455]. It is clear that in order for a cell to positively migrate in response to a signal gradient, this balance must be in place to control the localisation and expression levels of phospholipids in the cell membrane.

By introducing pharmacological tools to disrupt this balance, two outcomes may prevail, as illustrated in figure 5.12. Firstly, SHIP-1 activation will lead to enhanced dephosphorylation of $PI(3,4,5)P_3$ and accumulation of $PI(3,4)P_2$, leading to loss of localised $PI(3,4,5)P_3$-mediated Akt activation and signalling to drive cell motility. Additionally, SHIP-1 can also have a masking function, as it can block the recruitment of other key signalling enzymes [469]. It has been demonstrated that SHIP-1 can block PI3K activity at immune-activating receptors by preventing PI3K recruitment to DAP10 and DAP12 [470]. Secondly, SHIP-1 inhibition will limit the dephosphorylation of $PI(3,4,5)P_3$ and, as the inhibitor is applied exogenously, lead to a de-localised ‘global’ increase in PI3K activity, which is not polarised at the leading edge and therefore cannot support directed cell migration. This may also be true for the phenotype demonstrated by PTEN inhibition, again leading to $PI(3,4,5)P_3$ accumulation.

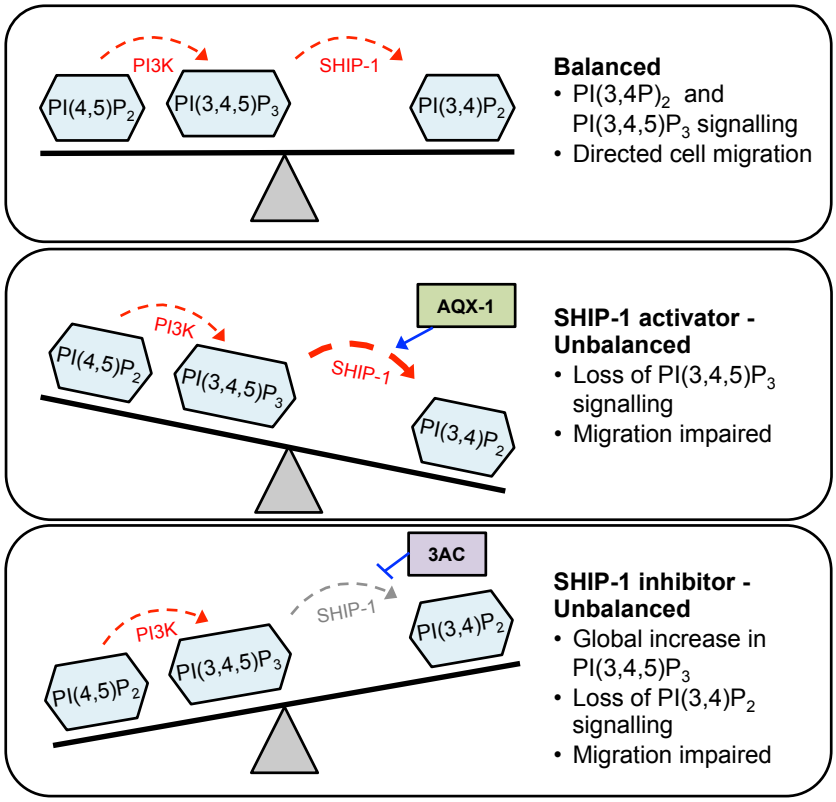


**Figure 5.12: Inhibition and activation of SHIP-1 lead to the same functional outcome.** Under normal conditions, PI3K and SHIP-1 regulate the levels and localisation of $PI(3,4,5)P_3$ and $PI(3,4)P_2$ to coordinate functional outcomes such as cell migration. The balance between $PI(3,4,5)P_3$ and $PI(3,4)P_2$ is vital. Activation of endogenous negative regulator SHIP-1 by pharmacological tools such as AQX-1 leads to upregulated dephosphorylation of $PI(3,4,5)P_3$, accumulation of $PI(3,4)P_2$ and inhibition of cell migration. Similarly, inhibition of SHIP-1 by 3AC leads to downregulation of $PI(3,4)P_2$ signalling and a global increase in $PI(3,4,5)P_3$, preventing the cell polarisation and impairing migration.

### PI3K class IA isoform characterisation in monocyte polarisation and spreading

Isoform-selective pharmacological inhibitors are becoming increasingly more influential not only in our quest for better understanding of PI3K signalling, but also in the development of therapeutic entities for use in the clinic. Using a 2D *in vitro* model of cell adhesion, actin organisation and spreading, we have confirmed that MCP-1-mediated actin reorganisation in THP-1 monocytes is dependent upon PI3K signalling. The concentrations of compounds used in these experiments are based upon published $IC_{50}$ values for the inhibitors against enzyme activity (see table 1.3). Treatment of cells with two separate pan-isoform inhibitors, LY294002 and ZSTK474, abrogated the MCP-1-mediated changes in F-actin and reduced mean surface area.

Vanhaesebroeck *et al* (1999) reported that LY294002 blocked CSF1-induced actin reorganisation and cell migration in a murine macrophage cell line [471], which is consistent with our findings in human THP-1 monocytes. We found that ZSTK474 decreased spreading of unstimulated cells and abrogated MCP-1-mediated elongation and spreading in THP-1 monocytes, in a comparable manner to LY294002. ZSTK474 has been reported to exhibit anti-migratory and anti-adhesive effects on prostate cancer cells *in vitro* [472]. Together with our ZSTK474 migration results, our observations provide more evidence for the anti-inflammatory effects of ZSTK474, and are consistent with other *in vitro* studies.

PI3K isoforms play important and non-redundant roles in immunology and are currently of great interest as therapeutic targets. It was therefore prudent to investigate the individual contributions of selective PI3K isoforms upon monocyte polarisation and spreading *in vitro*. The PI3Kα-selective inhibitor A66 did not affect basal THP-1 cell polarisation or surface area, nor did it affect MCP-1-stimulated responses. This result indicated that p110α is unlikely to be involved in regulating actin reorganisation and adhesion in monocytes. In support of these findings, Vanhaesebroeck *et al* (1999) reported a specific role of PI3Kδ, but not PI3Kα, in cytoskeletal reorganisation and chemotaxis of a macrophage like cell line in response to CSF1 [471].

PI3Kδ is preferentially expressed in cells of hematopoietic origin and has been shown to be important in fMLP-directed migration of human neutrophils in an under agarose migration assay, but is not involved in random motility [184]. THP-1 monocytes pre-treated with PI3Kδ-selective inhibitor IC87114 adopted a more rounded morphology with markedly fewer lamellipodia than untreated cells. Furthermore, prior exposure to IC87114 abrogated MCP-1 mediated actin reorganisation and decreased cell surface area. This result suggests that PI3Kδ plays an important role in MCP-1-stimulated monocyte spreading and polarisation. Ferreira *et al* (2006) reported that IC87114 inhibited diapedesis in human PBMCs and THP-1 cells, and that PI3Kδ activity was specifically required for the THP-1 cell adhesion and spreading on VCAM-1 [473]. Their flow cytometry analysis revealed that PI3Kδ inhibition decreased the amount of conformationally active $\beta_1$-integrins, and decreased the activation state of Rac1 and Cdc42. This report demonstrated the specific necessity of PI3Kδ in regulating monocytic integrin activation. Following this, another group reported that Syk-mediated translocation of p110δ to the leading edge was involved in $\beta_2$ integrin-mediated migration of neutrophil-like HL60 cells [474].

PI3Kβ is a class IA PI3K isoform that has reported roles in platelet activation and thrombosis [198], as well as in neutrophil activation by immune complexes [185]. It has been previously reported that antibodies against p110β reduced macrophage lamellipodium formation and membrane ruffling, and reduced directed chemotaxis in response to CSF-1 [471]. Indeed, we found that treatment of THP-1 cells with p110β-selective inhibitor GSK2636771 abrogated MCP-1-mediated actin reorganisation and cell spreading, but had no effect on unstimulated cells. These results indicate that, like PI3Kδ, PI3Kβ is also involved in mediating MCP-1-induced responses.

To summarise, our results confirm that p110β and p110δ are appropriate targets for therapeutics for inflammatory and autoimmune diseases. Kulkarni *et al* (2011) demonstrated that combined deficiency of p110β and p110δ resulted in near-complete protection against inflammatory arthritis in a mouse model, to an extent that was greater than just p110β deficiency alone [185]. This is indicative of a cooperative role for these PI3K isoforms, and represents a novel therapeutic strategy to target two contributing isoforms simultaneously.

**Proposed model of SFK and PI3K signalling in innate cell migration and actin reorganisation**

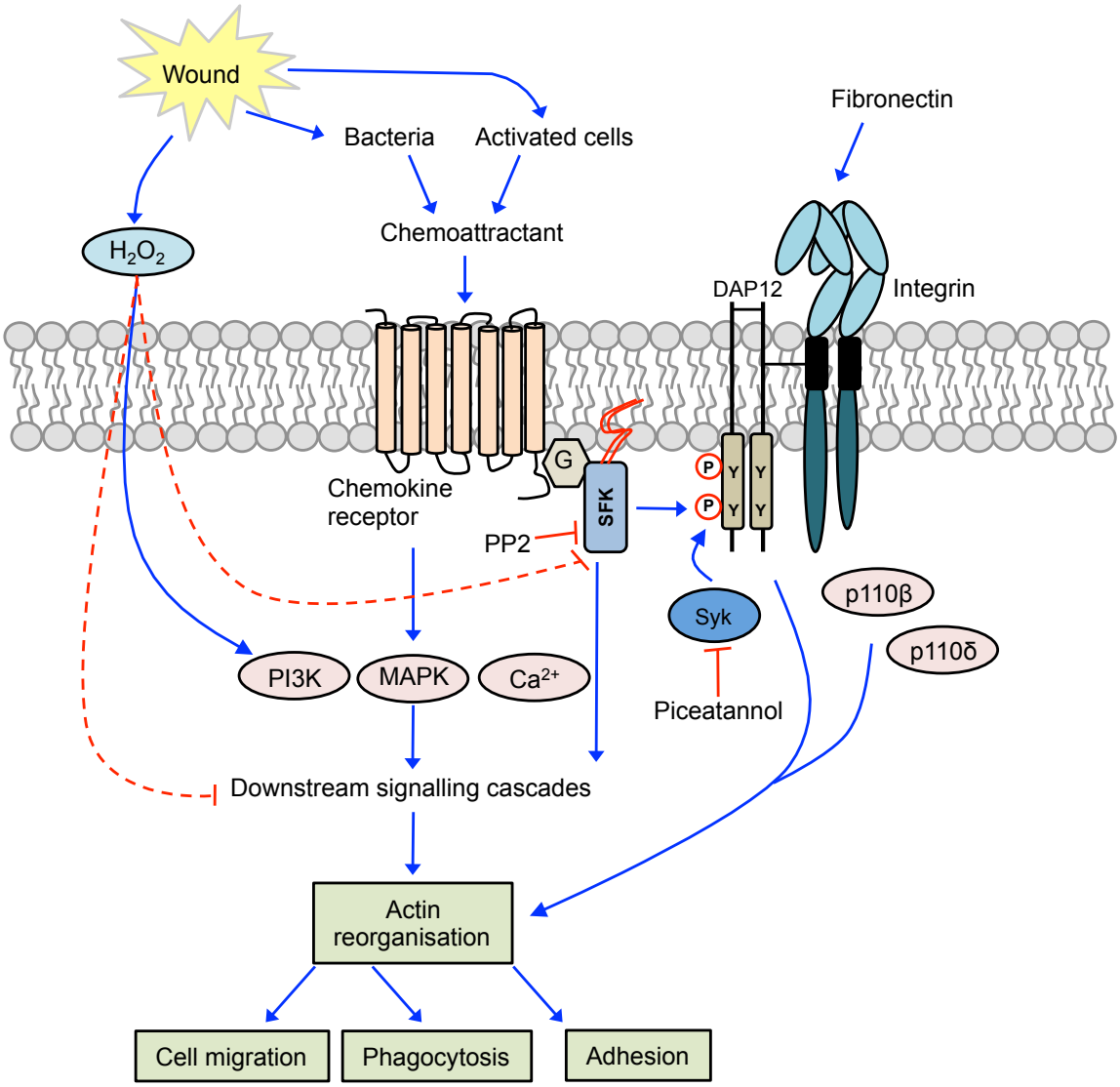


**Figure 5.13: Proposed model of SFK and PI3K signalling in innate cell migration and actin reorganisation.** Chemokine receptor activation by products of inflammation leads to association of SFKs with G proteins and subsequent phosphorylation of ITAM-containing motifs associated with integrin receptors. Phosphorylated tyrosine residues are recognised and bound by the Syk kinase adaptor enzyme. Signalling from GPCRs and integrin receptors leads to actin reorganisation and promotes functional processes including migration, phagocytosis and adhesion. p110β and p110δ are involved in driving actin-mediated processes downstream of chemoattractant receptor activation in cells seeded on fibronectin. While $H_2O_2$ can activate PI3K and MAPK signalling cascades, it can inhibit migration, possibly by inhibiting signalling mediators involve in actin reorganisation, or by directly targeting SFKs.

# CHAPTER 6: GENERAL DISCUSSION

**Overview**

Using a *Drosophila melanogaster* embryonic model of tissue damage, we have shown that Src42A activity is involved in driving directed immune cell recruitment to a wound, but is not necessary for general cell motility in the absence of a wound. The adaptor kinase Shark is also required for directed migration to a wound. Src42A activation may lead to Shark activation and signalling as these two kinases have previously been shown to interact [287]. We can hypothesise that kinase activity is upregulated following inflammatory events because phosphorylated tyrosine residues were identified in the vicinity of a wound. This investigation has not directly identified the damage-associated signals generated upon wounding. However, based on previously reported studies we can assume that a tissue scale gradient of $H_2O_2$ is likely to be generated [233], [270]. The formation of a defined gradient of $H_2O_2$ is likely to be a key factor in driving directed migration, as incubation of unwounded embryos in uniform gradients of exogenous $H_2O_2$ abrogated immune cell random motility.

The effect of damage-associated signals on human innate immune cells was investigated to explore how these processes are conserved across species. $H_2O_2$ did not induce chemotaxis and inhibited chemoattractant-mediated migration in a transwell *in vitro* model of migration. However, in an under agarose migration assay, $H_2O_2$ induced neutrophil chemotaxis but did not affect chemoattractant-mediated migration. Exogenous $H_2O_2$ abrogated actin reorganisation and spreading on fibronectin, and phagocytosis *in vitro*. The effect was consistent regardless of cell type, or the ligand-receptor pathway it was acting on. However, $H_2O_2$ induced intracellular calcium mobilisation and kinase activity without compromising cell viability. Furthermore, we have shown that endogenous ROS formation regulated cell motility and it is possible that autocrine $H_2O_2$ signalling has important regulatory roles in many cell processes. Our studies demonstrate that the effect of $H_2O_2$ on human innate cells *in vitro* is distinct from immune cells *in vivo* following tissue damage. In contrast to exogenous $H_2O_2$, extracellular ATP activated dynamic chemokinesis, cytoskeletal rearrangement, and spreading *in vitro*, even in the absence of a gradient. Therefore, ATP is a significant determinant of the leukocyte contribution to the inflammatory microenvironment by influencing migration and recruitment of leukocytes. Our results demonstrate that $H_2O_2$ and ATP are distinct in their effect on cell migration and function, and this could be due to sensitivity to gradient formation of either signal.

Our results indicate that SFK activity in human innate cells is important for chemotaxis, chemokinesis, actin remodelling and phagocytosis. This demonstrates conservation of SFK activity in directed cell migration between zebrafish, *Drosophila* and human cells in response to chemoattractant signals. We have been unable to demonstrate that SFKs are involved in human innate cell migration towards $H_2O_2$. We can hypothesise that $H_2O_2$ may inhibit SFK activity resulting in inhibition of migration due to their presence in similar pathways. Our results indicate that Syk kinase has different roles in monocytes and neutrophils, and is important in mediating responses to chemoattractants and the integrin ligand fibronectin. We have demonstrated that PI3K signalling is also important in driving directed chemotaxis, and that class IA isoforms p110β and p110δ, but not p110α, make a considerable contribution to monocyte MCP-1-mediated actin reorganisation and spreading on fibronectin *in vitro*.

**The *Drosophila melanogaster* embryonic wound model**

Embryo-wide mutation is a considerable drawback of the mutant *Drosophila* embryos used in this thesis. However, several alternative genetic strategies can be used to study the roles of Src42A and Shark specifically in hemocytes. Firstly, tissue specific re-expression of the wild type gene within the mutant background can generate rescue fly lines. Rescue of the wild type hemocyte migration phenotype would imply that gene disruption specifically in hemocytes is responsible for impaired migration. Secondly, dominant negative fly lines could be engineered. This involves expressing a form of the protein of interest that out-competes the resident protein in the same cell, but is functionally inactive. This occurs if the dominant negative version can still interact with the same elements as the wild type protein, but blocks some aspect of its function. The use of dominant negative lines also removes problems associated with embryo-wide gene disruption. Finally, using RNAi constructs and the Gal4-UAS system could silence the transcription of specific genes in a cell type specific manner.

Pharmacological inhibition of Src42A activity using SFK inhibitor PP2 offers an alternative approach to disrupting Src42A activity in *Drosophila* embryos. PP2 can be injected into the embryo before wounding, or incubated following membrane permeablisation and the resulting response of hemocytes imaged. However, this approach does not selectively target the hemocyte Src42A, so genetic rescue experiments will probably be more valuable. Alternatively, Src42A rescue embryos could be treated with PP2. Here the mutant background results in inhibition of Src42A activity only being possible in the hemocytes.

We have not used ROS reporters (e.g. HyPer) to identify the $H_2O_2$ gradient at the wound site, or any indicators of redox signalling. Therefore we cannot assume that $H_2O_2$ is driving Src activity in *Drosophila* hemocytes. Yoo *et al* (2011) used an *in vitro* kinase assay to show that Lyn Cys466 was directly activated by oxidation. After immunoprecipitation of Lyn, and treatment with 15μM $H_2O_2$, only wild type Lyn, but not C466A Lyn, could activate the Lyn substrate pSAM68 [282]. We can predict that due to the conservation of components between species, it is highly likely that this mechanism is operating in *Drosophila*. An elegant approach would be to use dynamic imaging with embryos encoding HyPer to study the $H_2O_2$ signal and subsequent activation of protein kinase mediators in hemocytes in response to a wound. Additionally, to identify whether *Drosophila* Cys466 coordinates directed hemocyte migration, mutants encoding an inactivating point mutation in Cys466 (similar to Yoo *et al*) could be studied in the *Drosophila* wounding assay.

To establish whether Src42A and Shark have a role in coordinating migration in the absence of damage-associated signals, but in the presence of developmental guidance cues, it will be essential to also study developmental migration of hemocytes in mutant embryos. In light of our observation that the correlation between wound size and hemocyte recruitment is weaker in Src42A and Shark mutant embryos, it will be useful to count the total hemocyte number in these embryos to establish whether cell number is compromised. This may arise due to disruption of hemocyte development and may account for the impaired migratory phenotype in the wounding assay.

*In vitro* studies using human cells described in this thesis have demonstrated that PI3K signalling makes a comparable contribution to SFK signalling in leukocyte migration. Importantly, others have shown that PI3K is also important in hemocyte chemotaxis to wounds in the *Drosophila* embryonic wound model. *Drosophila* has one class I PI3K, termed Dp110. Its role in cell growth and cell survival has been well characterised [475]. Using genetic and pharmacological approaches, Wood *et al* (2006) demonstrated that PI3K was essential for chemotaxis towards wounds, but was not required for normal dispersal of hemocytes during development [269]. This group suggest that in this setting PI3K is required for gradient sensing from a wound and subsequent cell polarisation. In light of this it would be interesting to investigate the molecular mechanisms that underlie how damage-associate signals lead to PI3K activation in hemocytes, and whether this is driven by cooperation with SFK signalling.

**Limitations of damage-associated signals in *in vitro* models**

$H_2O_2$ is a very small, highly diffusible molecule with a short half-life due to its rapid reactivity and degradation. Therefore, in migration assays, especially the liquid-phase ChemoTx assay, stable gradients of $H_2O_2$ are likely to be short-lived. We have not monitored the decay of $H_2O_2$ in our experiments and therefore it is unclear for how long and to what extent $H_2O_2$ levels remain elevated after treatment. The differences in $H_2O_2$ gradient formation between *in vivo* and *in vitro* models are likely to greatly influence our results, and may account for the contrasting observations we have made. Tissue-scale gradients of $H_2O_2$ *in vivo* will activate localised intracellular signalling networks that are fundamental to driving directed migration. 'Global' stimulation with $H_2O_2$ will evade the precise nature of localised responses and is unlikely to activate defined signalling cascades in a process that is highly dependent on the cells' ability to rearrange intracellular components in one overriding direction. In this case, *in vitro* assays that generate continuous gradients, such as the micropipette chemotaxis assay [418], may be more appropriate.

Because we couldn't be certain that $H_2O_2$ gradients were remaining intact during the experimental period, we have used bolus-based treatment with uniform concentrations of $H_2O_2$. A limitation of this approach is that bolus-based studies are typically performed with $H_2O_2$ concentrations in the upper micromolar or even milimolar range in order to overcome high degradation rates and induce a response. This is in contrast to the much lower $H_2O_2$ concentrations found under physiological conditions *in vivo*, where exogenous concentrations rarely exceed the low micromolar range [305]. The sudden and relatively short-lived exposure of cells to high concentrations of $H_2O_2$ in a bolus experiment may be rather atypical of what happens *in vivo*. It has been shown that bolus and continuous low-level $H_2O_2$ exposure can lead to substantially different signal transduction and cellular responses [476], [477]. Tang *et al* (2005) also show that milimolar concentrations of $H_2O_2$ may have pleiotropic effects on the intracellular signalling network and produce highly artificial results [478].

Extracellular ATP activates chemokinesis and causes immediate and dynamic responses so it is likely that extracellular ATP is involved in the immediate cellular responses to wounds, not only in immune cells but probably also in remaining intact epithelial cells that subsequently produce $H_2O_2$ and the calcium wave. Because ATP

responses are so dynamic they are less likely to rely on gradient formation, compared to $H_2O_2$ responses where graded signals are possibly more important. However, as ATP is a larger molecule than $H_2O_2$, and less diffusible/reactive, we may achieve longer-lived and more defined gradients of ATP in our migration assay. Compared to $H_2O_2$, ATP has defined sites of action, ATP-selective receptors, plasma membrane ion channels and pumps, and initiates rapid calcium influx. We have also demonstrated that ATP-mediated chemokinesis is abrogated by treatment with exogenous $H_2O_2$.

There are limitations to current chemotaxis assays that restrict the types of biological questions that can be addressed. For example, plate based transmigration chambers create unstable chemical gradients, filter cells by size and deformability and make it difficult to differentiate between chemokinesis and chemotaxis. The under agarose migration assay generates unstable chemical gradients that form in all directions. Finally, qualitative analysis is only appropriate for the micropipette assay, because of time-lapse imaging and high labour/low throughput. These assays require high cell numbers, and, if primary human cells are needed, high volumes of blood, which is unsustainable. Recently, more suitable microfluidic platforms have been engineered to provide better spatiotemporal control of gradients by decoupling the gradient generation and migration aspects of the assay. One example is the kit-on-a-lid-assay (KOALA), first reported by Sackmann *et al* (2012), which uses hydrogel to continuously diffuse chemokine without inducing undesired flows [479]. This assay uses cells directly from small blood samples, which reduces purification steps and reduces cell stress.

**Potential mechanisms of $H_2O_2$-induced inhibition of motility**

Deformability, the ability to change shape, is driven by reorganisation of the cytoskeletal network. Our results indicate that $H_2O_2$ could have negative effects on deformability because $H_2O_2$ inhibits all actin-mediated processes we have studied, but $H_2O_2$ can activate intracellular signalling cascades, including calcium mobilisation and protein phosphorylation. $H_2O_2$ does not appear to discriminate between cell types, ligands or receptors, or affect receptor expression. Additionally, $H_2O_2$ inhibits both basal and chemoattractant-mediated chemotaxis, which suggests that $H_2O_2$ is unlikely to be acting via a receptor (e.g. a GPCR). We can therefore hypothesise that $H_2O_2$ is affecting a global signalling network that is common to most activating pathways regardless of the initiating ligand. The targets of $H_2O_2$ are likely to be involved in mechanisms that act independently of a signal gradient or polarised intracellular signalling network. These include Rac1, which is involved in random motility [228], and other members of the Rho family of GTPases and their downstream mediators.

$H_2O_2$ can cross cell membranes and rapidly react with iron-rich molecules to yield very reactive radicals. Oxygen radicals react with polyunsaturated fatty acids and proteins in neutrophils and other cells causing lipid peroxidation and protein degradation [410]. Tang *et al* (2005) report that the cellular localisation of a kinase will affect whether the outcome of $H_2O_2$-mediated oxidation is positive or negative [478]. SFKs in focal adhesion complexes or at the plasma membrane become inactivated after the addition of $H_2O_2$, whereas those localised to the cytoplasm compartments such as the endosome become activated [478]. In light of this, biochemical analysis of the activity,

localisation and trafficking of these proteins in response to exogenous, uniform concentrations of $H_2O_2$ will help to explain the differences we have observed between our models. Additionally, more informative viability assays, such as the Annexin V-PI assay, which provide more information about the apoptotic or necrotic state of cells, will identify any damaging effects of $H_2O_2$.

**Caveats of pharmacological kinase inhibition**

We have shown that pharmacological inhibition of SFKs, Syk or PI3K affects innate cell responses to inflammatory signals. In general, this pharmacological approach is limited by the non-selective nature of the compounds, in particular with regard to the inhibition of several SFK members, and potentially other kinases, by PP2. The conserved nature of SFK domains makes the design of isoform-specific inhibitors challenging [116]. However, other inhibitors of specific protein tyrosine kinases, such as Brc-Abl inhibitor imatinib [480], provide hope that specificity can be achieved. In contrast, the development of p110-selective inhibitors is encouraging. We have used pan-isoform and isoform-selective PI3K inhibitors to characterise the contribution of class IA isoforms in monocyte polarisation. As polarisation is a pre-requisite for migration, we can infer that p110β and p110δ are likely to be involved in cell motility during inflammation.

Selectivity of ATP-competitive inhibitors is restricted by the homology of ATP binding pocket across kinases. In addition, ATP-competitors must compete with milimolar concentrations of ATP in cells, thus necessitating difficult to obtain affinity and/or very high doses to obtain potency *in vivo* [481]. Kinase inhibitors that bind outside of the ATP pocket are of increasing interest, such as one described by Brandvold *et al* (2012) [444]. In addition, Src-I1 is a dual site Src kinase inhibitor that is competitive for both ATP- and kinase-binding sites. It has $IC_{50}$ values of 44nM for Src and 88nM for Lck and inhibits VEGFR2 at higher concentrations ($IC_{50}$ value of 0.32μM) [443].

Genetic silencing of individual kinase isoforms represents an alternative model for global suppression of kinase signalling, and could improve selectivity compared to pharmacological inhibitors. This may be difficult to achieve in short-lived primary cells. However, siRNA-mediated knockdown of Lyn has previously been achieved in the THP-1 monocytic cell line [482]. siRNA-mediated knockdown of p110δ has been demonstrated in mouse bone marrow-derived eosinophils [483].

**The role of damage-associated signals in adhesion-dependent mechanisms**

It is possible that the damage-associated signals and kinases investigated in this thesis could also be affecting the role of cell adhesion molecules and their signalling cascades in our assays. Adhesive cells will engage integrins even in 2D systems, and therefore integrins may be an alternative target, for example of $H_2O_2$, alongside protein kinases in the regulation of cell shape and motility *in vitro*. Our results show that certain integrin-dependent processes, such as spreading and elongation on fibronectin, are affected by treatment with a range of chemoattractants. However, these effects are also observed in assays that do not contain the integrin ligand fibronectin. Furthermore,

while our results indicate that $H_2O_2$ does not affect endothelial ICAM-1 expression, this is in contrast with many other reports and could be an artefact of our *in vitro* models. In general, the effect of damage-associated signals on leukocyte adhesion is an important aspect of immune cell migration and function that should be explored further.

### Distinctive responses between cell types

| Human monocytic cell lines | Primary human neutrophils |
|---|---|
| • Catalase inhibits chemotaxis to MCP-1 | • Catalase potentiates chemotaxis to IL-8 |
| • $H_2O_2$ does not induce transient mobilisation of intracellular calcium | • $H_2O_2$ induces a transient increase in intracellular calcium |
| • MCP-1/LTB4 does not induce intracellular ROS generation | • fMLP induces an increase in intracellular ROS |
| • ATP pre-treatment potentiates migration to MCP-1 | • ATP pre-treatment inhibits migration to IL-8 |
| • Piceatannol pre-treatment potentiates migration to MCP-1 | • Piceatannol pre-treatment inhibits migration to IL-8 |

**Table 6.1 Differences between monocytic cells and neutrophils**

Our results show that signal prioritisation is distinct between monocytic cells and neutrophils. The key differences are summarised in table 6.1. Briefly, monocytic cell chemotaxis was inhibited by catalase, suggesting that migration to MCP-1 requires parallel autocrine signalling of $H_2O_2$ (similar to a reported case in T cells [327]). However, this was not the case with neutrophils, whose response to intermediary chemokine IL-8 was potentiated when catalase was present. This indicates that endogenously produced $H_2O_2$ could skew neutrophil migration prioritisation towards end-target or damage-associated cues. We could only generate transient calcium signalling in neutrophils in response to $H_2O_2$, which suggests that neutrophil intracellular calcium signalling mechanisms are more sensitive to redox regulation than monocytic cells. Additionally, fMLP-stimulated neutrophils generated considerable intracellular ROS, which suggest that FPR activation is linked to NADPH oxidase. However, neither MCP-1 nor $LTB_4$ could induce ROS generation in the monocytic cell lines. This could be due to inactivity of NOX or lack of coupling between CCR2/BLT1 and NOX in these cell types. In monocytic cells, co-activation of CCR2 receptors by MCP-1 and ATP-receptors by ATP leads to cooperative enhancement of migration compared to either stimulus alone. In neutrophils, co-activation of CXCL1/2 receptors by IL-8 and ATP-receptors by ATP leads to inhibition of the CXCR1/2-mediated migratory response. These distinct results imply that in neutrophils, damage-associated extracellular ATP outcompetes intermediary chemokine IL-8. However, in monocytes, ATP positively reinforces MCP-1 signalling, leading to greater chemotaxis. Finally, our results suggest that Syk is active downstream of neutrophil CXCR1/2 but not monocyte CCR2. This implies that CXCL1/2 may cooperate with ITAM-containing motifs through which Syk is recruited and signals to promote migration.

These differences could also be due to disparities between immortalised cell lines and primary cells. THP-1 and U937 monocytic cell lines are only partially representative of

the nature of primary monocytes. These cells lack several important receptors and have different cell cycle properties [382], [383], all of which could impact responses in this investigation. However, the use of primary human cells carries the risk of donor variation, which is sensitive to health, age and genetics. While we have used blood from healthy volunteers, we cannot screen for health history or genetic factors, all of which could impact responses in this investigation.

**Summary and future directions**

The role of SFKs in mediating immune cell migration to a wound is conserved in zebrafish and flies. We have shown that SFKs are important in regulating the *in vitro* effects of immune-related ligands in human immune cells. Our results demonstrate that $H_2O_2$ inhibits the *in vitro* effects of immune-related ligands, particularly actin-mediated processes. This may be due to redox regulation of downstream mediators that are involved in actin regulation. $H_2O_2$ did not affect signal prioritisation in opposing gradients of chemoattractant. $H_2O_2$ and ATP are distinct in their abilities to activate immune cells and regulate motility. SFKs and PI3Ks, particularly class IA isoforms p110β and p110δ, are likely to be useful therapeutic targets for the treatment of inflammatory and autoimmune diseases.

In light of investigations described in this thesis, future experiments should seek to address several objectives:

A) Determine the mechanisms by which damage signals activate Src42A in *Drosophila* following tissue damage. Explore the influence of multiple cues and how they may be prioritised in this setting.
B) Determine the interactions of Src42A, Syk and other inflammatory mediators in *Drosophila* hemocytes following tissue damage.
C) Optimise *in vitro* models of leukocyte chemotaxis for the study of small, highly diffusible molecules, such as $H_2O_2$.
D) Characterise the signalling properties of kinases in the presence of defined gradients of damage-associated signals. How are protein activation, localisation and substrate binding capacity regulated?
E) Investigate the contribution of adhesion molecules in processes activated by damage-associated signals. How are integrins regulated by redox signalling in leukocytes?

# REFERENCES

## References


[1] R. P. Tracy, “The five cardinal signs of inflammation: Calor, Dolor, Rubor, Tumor ... and Penuria (Apologies to Aulus Cornelius Celsus, De medicina, c. A.D. 25).,” *J. Gerontol. A Biol. Sci. Med. Sci.*, vol. 61, no. 10, pp. 1051–1052, Oct. 2006.

[2] C. Auffray, D. Fogg, M. Garfa, G. Elain, O. Join-Lambert, S. Kayal, S. Sarnacki, A. Cumano, G. Lauvau, and F. Geissmann, “Monitoring of blood vessels and tissues by a population of monocytes with patrolling behavior.,” *Science*, vol. 317, no. 5838, pp. 666–670, Aug. 2007.

[3] K. Newton and V. M. Dixit, “Signaling in innate immunity and inflammation.,” *Cold Spring Harbor Perspectives in Biology*, vol. 4, no. 3, pp. a006049–a006049, Mar. 2012.

[4] S. J. Galli, N. Borregaard, and T. A. Wynn, “Phenotypic and functional plasticity of cells of innate immunity: macrophages, mast cells and neutrophils,” *Nature Publishing Group*, vol. 12, no. 11, pp. 1035–1044, Nov. 2011.

[5] S. Lipinski, L. Bremer, T. Lammers, F. Thieme, S. Schreiber, and P. Rosenstiel, “Coagulation and inflammation. Molecular insights and diagnostic implications.,” *Hamostaseologie*, vol. 31, no. 2, pp. 94–102– 104, May 2011.

[6] W. A. Muller, “Getting Leukocytes to the Site of Inflammation,” *Veterinary Pathology*, vol. 50, no. 1, pp. 7–22, Jan. 2013.

[7] Y. Tanino, D. R. Coombe, S. E. Gill, W. C. Kett, O. Kajikawa, A. E. I. Proudfoot, T. N. C. Wells, W. C. Parks, T. N. Wight, T. R. Martin, and C. W. Frevert, “Kinetics of chemokine-glycosaminoglycan interactions control neutrophil migration into the airspaces of the lungs.,” *J. Immunol.*, vol. 184, no. 5, pp. 2677–2685, Mar. 2010.

[8] A. D. Luster, R. Alon, and U. H. von Andrian, “Immune cell migration in inflammation: present and future therapeutic targets,” *Nat Immunol*, vol. 6, no. 12, pp. 1182–1190, Dec. 2005.

[9] M. Sperandio, C. A. Gleissner, and K. Ley, “Glycosylation in immune cell trafficking.,” *Immunological Reviews*, vol. 230, no. 1, pp. 97–113, Jul. 2009.

[10] M. L. Arbonés, D. C. Ord, K. Ley, H. Ratech, C. Maynard-Curry, G. Otten, D. J. Capon, and T. F. Tedder, “Lymphocyte homing and leukocyte rolling and migration are impaired in L-selectin-deficient mice.,” *Immunity*, vol. 1, no. 4, pp. 247–260, Jul. 1994.

[11] B. Petri, M. Phillipson, and P. Kubes, “The physiology of leukocyte recruitment: an in vivo perspective.,” *The Journal of Immunology*, vol. 180, no. 10, pp. 6439–6446, May 2008.

[12] D. A. Carlow, K. Gossens, S. Naus, K. M. Veerman, W. Seo, and H. J. Ziltener, “PSGL-1 function in immunity and steady state homeostasis.,” *Immunological Reviews*, vol. 230, no. 1, pp. 75–96, Jul. 2009.

[13] Y. Kuwano, O. Spelten, H. Zhang, K. Ley, and A. Zarbock, “Rolling on E- or P-selectin induces the extended but not high-affinity conformation of LFA-1 in neutrophils,” *Blood*, vol. 116, no. 4, pp. 617–624, Jul. 2010.

[14] A. Mócsai, C. L. Abram, Z. Jakus, Y. Hu, L. L. Lanier, and C. A. Lowell, “Integrin signaling in neutrophils and macrophages uses adaptors containing immunoreceptor tyrosine-based activation motifs,” *Nat Immunol*, vol. 7, no. 12, pp. 1326–1333, Nov. 2006.

[15] K. Futosi, S. Fodor, and A. Mócsai, “Neutrophil cell surface receptors and their intracellular signal transduction pathways,” *International Immunopharmacology*, pp. 1–13, Aug. 2013.

[16] M. Phillipson, B. Heit, P. Colarusso, L. Liu, C. M. Ballantyne, and P. Kubes, “Intraluminal crawling of neutrophils to emigration sites: a molecularly distinct process from adhesion in the recruitment cascade.,” *Journal of Experimental Medicine*, vol. 203, no. 12, pp. 2569–2575, Nov. 2006.

[17] C. F. Nathan, “Neutrophil activation on biological surfaces. Massive secretion of hydrogen peroxide in response to products of macrophages and lymphocytes.,” *J. Clin. Invest.*, vol. 80, no. 6, pp. 1550–1560, Dec. 1987.

[18] E. Kolaczkowska and P. Kubes, “Neutrophil recruitment and function in health and inflammation,” *Nature Publishing Group*, vol. 13, no. 3, pp. 159–175, Mar. 2013.

[19] S. A. Parsons, R. Sharma, D. L. Roccamatisi, H. Zhang, B. Petri, P. Kubes, P. Colarusso, and K. D. Patel, “Endothelial paxillin and focal adhesion kinase (FAK) play a critical role in neutrophil transmigration,” *Eur. J. Immunol.*, vol. 42, no. 2, pp. 436–446, Jan. 2012.

[20] M. Häger, J. B. Cowland, and N. Borregaard, “Neutrophil granules in health and disease,” *Journal of Internal Medicine*, pp. no–no, Apr. 2010.

[21] S. Wang, “Venular basement membranes contain specific matrix protein low expression regions that act as exit points for emigrating neutrophils,” *Journal of Experimental Medicine*, vol. 203, no. 6, pp. 1519–1532, Jun. 2006.

[22] D. Proebstl, M. B. Voisin, A. Woodfin, J. Whiteford, F. D'Acquisto, G. E. Jones, D. Rowe, and S. Nourshargh, “Pericytes support neutrophil subendothelial cell crawling and breaching of venular walls in vivo,” *Journal of Experimental Medicine*, vol. 209, no. 6, pp. 1219–1234, Jun. 2012.

[23] E. F. Foxman, J. J. Campbell, and E. C. Butcher, “Multistep navigation and the combinatorial control of leukocyte chemotaxis.,” *The Journal of Cell Biology*, vol. 139, no. 5, pp. 1349–1360, Dec. 1997.

[24] R. S. Flannagan, V. Jaumouillé, and S. Grinstein, “The cell biology of phagocytosis.,” *Annu Rev Pathol*, vol. 7, no. 1, pp. 61–98, 2012.

[25] S. E. Doyle, R. M. O'Connell, G. A. Miranda, S. A. Vaidya, E. K. Chow, P. T. Liu, S. Suzuki, N. Suzuki, R. L. Modlin, W.-C. Yeh, T. F. Lane, and G. Cheng, “Toll-like receptors induce a phagocytic gene program through p38.,” *Journal of Experimental Medicine*, vol. 199, no. 1, pp. 81–90, Jan. 2004.

[26] C. L. Anderson, L. Shen, D. M. Eicher, M. D. Wewers, and J. K. Gill, “Phagocytosis mediated by three distinct Fc gamma receptor classes on human leukocytes.,” *Journal of Experimental Medicine*, vol. 171, no. 4, pp. 1333–1345, Apr. 1990.

[27] F. Niedergang and P. Chavrier, “Regulation of phagocytosis by Rho GTPases.,” *Curr. Top. Microbiol. Immunol.*, vol. 291, pp. 43–60, 2005.

[28] N. Kobayashi, P. Karisola, V. Peña-Cruz, D. M. Dorfman, M. Jinushi, S. E. Umetsu, M. J. Butte, H. Nagumo, I. Chernova, B. Zhu, A. H. Sharpe, S. Ito, G. Dranoff, G. G. Kaplan, J. M. Casasnovas, D. T. Umetsu, R. H. DeKruyff, and G. J. Freeman, “TIM-1 and TIM-4 glycoproteins bind phosphatidylserine and mediate uptake of apoptotic cells.,” *Immunity*, vol. 27, no. 6, pp. 927–940, Dec. 2007.

[29] F. M. Griffin, J. A. Griffin, J. E. Leider, and S. C. Silverstein, “Studies on the mechanism of phagocytosis. I. Requirements for circumferential attachment of particle-bound ligands to specific receptors on the macrophage plasma membrane.,” *Journal of Experimental Medicine*, vol. 142, no. 5, pp. 1263–1282, Nov. 1975.

[30] G. L. Lukacs, O. D. Rotstein, and S. Grinstein, “Determinants of the phagosomal pH in macrophages. In situ assessment of vacuolar H(+)-ATPase activity, counterion conductance, and H+ "leak".,” *Journal of Biological Chemistry*, vol. 266, no. 36, pp. 24540–24548, Dec. 1991.

[31] K. E. Anderson, T. A. M. Chessa, K. Davidson, R. B. Henderson, S. Walker, T. Tolmachova, K. Grys, O. Rausch, M. C. Seabra, V. L. J. Tybulewicz, L. R. Stephens, and P. T. Hawkins, “PtdIns3P and Rac direct the assembly of the NADPH oxidase on a novel, pre-phagosomal compartment during FcR-mediated phagocytosis in primary mouse neutrophils.,” *Blood*, vol. 116, no. 23, pp. 4978–4989, Dec. 2010.

[32] R. S. Flannagan, G. Cosío, and S. Grinstein, “Antimicrobial mechanisms of phagocytes and bacterial evasion strategies.,” *Nat. Rev. Microbiol.*, vol. 7, no. 5, pp. 355–366, May 2009.

[33] C. N. Serhan, N. Chiang, and T. E. Van Dyke, “Resolving inflammation: dual anti-inflammatory and pro-resolution lipid mediators,” *Nature Reviews Immunology*, vol. 8, no. 5, pp. 349–361, May 2008.

[34] C. N. Serhan, “Novel Lipid Mediators and Resolution Mechanisms in Acute Inflammation,” *The American Journal of Pathology*, vol. 177, no. 4, pp. 1576–1591, Dec. 2010.

[35] O. Soehnlein and L. Lindbom, “Phagocyte partnership during the onset and resolution of inflammation,” *Nature Publishing Group*, vol. 10, no. 6, pp. 427–439, Jun. 2010.

[36] J. Shi, “Role of the liver in regulating numbers of circulating neutrophils,” *Blood*, vol. 98, no. 4, pp. 1226–1230, Aug. 2001.

[37] J. R. Mathias, B. J. Perrin, T. X. Liu, J. Kanki, A. T. Look, and A. Huttenlocher, “Resolution of inflammation by retrograde chemotaxis of neutrophils in transgenic zebrafish,” *Journal of Leukocyte Biology*, vol. 80, no. 6, pp. 1281–1288, Aug. 2006.

[38] B. A. Maletto, A. S. Ropolo, D. O. Alignani, M. V. Liscovsky, R. P. Ranocchia, V. G. Moron, and M. C. Pistoresi-Palencia, “Presence of neutrophil-bearing antigen in lymphoid organs of immune mice.,” *Blood*, vol. 108, no. 9, pp. 3094–3102, Nov. 2006.

[39] Q. Deng, S. K. Yoo, P. J. Cavnar, J. M. Green, and A. Huttenlocher, “Dual roles for Rac2 in neutrophil motility and active retention in zebrafish hematopoietic tissue.,” *Developmental Cell*, vol. 21, no. 4, pp. 735–745, Oct. 2011.

[40] Y. Liu, J. M. Cousin, J. Hughes, J. Van Damme, J. R. Seckl, C. Haslett, I. Dransfield, J. Savill, and A. G. Rossi, “Glucocorticoids promote nonphlogistic phagocytosis of apoptotic leukocytes.,” *The Journal of Immunology*, vol. 162, no. 6, pp. 3639–3646, Mar. 1999.

[41] M. Perretti, N. Chiang, M. La, I. M. Fierro, S. Marullo, S. J. Getting, E. Solito, and C. N. Serhan, “Endogenous lipid- and peptide-derived anti-inflammatory pathways generated with glucocorticoid and aspirin treatment activate the lipoxin A4 receptor.,” *Nat Med*, vol. 8, no. 11, pp. 1296–1302, Nov. 2002.

[42] G. J. Lieschke, D. Grail, G. Hodgson, D. Metcalf, E. Stanley, C. Cheers, K. J. Fowler, S. Basu, Y. F. Zhan, and A. R. Dunn, “Mice lacking granulocyte colony-stimulating factor have chronic neutropenia, granulocyte and macrophage progenitor cell deficiency, and impaired neutrophil mobilization.,” *Blood*, vol. 84, no. 6, pp. 1737–1746, Sep. 1994.

[43] N. Borregaard, “Neutrophils, from Marrow to Microbes,” *Immunity*, vol. 33, no. 5, pp. 657–670, Nov. 2010.

[44] D. Kreisel, R. G. Nava, W. Li, B. H. Zinselmeyer, B. Wang, J. Lai, R. Pless, A. E. Gelman, A. S. Krupnick, and M. J. Miller, “In vivo two-photon imaging reveals monocyte-dependent neutrophil extravasation during pulmonary inflammation.,” *Proc. Natl. Acad. Sci. U.S.A.*, vol. 107, no. 42, pp. 18073–18078, Oct. 2010.

[45] V. M. Kamp, J. Pillay, J. W. J. Lammers, P. Pickkers, L. H. Ulfman, and L. Koenderman, “Human suppressive neutrophils CD16bright/CD62Ldim exhibit decreased adhesion,” *Journal of Leukocyte Biology*, vol. 92, no. 5, pp. 1011–1020, Oct. 2012.

[46] J. Pillay, V. M. Kamp, E. van Hoffen, T. Visser, T. Tak, J.-W. Lammers, L. H. Ulfman, L. P. Leenen, P. Pickkers, and L. Koenderman, “A subset of neutrophils in human systemic inflammation inhibits T cell responses through Mac-1,” *J. Clin. Invest.*, vol. 122, no. 1, pp. 327–336, Jan. 2012.

[47] M. Faurschou, O. E. Sørensen, A. H. Johnsen, J. Askaa, and N. Borregaard, “Defensin-rich granules of human neutrophils: characterization of secretory properties.,” *Biochim. Biophys. Acta*, vol. 1591, no. 1, pp. 29–35, Aug. 2002.

[48] V. Papayannopoulos and A. Zychlinsky, “NETs: a new strategy for using old weapons,” *Trends in Immunology*, vol. 30, no. 11, pp. 513–521, Nov. 2009.

[49] B. M. Fournier and C. A. Parkos, “The role of neutrophils during intestinal inflammation,” vol. 5, no. 4, pp. 354–366, Apr. 2012.

[50] J. Jablonska, S. Leschner, K. Westphal, S. Lienenklaus, and S. Weiss, “Neutrophils responsive to endogenous IFN-β regulate tumor angiogenesis and growth in a mouse tumor model,” *J. Clin. Invest.*, vol. 120, no. 4, pp. 1151–1164, Apr. 2010.

[51] C. Beauvillain, P. Cunin, A. Doni, M. Scotet, S. Jaillon, M. L. Loiry, G. Magistrelli, K. Masternak, A. Chevailler, Y. Delneste, and P. Jeannin, “CCR7 is involved in the migration of neutrophils to lymph nodes,” *Blood*, vol. 117, no. 4, pp. 1196–1204, Jan. 2011.

[52] D. Duffy, H. Perrin, V. Abadie, N. Benhabiles, A. Boissonnas, C. Liard, B. Descours, D. Reboulleau, O. Bonduelle, B. Verrier, N. Van Rooijen, C. Combadière, and B. Combadière, “Neutrophils Transport Antigen from the Dermis to the Bone Marrow, Initiating a Source of Memory CD8+ T Cells,” *Immunity*, vol. 37, no. 5, pp. 917–929, Nov. 2012.

[53] G. Y. Chen and G. Nuñez, “Sterile inflammation: sensing and reacting to damage,” *Nature Publishing Group*, vol. 10, no. 12, pp. 826–837, Nov. 2010.

[54] C. Summers, S. M. Rankin, A. M. Condliffe, N. Singh, A. M. Peters, and E. R. Chilvers, “Neutrophil kinetics in health and disease.,” *Trends in Immunology*, vol. 31, no. 8, pp. 318–324, Aug. 2010.

[55] P. A. Monach, P. A. Nigrovic, M. Chen, H. Hock, D. M. Lee, C. Benoist, and D. Mathis, “Neutrophils in a mouse model of autoantibody-mediated arthritis: Critical producers of Fc receptor γ, the receptor for C5a, and lymphocyte function−associated antigen 1,” *Arthritis & Rheumatism*, vol. 62, no. 3, pp. 753–764, Feb. 2010.

[56] E. R. Elliott, J. A. Van Ziffle, P. Scapini, B. M. Sullivan, R. M. Locksley, and C. A. Lowell, “Deletion of Syk in neutrophils prevents immune complex arthritis.,” *J. Immunol.*, vol. 187, no. 8, pp. 4319–4330, Oct. 2011.

[57] W. W. ZUELZER, “‘MYELOKATHEXIS’--A NEW FORM OF CHRONIC GRANULOCYTOPENIA. REPORT OF A CASE.,” *N. Engl. J. Med.*, vol. 270, no. 14, pp. 699–704, Apr. 1964.

[58] C. Shi and E. G. Pamer, “Monocyte recruitment during infection and inflammation,” *Nature Publishing Group*, vol. 11, no. 11, pp. 762–774, Oct. 2011.

[59] S. Gordon and P. R. Taylor, “Monocyte and macrophage heterogeneity.,” *Nature Reviews Immunology*, vol. 5, no. 12, pp. 953–964, Dec. 2005.

[60] N. V. Serbina, T. Jia, T. M. Hohl, and E. G. Pamer, “Monocyte-mediated defense against microbial pathogens.,” *Annu. Rev. Immunol.*, vol. 26, no. 1, pp. 421–452, 2008.

[61] T. Kurihara, G. Warr, J. Loy, and R. Bravo, “Defects in macrophage recruitment and host defense in mice lacking the CCR2 chemokine receptor.,” *Journal of Experimental Medicine*, vol. 186, no. 10, pp. 1757–1762, Nov. 1997.

[62] F. Ginhoux and S. Jung, “Monocytes and macrophages: developmental pathways and tissue homeostasis.,” *Nature Reviews Immunology*, vol. 14, no. 6, pp. 392–404, Jun. 2014.

[63] F. O. Martinez and S. Gordon, “The M1 and M2 paradigm of macrophage activation: time for reassessment.,” *F1000Prime Rep*, vol. 6, no. 13, p. 13, 2014.

[64] J. Murphy, R. Summer, A. A. Wilson, D. N. Kotton, and A. Fine, “The prolonged life-span of alveolar macrophages.,” *Am J Respir Cell Mol Biol*, vol. 38, no. 4, pp. 380–385, Apr. 2008.

[65] A. B. van oud Alblas and R. van Furth, “Origin, Kinetics, and characteristics of pulmonary macrophages in the normal steady state.,” *Journal of Experimental Medicine*, vol. 149, no. 6, pp. 1504–1518, Jun. 1979.

[66] L. Landsman and S. Jung, “Lung macrophages serve as obligatory intermediate between blood monocytes and alveolar macrophages.,” *The Journal of Immunology*, vol. 179, no. 6, pp. 3488–3494, Sep. 2007.

[67] D. M. Mosser and J. P. Edwards, “Exploring the full spectrum of macrophage activation.,” *Nature Reviews Immunology*, vol. 8, no. 12, pp. 958–969, Dec. 2008.

[68] L. Ziegler-Heitbrock, P. Ancuta, S. Crowe, M. Dalod, V. Grau, D. N. Hart, P. J. M. Leenen, Y.-J. Liu, G. MacPherson, G. J. Randolph, J. Scherberich, J. Schmitz, K. Shortman, S. Sozzani, H. Strobl, M. Zembala, J. M. Austyn, and M. B. Lutz, “Nomenclature of monocytes and dendritic cells in blood.,” *Blood*, vol. 116, no. 16, pp. e74–80, Oct. 2010.

[69] H. Liu and R. M. Pope, “Phagocytes: mechanisms of inflammation and tissue destruction.,” *Rheum. Dis. Clin. North Am.*, vol. 30, no. 1, pp. 19–39– v, Feb. 2004.

[70] H. Y. Kim, H. J. Lee, Y.-J. Chang, M. Pichavant, S. A. Shore, K. A. Fitzgerald, Y. Iwakura, E. Israel, K. Bolger, J. Faul, R. H. DeKruyff, and D. T. Umetsu, “Interleukin-17-producing innate lymphoid cells and the NLRP3 inflammasome facilitate obesity-associated airway hyperreactivity.,” *Nat Med*, vol. 20, no. 1, pp. 54–61, Jan. 2014.

[71] M. L. Novak and T. J. Koh, “Macrophage phenotypes during tissue repair.,” *Journal of Leukocyte Biology*, vol. 93, no. 6, pp. 875–881, Jun. 2013.

[72] A. Sica and A. Mantovani, “Macrophage plasticity and polarization: in vivo veritas.,” *J. Clin. Invest.*, vol. 122, no. 3, pp. 787–795, Mar. 2012.

[73] A. Saccani, T. Schioppa, C. Porta, S. K. Biswas, M. Nebuloni, L. Vago, B. Bottazzi, M. P. Colombo, A. Mantovani, and A. Sica, “p50 nuclear factor-kappaB overexpression in tumor-associated macrophages inhibits M1 inflammatory responses and antitumor resistance.,” *Cancer Res.*, vol. 66, no. 23, pp. 11432–11440, Dec. 2006.

[74] C. Guiducci, A. P. Vicari, S. Sangaletti, G. Trinchieri, and M. P. Colombo, “Redirecting in vivo elicited tumor infiltrating macrophages and dendritic cells towards tumor rejection.,” *Cancer Res.*, vol. 65, no. 8, pp. 3437–3446, Apr. 2005.

[75] A. Mantovani, A. Vecchi, and P. Allavena, “Pharmacological modulation of monocytes and macrophages.,” *Curr Opin Pharmacol*, vol. 17, pp. 38–44, Jul. 2014.

[76] L. Li, B. Yan, Y.-Q. Shi, W.-Q. Zhang, and Z.-L. Wen, “Live imaging reveals differing roles of macrophages and neutrophils during zebrafish tail fin regeneration.,” *J. Biol. Chem.*, vol. 287, no. 30, pp. 25353–25360, Jul. 2012.

[77] M. Baggiolini and P. Loetscher, “Chemokines in inflammation and immunity.,” *Immunol. Today*, vol. 21, no. 9, pp. 418–420, Sep. 2000.

[78] S. L. Deshmane, S. Kremlev, S. Amini, and B. E. Sawaya, “Monocyte Chemoattractant Protein-1 (MCP-1): An Overview,” *Journal of Interferon & Cytokine Research*, vol. 29, no. 6, pp. 313–326, Jun. 2009.

[79] A. Zlotnik and O. Yoshie, “The chemokine superfamily revisited.,” *Immunity*, vol. 36, no. 5, pp. 705–716, May 2012.

[80] G. J. Graham, M. Locati, A. Mantovani, A. Rot, and M. Thelen, “The biochemistry and biology of the atypical chemokine receptors.,” *Immunology Letters*, vol. 145, no. 1, pp. 30–38, Jul. 2012.

[81] A. Mantovani, “The chemokine system: redundancy for robust outputs.,” *Immunol. Today*, vol. 20, no. 6, pp. 254–257, Jun. 1999.

[82] C. A. Hébert and J. B. Baker, “Interleukin-8: a review.,” *Cancer Invest.*, vol. 11, no. 6, pp. 743–750, 1993.

[83] M. W. Nasser, S. K. Raghuwanshi, D. J. Grant, V. R. Jala, K. Rajarathnam, and R. M. Richardson, “Differential activation and regulation of CXCR1 and CXCR2 by CXCL8 monomer and dimer.,” *J. Immunol.*, vol. 183, no. 5, pp. 3425–3432, Sep. 2009.

[84] R. M. Richardson, B. C. Pridgen, B. Haribabu, H. Ali, and R. Snyderman, “Differential cross-regulation of the human chemokine receptors CXCR1 and CXCR2. Evidence for time-dependent signal generation.,” *Journal of Biological Chemistry*, vol. 273, no. 37, pp. 23830–23836, Sep. 1998.

[85] R. M. Richardson, R. J. Marjoram, L. S. Barak, and R. Snyderman, “Role of the cytoplasmic tails of CXCR1 and CXCR2 in mediating leukocyte migration, activation, and regulation.,” *The Journal of Immunology*, vol. 170, no. 6, pp. 2904–2911, Mar. 2003.

[86] L. M. Campbell, P. J. Maxwell, and D. J. J. Waugh, “Rationale and Means to Target Pro-Inflammatory Interleukin-8 (CXCL8) Signaling in Cancer.,” *Pharmaceuticals (Basel)*, vol. 6, no. 8, pp. 929–959, 2013.

[87] K. Ina, K. Kusugami, T. Yamaguchi, A. Imada, T. Hosokawa, M. Ohsuga, M. Shinoda, T. Ando, K. Ito, and Y. Yokoyama, “Mucosal interleukin-8 is involved in neutrophil migration and binding to extracellular matrix in inflammatory bowel disease.,” *Am. J. Gastroenterol.*, vol. 92, no. 8, pp. 1342–1346, Aug. 1997.

[88] M. N. Ajuebor, R. J. Flower, R. Hannon, M. Christie, K. Bowers, A. Verity, and M. Perretti, “Endogenous monocyte chemoattractant protein-1 recruits monocytes in the zymosan peritonitis model.,” *Journal of Leukocyte Biology*, vol. 63, no. 1, pp. 108–116, Jan. 1998.

[89] C.-L. Tsou, W. Peters, Y. Si, S. Slaymaker, A. M. Aslanian, S. P. Weisberg, M. Mack, and I. F. Charo, “Critical roles for CCR2 and MCP-3 in monocyte mobilization from bone marrow and recruitment to inflammatory sites.,” *J. Clin. Invest.*, vol. 117, no. 4, pp. 902–909, Apr. 2007.

[90] M. A. Thacker, A. K. Clark, F. Marchand, and S. B. McMahon, “Pathophysiology of peripheral neuropathic pain: immune cells and molecules.,” *Anesth. Analg.*, vol. 105, no. 3, pp. 838–847, Sep. 2007.

[91] M. P. Quinones, S. K. Ahuja, F. Jimenez, J. Schaefer, E. Garavito, A. Rao, G. Chenaux, R. L. Reddick, W. A. Kuziel, and S. S. Ahuja, “Experimental arthritis in CC chemokine receptor 2-null mice closely mimics severe human rheumatoid arthritis.,” *J. Clin. Invest.*, vol. 113, no. 6, pp. 856–866, Mar. 2004.

[92] L. Gu, Y. Okada, S. K. Clinton, C. Gerard, G. K. Sukhova, P. Libby, and B. J. Rollins, “Absence of monocyte chemoattractant protein-1 reduces atherosclerosis in low density lipoprotein receptor-deficient mice.,” *Mol. Cell*, vol. 2, no. 2, pp. 275–281, Aug. 1998.

[93] J. E. Simpson, J. Newcombe, M. L. Cuzner, and M. N. Woodroofe, “Expression of monocyte chemoattractant protein-1 and other beta-chemokines by resident glia and inflammatory cells in multiple sclerosis lesions.,” *J. Neuroimmunol.*, vol. 84, no. 2, pp. 238–249, Apr. 1998.

[94] D. A. Dorward, C. D. Lucas, A. L. Alessandri, J. A. Marwick, F. Rossi, I. Dransfield, C. Haslett, K. Dhaliwal, and A. G. Rossi, “Technical advance: autofluorescence-based sorting: rapid and nonperturbing isolation of ultrapure neutrophils to determine cytokine production.,” *Journal of Leukocyte Biology*, vol. 94, no. 1, pp. 193–202, Jul. 2013.

[95] W. A. Marasco, S. H. Phan, H. Krutzsch, H. J. Showell, D. E. Feltner, R. Nairn, E. L. Becker, and P. A. Ward, “Purification and identification of formyl-methionyl-leucyl-phenylalanine as the major peptide neutrophil chemotactic factor produced by Escherichia coli.,” *Journal of Biological Chemistry*, vol. 259, no. 9, pp. 5430–5439, May 1984.

[96] R. Selvatici, S. Falzarano, A. Mollica, and S. Spisani, “Signal transduction pathways triggered by selective formylpeptide analogues in human neutrophils.,” *Eur. J. Pharmacol.*, vol. 534, no. 1, pp. 1–11, Mar. 2006.

[97] F. Boulay, M. Tardif, L. Brouchon, and P. Vignais, “Synthesis and use of a novel N-formyl peptide derivative to isolate a human N-formyl peptide receptor cDNA.,” *Biochemical and Biophysical Research Communications*, vol. 168, no. 3, pp. 1103–1109, May 1990.

[98] K. G. Lazzari, P. J. Proto, and E. R. Simons, “Simultaneous measurement of stimulus-induced changes in cytoplasmic Ca2+ and in membrane potential of human neutrophils.,” *Journal of Biological Chemistry*, vol. 261, no. 21, pp. 9710–9713, Jul. 1986.

[99] D. D. Browning, Z. K. Pan, E. R. Prossnitz, and R. D. Ye, “Cell type- and developmental stage-specific activation of NF-kappaB by fMet-Leu-Phe in myeloid cells.,” *Journal of Biological Chemistry*, vol. 272, no. 12, pp. 7995–8001, Mar. 1997.

[100] M. A. Panaro, A. Acquafredda, M. Sisto, S. Lisi, A. B. Maffione, and V. Mitolo, “Biological role of the N-formyl peptide receptors.,” *Immunopharmacol Immunotoxicol*, vol. 28, no. 1, pp. 103–127, 2006.

[101] N. Arbour, P. Tremblay, and D. Oth, “N-formyl-methionyl-leucyl-phenylalanine induces and modulates IL-1 and IL-6 in human PBMC.,” *Cytokine*, vol. 8, no. 6, pp. 468–475, Jun. 1996.

[102] E. Fernández-Segura, J. M. García, J. L. Santos, and A. Campos, “Shape, F-actin, and surface morphology changes during chemotactic peptide-induced polarity in human neutrophils.,” *Anat. Rec.*, vol. 241, no. 4, pp. 519–528, Apr. 1995.

[103] M. Raoof, Q. Zhang, K. Itagaki, and C. J. Hauser, “Mitochondrial peptides are potent immune activators that activate human neutrophils via FPR-1.,” *J Trauma*, vol. 68, no. 6, pp. 1328–32– discussion 1332–4, Jun. 2010.

[104] M. R. Gwinn, A. Sharma, and E. De Nardin, “Single nucleotide polymorphisms of the N-formyl peptide receptor in localized juvenile periodontitis.,” *J. Periodontol.*, vol. 70, no. 10, pp. 1194–1201, Oct. 1999.

[105] J. L. Gao, E. J. Lee, and P. M. Murphy, “Impaired antibacterial host defense in mice lacking the N-formylpeptide receptor.,” *Journal of Experimental Medicine*, vol. 189, no. 4, pp. 657–662, Feb. 1999.

[106] T. Yokomizo, “Leukotriene B4 receptors: novel roles in immunological regulations.,” *Adv. Enzyme Regul.*, vol. 51, no. 1, pp. 59–64, 2011.

[107] M. Peters-Golden and T. G. Brock, “5-lipoxygenase and FLAP.,” *Prostaglandins Leukotrienes & Essential Fatty Acids*, vol. 69, no. 2, pp. 99–109, Aug. 2003.

[108] T. Yokomizo, K. Kato, K. Terawaki, T. Izumi, and T. Shimizu, “A second leukotriene B(4) receptor, BLT2. A new therapeutic target in inflammation and immunological disorders.,” *Journal of Experimental Medicine*, vol. 192, no. 3, pp. 421–432, Aug. 2000.

[109] B. Yousefi, F. Jadidi-Niaragh, G. Azizi, F. Hajighasemi, and A. Mirshafiey, “The role of leukotrienes in immunopathogenesis of rheumatoid arthritis.,” *Mod Rheumatol*, vol. 24, no. 2, pp. 225–235, Mar. 2014.

[110] J. N. Sharma and L. A. Mohammed, “The role of leukotrienes in the pathophysiology of inflammatory disorders: is there a case for revisiting leukotrienes as therapeutic targets?,” *Inflammopharmacology*, vol. 14, no. 1, pp. 10–16, Mar. 2006.

[111] G. Warwick, P. S. Thomas, and D. H. Yates, “Non-invasive biomarkers in exacerbations of obstructive lung disease.,” *Respirology*, vol. 18, no. 5, pp. 874–884, Jul. 2013.
[112] C. A. Lowell, “Src-family and Syk Kinases in Activating and Inhibitory Pathways in Innate Immune Cells: Signaling Cross Talk,” *Cold Spring Harbor Perspectives in Biology*, vol. 3, no. 3, pp. a002352–a002352, Mar. 2011.
[113] D. Stehelin, H. E. Varmus, J. M. Bishop, and P. K. Vogt, “DNA related to the transforming gene(s) of avian sarcoma viruses is present in normal avian DNA.,” *Nature*, vol. 260, no. 5547, pp. 170–173, Mar. 1976.
[114] M. P. Kim, S. I. Park, S. Kopetz, and G. E. Gallick, “Src family kinases as mediators of endothelial permeability: effects on inflammation and metastasis,” *Cell Tissue Res*, vol. 335, no. 1, pp. 249–259, Sep. 2008.
[115] A. Baruzzi, E. Caveggion, and G. Berton, “Regulation of phagocyte migration and recruitment by Src-family kinases,” *Cell. Mol. Life Sci.*, vol. 65, no. 14, pp. 2175–2190, Apr. 2008.
[116] T. J. Boggon and M. J. Eck, “Structure and regulation of Src family kinases.,” *Oncogene*, vol. 23, no. 48, pp. 7918–7927, Oct. 2004.
[117] M. C. Frame, “Src in cancer: deregulation and consequences for cell behaviour.,” *Biochim. Biophys. Acta*, vol. 1602, no. 2, pp. 114–130, Jun. 2002.
[118] S. K. Hanks, A. M. Quinn, and T. Hunter, “The protein kinase family: conserved features and deduced phylogeny of the catalytic domains.,” *Science*, vol. 241, no. 4861, pp. 42–52, Jul. 1988.
[119] K. G. Birukov, C. Csortos, L. Marzilli, S. Dudek, S. F. Ma, A. R. Bresnick, A. D. Verin, R. J. Cotter, and J. G. Garcia, “Differential regulation of alternatively spliced endothelial cell myosin light chain kinase isoforms by p60(Src).,” *Journal of Biological Chemistry*, vol. 276, no. 11, pp. 8567–8573, Mar. 2001.
[120] W. Xu, A. Doshi, M. Lei, M. J. Eck, and S. C. Harrison, “Crystal structures of c-Src reveal features of its autoinhibitory mechanism.,” *Mol. Cell*, vol. 3, no. 5, pp. 629–638, May 1999.
[121] L. Alland, S. M. Peseckis, R. E. Atherton, L. Berthiaume, and M. D. Resh, “Dual myristylation and palmitylation of Src family member p59fyn affects subcellular localization.,” *Journal of Biological Chemistry*, vol. 269, no. 24, pp. 16701–16705, Jun. 1994.
[122] J. E. Smart, H. Oppermann, A. P. Czernilofsky, A. F. Purchio, R. L. Erikson, and J. M. Bishop, “Characterization of sites for tyrosine phosphorylation in the transforming protein of Rous sarcoma virus (pp60v-src) and its normal cellular homologue (pp60c-src).,” *Proc. Natl. Acad. Sci. U.S.A.*, vol. 78, no. 10, pp. 6013–6017, Oct. 1981.
[123] R. B. Irby and T. J. Yeatman, “Role of Src expression and activation in human cancer.,” *Oncogene*, vol. 19, no. 49, pp. 5636–5642, Nov. 2000.
[124] C. R. Hauck, C. K. Klingbeil, and D. D. Schlaepfer, “Focal adhesion kinase functions as a receptor-proximal signaling component required for directed cell migration.,” *Immunol. Res.*, vol. 21, no. 2, pp. 293–303, 2000.
[125] A. K. Chowdhury, T. Watkins, N. L. Parinandi, B. Saatian, M. E. Kleinberg, P. V. Usatyuk, and V. Natarajan, “Src-mediated tyrosine phosphorylation of p47phox in hyperoxia-induced activation of NADPH oxidase and generation of reactive oxygen species in lung endothelial cells.,” *Journal of Biological Chemistry*, vol. 280, no. 21, pp. 20700–20711, May 2005.
[126] S. Fodor, Z. Jakus, and A. Mócsai, “ITAM-based signaling beyond the adaptive immune response.,” *Immunology Letters*, vol. 104, no. 1, pp. 29–37, Apr. 2006.
[127] T. Kurosaki, H. Shinohara, and Y. Baba, “B cell signaling and fate decision.,” *Annu. Rev. Immunol.*, vol. 28, no. 1, pp. 21–55, 2010.
[128] J. E. Smith-Garvin, G. A. Koretzky, and M. S. Jordan, “T cell activation.,” *Annu. Rev. Immunol.*, vol. 27, no. 1, pp. 591–619, 2009.

[129] P. Scapini, S. Pereira, H. Zhang, and C. A. Lowell, “Multiple roles of Lyn kinase in myeloid cell signaling and function,” *Immunological Reviews*, vol. 228, no. 1, pp. 23–40, Mar. 2009.

[130] S. Hunter, M. M. Huang, Z. K. Indik, and A. D. Schreiber, “Fc gamma RIIA-mediated phagocytosis and receptor phosphorylation in cells deficient in the protein tyrosine kinase Src.,” *Exp. Hematol.*, vol. 21, no. 11, pp. 1492–1497, Oct. 1993.

[131] F. Hayakawa and T. Naoe, “SFK-STAT pathway: an alternative and important way to malignancies.,” *Ann. N. Y. Acad. Sci.*, vol. 1086, no. 1, pp. 213–222, Nov. 2006.

[132] M. Perugini, A. L. Brown, D. G. Salerno, G. W. Booker, C. Stojkoski, T. R. Hercus, A. F. Lopez, M. L. Hibbs, T. J. Gonda, and R. J. D'Andrea, “Alternative modes of GM-CSF receptor activation revealed using activated mutants of the common beta-subunit.,” *Blood*, vol. 115, no. 16, pp. 3346–3353, Apr. 2010.

[133] C. Bourgin-Hierle, S. Gobert-Gosse, J. Thérier, M.-F. Grasset, and G. Mouchiroud, “Src-family kinases play an essential role in differentiation signaling downstream of macrophage colony-stimulating factor receptors mediating persistent phosphorylation of phospholipase C-gamma2 and MAP kinases ERK1 and ERK2.,” *Leukemia*, vol. 22, no. 1, pp. 161–169, Jan. 2008.

[134] L. L. Lanier, “DAP10- and DAP12-associated receptors in innate immunity.,” *Immunological Reviews*, vol. 227, no. 1, pp. 150–160, Jan. 2009.

[135] S. Hida, S. Yamasaki, Y. Sakamoto, M. Takamoto, K. Obata, T. Takai, H. Karasuyama, K. Sugane, T. Saito, and S. Taki, “Fc receptor gamma-chain, a constitutive component of the IL-3 receptor, is required for IL-3-induced IL-4 production in basophils.,” *Nature Publishing Group*, vol. 10, no. 2, pp. 214–222, Feb. 2009.

[136] Y. C. Ma, J. Huang, S. Ali, W. Lowry, and X. Y. Huang, “Src tyrosine kinase is a novel direct effector of G proteins.,” *Cell*, vol. 102, no. 5, pp. 635–646, Sep. 2000.

[137] A. Ptasznik, E. Urbanowska, S. Chinta, M. A. Costa, B. A. Katz, M. A. Stanislaus, G. Demir, D. Linnekin, Z. K. Pan, and A. M. Gewirtz, “Crosstalk between BCR/ABL oncoprotein and CXCR4 signaling through a Src family kinase in human leukemia cells.,” *Journal of Experimental Medicine*, vol. 196, no. 5, pp. 667–678, Sep. 2002.

[138] B. Tomkowicz, C. Lee, V. Ravyn, R. Cheung, A. Ptasznik, and R. G. Collman, “The Src kinase Lyn is required for CCR5 signaling in response to MIP-1beta and R5 HIV-1 gp120 in human macrophages.,” *Blood*, vol. 108, no. 4, pp. 1145–1150, Aug. 2006.

[139] R. Cheung, M. Malik, V. Ravyn, B. Tomkowicz, A. Ptasznik, and R. G. Collman, “An arrestin-dependent multi-kinase signaling complex mediates MIP-1beta/CCL4 signaling and chemotaxis of primary human macrophages.,” *Journal of Leukocyte Biology*, vol. 86, no. 4, pp. 833–845, Oct. 2009.

[140] T. I. Arefieva, N. B. Kukhtina, O. A. Antonova, and T. L. Krasnikova, “MCP-1-stimulated chemotaxis of monocytic and endothelial cells is dependent on activation of different signaling cascades,” *Cytokine*, vol. 31, no. 6, pp. 439–446, Sep. 2005.

[141] J. Sai, D. Raman, Y. Liu, J. Wikswo, and A. Richmond, “Parallel phosphatidylinositol 3-kinase (PI3K)-dependent and Src-dependent pathways lead to CXCL8-mediated Rac2 activation and chemotaxis.,” *Journal of Biological Chemistry*, vol. 283, no. 39, pp. 26538–26547, Sep. 2008.

[142] L. Fumagalli, H. Zhang, A. Baruzzi, C. A. Lowell, and G. Berton, “The Src family kinases Hck and Fgr regulate neutrophil responses to N-formyl-methionyl-leucyl-phenylalanine.,” *The Journal of Immunology*, vol. 178, no. 6, pp. 3874–3885, Mar. 2007.

[143] K. Zen and Y. Liu, “Role of different protein tyrosine kinases in fMLP-induced neutrophil transmigration.,” *Immunobiology*, vol. 213, no. 1, pp. 13–23, 2008.
[144] A. Mocsai, E. Ligeti, C. A. Lowell, and G. Berton, “Adhesion-dependent degranulation of neutrophils requires the Src family kinases Fgr and Hck.,” *The Journal of Immunology*, vol. 162, no. 2, pp. 1120–1126, Jan. 1999.
[145] H. Zhang, F. Meng, C.-L. Chu, T. Takai, and C. A. Lowell, “The Src family kinases Hck and Fgr negatively regulate neutrophil and dendritic cell chemokine signaling via PIR-B.,” *Immunity*, vol. 22, no. 2, pp. 235–246, Feb. 2005.
[146] P. W. Suen, D. Ilic, E. Caveggion, G. Berton, C. H. Damsky, and C. A. Lowell, “Impaired integrin-mediated signal transduction, altered cytoskeletal structure and reduced motility in Hck/Fgr deficient macrophages.,” *Journal of Cell Science*, vol. 112, pp. 4067–4078, Nov. 1999.
[147] E. Caveggion, S. Continolo, F. J. Pixley, E. R. Stanley, D. D. L. Bowtell, C. A. Lowell, and G. Berton, “Expression and tyrosine phosphorylation of Cbl regulates macrophage chemokinetic and chemotactic movement.,” *J. Cell. Physiol.*, vol. 195, no. 2, pp. 276–289, May 2003.
[148] C. J. Fitzer-Attas, M. Lowry, M. T. Crowley, A. J. Finn, F. Meng, A. L. DeFranco, and C. A. Lowell, “Fcgamma receptor-mediated phagocytosis in macrophages lacking the Src family tyrosine kinases Hck, Fgr, and Lyn.,” *Journal of Experimental Medicine*, vol. 191, no. 4, pp. 669–682, Feb. 2000.
[149] F. Chiaradonna, L. Fontana, C. Iavarone, M. V. Carriero, G. Scholz, M. V. Barone, and M. P. Stoppelli, “Urokinase receptor-dependent and -independent p56/59(hck) activation state is a molecular switch between myelomonocytic cell motility and adherence.,” *The EMBO Journal*, vol. 18, no. 11, pp. 3013–3023, Jun. 1999.
[150] M. Ernst, M. Inglese, G. M. Scholz, K. W. Harder, F. J. Clay, S. Bozinovski, P. Waring, R. Darwiche, T. Kay, P. Sly, R. Collins, D. Turner, M. L. Hibbs, G. P. Anderson, and A. R. Dunn, “Constitutive activation of the SRC family kinase Hck results in spontaneous pulmonary inflammation and an enhanced innate immune response.,” *Journal of Experimental Medicine*, vol. 196, no. 5, pp. 589–604, Sep. 2002.
[151] A. Ptasznik, E. R. Prossnitz, D. Yoshikawa, A. Smrcka, A. E. Traynor-Kaplan, and G. M. Bokoch, “A tyrosine kinase signaling pathway accounts for the majority of phosphatidylinositol 3,4,5-trisphosphate formation in chemoattractant-stimulated human neutrophils.,” *Journal of Biological Chemistry*, vol. 271, no. 41, pp. 25204–25207, Oct. 1996.
[152] A. Ptasznik, A. Traynor-Kaplan, and G. M. Bokoch, “G protein-coupled chemoattractant receptors regulate Lyn tyrosine kinase.Shc adapter protein signaling complexes.,” *Journal of Biological Chemistry*, vol. 270, no. 34, pp. 19969–19973, Aug. 1995.
[153] S. Pereira and C. Lowell, “The Lyn tyrosine kinase negatively regulates neutrophil integrin signaling.,” *The Journal of Immunology*, vol. 171, no. 3, pp. 1319–1327, Aug. 2003.
[154] L. A. Samayawardhena, J. Hu, P. L. Stein, and A. W. B. Craig, “Fyn kinase acts upstream of Shp2 and p38 mitogen-activated protein kinase to promote chemotaxis of mast cells towards stem cell factor.,” *Cellular Signalling*, vol. 18, no. 9, pp. 1447–1454, Sep. 2006.
[155] L. A. Samayawardhena, R. Kapur, and A. W. B. Craig, “Involvement of Fyn kinase in Kit and integrin-mediated Rac activation, cytoskeletal reorganization, and chemotaxis of mast cells.,” *Blood*, vol. 109, no. 9, pp. 3679–3686, May 2007.
[156] E. Gaudreault, C. Thompson, J. Stankova, and M. Rola-Pleszczynski, “Involvement of BLT1 endocytosis and Yes kinase activation in leukotriene B4-induced neutrophil degranulation.,” *The Journal of Immunology*, vol. 174, no. 6, pp. 3617–3625, Mar. 2005.

[157] J.-C. Gevrey, B. M. Isaac, and D. Cox, “Syk is required for monocyte/macrophage chemotaxis to CX3CL1 (Fractalkine).,” *The Journal of Immunology*, vol. 175, no. 6, pp. 3737–3745, Sep. 2005.

[158] A. Tomar and D. D. Schlaepfer, “Focal adhesion kinase: switching between GAPs and GEFs in the regulation of cell motility.,” *Current Opinion in Cell Biology*, vol. 21, no. 5, pp. 676–683, Oct. 2009.

[159] Y. Calle, S. Burns, A. J. Thrasher, and G. E. Jones, “The leukocyte podosome.,” *Eur. J. Cell Biol.*, vol. 85, no. 3, pp. 151–157, Apr. 2006.

[160] M. Okigaki, C. Davis, M. Falasca, S. Harroch, D. P. Felsenfeld, M. P. Sheetz, and J. Schlessinger, “Pyk2 regulates multiple signaling events crucial for macrophage morphology and migration.,” *Proc. Natl. Acad. Sci. U.S.A.*, vol. 100, no. 19, pp. 10740–10745, Sep. 2003.

[161] K. A. Owen, F. J. Pixley, K. S. Thomas, M. Vicente-Manzanares, B. J. Ray, A. F. Horwitz, J. T. Parsons, H. E. Beggs, E. R. Stanley, and A. H. Bouton, “Regulation of lamellipodial persistence, adhesion turnover, and motility in macrophages by focal adhesion kinase.,” *The Journal of Cell Biology*, vol. 179, no. 6, pp. 1275–1287, Dec. 2007.

[162] K. A. Owen, K. S. Thomas, and A. H. Bouton, “The differential expression of Yersinia pseudotuberculosis adhesins determines the requirement for FAK and/or Pyk2 during bacterial phagocytosis by macrophages.,” *Cell. Microbiol.*, vol. 9, no. 3, pp. 596–609, Mar. 2007.

[163] A. Kasorn, P. Alcaide, Y. Jia, K. K. Subramanian, B. Sarraj, Y. Li, F. Loison, H. Hattori, L. E. Silberstein, W. F. Luscinskas, and H. R. Luo, “Focal adhesion kinase regulates pathogen-killing capability and life span of neutrophils via mediating both adhesion-dependent and -independent cellular signals.,” *J. Immunol.*, vol. 183, no. 2, pp. 1032–1043, Jul. 2009.

[164] H. Han, M. Fuortes, and C. Nathan, “Critical role of the carboxyl terminus of proline-rich tyrosine kinase (Pyk2) in the activation of human neutrophils by tumor necrosis factor: separation of signals for the respiratory burst and degranulation.,” *Journal of Experimental Medicine*, vol. 197, no. 1, pp. 63–75, Jan. 2003.

[165] M. T. Crowley, P. S. Costello, C. J. Fitzer-Attas, M. Turner, F. Meng, C. Lowell, V. L. Tybulewicz, and A. L. DeFranco, “A critical role for Syk in signal transduction and phagocytosis mediated by Fcgamma receptors on macrophages.,” *Journal of Experimental Medicine*, vol. 186, no. 7, pp. 1027–1039, Oct. 1997.

[166] O. Gross, H. Poeck, M. Bscheider, C. Dostert, N. Hannesschläger, S. Endres, G. Hartmann, A. Tardivel, E. Schweighoffer, V. Tybulewicz, A. Mócsai, J. Tschopp, and J. Ruland, “Syk kinase signalling couples to the Nlrp3 inflammasome for anti-fungal host defence.,” *Nature*, vol. 459, no. 7245, pp. 433–436, May 2009.

[167] A. Mócsai, H. Zhang, Z. Jakus, J. Kitaura, T. Kawakami, and C. A. Lowell, “G-protein-coupled receptor signaling in Syk-deficient neutrophils and mast cells.,” *Blood*, vol. 101, no. 10, pp. 4155–4163, May 2003.

[168] S. Cohen and R. Fleischmann, “Kinase inhibitors: a new approach to rheumatoid arthritis treatment.,” *Curr Opin Rheumatol*, vol. 22, no. 3, pp. 330–335, May 2010.

[169] L. Colonna, G. Catalano, C. Chew, V. D'Agati, J. W. Thomas, F. S. Wong, J. Schmitz, E. S. Masuda, B. Reizis, A. Tarakhovsky, and R. Clynes, “Therapeutic targeting of Syk in autoimmune diabetes.,” *J. Immunol.*, vol. 185, no. 3, pp. 1532–1543, Aug. 2010.

[170] S. F. Doisneau-Sixou, P. Cestac, S. Chouini, J. S. Carroll, A. D. Hamilton, S. M. Sebti, M. Poirot, P. Balaguer, J.-C. Faye, R. L. Sutherland, and G. Favre, “Contrasting effects of prenyltransferase inhibitors on estrogen-dependent cell cycle progression and estrogen receptor-mediated transcriptional activity in MCF-7 cells.,” *Endocrinology*, vol. 144, no. 3, pp. 989–998, Mar. 2003.

[171] M. E. Weinblatt, A. Kavanaugh, M. C. Genovese, T. K. Musser, E. B. Grossbard, and D. B. Magilavy, “An oral spleen tyrosine kinase (Syk) inhibitor for rheumatoid arthritis.,” *N. Engl. J. Med.*, vol. 363, no. 14, pp. 1303–1312, Sep. 2010.

[172] K. Futosi, T. Nemeth, R. Pick, T. Vantus, B. Walzog, and A. Mocsai, “Dasatinib inhibits proinflammatory functions of mature human neutrophils,” *Blood*, vol. 119, no. 21, pp. 4981–4991, May 2012.

[173] B. Vanhaesebroeck, J. Guillermet-Guibert, M. Graupera, and B. Bilanges, “The emerging mechanisms of isoform-specific PI3K signalling.,” *Nat Rev Mol Cell Biol*, vol. 11, no. 5, pp. 329–341, May 2010.

[174] J. G. Foster, M. D. Blunt, E. Carter, and S. G. Ward, “Inhibition of PI3K signaling spurs new therapeutic opportunities in inflammatory/autoimmune diseases and hematological malignancies.,” *Pharmacol. Rev.*, vol. 64, no. 4, pp. 1027–1054, Oct. 2012.

[175] W. G. Kerr, “Inhibitor and activator: dual functions for SHIP in immunity and cancer.,” *Ann. N. Y. Acad. Sci.*, vol. 1217, no. 1, pp. 1–17, Jan. 2011.

[176] M. C. Schmid, C. J. Avraamides, H. C. Dippold, I. Franco, P. Foubert, L. G. Ellies, L. M. Acevedo, J. R. E. Manglicmot, X. Song, W. Wrasidlo, S. L. Blair, M. H. Ginsberg, D. A. Cheresh, E. Hirsch, S. J. Field, and J. A. Varner, “Receptor tyrosine kinases and TLR/IL1Rs unexpectedly activate myeloid cell PI3kγ, a single convergent point promoting tumor inflammation and progression.,” *Cancer Cell*, vol. 19, no. 6, pp. 715–727, Jun. 2011.

[177] J. Guillermet-Guibert, K. Bjorklof, A. Salpekar, C. Gonella, F. Ramadani, A. Bilancio, S. Meek, A. J. H. Smith, K. Okkenhaug, and B. Vanhaesebroeck, “The p110beta isoform of phosphoinositide 3-kinase signals downstream of G protein-coupled receptors and is functionally redundant with p110gamma.,” *Proc. Natl. Acad. Sci. U.S.A.*, vol. 105, no. 24, pp. 8292–8297, Jun. 2008.

[178] S. J. Harris, R. V. Parry, J. G. Foster, M. D. Blunt, A. Wang, F. Marelli-Berg, J. Westwick, and S. G. Ward, “Evidence That the Lipid Phosphatase SHIP-1 Regulates T Lymphocyte Morphology and Motility,” *The Journal of Immunology*, vol. 186, no. 8, pp. 4936–4945, Apr. 2011.

[179] D. D. Sarbassov, D. A. Guertin, S. M. Ali, and D. M. Sabatini, “Phosphorylation and regulation of Akt/PKB by the rictor-mTOR complex.,” *Science*, vol. 307, no. 5712, pp. 1098–1101, Feb. 2005.

[180] W. G. Kerr, “A role for SHIP in stem cell biology and transplantation.,” *Curr Stem Cell Res Ther*, vol. 3, no. 2, pp. 99–106, May 2008.

[181] S. J. Harris, R. V. Parry, J. Westwick, and S. G. Ward, “Phosphoinositide Lipid Phosphatases: Natural Regulators of Phosphoinositide 3-Kinase Signaling in T Lymphocytes,” *Journal of Biological Chemistry*, vol. 283, no. 5, pp. 2465–2469, Jan. 2008.

[182] S. G. Ward, J. Westwick, and S. Harris, “Sat-Nav for T cells: Role of PI3K isoforms and lipid phosphatases in migration of T lymphocytes,” *Immunology Letters*, vol. 138, no. 1, pp. 15–18, Jul. 2011.

[183] K. D. Puri, T. A. Doggett, J. Douangpanya, Y. Hou, W. T. Tino, T. Wilson, T. Graf, E. Clayton, M. Turner, J. S. Hayflick, and T. G. Diacovo, “Mechanisms and implications of phosphoinositide 3-kinase delta in promoting neutrophil trafficking into inflamed tissue.,” *Blood*, vol. 103, no. 9, pp. 3448–3456, May 2004.

[184] C. Sadhu, B. Masinovsky, K. Dick, C. G. Sowell, and D. E. Staunton, “Essential role of phosphoinositide 3-kinase delta in neutrophil directional movement.,” *The Journal of Immunology*, vol. 170, no. 5, pp. 2647–2654, Mar. 2003.

[185] S. Kulkarni, C. Sitaru, Z. Jakus, K. E. Anderson, G. Damoulakis, K. Davidson, M. Hirose, J. Juss, D. Oxley, T. A. M. Chessa, F. Ramadani, H. Guillou, A. Segonds-Pichon, A. Fritsch, G. E. Jarvis, K. Okkenhaug, R. Ludwig, D. Zillikens, A. Mócsai, B. Vanhaesebroeck, L. R. Stephens, and P. T. Hawkins, "PI3Kβ plays a critical role in neutrophil activation by immune complexes.," *Science Signaling*, vol. 4, no. 168, pp. ra23–ra23, 2011.

[186] L. Liu, K. D. Puri, J. M. Penninger, and P. Kubes, "Leukocyte PI3Kgamma and PI3Kdelta have temporally distinct roles for leukocyte recruitment in vivo.," *Blood*, vol. 110, no. 4, pp. 1191–1198, Aug. 2007.

[187] T. M. Randis, K. D. Puri, H. Zhou, and T. G. Diacovo, "Role of PI3Kdelta and PI3Kgamma in inflammatory arthritis and tissue localization of neutrophils.," *Eur. J. Immunol.*, vol. 38, no. 5, pp. 1215–1224, May 2008.

[188] G. J. Ferguson, L. Milne, S. Kulkarni, T. Sasaki, S. Walker, S. Andrews, T. Crabbe, P. Finan, G. Jones, S. Jackson, M. Camps, C. Rommel, M. Wymann, E. Hirsch, P. Hawkins, and L. Stephens, "PI(3)Kgamma has an important context-dependent role in neutrophil chemokinesis.," *Nat Cell Biol*, vol. 9, no. 1, pp. 86–91, Jan. 2007.

[189] B. Heit, "An intracellular signaling hierarchy determines direction of migration in opposing chemotactic gradients," *The Journal of Cell Biology*, vol. 159, no. 1, pp. 91–102, Oct. 2002.

[190] S. K. Yoo, Q. Deng, P. J. Cavnar, Y. I. Wu, K. M. Hahn, and A. Huttenlocher, "Differential Regulation of Protrusion and Polarity by PI(3)K during Neutrophil Motility in Live Zebrafish," *Developmental Cell*, vol. 18, no. 2, pp. 226–236, Feb. 2010.

[191] T. L. Yuan and L. C. Cantley, "PI3K pathway alterations in cancer: variations on a theme.," *Oncogene*, vol. 27, no. 41, pp. 5497–5510, Sep. 2008.

[192] J. A. Engelman, "Targeting PI3K signalling in cancer: opportunities, challenges and limitations.," *Nat Rev Cancer*, vol. 9, no. 8, pp. 550–562, Aug. 2009.

[193] J. Ball, S. Archer, and S. Ward, "PI3K inhibitors as potential therapeutics for autoimmune disease.," *Drug Discovery Today*, Apr. 2014.

[194] W.-H. Leung, T. Tarasenko, and S. Bolland, "Differential roles for the inositol phosphatase SHIP in the regulation of macrophages and lymphocytes.," *Immunol. Res.*, vol. 43, no. 1, pp. 243–251, 2009.

[195] B. J. Lannutti, S. A. Meadows, S. E. M. Herman, A. Kashishian, B. Steiner, A. J. Johnson, J. C. Byrd, J. W. Tyner, M. M. Loriaux, M. Deininger, B. J. Druker, K. D. Puri, R. G. Ulrich, and N. A. Giese, "CAL-101, a p110delta selective phosphatidylinositol-3-kinase inhibitor for the treatment of B-cell malignancies, inhibits PI3K signaling and cellular viability.," *Blood*, vol. 117, no. 2, pp. 591–594, Jan. 2011.

[196] G. J. Brunn, J. Williams, C. Sabers, G. Wiederrecht, J. C. Lawrence, and R. T. Abraham, "Direct inhibition of the signaling functions of the mammalian target of rapamycin by the phosphoinositide 3-kinase inhibitors, wortmannin and LY294002.," *The EMBO Journal*, vol. 15, no. 19, pp. 5256–5267, Oct. 1996.

[197] D. Kong and T. Yamori, "ZSTK474 is an ATP-competitive inhibitor of class I phosphatidylinositol 3 kinase isoforms.," *Cancer Sci.*, vol. 98, no. 10, pp. 1638–1642, Oct. 2007.

[198] S. P. Jackson, S. M. Schoenwaelder, I. Goncalves, W. S. Nesbitt, C. L. Yap, C. E. Wright, V. Kenche, K. E. Anderson, S. M. Dopheide, Y. Yuan, S. A. Sturgeon, H. Prabaharan, P. E. Thompson, G. D. Smith, P. R. Shepherd, N. Daniele, S. Kulkarni, B. Abbott, D. Saylik, C. Jones, L. Lu, S. Giuliano, S. C. Hughan, J. A. Angus, A. D. Robertson, and H. H. Salem, "PI 3-kinase p110beta: a new target for antithrombotic therapy.," *Nat Med*, vol. 11, no. 5, pp. 507–514, May 2005.

[199] R. M. Sanchez, K. Erhard, M. A. Hardwicke, H. Lin, J. McSurdy-Freed, R. Plant, K. Raha, C. M. Rominger, M. D. Schaber, M. D. Spengler, M. L. Moore, H. Yu, J. I. Luengo, R. Tedesco, and R. A. Rivero, “Synthesis and structure-activity relationships of 1,2,4-triazolo[1,5-a]pyrimidin-7(3H)-ones as novel series of potent β isoform selective phosphatidylinositol 3-kinase inhibitors.,” *Bioorg. Med. Chem. Lett.*, vol. 22, no. 9, pp. 3198–3202, May 2012.

[200] A. Bilancio, K. Okkenhaug, M. Camps, J. L. Emery, T. Ruckle, C. Rommel, and B. Vanhaesebroeck, “Key role of the p110delta isoform of PI3K in B-cell antigen and IL-4 receptor signaling: comparative analysis of genetic and pharmacologic interference with p110delta function in B cells.,” *Blood*, vol. 107, no. 2, pp. 642–650, Jan. 2006.

[201] G. R. Stenton, L. F. Mackenzie, P. Tam, J. L. Cross, C. Harwig, J. Raymond, J. Toews, J. Wu, N. Ogden, T. MacRury, and C. Szabo, “Characterization of AQX-1125, a small-molecule SHIP1 activator: Part 1. Effects on inflammatory cell activation and chemotaxis in vitro and pharmacokinetic characterization in vivo.,” *Br. J. Pharmacol.*, vol. 168, no. 6, pp. 1506–1518, Mar. 2013.

[202] R. Brooks, G. M. Fuhler, S. Iyer, M. J. Smith, M.-Y. Park, K. H. T. Paraiso, R. W. Engelman, and W. G. Kerr, “SHIP1 inhibition increases immunoregulatory capacity and triggers apoptosis of hematopoietic cancer cells.,” *J. Immunol.*, vol. 184, no. 7, pp. 3582–3589, Apr. 2010.

[203] S. Etienne-Manneville and A. Hall, “Rho GTPases in cell biology.,” *Nature*, vol. 420, no. 6916, pp. 629–635, Dec. 2002.

[204] G. A. Hobbs, B. Zhou, A. D. Cox, and S. L. Campbell, “Rho GTPases, oxidation, and cell redox control.,” *Small GTPases*, vol. 5, no. 1, p. e28579, 2014.

[205] A. J. Ridley, H. F. Paterson, C. L. Johnston, D. Diekmann, and A. Hall, “The small GTP-binding protein rac regulates growth factor-induced membrane ruffling.,” *Cell*, vol. 70, no. 3, pp. 401–410, Aug. 1992.

[206] C. D. Nobes and A. Hall, “Rho, rac, and cdc42 GTPases regulate the assembly of multimolecular focal complexes associated with actin stress fibers, lamellipodia, and filopodia.,” *Cell*, vol. 81, no. 1, pp. 53–62, Apr. 1995.

[207] G. O. C. Cory and A. J. Ridley, “Cell motility: braking WAVEs.,” *Nature*, vol. 418, no. 6899, pp. 732–733, Aug. 2002.

[208] M. D. Welch and R. D. Mullins, “Cellular control of actin nucleation.,” *Annu. Rev. Cell Dev. Biol.*, vol. 18, no. 1, pp. 247–288, 2002.

[209] A. J. Ridley, M. A. Schwartz, K. Burridge, R. A. Firtel, M. H. Ginsberg, G. Borisy, J. T. Parsons, and A. R. Horwitz, “Cell migration: integrating signals from front to back.,” *Science*, vol. 302, no. 5651, pp. 1704–1709, Dec. 2003.

[210] D. W. Sawyer, J. A. Sullivan, and G. L. Mandell, “Intracellular free calcium localization in neutrophils during phagocytosis.,” *Science*, vol. 230, no. 4726, pp. 663–666, Nov. 1985.

[211] M. Camps, A. Carozzi, P. Schnabel, A. Scheer, P. J. Parker, and P. Gierschik, “Isozyme-selective stimulation of phospholipase C-beta 2 by G protein beta gamma-subunits.,” *Nature*, vol. 360, no. 6405, pp. 684–686, Dec. 1992.

[212] M. D. Bootman, “Calcium signaling.,” *Cold Spring Harbor Perspectives in Biology*, vol. 4, no. 7, pp. a011171–a011171, Jul. 2012.

[213] S. Bréchard, C. Melchior, S. Plançon, V. Schenten, and E. J. Tschirhart, “Store-operated Ca2+ channels formed by TRPC1, TRPC6 and Orai1 and non-store-operated channels formed by TRPC3 are involved in the regulation of NADPH oxidase in HL-60 granulocytes,” *Cell Calcium*, vol. 44, no. 5, pp. 492–506, Nov. 2008.

[214] Z. Li, H. Jiang, W. Xie, Z. Zhang, A. V. Smrcka, and D. Wu, “Roles of PLC-beta2 and -beta3 and PI3Kgamma in chemoattractant-mediated signal transduction.,” *Science*, vol. 287, no. 5455, pp. 1046–1049, Feb. 2000.

[215] S. Qin, T. Inazu, M. Takata, T. Kurosaki, Y. Homma, and H. Yamamura, “Cooperation of tyrosine kinases p72syk and p53/56lyn regulates calcium mobilization in chicken B cell oxidant stress signaling.,” *Eur. J. Biochem.*, vol. 236, no. 2, pp. 443–449, Mar. 1996.

[216] L. E. Hinman, G. J. Beilman, K. E. Groehler, and P. J. Sammak, “Wound-induced calcium waves in alveolar type II cells.,” *Am. J. Physiol.*, vol. 273, no. 6, pp. L1242–8, Dec. 1997.

[217] S. Shabir and J. Southgate, “Calcium signalling in wound-responsive normal human urothelial cell monolayers.,” *Cell Calcium*, vol. 44, no. 5, pp. 453–464, Nov. 2008.

[218] S. Xu and A. D. Chisholm, “A Gαq-Ca2+ Signaling Pathway Promotes Actin-Mediated Epidermal Wound Closure in C. elegans,” *Current Biology*, vol. 21, no. 23, pp. 1960–1967, Dec. 2011.

[219] S. K. Yoo, C. M. Freisinger, D. C. LeBert, and A. Huttenlocher, “Early redox, Src family kinase, and calcium signaling integrate wound responses and tissue regeneration in zebrafish,” *The Journal of Cell Biology*, vol. 199, no. 2, pp. 225–234, Oct. 2012.

[220] W. Razzell, I. R. Evans, P. Martin, and W. Wood, “Calcium flashes orchestrate the wound inflammatory response through DUOX activation and hydrogen peroxide release.,” *Curr. Biol.*, vol. 23, no. 5, pp. 424–429, Mar. 2013.

[221] K. Paemeleire, P. E. Martin, S. L. Coleman, K. E. Fogarty, W. A. Carrington, L. Leybaert, R. A. Tuft, W. H. Evans, and M. J. Sanderson, “Intercellular calcium waves in HeLa cells expressing GFP-labeled connexin 43, 32, or 26.,” *Molecular Biology of the Cell*, vol. 11, no. 5, pp. 1815–1827, May 2000.

[222] P. De Smet, J. B. Parys, G. Callewaert, A. F. Weidema, E. Hill, H. De Smedt, C. Erneux, V. Sorrentino, and L. Missiaen, “Xestospongin C is an equally potent inhibitor of the inositol 1,4,5-trisphosphate receptor and the endoplasmic-reticulum Ca(2+) pumps.,” *Cell Calcium*, vol. 26, no. 1, pp. 9–13, Jul. 1999.

[223] M. Treiman, C. Caspersen, and S. B. Christensen, “A tool coming of age: thapsigargin as an inhibitor of sarco-endoplasmic reticulum Ca(2+)-ATPases.,” *Trends Pharmacol. Sci.*, vol. 19, no. 4, pp. 131–135, Apr. 1998.

[224] P. Nicotera, G. Bellomo, and S. Orrenius, “Calcium-mediated mechanisms in chemically induced cell death.,” *Annu. Rev. Pharmacol. Toxicol.*, vol. 32, no. 1, pp. 449–470, 1992.

[225] M. Sixt, “Interstitial locomotion of leukocytes.,” *Immunology Letters*, vol. 138, no. 1, pp. 32–34, Jul. 2011.

[226] S. Massberg, P. Schaerli, I. Knezevic-Maramica, M. Köllnberger, N. Tubo, E. A. Moseman, I. V. Huff, T. Junt, A. J. Wagers, I. B. Mazo, and U. H. von Andrian, “Immunosurveillance by hematopoietic progenitor cells trafficking through blood, lymph, and peripheral tissues.,” *Cell*, vol. 131, no. 5, pp. 994–1008, Nov. 2007.

[227] E. Metchnikoff, *Lectures on the Comparative Pathology of Inflammation.* London: Kegan Paul, Trench, Trubner & Co. Ltd, 1893.

[228] G. Reig, E. Pulgar, and M. L. Concha, “Cell migration: from tissue culture to embryos.,” *Development*, vol. 141, no. 10, pp. 1999–2013, May 2014.

[229] R. Majumdar, M. Sixt, and C. A. Parent, “New paradigms in the establishment and maintenance of gradients during directed cell migration.,” *Current Opinion in Cell Biology*, vol. 30, pp. 33–40, Jun. 2014.

[230] M. Weber, R. Hauschild, J. Schwarz, C. Moussion, I. de Vries, D. F. Legler, S. A. Luther, T. Bollenbach, and M. Sixt, “Interstitial dendritic cell guidance by haptotactic chemokine gradients.,” *Science*, vol. 339, no. 6117, pp. 328–332, Jan. 2013.

[231] B. McDonald and P. Kubes, “Chemokines: sirens of neutrophil recruitment-but is it just one song?,” *Immunity*, vol. 33, no. 2, pp. 148–149, Aug. 2010.

[232] T. Lämmermann, P. V. Afonso, B. R. Angermann, J. M. Wang, W. Kastenmüller, C. A. Parent, and R. N. Germain, “Neutrophil swarms require LTB4 and integrins at sites of cell death in vivo ,” *Nature*, pp. 1–7, May 2013.

[233] P. Niethammer, C. Grabher, A. T. Look, and T. J. Mitchison, “A tissue-scale gradient of hydrogen peroxide mediates rapid wound detection in zebrafish,” *Nature*, vol. 459, no. 7249, pp. 996–999, Jun. 2009.

[234] G. Helmlinger, F. Yuan, M. Dellian, and R. K. Jain, “Interstitial pH and pO2 gradients in solid tumors in vivo: high-resolution measurements reveal a lack of correlation.,” *Nat Med*, vol. 3, no. 2, pp. 177–182, Feb. 1997.

[235] F. Wang, “The Signaling Mechanisms Underlying Cell Polarity and Chemotaxis,” *Cold Spring Harbor Perspectives in Biology*, vol. 1, no. 4, pp. a002980–a002980, Oct. 2009.

[236] K. F. Swaney, C.-H. Huang, and P. N. Devreotes, “Eukaryotic chemotaxis: a network of signaling pathways controls motility, directional sensing, and polarity.,” *Annu Rev Biophys*, vol. 39, no. 1, pp. 265–289, 2010.

[237] R. H. Insall, “Understanding eukaryotic chemotaxis: a pseudopod-centred view.,” *Nat Rev Mol Cell Biol*, vol. 11, no. 6, pp. 453–458, Jun. 2010.

[238] A. R. Houk, A. Jilkine, C. O. Mejean, R. Boltyanskiy, E. R. Dufresne, S. B. Angenent, S. J. Altschuler, L. F. Wu, and O. D. Weiner, “Membrane tension maintains cell polarity by confining signals to the leading edge during neutrophil migration.,” *Cell*, vol. 148, no. 1, pp. 175–188, Jan. 2012.

[239] M. C. Weiger and C. A. Parent, “Phosphoinositides in chemotaxis.,” *Subcell. Biochem.*, vol. 59, pp. 217–254, 2012.

[240] S. Etienne-Manneville and A. Hall, “Integrin-mediated activation of Cdc42 controls cell polarity in migrating astrocytes through PKCzeta.,” *Cell*, vol. 106, no. 4, pp. 489–498, Aug. 2001.

[241] K. Riento and A. J. Ridley, “Rocks: multifunctional kinases in cell behaviour.,” *Nat Rev Mol Cell Biol*, vol. 4, no. 6, pp. 446–456, Jun. 2003.

[242] M. Vicente-Manzanares, C. K. Choi, and A. R. Horwitz, “Integrins in cell migration--the actin connection.,” *Journal of Cell Science*, vol. 122, no. 2, pp. 199–206, Jan. 2009.

[243] F. P. L. Lai, M. Szczodrak, J. Block, J. Faix, D. Breitsprecher, H. G. Mannherz, T. E. B. Stradal, G. A. Dunn, J. V. Small, and K. Rottner, “Arp2/3 complex interactions and actin network turnover in lamellipodia.,” *The EMBO Journal*, vol. 27, no. 7, pp. 982–992, Apr. 2008.

[244] J. Renkawitz, K. Schumann, M. Weber, T. Lämmermann, H. Pflicke, M. Piel, J. Polleux, J. P. Spatz, and M. Sixt, “Adaptive force transmission in amoeboid cell migration.,” *Nat Cell Biol*, vol. 11, no. 12, pp. 1438–1443, Dec. 2009.

[245] E. Paluch, M. Piel, J. Prost, M. Bornens, and C. Sykes, “Cortical actomyosin breakage triggers shape oscillations in cells and cell fragments.,” *Biophys. J.*, vol. 89, no. 1, pp. 724–733, Jul. 2005.

[246] R. J. Hawkins, M. Piel, G. Faure-Andre, A. M. Lennon-Dumenil, J. F. Joanny, J. Prost, and R. Voituriez, “Pushing off the walls: a mechanism of cell motility in confinement.,” *Phys. Rev. Lett.*, vol. 102, no. 5, p. 058103, Feb. 2009.

[247] J. Werr, X. Xie, P. Hedqvist, E. Ruoslahti, and L. Lindbom, “beta1 integrins are critically involved in neutrophil locomotion in extravascular tissue In vivo.,” *Journal of Experimental Medicine*, vol. 187, no. 12, pp. 2091–2096, Jun. 1998.

[248] J. Renkawitz and M. Sixt, “Mechanisms of force generation and force transmission during interstitial leukocyte migration.,” *EMBO Rep*, vol. 11, no. 10, pp. 744–750, Oct. 2010.

[249] M. Phillipson and P. Kubes, “The neutrophil in vascular inflammation.,” *Nat Med*, vol. 17, no. 11, pp. 1381–1390, 2011.

[250] R. Pankov, Y. Endo, S. Even-Ram, M. Araki, K. Clark, E. Cukierman, K. Matsumoto, and K. M. Yamada, “A Rac switch regulates random versus directionally persistent cell migration.,” *The Journal of Cell Biology*, vol. 170, no. 5, pp. 793–802, Aug. 2005.

[251] S. Woo, M. P. Housley, O. D. Weiner, and D. Y. R. Stainier, “Nodal signaling regulates endodermal cell motility and actin dynamics via Rac1 and Prex1.,” *The Journal of Cell Biology*, vol. 198, no. 5, pp. 941–952, Sep. 2012.

[252] R. J. Petrie, A. D. Doyle, and K. M. Yamada, “Random versus directionally persistent cell migration.,” *Nat Rev Mol Cell Biol*, vol. 10, no. 8, pp. 538–549, Aug. 2009.

[253] B. Geiger and K. M. Yamada, “Molecular architecture and function of matrix adhesions.,” *Cold Spring Harbor Perspectives in Biology*, vol. 3, no. 5, pp. a005033–a005033, May 2011.

[254] R. J. Pelham and Y. L. Wang, “Cell locomotion and focal adhesions are regulated by substrate flexibility.,” *Proc. Natl. Acad. Sci. U.S.A.*, vol. 94, no. 25, pp. 13661–13665, Dec. 1997.

[255] M. Bokstad, H. Sabanay, I. Dahan, B. Geiger, and O. Medalia, “Reconstructing adhesion structures in tissues by cryo-electron tomography of vitrified frozen sections.,” *J. Struct. Biol.*, vol. 178, no. 2, pp. 76–83, May 2012.

[256] T. Lämmermann, B. L. Bader, S. J. Monkley, T. Worbs, R. Wedlich-Söldner, K. Hirsch, M. Keller, R. Förster, D. R. Critchley, R. Fässler, and M. Sixt, “Rapid leukocyte migration by integrin-independent flowing and squeezing.,” *Nature*, vol. 453, no. 7191, pp. 51–55, May 2008.

[257] W. S. Haston, J. M. Shields, and P. C. Wilkinson, “Lymphocyte locomotion and attachment on two-dimensional surfaces and in three-dimensional matrices.,” *The Journal of Cell Biology*, vol. 92, no. 3, pp. 747–752, Mar. 1982.

[258] P. Friedl, P. B. Noble, and K. S. Zänker, “T lymphocyte locomotion in a three-dimensional collagen matrix. Expression and function of cell adhesion molecules.,” *The Journal of Immunology*, vol. 154, no. 10, pp. 4973–4985, May 1995.

[259] P. Friedl, F. Entschladen, C. Conrad, B. Niggemann, and K. S. Zänker, “CD4+ T lymphocytes migrating in three-dimensional collagen lattices lack focal adhesions and utilize beta1 integrin-independent strategies for polarization, interaction with collagen fibers and locomotion.,” *Eur. J. Immunol.*, vol. 28, no. 8, pp. 2331–2343, Aug. 1998.

[260] K. B. Walters, J. M. Green, J. C. Surfus, S. K. Yoo, and A. Huttenlocher, “Live imaging of neutrophil motility in a zebrafish model of WHIM syndrome.,” *Blood*, vol. 116, no. 15, pp. 2803–2811, Oct. 2010.

[261] Q. Deng and A. Huttenlocher, “Leukocyte migration from a fish eye's view,” *Journal of Cell Science*, vol. 125, no. 17, pp. 3949–3956, Oct. 2012.

[262] G. J. Lieschke and N. S. Trede, “Fish immunology.,” *Curr. Biol.*, vol. 19, no. 16, pp. R678–82, Aug. 2009.

[263] G. J. Lieschke, A. C. Oates, M. O. Crowhurst, A. C. Ward, and J. E. Layton, “Morphologic and functional characterization of granulocytes and macrophages in embryonic and adult zebrafish.,” *Blood*, vol. 98, no. 10, pp. 3087–3096, Nov. 2001.

[264] P. A. Morcos, “Achieving targeted and quantifiable alteration of mRNA splicing with Morpholino oligos.,” *Biochemical and Biophysical Research Communications*, vol. 358, no. 2, pp. 521–527, Jun. 2007.

[265] S. A. Renshaw, C. A. Loynes, D. M. I. Trushell, S. Elworthy, P. W. Ingham, and M. K. B. Whyte, “A transgenic zebrafish model of neutrophilic inflammation.,” *Blood*, vol. 108, no. 13, pp. 3976–3978, Dec. 2006.

[266] S. K. Yoo and A. Huttenlocher, “Spatiotemporal photolabeling of neutrophil trafficking during inflammation in live zebrafish.,” *Journal of Leukocyte Biology*, vol. 89, no. 5, pp. 661–667, May 2011.

[267] F. Ellett, L. Pase, J. W. Hayman, A. Andrianopoulos, and G. J. Lieschke, “mpeg1 promoter transgenes direct macrophage-lineage expression in zebrafish.,” *Blood*, vol. 117, no. 4, pp. e49–56, Jan. 2011.

[268] I. R. Evans and W. Wood, “Drosophila embryonic hemocytes,” *Current Biology*, vol. 21, no. 5, pp. R173–R174, Mar. 2011.

[269] W. Wood, “Distinct mechanisms regulate hemocyte chemotaxis during development and wound healing in Drosophila melanogaster,” *The Journal of Cell Biology*, vol. 173, no. 3, pp. 405–416, May 2006.

[270] S. Moreira, B. Stramer, I. Evans, W. Wood, and P. Martin, “Prioritization of Competing Damage and Developmental Signals by Migrating Macrophages in the Drosophila Embryo,” *Current Biology*, vol. 20, no. 5, pp. 464–470, Mar. 2010.

[271] B. Stramer, “Live imaging of wound inflammation in Drosophila embryos reveals key roles for small GTPases during in vivo cell migration,” *The Journal of Cell Biology*, vol. 168, no. 4, pp. 567–573, Feb. 2005.

[272] M. L. Orozco-Cárdenas, J. Narváez-Vásquez, and C. A. Ryan, “Hydrogen peroxide acts as a second messenger for the induction of defense genes in tomato plants in response to wounding, systemin, and methyl jasmonate.,” *Plant Cell*, vol. 13, no. 1, pp. 179–191, Jan. 2001.

[273] S. Roy, S. Khanna, K. Nallu, T. K. Hunt, and C. K. Sen, “Dermal wound healing is subject to redox control.,” *Mol. Ther.*, vol. 13, no. 1, pp. 211–220, Jan. 2006.

[274] Y. Feng, C. Santoriello, M. Mione, A. Hurlstone, and P. Martin, “Live Imaging of Innate Immune Cell Sensing of Transformed Cells in Zebrafish Larvae: Parallels between Tumor Initiation and Wound Inflammation,” *PLoS Biol*, vol. 8, no. 12, p. e1000562, Dec. 2010.

[275] S. de Oliveira, A. López-Muñoz, S. Candel, P. Pelegrín, Â. Calado, and V. Mulero, “ATP modulates acute inflammation in vivo through dual oxidase 1-derived H2O2 production and NF-κB activation.,” *J. Immunol.*, vol. 192, no. 12, pp. 5710–5719, Jun. 2014.

[276] V. V. Belousov, A. F. Fradkov, K. A. Lukyanov, D. B. Staroverov, K. S. Shakhbazov, A. V. Terskikh, and S. Lukyanov, “Genetically encoded fluorescent indicator for intracellular hydrogen peroxide.,” *Nat. Methods*, vol. 3, no. 4, pp. 281–286, Apr. 2006.

[277] J. Kwon, S.-R. Lee, K.-S. Yang, Y. Ahn, Y. J. Kim, E. R. Stadtman, and S. G. Rhee, “Reversible oxidation and inactivation of the tumor suppressor PTEN in cells stimulated with peptide growth factors.,” *Proc. Natl. Acad. Sci. U.S.A.*, vol. 101, no. 47, pp. 16419–16424, Nov. 2004.

[278] M. T. Juarez, R. A. Patterson, E. Sandoval-Guillen, and W. McGinnis, “Duox, Flotillin-2, and Src42A Are Required to Activate or Delimit the Spread of the Transcriptional Response to Epidermal Wounds in Drosophila,” *PLoS Genet*, vol. 7, no. 12, p. e1002424, Dec. 2011.

[279] L. Pase, J. E. Layton, C. Wittmann, F. Ellett, C. J. Nowell, C. C. Reyes-Aldasoro, S. Varma, K. L. Rogers, C. J. Hall, M. C. Keightley, P. S. Crosier, C. Grabher, J. K. Heath, S. A. Renshaw, and G. J. Lieschke, “Neutrophil-Delivered Myeloperoxidase Dampens the Hydrogen Peroxide Burst after Tissue Wounding in Zebrafish,” *Current Biology*, pp. 1–7, Aug. 2012.

[280] J. L. Koff, M. X. G. Shao, I. F. Ueki, and J. A. Nadel, “Multiple TLRs activate EGFR via a signaling cascade to produce innate immune responses in airway epithelium.,” *Am. J. Physiol. Lung Cell Mol. Physiol.*, vol. 294, no. 6, pp. L1068–75, Jun. 2008.

[281] Q. Deng, E. A. Harvie, and A. Huttenlocher, “Distinct signalling mechanisms mediate neutrophil attraction to bacterial infection and tissue injury.,” *Cell. Microbiol.*, vol. 14, no. 4, pp. 517–528, Apr. 2012.

[282] S. K. Yoo, T. W. Starnes, Q. Deng, and A. Huttenlocher, “Lyn is a redox sensor that mediates leukocyte wound attraction in vivo,” *Nature*, vol. 480, no. 7375, pp. 109–112, Nov. 2011.

[283] C. M. Pleiman, W. M. Hertz, and J. C. Cambier, “Activation of phosphatidylinositol-3' kinase by Src-family kinase SH3 binding to the p85 subunit.,” *Science*, vol. 263, no. 5153, pp. 1609–1612, Mar. 1994.

[284] J. Savill, I. Dransfield, C. Gregory, and C. Haslett, “A blast from the past: clearance of apoptotic cells regulates immune responses.,” *Nature Reviews Immunology*, vol. 2, no. 12, pp. 965–975, Dec. 2002.

[285] T. Kuraishi, Y. Nakagawa, K. Nagaosa, Y. Hashimoto, T. Ishimoto, T. Moki, Y. Fujita, H. Nakayama, N. Dohmae, A. Shiratsuchi, N. Yamamoto, K. Ueda, M. Yamaguchi, T. Awasaki, and Y. Nakanishi, “Pretaporter, a Drosophila protein serving as a ligand for Draper in the phagocytosis of apoptotic cells,” *The EMBO Journal*, vol. 28, no. 24, pp. 3868–3878, Nov. 2009.

[286] Y. Hashimoto, Y. Tabuchi, K. Sakurai, M. Kutsuna, K. Kurokawa, T. Awasaki, K. Sekimizu, Y. Nakanishi, and A. Shiratsuchi, “Identification of lipoteichoic acid as a ligand for draper in the phagocytosis of Staphylococcus aureus by Drosophila hemocytes.,” *J. Immunol.*, vol. 183, no. 11, pp. 7451–7460, Dec. 2009.

[287] J. S. Ziegenfuss, R. Biswas, M. A. Avery, K. Hong, A. E. Sheehan, Y.-G. Yeung, E. R. Stanley, and M. R. Freeman, “Draper-dependent glial phagocytic activity is mediated by Src and Syk family kinase signalling,” *Nature*, vol. 453, no. 7197, pp. 935–939, Apr. 2008.

[288] H. Aldskogius and E. N. Kozlova, “Central neuron-glial and glial-glial interactions following axon injury.,” *Prog. Neurobiol.*, vol. 55, no. 1, pp. 1–26, May 1998.

[289] R. Fernandez, F. Takahashi, Z. Liu, R. Steward, D. Stein, and E. R. Stanley, “The Drosophila shark tyrosine kinase is required for embryonic dorsal closure.,” *Genes Dev.*, vol. 14, no. 5, pp. 604–614, Mar. 2000.

[290] A. W. Ferrante, R. Reinke, and E. R. Stanley, “Shark, a Src homology 2, ankyrin repeat, tyrosine kinase, is expressed on the apical surfaces of ectodermal epithelia.,” *Proc. Natl. Acad. Sci. U.S.A.*, vol. 92, no. 6, pp. 1911–1915, Mar. 1995.

[291] C. C. Winterbourn, “Reconciling the chemistry and biology of reactive oxygen species,” *Nat Chem Biol*, vol. 4, no. 5, pp. 278–286, May 2008.

[292] O. Sareila, T. Kelkka, A. Pizzolla, H. M, and R. Holmdahl, “NOX2 Complex–Derived ROS as Immune Regulators,” *Antioxidants Redox Signaling*, vol. 15, no. 8, pp. 2197–2208, Aug. 2011.

[293] C. C. Winterbourn, “Free-Radical Production and Oxidative Reactions of Hemoglobin,” *Environmental Health Perspectives*, vol. 64, pp. 321–330, 1985.

[294] R. Ameziane-El-Hassani, “Dual Oxidase-2 Has an Intrinsic Ca2+-dependent H2O2-generating Activity,” *Journal of Biological Chemistry*, vol. 280, no. 34, pp. 30046–30054, Jul. 2005.

[295] C. Wittmann, P. Chockley, S. K. Singh, L. Pase, G. J. Lieschke, and C. Grabher, “Hydrogen Peroxide in Inflammation: Messenger, Guide, and Assassin,” *Advances in Hematology*, vol. 2012, no. 2, pp. 1–6, 2012.

[296] M. Hultqvist, L. M. Olsson, K. A. Gelderman, and R. Holmdahl, “The protective role of ROS in autoimmune disease.,” *Trends in Immunology*, vol. 30, no. 5, pp. 201–208, May 2009.

[297] O. N. Oktyabrsky and G. V. Smirnova, “Redox regulation of cellular functions.,” *Biochemistry Mosc.*, vol. 72, no. 2, pp. 132–145, Feb. 2007.

[298] M. P. Granados, G. M. Salido, J. A. Pariente, and A. González, “Generation of ROS in response to CCK-8 stimulation in mouse pancreatic acinar cells.,” *Mitochondrion*, vol. 3, no. 5, pp. 285–296, Apr. 2004.

[299] J. A. Rosado, P. C. Redondo, G. M. Salido, E. Gómez-Arteta, S. O. Sage, and J. A. Pariente, “Hydrogen peroxide generation induces pp60src activation in human platelets: evidence for the involvement of this pathway in store-mediated calcium entry.,” *Journal of Biological Chemistry*, vol. 279, no. 3, pp. 1665–1675, Jan. 2004.

[300] S. G. Rhee, Y. S. Bae, S. R. Lee, and J. Kwon, “Hydrogen Peroxide: A Key Messenger That Modulates Protein Phosphorylation Through Cysteine Oxidation,” *Science Signaling*, vol. 2000, no. 53, pp. pe1–pe1, Oct. 2000.

[301] J. Fetrow, N. Siew, and J. Skolnick, “Structure-based functional motif identifies a potential disulfide oxidoreductase active site in the serine/ threonine protein phosphatase-1 subfamily,” *FASEB*, vol. 13, pp. 1866–1874, Sep. 1999.

[302] Y. S. Bae, S. W. Kang, M. S. Seo, I. C. Baines, E. Tekle, P. B. Chock, and S. G. Rhee, “Epidermal Growth Factor (EGF)-induced Generation of Hydrogen Peroxide. ROLE IN EGF RECEPTOR-MEDIATED TYROSINE PHOSPHORYLATION,” *Journal of Biological Chemistry*, vol. 272, no. 1, pp. 217–221, Jan. 1997.

[303] M. Yoshizumi, J. Abe, J. Haendeler, Q. Huang, and B. C. Berk, “Src and Cas mediate JNK activation but not ERK1/2 and p38 kinases by reactive oxygen species.,” *Journal of Biological Chemistry*, vol. 275, no. 16, pp. 11706–11712, Apr. 2000.

[304] M. J. Davies, “The oxidative environment and protein damage.,” *Biochim. Biophys. Acta*, vol. 1703, no. 2, pp. 93–109, Jan. 2005.

[305] A. Corcoran and T. G. Cotter, “Redox regulation of protein kinases.,” *FEBS J.*, vol. 280, no. 9, pp. 1944–1965, May 2013.

[306] Y. M. W. Janssen-Heininger, B. T. Mossman, N. H. Heintz, H. J. Forman, B. Kalyanaraman, T. Finkel, J. S. Stamler, S. G. Rhee, and A. van der Vliet, “Redox-based regulation of signal transduction: principles, pitfalls, and promises.,” *Free Radical Biology and Medicine*, vol. 45, no. 1, pp. 1–17, Jul. 2008.

[307] A. Ostman, J. Frijhoff, A. Sandin, and F.-D. Böhmer, “Regulation of protein tyrosine phosphatases by reversible oxidation.,” *J. Biochem.*, vol. 150, no. 4, pp. 345–356, Oct. 2011.

[308] L. B. Poole and K. J. Nelson, “Discovering mechanisms of signaling-mediated cysteine oxidation,” *Current Opinion in Chemical Biology*, vol. 12, no. 1, pp. 18–24, Feb. 2008.

[309] J. M. Denu and J. E. Dixon, “Protein tyrosine phosphatases: mechanisms of catalysis and regulation.,” *Current Opinion in Chemical Biology*, vol. 2, no. 5, pp. 633–641, Oct. 1998.

[310] S. R. Lee, K. S. Kwon, S. R. Kim, and S. G. Rhee, “Reversible inactivation of protein-tyrosine phosphatase 1B in A431 cells stimulated with epidermal growth factor.,” *Journal of Biological Chemistry*, vol. 273, no. 25, pp. 15366–15372, Jun. 1998.

[311] J. M. Denu and K. G. Tanner, “Specific and reversible inactivation of protein tyrosine phosphatases by hydrogen peroxide: evidence for a sulfenic acid intermediate and implications for redox regulation.,” *Biochemistry*, vol. 37, no. 16, pp. 5633–5642, Apr. 1998.

[312] J. M. Cunnick, J. F. Dorsey, L. Mei, and J. Wu, “Reversible regulation of SHP-1 tyrosine phosphatase activity by oxidation.,” *Biochem. Mol. Biol. Int.*, vol. 45, no. 5, pp. 887–894, Aug. 1998.

[313] T. H. Truong and K. S. Carroll, “Redox regulation of protein kinases.,” *Crit. Rev. Biochem. Mol. Biol.*, vol. 48, no. 4, pp. 332–356, Jul. 2013.

[314] J. Heo, “Redox control of GTPases: from molecular mechanisms to functional significance in health and disease.,” *Antioxid. Redox Signal.*, vol. 14, no. 4, pp. 689–724, Feb. 2011.

[315] R. P. Guttmann and S. Ghoshal, “Thiol-protease oxidation in age-related neuropathology.,” *Free Radical Biology and Medicine*, vol. 51, no. 2, pp. 282–288, Jul. 2011.

[316] I. Nakashima, M. Kato, A. A. Akhand, H. Suzuki, K. Takeda, K. Hossain, and Y. Kawamoto, “Redox-linked signal transduction pathways for protein tyrosine kinase activation.,” *Antioxid. Redox Signal.*, vol. 4, no. 3, pp. 517–531, Jun. 2002.

[317] K. M. Humphries, M. S. Deal, and S. S. Taylor, “Enhanced dephosphorylation of cAMP-dependent protein kinase by oxidation and thiol modification.,” *Journal of Biological Chemistry*, vol. 280, no. 4, pp. 2750–2758, Jan. 2005.

[318] Y.-J. Lee, H.-N. Cho, J.-W. Soh, G. J. Jhon, C.-K. Cho, H.-Y. Chung, S. Bae, S.-J. Lee, and Y.-S. Lee, “Oxidative stress-induced apoptosis is mediated by ERK1/2 phosphorylation.,” *Exp. Cell Res.*, vol. 291, no. 1, pp. 251–266, Nov. 2003.

[319] V. V. Sumbayev and I. M. Yasinska, “Regulation of MAP kinase-dependent apoptotic pathway: implication of reactive oxygen and nitrogen species.,” *Archives of Biochemistry and Biophysics*, vol. 436, no. 2, pp. 406–412, Apr. 2005.

[320] S. Galli, V. G. Antico Arciuch, C. Poderoso, D. P. Converso, Q. Zhou, E. Bal de Kier Joffé, E. Cadenas, J. Boczkowski, M. C. Carreras, and J. J. Poderoso, “Tumor cell phenotype is sustained by selective MAPK oxidation in mitochondria.,” *PLoS ONE*, vol. 3, no. 6, p. e2379, 2008.

[321] Y. S. Bae, H. Oh, S. G. Rhee, and Y. D. Yoo, “Regulation of reactive oxygen species generation in cell signaling,” *Mol Cells*, vol. 32, no. 6, pp. 491–509, Dec. 2011.

[322] Y. S. Bae, J. Y. Sung, O. S. Kim, Y. J. Kim, K. C. Hur, A. Kazlauskas, and S. G. Rhee, “Platelet-derived growth factor-induced H(2)O(2) production requires the activation of phosphatidylinositol 3-kinase.,” *Journal of Biological Chemistry*, vol. 275, no. 14, pp. 10527–10531, Apr. 2000.

[323] I. Bejarano, M. P. Terrón, S. D. Paredes, C. Barriga, A. B. Rodríguez, and J. A. Pariente, “Hydrogen peroxide increases the phagocytic function of human neutrophils by calcium mobilisation.,” *Mol. Cell. Biochem.*, vol. 296, no. 1, pp. 77–84, Feb. 2007.

[324] S. K. Lo, K. Janakidevi, L. Lai, and A. B. Malik, “Hydrogen peroxide-induced increase in endothelial adhesiveness is dependent on ICAM-1 activation.,” *Am. J. Physiol.*, vol. 264, no. 4, pp. L406–12, Apr. 1993.

[325] I. V. Klyubin, K. M. Kirpichnikova, and I. A. Gamaley, “Hydrogen peroxide-induced chemotaxis of mouse peritoneal neutrophils.,” *Eur. J. Cell Biol.*, vol. 70, no. 4, pp. 347–351, Aug. 1996.

[326] H. Nakamura, L. A. Herzenberg, J. Bai, S. Araya, N. Kondo, Y. Nishinaka, and J. Yodoi, “Circulating thioredoxin suppresses lipopolysaccharide-induced neutrophil chemotaxis.,” *Proc. Natl. Acad. Sci. U.S.A.*, vol. 98, no. 26, pp. 15143–15148, Dec. 2001.

[327] E. W. Miller, B. C. Dickinson, and C. J. Chang, “Aquaporin-3 mediates hydrogen peroxide uptake to regulate downstream intracellular signaling.,” *Proc. Natl. Acad. Sci. U.S.A.*, vol. 107, no. 36, pp. 15681–15686, Sep. 2010.

[328] M. Hara-Chikuma, S. Chikuma, Y. Sugiyama, K. Kabashima, A. S. Verkman, S. Inoue, and Y. Miyachi, “Chemokine-dependent T cell migration requires aquaporin-3-mediated hydrogen peroxide uptake,” *Journal of Experimental Medicine*, vol. 209, no. 10, pp. 1743–1752, Sep. 2012.

[329] E. Giannoni, M. L. Taddei, and P. Chiarugi, “Src redox regulation: again in the front line.,” *Free Radical Biology and Medicine*, vol. 49, no. 4, pp. 516–527, Aug. 2010.

[330] K. Nakamura, T. Hori, N. Sato, K. Sugie, T. Kawakami, and J. Yodoi, “Redox regulation of a src family protein tyrosine kinase p56lck in T cells.,” *Oncogene*, vol. 8, no. 11, pp. 3133–3139, Nov. 1993.

[331] S. Rigutto, C. Hoste, H. Grasberger, M. Milenkovic, D. Communi, J. E. Dumont, B. Corvilain, F. Miot, and X. De Deken, “Activation of dual oxidases Duox1 and Duox2: differential regulation mediated by camp-dependent protein kinase and protein kinase C-dependent phosphorylation.,” *Journal of Biological Chemistry*, vol. 284, no. 11, pp. 6725–6734, Mar. 2009.

[332] X. Wang, S. Takeda, S. Mochizuki, R. Jindal, and N. Dhalla, “Mechanisms of Hydrogen Peroxide-Induced Increase in Intracellular Calcium in Cardiomyocytes.,” *J. Cardiovasc. Pharmacol. Ther.*, vol. 4, no. 1, pp. 41–48, Jan. 1999.

[333] P. Krippeit-Drews, C. Haberland, J. Fingerle, G. Drews, and F. Lang, “Effects of H2O2 on membrane potential and [Ca2+]i of cultured rat arterial smooth muscle cells.,” *Biochemical and Biophysical Research Communications*, vol. 209, no. 1, pp. 139–145, Apr. 1995.

[334] A. Korzets, A. Chagnac, T. Weinstein, Y. Ori, T. Malachi, and U. Gafter, “H2O2 induces DNA repair in mononuclear cells: evidence for association with cytosolic Ca2+ fluxes.,” *J. Lab. Clin. Med.*, vol. 133, no. 4, pp. 362–369, Apr. 1999.

[335] P. S. Herson, K. Lee, R. D. Pinnock, J. Hughes, and M. L. Ashford, “Hydrogen peroxide induces intracellular calcium overload by activation of a non-selective cation channel in an insulin-secreting cell line.,” *Journal of Biological Chemistry*, vol. 274, no. 2, pp. 833–841, Jan. 1999.

[336] A. Mata, D. Marques, M. A. Martínez-Burgos, J. Silveira, J. Marques, M. F. Mesquita, J. A. Pariente, G. M. Salido, and J. Singh, “Effect of hydrogen peroxide on secretory response, calcium mobilisation and caspase-3 activity in the isolated rat parotid gland.,” *Mol. Cell. Biochem.*, vol. 319, no. 1, pp. 23–31, Dec. 2008.

[337] V. H. Moreau, R. F. Castilho, S. T. Ferreira, and P. C. Carvalho-Alves, “Oxidative damage to sarcoplasmic reticulum Ca2+-ATPase AT submicromolar iron concentrations: evidence for metal-catalyzed oxidation.,” *Free Radical Biology and Medicine*, vol. 25, no. 4, pp. 554–560, Sep. 1998.

[338] J. A. Pariente, C. Camello, P. J. Camello, and G. M. Salido, “Release of calcium from mitochondrial and nonmitochondrial intracellular stores in mouse pancreatic acinar cells by hydrogen peroxide.,” *J. Membr. Biol.*, vol. 179, no. 1, pp. 27–35, Jan. 2001.

[339] J. D. Lambeth, K.-H. Krause, and R. A. Clark, “NOX enzymes as novel targets for drug development.,” *Semin Immunopathol*, vol. 30, no. 3, pp. 339–363, Jul. 2008.

[340] L. I. Filippin, R. Vercelino, N. P. Marroni, and R. M. Xavier, “Redox signalling and the inflammatory response in rheumatoid arthritis.,” *Clin Exp Immunol*, vol. 152, no. 3, pp. 415–422, Jun. 2008.

[341] Y. Gilgun-Sherki, E. Melamed, and D. Offen, “The role of oxidative stress in the pathogenesis of multiple sclerosis: the need for effective antioxidant therapy.,” *J. Neurol.*, vol. 251, no. 3, pp. 261–268, Mar. 2004.

[342] C. L. Burek and N. R. Rose, “Autoimmune thyroiditis and ROS.,” *Autoimmun Rev*, vol. 7, no. 7, pp. 530–537, Jul. 2008.

[343] J. Chen, A. M. Gusdon, T. C. Thayer, and C. E. Mathews, “Role of increased ROS dissipation in prevention of T1D.,” *Ann. N. Y. Acad. Sci.*, vol. 1150, no. 1, pp. 157–166, Dec. 2008.

[344] K. Murata, K. Fujimoto, Y. Kitaguchi, T. Horiuchi, K. Kubo, and T. Honda, “Hydrogen peroxide content and pH of expired breath condensate from patients with asthma and COPD.,” *COPD*, vol. 11, no. 1, pp. 81–87, Feb. 2014.

[345] W. Yang, L. Zou, C. Huang, and Y. Lei, “Redox Regulation of Cancer Metastasis: Molecular Signaling and Therapeutic Opportunities.,” *Drug Dev. Res.*, vol. 75, no. 5, pp. 331–341, Aug. 2014.

[346] K. A. Gelderman, M. Hultqvist, L. M. Olsson, K. Bauer, A. Pizzolla, P. Olofsson, and R. Holmdahl, “Rheumatoid arthritis: the role of reactive oxygen species in disease development and therapeutic strategies.,” *Antioxid. Redox Signal.*, vol. 9, no. 10, pp. 1541–1567, Oct. 2007.

[347] K. R. Higgins and H. R. Ashry, “Wound dressings and topical agents.,” *Clin Podiatr Med Surg*, vol. 12, no. 1, pp. 31–40, Jan. 1995.

[348] J. I. Keenan, R. A. Peterson, and M. B. Hampton, “NADPH oxidase involvement in the pathology of Helicobacter pylori infection.,” *Free Radical Biology and Medicine*, vol. 38, no. 9, pp. 1188–1196, May 2005.

[349] J. Komatsu, H. Koyama, N. Maeda, and Y. Aratani, “Earlier onset of neutrophil-mediated inflammation in the ultraviolet-exposed skin of mice deficient in myeloperoxidase and NADPH oxidase.,” *Inflamm. Res.*, vol. 55, no. 5, pp. 200–206, May 2006.

[350] H. Yao, I. Edirisinghe, S.-R. Yang, S. Rajendrasozhan, A. Kode, S. Caito, D. Adenuga, and I. Rahman, “Genetic ablation of NADPH oxidase enhances susceptibility to cigarette smoke-induced lung inflammation and emphysema in mice.,” *The American Journal of Pathology*, vol. 172, no. 5, pp. 1222–1237, May 2008.

[351] D. C. Hohn and R. I. Lehrer, “NADPH oxidase deficiency in X-linked chronic granulomatous disease.,” *J. Clin. Invest.*, vol. 55, no. 4, pp. 707–713, Apr. 1975.

[352] A. C. Battersby, A. M. Cale, D. Goldblatt, and A. R. Gennery, “Clinical manifestations of disease in X-linked carriers of chronic granulomatous disease.,” *J. Clin. Immunol.*, vol. 33, no. 8, pp. 1276–1284, Nov. 2013.

[353] C. E. Paulsen, T. H. Truong, F. J. Garcia, A. Homann, V. Gupta, S. E. Leonard, and K. S. Carroll, “Peroxide-dependent sulfenylation of the EGFR catalytic site enhances kinase activity.,” *Nat Chem Biol*, vol. 8, no. 1, pp. 57–64, Jan. 2012.

[354] C. Persson, K. Kappert, U. Engström, A. Ostman, and T. Sjöblom, “An antibody-based method for monitoring in vivo oxidation of protein tyrosine phosphatases.,” *Methods*, vol. 35, no. 1, pp. 37–43, Jan. 2005.

[355] M. P. Murphy, A. Holmgren, N.-G. Larsson, B. Halliwell, C. J. Chang, B. Kalyanaraman, S. G. Rhee, P. J. Thornalley, L. Partridge, D. Gems, T. Nyström, V. Belousov, P. T. Schumacker, and C. C. Winterbourn, “Unraveling the Biological Roles of Reactive Oxygen Species,” *Cell Metabolism*, vol. 13, no. 4, pp. 361–366, Apr. 2011.

[356] J.-S. Kim, T. Y. Huang, and G. M. Bokoch, “Reactive Oxygen Species Regulate a Slingshot-Cofilin Activation Pathway,” *Molecular Biology of the Cell*, vol. 20, pp. 2650–2660, May 2009.

[357] M. J. L. Bours, E. L. R. Swennen, F. Di Virgilio, B. N. Cronstein, and P. C. Dagnelie, “Adenosine 5′-triphosphate and adenosine as endogenous signaling molecules in immunity and inflammation,” *Pharmacology & Therapeutics*, vol. 112, no. 2, pp. 358–404, Nov. 2006.

[358] F. Di Virgilio, O. R. Baricordi, R. Romagnoli, and P. G. Baraldi, “Leukocyte P2 receptors: a novel target for anti-inflammatory and anti-tumor therapy.,” *Curr Drug Targets Cardiovasc Haematol Disord*, vol. 5, no. 1, pp. 85–99, Feb. 2005.

[359] Y. Dou, H.-J. Wu, H.-Q. Li, S. Qin, Y.-E. Wang, J. Li, H.-F. Lou, Z. Chen, X.-M. Li, Q.-M. Luo, and S. Duan, “Microglial migration mediated by ATP-induced ATP release from lysosomes.,” *Cell Res.*, vol. 22, no. 6, pp. 1022–1033, Jun. 2012.

[360] W. G. Junger, “Immune cell regulation by autocrine purinergic signalling.,” *Nature Reviews Immunology*, vol. 11, no. 3, pp. 201–212, Mar. 2011.

[361] R. Nandigama, M. Padmasekar, M. Wartenberg, and H. Sauer, “Feed forward cycle of hypotonic stress-induced ATP release, purinergic receptor activation, and growth stimulation of prostate cancer cells.,” *Journal of Biological Chemistry*, vol. 281, no. 9, pp. 5686–5693, Mar. 2006.

[362] D. S. Cowen, H. M. Lazarus, S. B. Shurin, S. E. Stoll, and G. R. Dubyak, “Extracellular adenosine triphosphate activates calcium mobilization in human phagocytic leukocytes and neutrophil/monocyte progenitor cells.,” *J. Clin. Invest.*, vol. 83, no. 5, pp. 1651–1660, May 1989.

[363] F. Di Virgilio, P. Chiozzi, D. Ferrari, S. Falzoni, J. M. Sanz, A. Morelli, M. Torboli, G. Bolognesi, and O. R. Baricordi, “Nucleotide receptors: an emerging family of regulatory molecules in blood cells.,” *Blood*, vol. 97, no. 3, pp. 587–600, Feb. 2001.

[364] V. Sivaramakrishnan, S. Bidula, H. Campwala, D. Katikaneni, and S. J. Fountain, “Constitutive lysosome exocytosis releases ATP and engages P2Y receptors in human monocytes.,” *Journal of Cell Science*, vol. 125, no. 19, pp. 4567–4575, Oct. 2012.

[365] P. Bodin and G. Burnstock, “Increased release of ATP from endothelial cells during acute inflammation.,” *Inflamm. Res.*, vol. 47, no. 8, pp. 351–354, Aug. 1998.

[366] F. B. Chekeni, M. R. Elliott, J. K. Sandilos, S. F. Walk, J. M. Kinchen, E. R. Lazarowski, A. J. Armstrong, S. Penuela, D. W. Laird, G. S. Salvesen, B. E. Isakson, D. A. Bayliss, and K. S. Ravichandran, “Pannexin 1 channels mediate ‘find-me’ signal release and membrane permeability during apoptosis.,” *Nature*, vol. 467, no. 7317, pp. 863–867, Oct. 2010.

[367] H. K. Eltzschig, T. Eckle, A. Mager, N. Küper, C. Karcher, T. Weissmüller, K. Boengler, R. Schulz, S. C. Robson, and S. P. Colgan, “ATP release from activated neutrophils occurs via connexin 43 and modulates adenosine-dependent endothelial cell function.,” *Circ. Res.*, vol. 99, no. 10, pp. 1100–1108, Nov. 2006.

[368] M. Idzko, D. Ferrari, and H. K. Eltzschig, “Nucleotide signalling during inflammation.,” *Nature*, vol. 509, no. 7500, pp. 310–317, May 2014.

[369] P. A. Ward, T. W. Cunningham, K. K. McCulloch, and K. J. Johnson, “Regulatory effects of adenosine and adenine nucleotides on oxygen radical responses of neutrophils.,” *Lab. Invest.*, vol. 58, no. 4, pp. 438–447, Apr. 1988.

[370] C. Goepfert, M. Imai, S. Brouard, E. Csizmadia, E. Kaczmarek, and S. C. Robson, “CD39 modulates endothelial cell activation and apoptosis.,” *Mol. Med.*, vol. 6, no. 7, pp. 591–603, Jul. 2000.

[371] D. C. Altieri and T. S. Edgington, “The saturable high affinity association of factor X to ADP-stimulated monocytes defines a novel function of the Mac-1 receptor.,” *Journal of Biological Chemistry*, vol. 263, no. 15, pp. 7007–7015, May 1988.

[372] K. A. Aziz and M. Zuzel, “Regulation of polymorphonuclear leukocyte function by platelets.,” *Saudi Med J*, vol. 22, no. 6, pp. 526–530, Jun. 2001.

[373] J. G. Elferink, B. M. de Koster, G. J. Boonen, and W. de Priester, “Inhibition of neutrophil chemotaxis by purinoceptor agonists.,” *Arch Int Pharmacodyn Ther*, vol. 317, pp. 93–106, May 1992.

[374] M. W. Verghese, T. B. Kneisler, and J. A. Boucheron, “P2U agonists induce chemotaxis and actin polymerization in human neutrophils and differentiated HL60 cells.,” *Journal of Biological Chemistry*, vol. 271, no. 26, pp. 15597–15601, Jun. 1996.

[375] H. K. Eltzschig, L. F. Thompson, J. Karhausen, R. J. Cotta, J. C. Ibla, S. C. Robson, and S. P. Colgan, “Endogenous adenosine produced during hypoxia attenuates neutrophil accumulation: coordination by extracellular nucleotide metabolism.,” *Blood*, vol. 104, no. 13, pp. 3986–3992, Dec. 2004.

[376] S. Cockcroft and J. Stutchfield, “ATP stimulates secretion in human neutrophils and HL60 cells via a pertussis toxin-sensitive guanine nucleotide-binding protein coupled to phospholipase C.,” *FEBS Lett.*, vol. 245, no. 1, pp. 25–29, Mar. 1989.

[377] M. Idzko, S. Dichmann, D. Ferrari, F. Di Virgilio, A. la Sala, G. Girolomoni, E. Panther, and J. Norgauer, “Nucleotides induce chemotaxis and actin polymerization in immature but not mature human dendritic cells via activation of pertussis toxin-sensitive P2y receptors.,” *Blood*, vol. 100, no. 3, pp. 925–932, Aug. 2002.

[378] R. A. North and M. F. Jarvis, “P2X receptors as drug targets.,” *Mol. Pharmacol.*, vol. 83, no. 4, pp. 759–769, Apr. 2013.

[379] J. Li and S. J. Fountain, “Fluvastatin suppresses native and recombinant human P2X4 receptor function.,” *Purinergic Signalling*, vol. 8, no. 2, pp. 311–316, Jun. 2012.

[380] I. von Kügelgen, “Pharmacological profiles of cloned mammalian P2Y-receptor subtypes.,” *Pharmacology & Therapeutics*, vol. 110, no. 3, pp. 415–432, Jun. 2006.

[381] F. Ratjen, T. Durham, T. Navratil, A. Schaberg, F. J. Accurso, C. Wainwright, M. Barnes, R. B. Moss, TIGER-2 Study Investigator Group, “Long term effects of denufosol tetrasodium in patients with cystic fibrosis.,” *J. Cyst. Fibros.*, vol. 11, no. 6, pp. 539–549, Dec. 2012.

[382] S. Tsuchiya, M. Yamabe, Y. Yamaguchi, Y. Kobayashi, T. Konno, and K. Tada, “Establishment and characterization of a human acute monocytic leukemia cell line (THP-1).,” *Int. J. Cancer*, vol. 26, no. 2, pp. 171–176, Aug. 1980.

[383] C. Sundström and K. Nilsson, “Establishment and characterization of a human histiocytic lymphoma cell line (U-937).,” *Int. J. Cancer*, vol. 17, no. 5, pp. 565–577, May 1976.

[384] C. J. Edgell, C. C. McDonald, and J. B. Graham, “Permanent cell line expressing human factor VIII-related antigen established by hybridization.,” *Proc. Natl. Acad. Sci. U.S.A.*, vol. 80, no. 12, pp. 3734–3737, Jun. 1983.

[385] M. Daigneault, J. A. Preston, H. M. Marriott, M. K. B. Whyte, and D. H. Dockrell, “The Identification of Markers of Macrophage Differentiation in PMA-Stimulated THP-1 Cells and Monocyte-Derived Macrophages,” *PLoS ONE*, vol. 5, no. 1, p. e8668, Jan. 2010.

[386] A. Böyum, “Isolation of mononuclear cells and granulocytes from human blood. Isolation of monuclear cells by one centrifugation, and of granulocytes by combining centrifugation and sedimentation at 1 g.,” *Scand. J. Clin. Lab. Invest. Suppl.*, vol. 97, pp. 77–89, 1968.

[387] A. B. Lyons, “Analysing cell division in vivo and in vitro using flow cytometric measurement of CFSE dye dilution.,” *J. Immunol. Methods*, vol. 243, no. 1, pp. 147–154, Sep. 2000.

[388] S. Sakamoto, “[Morphological studies of lymphocytes using Wright-Giemsa stains].,” *Rinsho Byori*, vol. 44, pp. 7–22, Mar. 1981.

[389] D. A. Bass, J. W. Parce, L. R. Dechatelet, P. Szejda, M. C. Seeds, and M. Thomas, “Flow cytometric studies of oxidative product formation by neutrophils: a graded response to membrane stimulation.,” *The Journal of Immunology*, vol. 130, no. 4, pp. 1910–1917, Apr. 1983.

[390] K. R. Gee, K. A. Brown, W. N. Chen, J. Bishop-Stewart, D. Gray, and I. Johnson, “Chemical and physiological characterization of fluo-4 Ca(2+)-indicator dyes.,” *Cell Calcium*, vol. 27, no. 2, pp. 97–106, Feb. 2000.

[391] C. A. Schneider, W. S. Rasband, and K. W. Eliceiri, “NIH Image to ImageJ: 25 years of image analysis.,” *Nat. Methods*, vol. 9, no. 7, pp. 671–675, Jul. 2012.

[392] A. E. Carpenter, T. R. Jones, M. R. Lamprecht, C. Clarke, I. H. Kang, O. Friman, D. A. Guertin, J. H. Chang, R. A. Lindquist, J. Moffat, P. Golland, and D. M. Sabatini, “CellProfiler: image analysis software for identifying and quantifying cell phenotypes.,” *Genome Biol.*, vol. 7, no. 10, p. R100, 2006.

[393] B. Heit and P. Kubes, “Measuring Chemotaxis and Chemokinesis: The Under-Agarose Cell Migration Assay,” *Science Signaling*, vol. 2003, no. 170, pp. pl5–pl5, Feb. 2003.

[394] M. Tateno, Y. Nishida, and T. Adachi-Yamada, “Regulation of JNK by Src during Drosophila development.,” *Science*, vol. 287, no. 5451, pp. 324–327, Jan. 2000.

[395] A. C. Spradling, D. Stern, A. Beaton, E. J. Rhem, T. Laverty, N. Mozden, S. Misra, and G. M. Rubin, “The Berkeley Drosophila Genome Project gene disruption project: Single P-element insertions mutating 25% of vital Drosophila genes.,” *Genetics*, vol. 153, no. 1, pp. 135–177, Sep. 1999.

[396] V. Tsarouhas, L. Yao, and C. Samakovlis, “Src kinases and ERK activate distinct responses to Stitcher receptor tyrosine kinase signaling during wound healing in Drosophila.,” *Journal of Cell Science*, vol. 127, no. 8, pp. 1829–1839, Apr. 2014.

[397] T. Takano, K. Sada, and H. Yamamura, “Role of protein-tyrosine kinase syk in oxidative stress signaling in B cells.,” *Antioxid. Redox Signal.*, vol. 4, no. 3, pp. 533–541, Jun. 2002.

[398] F. Tabet, E. L. Schiffrin, and R. M. Touyz, “Mitogen-activated protein kinase activation by hydrogen peroxide is mediated through tyrosine kinase-dependent, protein kinase C-independent pathways in vascular smooth muscle cells: upregulation in spontaneously hypertensive rats.,” *J. Hypertens.*, vol. 23, no. 11, pp. 2005–2012, Nov. 2005.

[399] Y. Takada, A. Mukhopadhyay, G. C. Kundu, G. H. Mahabeleshwar, S. Singh, and B. B. Aggarwal, “Hydrogen peroxide activates NF-kappa B through tyrosine phosphorylation of I kappa B alpha and serine phosphorylation of p65: evidence for the involvement of I kappa B alpha kinase and Syk protein-tyrosine kinase.,” *Journal of Biological Chemistry*, vol. 278, no. 26, pp. 24233–24241, Jun. 2003.

[400] X. Lu and Y. Li, “Drosophila Src42A is a negative regulator of RTK signaling.,” *Dev. Biol.*, vol. 208, no. 1, pp. 233–243, Apr. 1999.

[401] F. Takahashi, S. Endo, T. Kojima, and K. Saigo, “Regulation of cell-cell contacts in developing Drosophila eyes by Dsrc41, a new, close relative of vertebrate c-src.,” *Genes Dev.*, vol. 10, no. 13, pp. 1645–1656, Jul. 1996.

[402] K. A. Mace, J. C. Pearson, and W. McGinnis, “An epidermal barrier wound repair pathway in Drosophila is mediated by grainy head.,” *Science*, vol. 308, no. 5720, pp. 381–385, Apr. 2005.

[403] M. Rämet, R. Lanot, D. Zachary, and P. Manfruelli, “JNK signaling pathway is required for efficient wound healing in Drosophila.,” *Dev. Biol.*, vol. 241, no. 1, pp. 145–156, Jan. 2002.

[404] S. Rieger and A. Sagasti, “Hydrogen peroxide promotes injury-induced peripheral sensory axon regeneration in the zebrafish skin.,” *PLoS Biol*, vol. 9, no. 5, p. e1000621, May 2011.

[405] D. Grover, D. Ford, C. Brown, N. Hoe, A. Erdem, S. Tavaré, and J. Tower, “Hydrogen peroxide stimulates activity and alters behavior in Drosophila melanogaster.,” *PLoS ONE*, vol. 4, no. 10, p. e7580, 2009.

[406] A. Trautmann, “Extracellular ATP in the Immune System: More Than Just a ‘Danger Signal’,” *Science Signaling*, vol. 2, no. 56, pp. pe6–pe6, Feb. 2009.

[407] B. V. O'Donnell, D. G. Tew, O. T. Jones, and P. J. England, “Studies on the inhibitory mechanism of iodonium compounds with special reference to neutrophil NADPH oxidase.,” *Biochem. J.*, vol. 290, pp. 41–49, Feb. 1993.

[408] L. Fantuzzi, P. Borghi, V. Ciolli, G. Pavlakis, F. Belardelli, and S. Gessani, “Loss of CCR2 expression and functional response to monocyte chemotactic protein (MCP-1) during the differentiation of human monocytes: role of secreted MCP-1 in the regulation of the chemotactic response.,” *Blood*, vol. 94, no. 3, pp. 875–883, Aug. 1999.

[409] C.-Y. Chao, C.-K. Lii, I.-T. Tsai, C. C. Li, K.-L. Liu, C.-W. Tsai, and H.-W. Chen, “Andrographolide Inhibits ICAM-1 Expression and NF-κB Activation in TNF-α-Treated EA.hy926 Cells,” *J. Agric. Food Chem.*, vol. 59, no. 10, pp. 5263–5271, May 2011.

[410] A. A. Abu-Khader and Y. Y. Bilto, “Exposure of human neutrophils to oxygen radicals causes loss of deformability, lipid peroxidation, protein degradation, respiratory burst activation and loss of migration.,” *Clin. Hemorheol. Microcirc.*, vol. 27, no. 1, pp. 57–66, 2002.

[411] Y. Wu, X. Zhang, X. Kang, N. Li, R. Wang, T. Hu, M. Xiang, X. Wang, W. Yuan, A. Chen, D. Meng, and S. Chen, “Oxidative stress inhibits adhesion and transendothelial migration, and induces apoptosis and senescence of induced pluripotent stem cells.,” *Clin. Exp. Pharmacol. Physiol.*, vol. 40, no. 9, pp. 626–634, Sep. 2013.

[412] M. J. Grimshaw and F. R. Balkwill, “Inhibition of monocyte and macrophage chemotaxis by hypoxia and inflammation--a potential mechanism.,” *Eur. J. Immunol.*, vol. 31, no. 2, pp. 480–489, Feb. 2001.

[413] A. Sica, A. Saccani, A. Borsatti, C. A. Power, T. N. Wells, W. Luini, N. Polentarutti, S. Sozzani, and A. Mantovani, “Bacterial lipopolysaccharide rapidly inhibits expression of C-C chemokine receptors in human monocytes.,” *Journal of Experimental Medicine*, vol. 185, no. 5, pp. 969–974, Mar. 1997.

[414] L. Xu, M. H. Khandaker, J. Barlic, L. Ran, M. L. Borja, J. Madrenas, R. Rahimpour, K. Chen, G. Mitchell, C. M. Tan, M. DeVries, R. D. Feldman, and D. J. Kelvin, “Identification of a novel mechanism for endotoxin-mediated down-modulation of CC chemokine receptor expression.,” *Eur. J. Immunol.*, vol. 30, no. 1, pp. 227–235, Jan. 2000.

[415] A. Saccani, S. Saccani, S. Orlando, M. Sironi, S. Bernasconi, P. Ghezzi, A. Mantovani, and A. Sica, “Redox regulation of chemokine receptor expression.,” *Proc. Natl. Acad. Sci. U.S.A.*, vol. 97, no. 6, pp. 2761–2766, Mar. 2000.

[416] T. R. Hurd, M. DeGennaro, and R. Lehmann, “Redox regulation of cell migration and adhesion,” *Trends in Cell Biology*, vol. 22, no. 2, pp. 107–115, Feb. 2012.

[417] C. F. Lee, S. Ullevig, H. S. Kim, and R. Asmis, “Regulation of Monocyte Adhesion and Migration by Nox4.,” *PLoS ONE*, vol. 8, no. 6, p. e66964, 2013.

[418] G. Gerisch and H. U. Keller, “Chemotactic reorientation of granulocytes stimulated with micropipettes containing fMet-Leu-Phe.,” *Journal of Cell Science*, vol. 52, pp. 1–10, Dec. 1981.

[419] R. K. Root, J. Metcalf, N. Oshino, and B. Chance, “H2O2 release from human granulocytes during phagocytosis. I. Documentation, quantitation, and some regulating factors.,” *J. Clin. Invest.*, vol. 55, no. 5, pp. 945–955, May 1975.

[420] A. Magenau, C. Benzing, N. Proschogo, A. S. Don, L. Hejazi, D. Karunakaran, W. Jessup, and K. Gaus, “Phagocytosis of IgG-coated polystyrene beads by macrophages induces and requires high membrane order.,” *Traffic*, vol. 12, no. 12, pp. 1730–1743, Dec. 2011.

[421] A. A. Voetman and D. Roos, “Endogenous catalase protects human blood phagocytes against oxidative damage by extracellularly generated hydrogen peroxide.,” *Blood*, vol. 56, no. 5, pp. 846–852, Nov. 1980.

[422] R. L. Baehner, L. A. Boxer, J. M. Allen, and J. Davis, “Autooxidation as a basis for altered function by polymorphonuclear leukocytes.,” *Blood*, vol. 50, no. 2, pp. 327–335, Aug. 1977.

[423] S. B. Dillon, M. W. Verghese, and R. Snyderman, “Signal transduction in cells following binding of chemoattractants to membrane receptors.,” *Virchows Arch., B, Cell Pathol.*, vol. 55, no. 2, pp. 65–80, 1988.

[424] J. Cuschieri, E. Bulger, I. Garcia, and R. V. Maier, “Oxidative-induced calcium mobilization is dependent on annexin VI release from lipid rafts.,” *Surgery*, vol. 138, no. 2, pp. 158–164, Aug. 2005.

[425] B. A. Miller, “The role of TRP channels in oxidative stress-induced cell death.,” *J. Membr. Biol.*, vol. 209, no. 1, pp. 31–41, Jan. 2006.

[426] M. A. Panaro and V. Mitolo, “Cellular responses to FMLP challenging: a mini-review.,” *Immunopharmacol Immunotoxicol*, vol. 21, no. 3, pp. 397–419, Aug. 1999.

[427] N. Y. Bhatt, T. W. Kelley, V. V. Khramtsov, Y. Wang, G. K. Lam, T. L. Clanton, and C. B. Marsh, “Macrophage-colony-stimulating factor-induced activation of extracellular-regulated kinase involves phosphatidylinositol 3-kinase and reactive oxygen species in human monocytes.,” *The Journal of Immunology*, vol. 169, no. 11, pp. 6427–6434, Dec. 2002.

[428] S. Carta, S. Tassi, I. Pettinati, L. Delfino, C. A. Dinarello, and A. Rubartelli, “The rate of interleukin-1beta secretion in different myeloid cells varies with the extent of redox response to Toll-like receptor triggering.,” *J. Biol. Chem.*, vol. 286, no. 31, pp. 27069–27080, Aug. 2011.

[429] J. A. Ellis, S. J. Mayer, and O. T. Jones, “The effect of the NADPH oxidase inhibitor diphenyleneiodonium on aerobic and anaerobic microbicidal activities of human neutrophils.,” *Biochem. J.*, vol. 251, no. 3, pp. 887–891, May 1988.

[430] J. Wilson, M. Winter, and D. M. Shasby, “Oxidants, ATP depletion, and endothelial permeability to macromolecules.,” *Blood*, vol. 76, no. 12, pp. 2578–2582, Dec. 1990.

[431] M. S. Lewis, R. E. Whatley, P. Cain, T. M. McIntyre, S. M. Prescott, and G. A. Zimmerman, “Hydrogen peroxide stimulates the synthesis of platelet-activating factor by endothelium and induces endothelial cell-dependent neutrophil adhesion.,” *J. Clin. Invest.*, vol. 82, no. 6, pp. 2045–2055, Dec. 1988.

[432] A. C. Gasic, G. McGuire, S. Krater, A. I. Farhood, M. A. Goldstein, C. W. Smith, M. L. Entman, and A. A. Taylor, “Hydrogen peroxide pretreatment of perfused canine vessels induces ICAM-1 and CD18-dependent neutrophil adherence.,” *Circulation*, vol. 84, no. 5, pp. 2154–2166, Nov. 1991.

[433] J. R. Bradley, D. R. Johnson, and J. S. Pober, “Endothelial activation by hydrogen peroxide. Selective increases of intercellular adhesion molecule-1 and major histocompatibility complex class I.,” *The American Journal of Pathology*, vol. 142, no. 5, pp. 1598–1609, May 1993.

[434] M. Gülden, A. Jess, J. Kammann, E. Maser, and H. Seibert, “Cytotoxic potency of H2O2 in cell cultures: impact of cell concentration and exposure time.,” *Free Radical Biology and Medicine*, vol. 49, no. 8, pp. 1298–1305, Nov. 2010.

[435] J. Nakamura, E. R. Purvis, and J. A. Swenberg, “Micromolar concentrations of hydrogen peroxide induce oxidative DNA lesions more efficiently than millimolar concentrations in mammalian cells.,” *Nucleic Acids Research*, vol. 31, no. 6, pp. 1790–1795, Mar. 2003.

[436] F. Bianco, S. Ceruti, A. Colombo, M. Fumagalli, D. Ferrari, C. Pizzirani, M. Matteoli, F. Di Virgilio, M. P. Abbracchio, and C. Verderio, “A role for P2X7 in microglial proliferation.,” *Journal of Neurochemistry*, vol. 99, no. 3, pp. 745–758, Nov. 2006.

[437] C. Lambert, A. R. Ase, P. Séguéla, and J. P. Antel, “Distinct migratory and cytokine responses of human microglia and macrophages to ATP.,” *Brain Behav. Immun.*, vol. 24, no. 8, pp. 1241–1248, Nov. 2010.

[438] Y. Chen, R. Corriden, Y. Inoue, L. Yip, N. Hashiguchi, A. Zinkernagel, V. Nizet, P. A. Insel, and W. G. Junger, “ATP release guides neutrophil chemotaxis via P2Y2 and A3 receptors.,” *Science*, vol. 314, no. 5806, pp. 1792–1795, Dec. 2006.

[439] F. Kukulski, F. Ben Yebdri, J. Lecka, G. Kauffenstein, S. A. Lévesque, M. Martín-Satué, and J. Sévigny, “Extracellular ATP and P2 receptors are required for IL-8 to induce neutrophil migration.,” *Cytokine*, vol. 46, no. 2, pp. 166–170, May 2009.

[440] R. Corriden and P. A. Insel, “New insights regarding the regulation of chemotaxis by nucleotides, adenosine, and their receptors.,” *Purinergic Signalling*, vol. 8, no. 3, pp. 587–598, Sep. 2012.

[441] J. T. Neary, L. Baker, S. L. Jorgensen, and M. D. Norenberg, “Extracellular ATP induces stellation and increases glial fibrillary acidic protein content and DNA synthesis in primary astrocyte cultures.,” *Acta Neuropathol.*, vol. 87, no. 1, pp. 8–13, 1994.

[442] J. H. Hanke, J. P. Gardner, R. L. Dow, P. S. Changelian, W. H. Brissette, E. J. Weringer, B. A. Pollok, and P. A. Connelly, “Discovery of a novel, potent, and Src family-selective tyrosine kinase inhibitor. Study of Lck- and FynT-dependent T cell activation.,” *Journal of Biological Chemistry*, vol. 271, no. 2, pp. 695–701, Jan. 1996.

[443] J. Bain, L. Plater, M. Elliott, N. Shpiro, C. J. Hastie, H. Mclauchlan, I. Klevernic, J. S. C. Arthur, D. R. Alessi, and P. Cohen, “The selectivity of protein kinase inhibitors: a further update,” *Biochem. J.*, vol. 408, no. 3, p. 297, Dec. 2007.

[444] K. R. Brandvold, M. E. Steffey, C. C. Fox, and M. B. Soellner, “Development of a highly selective c-Src kinase inhibitor.,” *ACS Chem. Biol.*, vol. 7, no. 8, pp. 1393–1398, Aug. 2012.

[445] R. Karni, S. Mizrachi, E. Reiss-Sklan, A. Gazit, O. Livnah, and A. Levitzki, “The pp60c-Src inhibitor PP1 is non-competitive against ATP.,” *FEBS Lett.*, vol. 537, no. 1, pp. 47–52, Feb. 2003.

[446] R. L. Geahlen and J. L. McLaughlin, “Piceatannol (3,4,3‘,5’-tetrahydroxy-trans-stilbene) is a naturally occurring protein-tyrosine kinase inhibitor.,” *Biochemical and Biophysical Research Communications*, vol. 165, no. 1, pp. 241–245, Nov. 1989.

[447] J. M. Oliver, D. L. Burg, B. S. Wilson, J. L. McLaughlin, and R. L. Geahlen, “Inhibition of mast cell Fc epsilon R1-mediated signaling and effector function by the Syk-selective inhibitor, piceatannol.,” *Journal of Biological Chemistry*, vol. 269, no. 47, pp. 29697–29703, Nov. 1994.

[448] C. J. Vlahos, W. F. Matter, K. Y. Hui, and R. F. Brown, “A specific inhibitor of phosphatidylinositol 3-kinase, 2-(4-morpholinyl)-8-phenyl-4H-1-benzopyran-4-one (LY294002).,” *Journal of Biological Chemistry*, vol. 269, no. 7, pp. 5241–5248, Feb. 1994.

[449] S.-I. Yaguchi, Y. Fukui, I. Koshimizu, H. Yoshimi, T. Matsuno, H. Gouda, S. Hirono, K. Yamazaki, and T. Yamori, “Antitumor activity of ZSTK474, a new phosphatidylinositol 3-kinase inhibitor.,” *J. Natl. Cancer Inst.*, vol. 98, no. 8, pp. 545–556, Apr. 2006.

[450] S. Toyama, N. Tamura, K. Haruta, T. Karakida, S. Mori, T. Watanabe, T. Yamori, and Y. Takasaki, “Inhibitory effects of ZSTK474, a novel phosphoinositide 3-kinase inhibitor, on osteoclasts and collagen-induced arthritis in mice.,” *Arthritis Res. Ther.*, vol. 12, no. 3, p. R92, 2010.

[451] K. Haruta, S. Mori, N. Tamura, A. Sasaki, M. Nagamine, S.-I. Yaguchi, F. Kamachi, J. Enami, S. Kobayashi, T. Yamori, and Y. Takasaki, “Inhibitory effects of ZSTK474, a phosphatidylinositol 3-kinase inhibitor, on adjuvant-induced arthritis in rats,” *Inflamm. Res.*, vol. 61, no. 6, pp. 551–562, Feb. 2012.

[452] B. R. Leaker, P. J. Barnes, B. J. O'Connor, F. Y. Ali, P. Tam, J. Neville, L. F. Mackenzie, and T. MacRury, “The effects of the novel SHIP1 activator AQX-1125 on allergen-induced responses in mild-to-moderate asthma.,” *Clin. Exp. Allergy*, vol. 44, no. 9, pp. 1146–1153, Sep. 2014.

[453] A. C. Schmid, R. D. Byrne, R. Vilar, and R. Woscholski, “Bisperoxovanadium compounds are potent PTEN inhibitors.,” *FEBS Lett.*, vol. 566, no. 1, pp. 35–38, May 2004.

[454] M. Iijima and P. Devreotes, “Tumor suppressor PTEN mediates sensing of chemoattractant gradients.,” *Cell*, vol. 109, no. 5, pp. 599–610, May 2002.

[455] S. Funamoto, R. Meili, S. Lee, L. Parry, and R. A. Firtel, “Spatial and temporal regulation of 3-phosphoinositides by PI 3-kinase and PTEN mediates chemotaxis.,” *Cell*, vol. 109, no. 5, pp. 611–623, May 2002.

[456] C. Feistritzer, B. A. Mosheimer, I. Tancevski, N. C. Kaneider, D. H. Sturn, J. R. Patsch, and C. J. Wiedermann, “Src tyrosine kinase-dependent migratory effects of antithrombin in leukocytes.,” *Exp. Cell Res.*, vol. 305, no. 1, pp. 214–220, Apr. 2005.

[457] J. B. Bolen and J. S. Brugge, “Leukocyte protein tyrosine kinases: potential targets for drug discovery.,” *Annu. Rev. Immunol.*, vol. 15, no. 1, pp. 371–404, 1997.

[458] S. Carréno, E. Caron, C. Cougoule, L. J. Emorine, and I. Maridonneau-Parini, “p59Hck isoform induces F-actin reorganization to form protrusions of the plasma membrane in a Cdc42- and Rac-dependent manner.,” *Journal of Biological Chemistry*, vol. 277, no. 23, pp. 21007–21016, Jun. 2002.

[459] M. Resnati, M. Guttinger, S. Valcamonica, N. Sidenius, F. Blasi, and F. Fazioli, “Proteolytic cleavage of the urokinase receptor substitutes for the agonist-induced chemotactic effect.,” *The EMBO Journal*, vol. 15, no. 7, pp. 1572–1582, Apr. 1996.

[460] T. Suzuki, H. Kono, N. Hirose, M. Okada, T. Yamamoto, K. Yamamoto, and Z. Honda, “Differential involvement of Src family kinases in Fc gamma receptor-mediated phagocytosis.,” *The Journal of Immunology*, vol. 165, no. 1, pp. 473–482, Jul. 2000.

[461] V. Le Cabec, S. Carréno, A. Moisand, C. Bordier, and I. Maridonneau-Parini, “Complement receptor 3 (CD11b/CD18) mediates type I and type II phagocytosis during nonopsonic and opsonic phagocytosis, respectively.,” *The Journal of Immunology*, vol. 169, no. 4, pp. 2003–2009, Aug. 2002.

[462] G. Scholz, K. Cartledge, and A. R. Dunn, “Hck enhances the adherence of lipopolysaccharide-stimulated macrophages via Cbl and phosphatidylinositol 3-kinase.,” *Journal of Biological Chemistry*, vol. 275, no. 19, pp. 14615–14623, May 2000.

[463] M. A. Sanjuan, N. Rao, K.-T. A. Lai, Y. Gu, S. Sun, A. Fuchs, W.-P. Fung-Leung, M. Colonna, and L. Karlsson, “CpG-induced tyrosine phosphorylation occurs via a TLR9-independent mechanism and is required for cytokine secretion.,” *The Journal of Cell Biology*, vol. 172, no. 7, pp. 1057–1068, Mar. 2006.

[464] V. L. J. Tybulewicz, L. Ardouin, A. Prisco, and L. F. Reynolds, “Vav1: a key signal transducer downstream of the TCR.,” *Immunological Reviews*, vol. 192, pp. 42–52, Apr. 2003.

[465] J. Schymeinsky, A. Sindrilaru, D. Frommhold, M. Sperandio, R. Gerstl, C. Then, A. Mócsai, K. Scharffetter-Kochanek, and B. Walzog, “The Vav binding site of the non-receptor tyrosine kinase Syk at Tyr 348 is critical for beta2 integrin (CD11/CD18)-mediated neutrophil migration.,” *Blood*, vol. 108, no. 12, pp. 3919–3927, Dec. 2006.

[466] D. Frommhold, I. Mannigel, J. Schymeinsky, A. Mócsai, J. Poeschl, B. Walzog, and M. Sperandio, “Spleen tyrosine kinase Syk is critical for sustained leukocyte adhesion during inflammation in vivo.,” *BMC Immunol.*, vol. 8, no. 1, p. 31, 2007.

[467] M. Nishio, K.-I. Watanabe, J. Sasaki, C. Taya, S. Takasuga, R. Iizuka, T. Balla, M. Yamazaki, H. Watanabe, R. Itoh, S. Kuroda, Y. Horie, I. Förster, T. W. Mak, H. Yonekawa, J. M. Penninger, Y. Kanaho, A. Suzuki, and T. Sasaki, “Control of cell polarity and motility by the PtdIns(3,4,5)P3 phosphatase SHIP1.,” *Nat Cell Biol*, vol. 9, no. 1, pp. 36–44, Jan. 2007.

[468] V. Vedham, H. Phee, and K. M. Coggeshall, “Vav activation and function as a rac guanine nucleotide exchange factor in macrophage colony-stimulating factor-induced macrophage chemotaxis.,” *Molecular and Cellular Biology*, vol. 25, no. 10, pp. 4211–4220, May 2005.

[469] J. A. Wahle, K. H. T. Paraiso, R. D. Kendig, H. R. Lawrence, L. Chen, J. Wu, and W. G. Kerr, “Inappropriate recruitment and activity by the Src homology region 2 domain-containing phosphatase 1 (SHP1) is responsible for receptor dominance in the SHIP-deficient NK cell.,” *The Journal of Immunology*, vol. 179, no. 12, pp. 8009–8015, Dec. 2007.

[470] Q. Peng, S. Malhotra, J. A. Torchia, W. G. Kerr, K. M. Coggeshall, and M. B. Humphrey, “TREM2- and DAP12-dependent activation of PI3K requires DAP10 and is inhibited by SHIP1.,” *Science Signaling*, vol. 3, no. 122, pp. ra38–ra38, 2010.

[471] B. Vanhaesebroeck, G. E. Jones, W. E. Allen, D. Zicha, R. Hooshmand-Rad, C. Sawyer, C. Wells, M. D. Waterfield, and A. J. Ridley, “Distinct PI(3)Ks mediate mitogenic signalling and cell migration in macrophages.,” *Nat Cell Biol*, vol. 1, no. 1, pp. 69–71, May 1999.

[472] W. Zhao, W. Guo, Q. Zhou, S.-N. Ma, R. Wang, Y. Qiu, M. Jin, H.-Q. Duan, and D. Kong, “In Vitro Antimetastatic Effect of Phosphatidylinositol 3-Kinase Inhibitor ZSTK474 on Prostate Cancer PC3 Cells.,” *Int J Mol Sci*, vol. 14, no. 7, pp. 13577–13591, 2013.

[473] A. M. Ferreira, H. Isaacs, J. S. Hayflick, K. A. Rogers, and M. Sandig, “The p110delta isoform of PI3K differentially regulates beta1 and beta2 integrin-mediated monocyte adhesion and spreading and modulates diapedesis.,” *Microcirculation*, vol. 13, no. 6, pp. 439–456, Sep. 2006.

[474] J. Schymeinsky, C. Then, A. Sindrilaru, R. Gerstl, Z. Jakus, V. L. J. Tybulewicz, K. Scharffetter-Kochanek, and B. Walzog, “Syk-mediated translocation of PI3Kdelta to the leading edge controls lamellipodium formation and migration of leukocytes.,” *PLoS ONE*, vol. 2, no. 11, p. e1132, 2007.

[475] S. J. Leevers, D. Weinkove, L. K. MacDougall, E. Hafen, and M. D. Waterfield, “The Drosophila phosphoinositide 3-kinase Dp110 promotes cell growth.,” *The EMBO Journal*, vol. 15, no. 23, pp. 6584–6594, Dec. 1996.

[476] G. Millonig, I. Ganzleben, T. Peccerella, G. Casanovas, L. Brodziak-Jarosz, K. Breitkopf-Heinlein, T. P. Dick, H.-K. Seitz, M. U. Muckenthaler, and S. Mueller, “Sustained submicromolar H2O2 levels induce hepcidin via signal transducer and activator of transcription 3 (STAT3).,” *J. Biol. Chem.*, vol. 287, no. 44, pp. 37472–37482, Oct. 2012.

[477] M. C. Sobotta, A. G. Barata, U. Schmidt, S. Mueller, G. Millonig, and T. P. Dick, “Exposing cells to H2O2: a quantitative comparison between continuous low-dose and one-time high-dose treatments.,” *Free Radical Biology and Medicine*, vol. 60, pp. 325–335, Jul. 2013.

[478] H. Tang, Q. Hao, S. A. Rutherford, B. Low, and Z. J. Zhao, “Inactivation of SRC family tyrosine kinases by reactive oxygen species in vivo.,” *Journal of Biological Chemistry*, vol. 280, no. 25, pp. 23918–23925, Jun. 2005.

[479] E. K. Sackmann, E. Berthier, E. W. K. Young, M. A. Shelef, S. A. Wernimont, A. Huttenlocher, and D. J. Beebe, “Microfluidic kit-on-a-lid: a versatile platform for neutrophil chemotaxis assays.,” *Blood*, vol. 120, no. 14, pp. e45–53, Oct. 2012.

[480] R. Capdeville, E. Buchdunger, J. Zimmermann, and A. Matter, “Glivec (STI571, imatinib), a rationally developed, targeted anticancer drug.,” *Nat Rev Drug Discov*, vol. 1, no. 7, pp. 493–502, Jul. 2002.

[481] M. E. Breen, M. E. Steffey, E. J. Lachacz, F. E. Kwarcinski, C. C. Fox, and M. B. Soellner, “Substrate activity screening with kinases: discovery of small-molecule substrate-competitive c-Src inhibitors.,” *Angew. Chem. Int. Ed. Engl.*, vol. 53, no. 27, pp. 7010–7013, Jul. 2014.

[482] A. Nijnik, J. Pistolic, P. Cho, N. C. J. Filewod, R. Falsafi, A. Ramin, K. W. Harder, and R. E. W. Hancock, “The role of the Src family kinase Lyn in the immunomodulatory activities of cathelicidin peptide LL-37 on monocytic cells.,” *Journal of Leukocyte Biology*, vol. 91, no. 4, pp. 599–607, Apr. 2012.

[483] B. N. Kang, S. G. Ha, X. N. Ge, M. Reza Hosseinkhani, N. S. Bahaie, Y. Greenberg, M. N. Blumenthal, K. D. Puri, S. P. Rao, and P. Sriramarao, “The p110δ subunit of PI3K regulates bone marrow-derived eosinophil trafficking and airway eosinophilia in allergen-challenged mice.,” *Am. J. Physiol. Lung Cell Mol. Physiol.*, vol. 302, no. 11, pp. L1179–91, Jun. 2012.

# APPENDIX

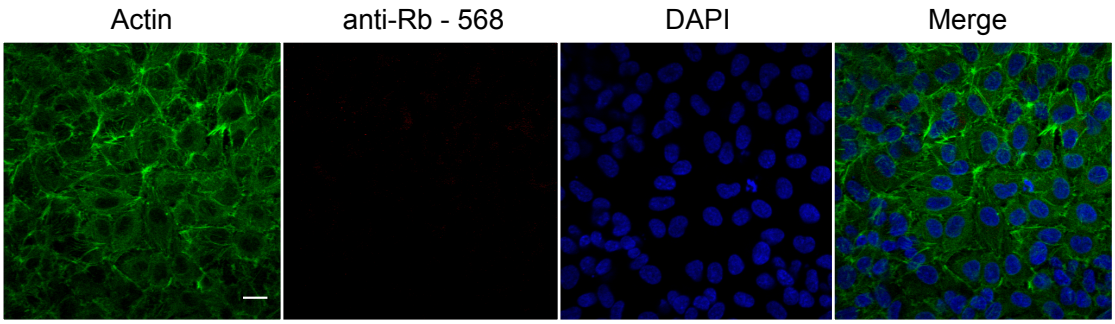


**Figure A1: No primary controls for endothelial EA.hy926 monolayer ICAM-1 expression.** Confocal images of indicated fluorescent secondary antibodies from EA.hy926 monolayers. Monolayers were processed for immunofluorescence as outlined in chapter 2.2.8 with the exception that there was no primary antibody step. Images are representative of three independent experiments. Scale bar = 20µm.

**Movie legends**

**Movie S3.2(a-d):** Time lapse movies of developmental stage 15 *Drosophila* embryonic hemocyte wound response in (a) WT, (b) $Src42A^{myri}$, (c) $Src42A^{K10108}$ and (d) $Src42A^{E1}$ fly lines. Images were captured every 2 minutes. Each movie is representative of at least three separate embryos per genotype. Scale bar = 100µm.
Stills from these movies are used in **Figure 3.2: Src42A mutant embryos show reduced hemocyte directionality and velocity in *Drosophila* embryos.**

**Movie S3.3(a-d):** Time lapse movies of developmental stage 15 *Drosophila* embryonic hemocyte random migration in (a) WT, (b) $Src42A^{myri}$, (c) $Src42A^{K10108}$ and (d) $Src42A^{E1}$ fly lines. Images were captured every 60 seconds. Each movie is representative of at least three separate embryos per genotype. Scale bar = 100µm.
Stills from these movies are used in **Figure 3.3: Random migration of hemocytes is not compromised in Src42A mutant *Drosophila* embryos.**

**Movie S3.6(a-d):** Time lapse movies of developmental stage 15 *Drosophila* embryonic hemocyte random migration in WT embryos treated with (a) PBS, (b) 10nM $H_2O_2$, (c) 10µM $H_2O_2$ and (d) 10mM $H_2O_2$. Images were captured every 30 seconds. Scale bar = 20µm.
Stills from these movies are used in **Figure 3.6: Exogenous $H_2O_2$ impairs hemocyte random migration in *Drosophila* embryos.**

**Movie S4.8(a-d):** Time lapse movies of primary human neutrophil chemokinesis on fibronectin-coated coverglass chambers in response to uniform gradients of (a) PBS, (b) 10nM IL-8, (c) 10nM fMLP and (d) 10µM $H_2O_2$. Images were captured every 30 seconds. Each movie is representative of at least three separate experiments per treatment group. Scale bar = 20µm.
Stills from these movies are used in **Figure 4.8: Neutrophil chemokinesis is increased by stimulation with IL-8 and fMLP but not with $H_2O_2$.**

**Movie S4.32(a-c):** Time lapse movies of THP-1 monocytic cells seeded on fibronectin coated coverglass chambers in response to uniform gradients of (a) 10nM MCP-1, (b) 0.3mM ATP and (c) 10µM $H_2O_2$. Images were captured every 30 seconds. Scale bar = 10µm.
Stills from these movies are used in **Figure 4.32: Time lapse imaging of THP-1 monocytes seeded on fibronectin reveals changes in shape following stimulation with different agonists.**